

# Anti-apoptotic and neuroprotective erythropoietin/CRLF3- signalling in insects and humans

Dissertation

for the award of the degree

"Doctor rerum naturalium" (Dr.rer.nat.)

of the Georg-August-Universität Göttingen

within the doctoral program Biology

of the Georg-August University School of Science (GAUSS)

submitted by

Debra Yasemin Knorr

From Cape Town

Göttingen, 2022

## **Thesis Committee**

Prof. Dr. Ralf Heinrich  
Department of Cellular Neurobiology;  
Georg-August-University Göttingen

Prof. Dr. Gregor Bucher  
Department of Evolutionary Developmental Genetics;  
Georg-August-University Göttingen

Prof. Dr. Rüdiger Behr  
Platform for Degenerative Diseases;  
German Primate Center Göttingen

## **Members of the Examination Board**

Reviewer: Prof. Dr. Ralf Heinrich  
Department of Cellular Neurobiology;  
Georg-August-University Göttingen

Second Reviewer: Prof. Dr. Gregor Bucher  
Department of Evolutionary Developmental Genetics;  
Georg-August-University Göttingen

## **Further Members of the Examination Board:**

Prof. Dr. Rüdiger Behr  
Platform for Degenerative Diseases;  
German Primate Center Göttingen

Prof. Dr. Tiago Outeiro  
Experimental Neurodegeneration;  
University Medical Center Göttingen

Prof. Dr. Susann Boretius  
Functional Imaging;  
German Primate Center

PD Dr. Sven Bradler  
Dep. Animal Evolution and Biodiversity;  
Georg-August-University Göttingen

Date of the oral examination: 25.05.2022

---

Of course it is happening inside your head, [...], but why on earth should that mean it is not real?

- Albus P. W. B. Dumbledore

## Summary

The cytokine receptor like factor 3 (CRLF3) evolved together with the eumetazoan nervous system and is present in all major groups of Animalia. Based on sequence similarities, CRLF3 was assigned to the family of class 1 cytokine receptors which also includes the classical erythropoietin receptor (EpoR). CRLF3 misregulation has been associated with several human diseases, but neither its ligand nor a particular function have been reported.

Erythropoietin (Epo) is a vertebrate-specific helical cytokine that regulates erythropoiesis and activates cytoprotective pathways in various tissues including the nervous system. Neuroprotective functions of Epo are partially mediated by EpoR but also by additional, partly unidentified receptors.

In insects, CRLF3 was identified to respond to human recombinant Epo and the naturally occurring Epo splice variant EV-3. Activation of CRLF3 in insects stimulates anti-apoptotic processes via JAK/STAT intracellular signalling. Even though many efforts were made in order to characterize CRLF3-mediated responses, downstream effectors beyond JAK/STAT remained elusive.

My thesis combines studies on CRLF3-mediated anti-apoptotic mechanisms in insects and the functional characterisation of human CRLF3 in iPSC (induced pluripotent stem cell) -derived neurons.

Studies on *Locusta migratoria* and *Tribolium castaneum* revealed a pro-apoptotic role of acetylcholinesterase (AChE coded by *ace*) that was previously reported for vertebrates. Similar to those studies, reduction of AChE levels and inhibition of AChE activity prevented apoptotic death in hypoxia-exposed primary neuron cultures. Moreover, apoptogenic stimuli increased *ace* expression supporting the association of AChE with increased apoptosis under challenging conditions. Experiments in *T. castaneum* indicated that both types of AChE (AChE-1 transcribed from *ace-1* and AChE-2 transcribed from *ace-2*) promote apoptosis and are upregulated by apoptogenic stimuli. However, stress-induced upregulation of AChE-1 was prevented by neuroprotective concentrations of Epo. This indicated that Epo/CRLF3-stimulated neuroprotection is mediated through suppression of pro-apoptotic *ace-1* expression. Whether this Epo-stimulated protective mechanism is specific to insects or also present in other species remains to be studied.

In order to determine the endogenous ligand of insect CRLF3 (insects do not possess Epo) I used locust hemolymph as potential source for its identification. I first demonstrated that locust hemolymph protects both *L. migratoria* and *T. castaneum* primary neurons from hypoxia-induced apoptosis. The protective effect was absent after RNAi-mediated knockdown of CRLF3 expression. Thus, locust hemolymph contains a ligand that is sufficiently conserved to activate CRLF3 in different insect species. Fractionation of locust hemolymph by size exclusion chromatography generated two (out of >11) fractions with particular neuroprotective potency. These hemolymph fractions will be used to separate and identify the CRLF3 ligand.

In order to determine the function of human CRLF3, I generated *CRLF3*-knockout lines from two fibroblast-derived human iPSC lines by CRISPR/Cas9 gene editing. *CRLF3* KO lines, along with wild type and isogenic controls, were differentiated into neuronal-like cells expressing cell type-specific markers and presenting characteristic morphology. After differentiation, neuronal-like cells were exposed to rotenone, an inhibitor of respiratory chain complex I, which induced apoptosis in all cell lines. The addition of the Epo splice variant EV-3 prevented rotenone-induced cell death in wild type and isogenic controls but not in *CRLF3* KO neurons. This demonstrates that human *CRLF3* is a neuroprotective receptor similar to its previously determined function in insects. Moreover, *CRLF3* is identified as the first known receptor for EV-3 and *vice versa*, human *CRLF3* is orphanized by identifying EV-3 as one of its endogenous ligands.

Taken together, my work has identified *CRLF3* as a new player in neuroprotection that may account for various previously described Epo-mediated cytoprotective functions in the nervous system and other tissues. Specific activation of *CRLF3*-mediated beneficial pathways may interfere with degenerative processes without coactivation of EpoR and its associated adverse side effects.



## Table of contents

<b>List of Abbreviations</b> .....	1
<b>General Introduction</b> .....	2
Apoptosis.....	2
Erythropoietin- The neuroprotective cytokine and its potential for clinical application.....	3
The orphan cytokine receptor-like factor 3 and its functions in Epo-mediated neuroprotection .....	3
Understanding the anti-apoptotic functions of insect CRLF3 .....	4
Epo/CRLF3: A possibility to tackle neurodegeneration?.....	5
Aims of Thesis.....	6
<b>Chapter 1- Acetylcholinesterase promotes apoptosis in insect neurons</b> .....	7
<b>Chapter 2- Protection of insect neurons by erythropoietin/CRLF3-mediated regulation of pro-apoptotic acetylcholinesterase</b> .....	25
<b>Chapter 3- Locust Hemolymph Conveys Erythropoietin-Like Cytoprotection via Activation of the Cytokine Receptor CRLF3</b> .....	51
Chapter 3.1- Follow up.....	67
<b>Chapter 4- Human Epo splice variant EV-3 mediates neuroprotective effects in human iPSC derived neurons by activation of CRLF3</b> .....	76
<b>General Discussion</b> .....	109
The missing link in Epo-mediated anti-apoptotic effects.....	110
Deorphanizing CRLF3 – A quest for an unknown cytokine .....	110
A new prospect for human Epo-mediated neuroprotection.....	111
The hypothetical cell – A model for cytokine/CRLF3 mediated neuroprotection .....	112
Final remarks.....	114
<b>References</b> .....	115
<b>Supplements</b> .....	120
Vector maps for recombinant protein expression.....	120
Mass spectrometry data .....	121
Methods iPSC molecular analysis .....	131
<b>Acknowledgements</b> .....	133
<b>Curriculum Vitae</b> .....	135

List of Abbreviations

aApt	Anti-Apoptotic
<i>ace</i>	AChE Gene
AChE	Acetylcholinesterase
AChE-E	Acetylcholinesterase-Erythrocytic
AChE-R	Acetylcholinesterase-Readthrough
AChE-S	Acetylcholinesterase-Synaptic
ACS	Anticoagulation Solution
Ampho/B	Amphotericin B
Apaf-1	Apoptotic Protease-Activating Factor 1
BDNF	Brain-Derived Neurotrophic Factor
BF	Brightfield
bFGF	Basic Fibroblast Growth Factor
BSA	Bovine Serum Albumin
CAD	Caspase-Activated Deoxyribonuclease
cAMP	Cyclic Adenosine Monophosphate
cDNA	Complementary DNA
ConA	Concanavalin A
CRISPR	Clustered Regularly Interspaced Short Palindrome Repeats
CRLF3	Cytokine Receptor-Like Factor 3
Ctrl	Control
DABCO	1,4-Diazabicyclo[2.2.2]Octane
DAPI	4',6-Diamidin-2-Phenylindol
ddH <sub>2</sub> O	Double Distilled Water
gDNA	Genomic DNA
dHL	Denatured Hemolymph
DMEM	Dulbecco's Modified Eagle Medium
DMSO	Dimethyl Sulfoxide
dsRNA	Double Stranded RNA
EB	Embryoid Bodies
EGF	Epidermal Growth Factor
ELC	Epo-Like Cytokine
Epo	Erythropoietin
EpoR	"classical" Epo Receptor
EtOH	Ethanol
F1/F2	Fragment 1 / 2
F10-F22	Fraction 10-22
FACS	Fluorescence Assisted Cell Sorting
FBS	Fetal Bovine Serum
FBSG	Fetal Bovine Serum Gold
GAPDH	Glyceraldehyde 3-Phosphate Dehydrogenase
GFP	Green Fluorescent Protein
GNBP3	Gram-Negative Bacteria-Binding Protein 3
GOI	Gene Of Interest
gRNA	Guide RNA
H	Hypoxia
HKG	Housekeeping Gene
HL	Hemolymph
HL Str	Hemolymph Stressed

Hyp	Hypoxia
Ig-Ctrl	Isogenic Control
INDEL	Insertion Or Deletion
iPSC	Induced Pluripotent Stem Cells
JAK	Janus Kinase
KLF2	Krüppel-Like-Factor 3
KO	Knock Out
KOS	Knock Out Serum
L15	Leibowitz 15 Medium
L-AA	L-Ascorbic Acid
Lm	<i>Locusta migratoria</i>
MMC	Mitomycin C
MOMP	Mitochondrial Outer Membrane Porin
MWCO	Molecular Weight Cut Off
N	Normoxia
NEAA	Non-Essential-Amino-Acids
NF200	Neurofilament 200
NF $\kappa$ B	Nuclear Factor 'Kappa-Light-Chain-Enhancer' Of Activated B-Cells
NSB	Neostigmine Bromide
NT-3	Neurotrophin 3
OCT4	Octamer Binding Transcription Factor 4
P/S	Penicillin/Streptomycin
PBS	Phosphate-Buffered Saline
PBST	Phosphate-Buffered Saline/ 0,1% Triton-X-100
PCR	Polymerase Chain Reaction
PFA	Paraformaldehyde
PI3K	Phosphoinositide 3-Kinase
PSC	Pluripotent Stem Cells
qRT-PCR/qPCR	Quantitative RT-PCR
rhEpo	Recombinant Human Epo
RNAi	RNA Interference
Rot	Rotenone
RPS	Ribosomal Protein S
rRNA	Ribosomal RNA
RT	Room Temperature
RT-PCR	Reverse Transcription PCR
SDS-PAGE	Sodium Dodecylsulfate Polyacrylamide Gel Electrophoresis
SEC	Size Exclusion Chromatogram
SOB	Super Optimal Broth
SOX2	Sex Determining Region Y-Box 2
$\beta$ cR	$\beta$ -Common-Receptor
STAT	Signal Transducers And Activators Of Transcription
Stdv	Standard Deviation
Tc	<i>Tribolium castaneum</i>
TF	Transcription Factor
TMB	Tris-Maleic-Buffer
TRB	Territrem B
TUNEL	Tdt-Mediated dUTP-Biotin Nick End Labeling
UPPS	Universal Primate Pluripotent Stem Cell
WT	Wild type

## General Introduction

Cells permanently monitor general conditions (pH, ion concentrations, etc.) and specific signals (transmitters, hormones, cell-to-cell contacts, etc.) to adjust their physiology in order to maintain their designated functions within tissues. Special or extreme conditions may cause cell death, which in the case of apoptosis involves evolutionarily conserved mechanisms to eliminate particular cells without generating additional stress for their neighbours. Cell survival and apoptotic death are regulated by a balance of pro-apoptotic and anti-apoptotic molecules whose expression depends on the activation of intrinsic sensors, cell membrane-located receptor molecules and transduction pathways activated by these. My doctoral thesis investigates two mechanisms involved in the regulation of apoptosis, (1) the pro-apoptotic function of acetylcholinesterase and (2) the anti-apoptotic neuroprotective mechanisms of the cytokine receptor CRLF3. After a brief general introduction, studies on specific aspects of the pro- and anti-apoptotic functions of acetylcholinesterase and CRLF3 will be presented and discussed regarding their implications for the evolution of apoptotic mechanisms, cytokine signalling systems and potential applications in medical treatment against degenerative cell loss. Some of the chapters are identical to existing publications or manuscripts submitted for review.

### ***Apoptosis***

Apoptosis describes a highly regulated cell suicide mechanism. Best described for developmental processes, apoptosis maintains tissue integrity by abolishing damaged or superfluous cells. In contrast to necrosis, the highly regulated apoptotic digestion of cellular compartments does not affect surrounding tissue.

In healthy vertebrate cells a fine balance between pro- and anti-apoptotic BCL-2 proteins allows cellular integrity. Physiological stressors (e.g. hypoxia) will induce upregulation of pro-apoptotic Bax and Bak, which in return mediate mitochondrial outer membrane pore (MOMP) formation (Sendoel and Hengartner, 2014). Opening of MOMP will lead to cytochrome c release into the cytosol, allowing interaction with the apoptotic protease activating factor 1 (Apaf-1). Apaf-1, in return, oligomerizes and recruits procaspase 9. The resulting multiprotein complex, termed the apoptosome, further facilitates caspase 9 dimerization, leading to caspase 3 activation (Riedl and Salvesen, 2007). Generally, apoptosome formation is considered as “the point of no return” in the apoptotic machinery, given the resulting activation of autocatalytic executioner caspase 3. Subsequently, DNA- and mitochondrial fragmentation, membrane blebbing and apoptotic body formation will destroy the cell within membrane-enclosed compartments.

In contrast to vertebrates, invertebrate and particularly insect apoptosis remains widely elusive. The nematode *C.elegans* has excessively been studied with regards to developmental apoptosis. Here, the Apaf-1 homologue CED-4 is actively inhibited in intact cells by binding to the BCL-2 protein CED-9 (anti-apoptotic). Apoptosis is initiated on upregulation of *EGL-1*, releasing CED-4, which in return forms a tetrameric apoptosome. The CED-4 apoptosome activates CED-3 (Caspase 3 homolog), leading to autocatalytic caspase activation. Interestingly no MOMP could be detected in *C.elegans* apoptosis (Bender *et al.*, 2012). This finding goes together with earlier studies, suggesting *C.elegans* apoptosis to be cytochrome c independent (Arnoult, 2007).

Even though a *Drosophila* apoptosome has been demonstrated, apoptosis in nearly all cells of the fly is also described to be cytochrome c independent (Pang *et al.*, 2015). Here, the Apaf-1 homolog Dark recruits the initiator caspase Dronc for activation. However, in contrast to *C.elegans* CED-3, Dronc stays associated with Dark, resulting in a holoenzyme with catalytic activity, leading to Drice (effector caspase) activation (Bender *et al.*, 2012). Given that the two main invertebrate model organisms, *C.elegans* and *D. melanogaster* show no evidence of mitochondrial involvement in apoptosis, it was widely accepted that the apoptotic machinery gained in complexity during evolution.

### *Acetylcholinesterase functions in apoptosis*

The enzyme acetylcholinesterase (AChE) is commonly known for its functions in synaptic transmission. In recent years, non-canonical functions of AChE in vertebrates have been reported. AChE plays a crucial role in multiple disease phenotypes and furthermore is implied to contribute to the vertebrate apoptotic machinery (Zhang *et al.*, 2002; Park, Kim and Yoo, 2004; Gilboa-geffen *et al.*, 2007; Park *et al.*, 2008; Härtel, Gleinich and Zimmermann, 2011; Zhang and Greenberg, 2012; Du *et al.*, 2015; Abdel-Aal *et al.*, 2021; Walczak-Nowicka and Herbet, 2021). Concerning apoptosis, vertebrate AChE is

crucially involved in apoptosome formation by facilitating cytochrome c and Apaf-1 interaction (Park et al., 2008; Park, Kim, & Yoo, 2004). Knock-down or inhibition of AChE in vertebrate cells significantly increases cell survival (Park, Kim and Yoo, 2004; Park *et al.*, 2008; Zhang and Greenberg, 2012). Du and coworkers (Du *et al.*, 2015) further demonstrated that AChE translocates to the nucleus during apoptosis and acts as a DNase similar to the designated DNases CAD and Endonuclease G.

While vertebrates express three distinct splice variants from a single gene locus, invertebrate species generally possess two distinct genes expressing two AChE enzymes (*ace-1* / AChE-1 and *ace-2* / AChE-2) (Hall and Spierer, 1986; Grisaru *et al.*, 1999; Ye *et al.*, 2010; Hicks *et al.*, 2011; Lu, Park, *et al.*, 2012; Zhang and Greenberg, 2012; Kim and Lee, 2013). Typically either AChE-1 or AChE-2 (which one may vary between insect species) elicits canonical synaptic functions while the functions of the second enzyme are largely unknown (Revuelta *et al.*, 2009; Zhou and Xia, 2009; Lu, Pang, *et al.*, 2012; Lu, Park, *et al.*, 2012; Kim and Lee, 2013).

### ***Erythropoietin-mediated neuroprotection and its potential for clinical application***

Erythropoietin (Epo) is a helical glycoprotein commonly known for its functions in vertebrate erythropoiesis, mediated by the classical Epo receptor (EpoR). In addition to kidney-derived hormonal Epo, local production of Epo has been reported for the brain, liver, lung and testis (Marti *et al.*, 1996; Bernaudin *et al.*, 2000; Jelkmann, 2011). Furthermore, EpoR expression has been observed in many non-hematopoietic tissues (Yamaji *et al.*, 1996; Vittori *et al.*, 2021). These observations led to the hypothesis that Epo might have functions beyond regulation of erythropoiesis. Indeed, many studies were able to describe cytoprotective actions of Epo in the heart, liver and brain, amongst others (Yilmaz *et al.*, 2004; Sepodes *et al.*, 2006 and reviewed in (Chateauvieux *et al.*, 2011).

Beneficial effects of Epo on cell survival after disturbance of the allostatic balance have been demonstrated in vitro (Yilmaz *et al.*, 2004; Brines and Cerami, 2005; Sepodes *et al.*, 2006; Noguchi *et al.*, 2007; Arcasoy, 2008; Ghezzi and Conklin, 2013). Additionally, clinical studies focused on Epo administration to treat neurodegenerative diseases (reviewed in (Vittori *et al.*, 2021)). However, the results of these studies are contradictory. While many clinical trials reported beneficial effects of Epo on patients treated for Parkinsons disease or multiple sclerosis (Ehrenreich *et al.*, 2007; Jang *et al.*, 2014), others had to be stopped prematurely due to severe side effects connected to Epo-initiated erythrocyte production (Ehrenreich *et al.*, 2009; Pedroso *et al.*, 2012). In light of these side effects, Epo cannot be safely administered within treatments outside of the hematopoietic system. Focusing on the beneficial effects of Epo, researchers began to synthesize and study effects of Epo-like molecules. Some of these Epo mimetics were able to separately activate the cytoprotective but not the erythropoietic functions of Epo (Brines *et al.*, 2008; Ueba *et al.*, 2010; Wu *et al.*, 2013; Bonnas *et al.*, 2017). Among the tissue-specific ligands was the naturally occurring Epo splice variant EV-3 (detected in mice and humans) that cannot activate classical homodimeric EpoR (Bonnas *et al.*, 2017). Studies covering the effects of Epo mimetics have demonstrated neuro- and cytoprotective effects following direct administration in vitro (Brines *et al.*, 2008; Ueba *et al.*, 2010; Wu *et al.*, 2013; Bonnas *et al.*, 2017). These effects were independent of homodimeric and heteromeric (with  $\beta$ -common chain receptor) EpoR activation, highlighting the presence of additional receptors for Epo (and Epo-mimetics) that mediate cytoprotective functions in various non-hematopoietic tissues (Brines *et al.*, 2004; Chamorro *et al.*, 2013; Miller *et al.*, 2015; Bonnas *et al.*, 2017; Ding *et al.*, 2017; Wakhloo *et al.*, 2020).

### ***The orphan cytokine receptor-like factor 3 and its functions in Epo-mediated neuroprotection***

EpoR belongs to class 1 of cytokine receptors (Liongue and Ward, 2007) together with the cytokine receptor-like factor 3 (CRLF3), the thrombopoietin receptor, prolactin receptor and growth hormone receptor (Liongue and Ward, 2007). CRLF3 is widely uncharacterized, however, it contains the classical properties of cytokine receptors, including the conserved WSXWS motif and constitutive JAK binding site (Boulay, O'Shea and Paul, 2003; Liongue and Ward, 2007). CRLF3 is phylogenetically conserved and present in most vertebrate and invertebrate species (Wyder *et al.*, 2007). Nonetheless, CRLF3 is termed as an orphan receptor since, presently, no endogenous ligand is known in any species and its functions are largely unknown.

Invertebrates do not express Epo and also lack any so far recognized Epo receptors. However, presence of the Epo/EpoR system in all vertebrates, including fish, hinted towards the emergence of precursors prior to the vertebrate lineage (Brines and Cerami, 2005; Chu *et al.*, 2008; Buchmann, 2014). Our own studies demonstrated that treatment of insect neuronal cell cultures with recombinant human Epo (rhEpo) elicits neuroprotective effects (Ostrowski, Ehrenreich and Heinrich, 2011; Miljus *et al.*, 2014;

Hahn *et al.*, 2017). However, neuroprotective effects were detected in orthopteran and coleopteran species but not in *Drosophila melanogaster*. While studying the underlying mechanisms of insect Epo-mediated neuroprotection, it was demonstrated that, similar to the vertebrate system, JAK/STAT signalling is involved (Miljus *et al.*, 2014). In light of these findings we aimed to identify receptors present in both insects and vertebrates, but not the fruit fly, which could potentially function as Epo-responsive receptors. In the course of this search, we identified CRLF3 as a potential candidate receptor. RNAi mediated knock down of the receptor in primary neuron cultures of the migratory locust *Locusta migratoria* and the red flour beetle *Tribolium castaneum* completely prevented Epo-mediated neuroprotective effects (Hahn *et al.*, 2017; Hahn *et al.*, 2019). Furthermore, we were able to show that CRLF3 is highly conserved throughout evolution and emerged together with the nervous system in cnidarians and is still present in humans (Hahn *et al.*, 2019). This data highlights the importance of CRLF3 in invertebrate neuroprotection and suggests a similarly crucial role in mammalian, including human, Epo-mediated cytoprotection. Albeit the first evidence of CRLF3 mediated neuroprotection in insects being published in 2017 (Hahn *et al.*, 2017), no studies in mammalian or any vertebrate species have been reported.

### ***Understanding the anti-apoptotic functions of CRLF3***

As mentioned above, CRLF3 is a widely uncharacterized cytokine receptor. CRLF3 expression has been confirmed in all major groups of eumetazoan animals (Boulay, O'Shea and Paul, 2003) and it is evolutionarily highly conserved (Hahn, et al., 2019). Even though altered expression of CRLF3 has been associated with various human diseases, studies covering its activation and mechanisms in neuroprotection are limited to locusts and beetles. To the present, there is no identified ligand activating CRLF3 endogenously in any species. Nonetheless, it is likely that endogenous CRLF3 ligands are helical cytokines, which are known to adapt cellular functions to unfavorable conditions elicited by hypoxia, infection, nutritional deprivation and challenges.

### *Cytokines*

Cytokines form a group of humoral factors which can act in paracrine, autocrine and endocrine fashion. Various invertebrate cytokines have been identified and many of them are involved in invertebrate innate immune responses (Beschin *et al.*, 2001; Ottaviani, Malagoli and Franchini, 2004; H. S. Wang *et al.*, 2007; Altincicek, Knorr and Vilcinskis, 2008; Duressa *et al.*, 2015; Kodrík *et al.*, 2015; Shears and Hayakawa, 2019; Watari *et al.*, 2019). Accordingly, it is believed that cytokine signalling evolved early and has become more complex during the course of evolution (Beschin *et al.*, 1999, 2001; Huising, Kruiswijk and Flik, 2006; Shears and Hayakawa, 2019). In connection with cytokine receptors, a single cytokine may activate various receptors, resulting in different cellular functions. Conversely, a single cytokine receptor can be activated by multiple cytokine ligands (Huising, Kruiswijk and Flik, 2006). These promiscuous cytokine ligand-receptor interactions typically mediate pleiotropic cellular responses, which may interfere with identification and mechanistic characterisation of cellular responses. Functions attributed to cytokine signalling primarily cover immune responses but also cell activation, proliferation, maturation and differentiation (Shields *et al.*, 1995; Beschin *et al.*, 1999, 2001; Oda *et al.*, 2010). While most cytokine receptors contain four conserved cysteines in their N-terminal regions and a tryptophan-serine doublet near the C-terminal end, they generally share little structural relatedness with each other (Boulay, O'Shea and Paul, 2003). Additionally, albeit considered a monophyletic group, cytokines and their receptors share little sequence similarities between different organisms, making the study of ancestral relations of cytokines challenging (Huising, Kruiswijk and Flik, 2006; Liongue and Ward, 2007). Based on this evidence, purely bioinformatic approaches concerning CRLF3 ligand identification pose limitations.

### *Induced pluripotent stem cells and their implications in biomedical research*

The study of human tissue and its physiology under normal and pathological conditions is the main part of translational research. When thinking about the establishment of potential treatments for any disease, *in vitro* studies build the basis for *in vivo* experiments and clinical trials. However, experiments with mammalian organisms are connected to high workload concerning ethics approval and laboratory security measures. In order to have a well-founded approximation of drug treatment effects, experiments in non-human primates, primates or humans have to be performed. Here again, ethical concerns must be taken into regard.

The discovery of induced pluripotency by Yamanaka and Takahashi in 2006 has been a milestone in modern science. By transfection of defined pluripotency factors, namely OCT4, SOX2, KLF2 and c-Myc, differentiated somatic cells can now be reprogrammed to reassume a fully pluripotent state (Takahashi and Yamanaka, 2006). Termed induced pluripotent stem cells (iPSC), these cells can be maintained in their newly acquired pluripotent state, characterized by the capacity to differentiate into close to any somatic cell and constant self-renewal (Rodriguez-Polo *et al.*, 2019; Stauske *et al.*, 2020; Doss and Sachinidis, 2019; Wiegand and Banerjee, 2019). The constant proliferation opens possibilities for genetic manipulation and the establishment of transgenic cell lines. These cells, upon differentiation to a specific cell type, allow functional studies related to the induced mutation in specific tissues. Taken together, iPSC form an important and highly valuable tool for loss-of/gain-of-function studies in close to any tissue.

### ***Epo/CRLF3: A possibility to tackle neurodegeneration?***

The cytokine Epo and its anti-apoptotic effects harbour great potential for the treatment of degenerative diseases, however, its functions in the erythropoietic system limit its application in the clinics. The evidence that receptor-selective Epo-mimetics activate neuroprotective mechanisms without stimulating erythropoiesis has boosted Epo-related research. However, the application herewith is limited without identifying and fully characterizing the receptors activated by Epo-mimetics.

To this point, we know that Epo-stimulated neuroprotection in insects is mediated by the orphan CRLF3, which is conserved throughout evolution. This evidence raises the hypothesis that CRLF3 might also act as an Epo-responsive cell-protective receptor in mammalian species. However, data verifying or falsifying this hypothesis was lacking to the present. In this thesis, I introduce CRLF3 as a human neuroprotective receptor which responds to EV-3 treatment in human iPSC-derived neurons.

Even though we know that insect CRLF3 is activated by rhEpo and that activated transduction pathways include JAK/STAT, we are still lacking a full understanding of how Epo rescues cells from apoptosis and promotes neuronal regeneration. In light of potential clinical applications, it is highly relevant to complete our understanding of the mechanisms underlying these beneficial effects.

After identifying AChE as a pro-apoptotic factor in insects, I demonstrated its regulation through Epo/CRLF3 signalling. Furthermore, I started the identification of the endogenous CRLF3 ligand from insect hemolymph. Initial studies demonstrated that locust hemolymph contains a Epo-like cytokine, which activates CRLF3-mediated neuroprotection in different insect species.

## Aims of Thesis

During my Ph.D. I aimed to study Epo/CRLF3-mediated neuroprotective effects in insect and human neurons. In order to characterize CRLF3-initiated anti-apoptotic mechanisms, I studied the pro-apoptotic function of insect AChE and a possible convergence of pro- and anti-apoptotic pathways involving these two molecules. Furthermore, I tried to identify and characterize the insect endogenous CRLF3 ligands.

The main aims are as follows:

- (1) Analysis of acetylcholinesterase as a pro-apoptotic factor and target of CRLF3-mediated neuroprotection in insects.
- (2) Identification of the endogenous CRLF3 ligand in insects.
- (3) Evaluation of human CRLF3 as an Epo-responsive receptor in human induced pluripotent stem cell-derived neurons.

(1) Pro-apoptotic functions of AChE were previously reported in vertebrates but not in insects. This was connected to the belief that invertebrates contain a rather simple apoptotic system (e.g., without contribution of cytochrome c) which evolved to higher complexity in vertebrates, including mammals. The studies presented in **Chapters 1 and 2** prove a pro-apoptotic function of AChE in locust and beetle neurons. I also demonstrate, that AChE expression is negatively regulated by Epo/CRLF3-stimulated transduction processes. While the locust genome is widely unannotated, *T. castaneum* sequences for both *ace-1* and *ace-2* are available. I report, that both AChE enzymes contribute to apoptosis in beetle neurons. However, predominantly *ace-1* expression was negatively regulated by Epo administration, demonstrating, that Epo/CRLF3 inhibit apoptosis by reduction of pro-apoptotic AChE-1 activity.

(2) Since insects (and other invertebrates) lack Epo I tried to identify their endogenous ligand for CRLF3. **Chapters 3 and 3.1** describe the efforts made and the results obtained from studying neuroprotective properties of insect hemolymph. I demonstrate that locust cell-free hemolymph protects both locust and beetle neurons from hypoxia-induced apoptosis. Importantly, these protective effects were mediated by activation of CRLF3, indicating that the endogenous CRLF3 ligand is contained in the hemolymph fluid. Together with Dr. Sonja Pribicevic (Max-Planck-Institute for Biophysical Chemistry) I performed size exclusion chromatography in order to separate proteins contained in the hemolymph by their size and complexity. In vitro application of the different fractions on hypoxia-exposed insect neurons highlighted two fractions with pronounced neuroprotective effects. Identification of the neuroprotective CRLF3 ligand has not yet been completed. The results gathered so far suggest an intermediate-sized protein whose expression is stimulated under physiologically harmful conditions such as hypoxia.

(3) In order to identify the function of human CRLF3 I studied its potential involvement in the protection of human iPSC-derived neurons. As described in **Chapter 4**, I generated CRLF3 knockouts (KO) in two independent human iPSC lines and investigated the beneficial effects of the human Epo splice variant EV-3 in iPSC-derived neurons with (wild type cells) or without (KO) CRLF3. EV-3 protected wild type neurons from chemical hypoxia-induced apoptosis but had no protective effect on CRLF3 KO cells. Expression analysis of pro- and anti-apoptotic factors in wild type and CRLF3 KO cells under normal conditions, apoptogenic conditions and EV-3 application provided hints about the apoptosis regulating mechanisms. This data represents the first report of CRLF3-mediated neuroprotective effects in human cells and identifies both an endogenous ligand for human CRLF3 and a neuroprotective receptor for EV-3.

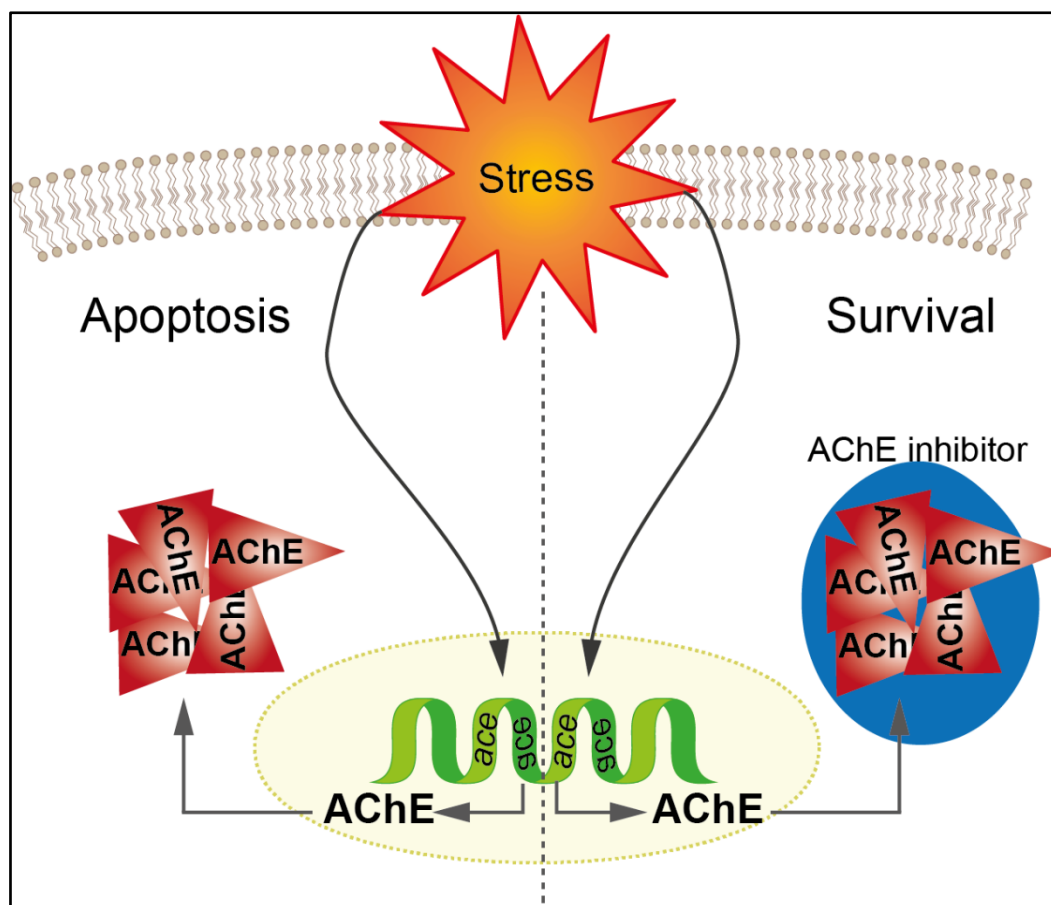


## Chapter 1

### Acetylcholinesterase promotes apoptosis in insect neurons

Debbra Y. Knorr, Nadine S. Georges, Stephanie Pauls, Ralf Heinrich

- Published in *Apoptosis*-



#### Author contribution statement

All authors contributed experimental data. Data was analysed by D.Y. Knorr, N. S. Georges and R. Heinrich. R. Heinrich and D.Y. Knorr designed and supervised the study and wrote and edited the final manuscript in correspondence with the other authors.

<b>Figure 1</b>	<b>DYK</b> performed literature review and figure design
<b>Figure 2</b>	<b>DYK</b> performed stainings and imaging; <b>SP</b> performed DNA fragmentation gels
<b>Figure 3</b>	<b>DYK</b> generated and analysed the data
<b>Figure 4</b>	<b>RH</b> performed stainings and imaging
<b>Figure 5</b>	<b>DYK</b> and <b>NS</b> (supervised by <b>DYK</b> ) generated and analysed the data
<b>Table 3</b>	<b>DYK</b> performed similarity analysis
<b>Table 4</b>	<b>DYK</b> performed similarity analysis
<b>Table 5</b>	<b>DYK</b> performed experiments and analysed the data
<b>Experimental design</b>	<b>RH</b> and <b>DYK</b>
<b>Manuscript writhing</b>	<b>RH</b> and <b>DYK</b> , with contribution of all authors



# Acetylcholinesterase promotes apoptosis in insect neurons

Debbra Y. Knorr<sup>1</sup> · Nadine S. Georges<sup>1</sup> · Stephanie Pauls<sup>1</sup> · Ralf Heinrich<sup>1</sup>

© The Author(s) 2020

## Abstract

Apoptosis plays a major role in development, tissue renewal and the progression of degenerative diseases. Studies on various types of mammalian cells reported a pro-apoptotic function of acetylcholinesterase (AChE), particularly in the formation of the apoptosome and the degradation of nuclear DNA. While three AChE splice variants are present in mammals, invertebrates typically express two *ache* genes that code for a synaptically located protein and a protein with non-synaptic functions respectively. In order to investigate a potential contribution of AChE to apoptosis in insects, we selected the migratory locust *Locusta migratoria*. We established primary neuronal cultures of locust brains and characterized apoptosis progression in vitro. Dying neurons displayed typical characteristics of apoptosis, including caspase-activation, nuclear condensation and DNA fragmentation visualized by TUNEL staining. Addition of the AChE inhibitors neostigmine and teritrem B reduced apoptotic cell death under normal culture conditions. Moreover, both inhibitors completely suppressed hypoxia-induced neuronal cell death. Exposure of live animals to severe hypoxia moderately increased the expression of *ace-1* in locust brains in vivo. Our results indicate a previously unreported role of AChE in insect apoptosis that parallels the pro-apoptotic role in mammalian cells. This similarity adds to the list of apoptotic mechanisms shared by mammals and insects, supporting the hypothesized existence of an ancient, complex apoptosis regulatory network present in common ancestors of vertebrates and insects.

**Keywords** Acetylcholinesterase · Non-synaptic · Apoptosis · Hypoxia · Insect · *Ace-1*

## Introduction

Apoptosis describes highly regulated processes that lead to death and elimination of individual cells with little or no negative impact on the surrounding tissue. It contributes to the development of structured organs, to the renewal of adult tissue by regular turnover of cells and to the removal of compromised or malfunctioning cells (Reviewed: [1–4]). Morphologically, apoptosis is characterized by loss of cellular volume, condensation of nuclear chromatin due to DNA fragmentation, plasma membrane blebbing and formation of apoptotic bodies. While these morphological features

are partly shared by other types of programmed cell death within and outside the animal phylum, apoptosis in its strict sense is executed by metazoan-specific cysteine proteases termed caspases [5–7]. Recent studies indicated that most components of the vertebrate-typical apoptosis regulatory network were already present in an early ancestor of all metazoans (Reviewed [5, 8]). Consequently, the well investigated comparatively simple apoptotic networks of *Caenorhabditis elegans* and *Drosophila melanogaster* resulted from a secondary reduction of ancient complexity. Whether this simplification is specific for these model organisms or whether it is a general feature of nematodes, insects and their last common ecdysozoan ancestors is not clear at the present state.

Caspases that mediate the final stages of apoptosis cleave various selected substrates, either to destabilize or degrade structural elements of the cell or to activate executors of downstream apoptotic processes [9, 10] (Fig. 1). This may imply sequential activation of initiator caspases and executioner caspases (caspase-9 and caspase-3 in vertebrates; dronc and drice in *D. melanogaster*) or direct

**Electronic supplementary material** The online version of this article (<https://doi.org/10.1007/s10495-020-01630-4>) contains supplementary material, which is available to authorized users.

✉ Ralf Heinrich  
rheinri1@gwdg.de

<sup>1</sup> Department of Cellular Neurobiology, Johann-Friedrich-Blumenbach-Institute for Zoology and Anthropology, Georg-August-University Göttingen, Göttingen, Germany

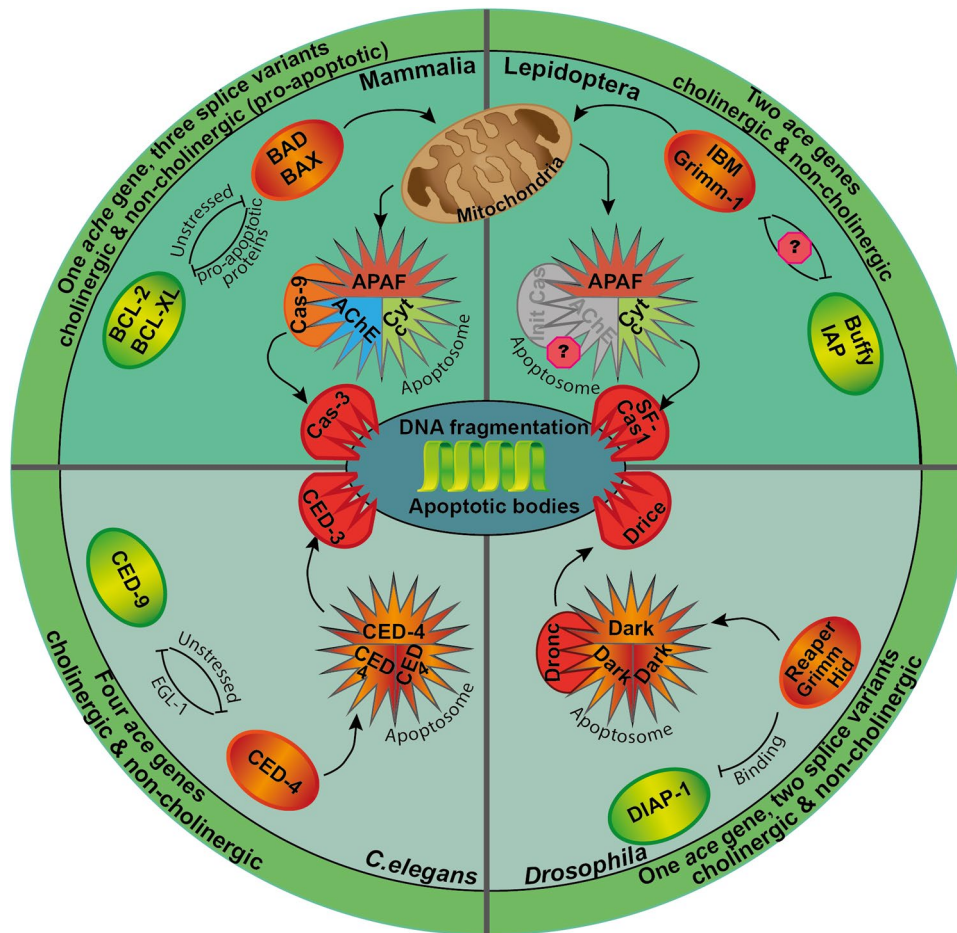


**Fig. 1** Apoptotic pathways in mammals, nematodes (*C. elegans*) and insects (*D. melanogaster* and lepidopteran species *S. frugiperda* and *B. mori*). Same colours depict similar functions mediated by orthologous or paralogous proteins. Top half of the circle depicts mitochondria-dependent apoptosis, bottom part illustrates mitochondria and cytochrome c independent apoptosis. Outer circle shows presence of *ache/ace* genes and their general functions in respective taxa. Mitochondria-dependent apoptosis is initiated by upregulation of pro-apoptotic proteins (BAD/BAX and IBM/Grimm-1; orange circles), release of cytochrome c into the cytosol, apoptosome formation (star-like structures) and activation of effector caspase (Cas-3 and SF-Cas 1) activation. AChE contributes to apoptosome formation in mamma-

lia. Mitochondria-independent apoptosis is executed by upregulation/activation of pro-apoptotic agents (EGL-1/CED-4; Reaper/Grimm/Hid) that counteract anti-apoptotic factors (CED-9; DIAP-1 green circles). The apoptosome is formed either by accumulation of pro-apoptotic proteins (nematode; CED-4) or activation of an APAF-like protein (fly; Dark). The apoptosome will eventually lead to effector caspase activation (CED-3; Dronc). Both mitochondria dependent and independent pathways will result in DNA fragmentation, membrane blebbing and apoptotic body formation. AChE acetylcholinesterase, APAF apoptotic protease activating factor; Cas caspase; Cyt cytochrome c, IAP inhibitor of apoptosis

activation of executioner caspases (CED-3 in *C. elegans*). Caspases also perform various non-apoptotic functions [11] and are typically produced as enzymatically inactive zymogens [9]. Activation of caspases is mediated by non-caspase proteases (e.g. granzyme B in virally induced apoptosis) or weak intrinsic catalytic activity of procaspases (mammalian procaspase-8 with death-receptors; CED-4 oligomerization leading to CED-3 caspase activation in *C. elegans*). Formation of the apoptosome, a protein complex that associates in the cytosol as part of the intrinsic or mitochondrial apoptotic pathway, can also cause caspase activation (Reviewed in: [2, 12]). The

vertebrate mitochondrial apoptotic pathway can be initiated by physiological stressors (hypoxia, toxins and others) that shift the balance of anti- and pro-apoptotic Bcl-2 proteins to the pro-apoptotic side by enhanced expression of BAX and BAD (Reviewed by [13]). This initiates the formation of mitochondrial outer membrane pores (MOMP) allowing cytochrome c (and other factors) release from the mitochondrial intermembrane space into the cytosol [14]. Cytochrome c associates with apoptotic protease activating factor-1 (Apaf-1) and procaspase 9. The resulting multi-protein complex, termed the apoptosome facilitates caspase 9 dimerization to release its function as initiator

caspace that activates effector caspase-3 [15, 16]. While apoptosome formation in *C. elegans* and most cell types of *D. melanogaster* is independent from mitochondria-derived factors [17] (Fig. 1), contribution of cytochrome c has been described in lepidopteran species [18, 19] and two cell types (interommatidial retina cells and sperm cells) of *D. melanogaster* [20, 21].

Promotion of apoptosis by acetylcholinesterase (AChE) has been demonstrated in several studies on various mammalian cell types, suggesting that AChE is commonly involved in apoptosis regulation (Review: [22]). Generally, AChE is known to terminate synaptic transmission at cholinergic synapses by hydrolytic cleavage of the transmitter acetylcholine. However, other non-canonical functions of AChE in cell growth, cellular differentiation, cell adhesion and amyloid fiber assembly (amongst others) have been reported [22–24]. Vertebrates express a single *AChE* gene by different cell types in various tissues either constitutively or stimulus-induced. Alternative splicing leads to three major variants with identical esterase domains and distinct carboxy-terminal domains that seem to determine specific biological and pathological functions [22, 25–27]. Expression of the synaptic form of AChE is increased in response to apoptotic stimuli [27–29]. The presence of AChE per se is not sufficient to induce apoptosis. However, overexpression of AChE has been demonstrated to sensitize cells towards apoptosis induction [30] while suppressing AChE expression or pharmacological inhibition of its activity can rescue cells from apoptotic death [23, 28, 29, 31–33]. Both cytosolic appearance and translocation into the nucleus have been associated with the execution of apoptosis (see below). Nevertheless, all isoforms of AChE are translated in the endoplasmic reticulum and are designated to become intramembraneous, membrane attached or secreted proteins. To our knowledge, the mechanisms by which AChE can accumulate in the cytosol remain unresolved (see [34] for a general discussion). In the cytosol, AChE interacts with components of the apoptosome including Apaf-1 and cytochrome c [35] and suppression of AChE expression inhibits apoptosome formation [31]. A detailed study on rat PC12 cells [36] demonstrated an increased AChE expression following apoptosis induction. Additionally, a caspase-mediated cleavage of cytosol-located AChE at its N-terminus and a subsequent translocation of cleaved and full-length AChE into the nucleus were observed. Prevention of AChE cleavage by caspase inhibitors or stimulation of Akt signalling interfered with apoptotic cell death [36]. Accumulation of AChE in the nucleus of apoptotic cells has been described in several studies on different cell types [28, 30, 37]. AChE has been shown to cleave DNA in nuclei of apoptotic cells independent of other nucleases [32]. Hence, AChE seems to promote apoptosis in mammalian cells by contributing to cytochrome c-triggered apoptosome formation and degradation of nuclear DNA.

Involvement of AChE in regulation of apoptosis has not been described for invertebrate species. Insects, with the exception of cyclorrhaphan flies including *Drosophila melanogaster*, express two AChE genes, *ace-1* and *ace-2* [38–41]. Depending on the species, either *ace-1* or *ace-2* is expressed at higher levels and serves as the major enzyme that hydrolyzes synaptically released acetylcholine. The other AChE has frequently been described to perform non-synaptic functions involved in the regulation of growth, reproduction and development [often described as “non-cholinergic functions” [38, 41–43]]. Since acetylcholine is a major transmitter of sensory neurons and excitatory central nervous system synapses in insects, a large number of pharmacological agents used for pest control target AChE activity [43, 44]. Though AChE expression in non-neuronal cells has been reported [45], non-synaptic functions of insect AChE have not been resolved in detail.

In this study we challenged primary brain cell cultures from the migratory locust *Locusta migratoria* by exposure to hypoxic conditions. Hypoxia-induced cell death was accompanied with the characteristic phenotypic alterations attributed to apoptosis. We demonstrate increased *ace-1* expression in vivo during hypoxia exposure and significant reduction of hypoxia-induced cell death in the presence of two different AChE inhibitors in vitro. These results indicate that AChE promotes apoptosis in locusts, as it has previously been described for mammalian cells. This similarity provides another piece of evidence for the presence of a complex “mammalian-like” apoptosis regulatory system in the evolutionary ancestors of mammals and insects.

## Methods

Studies were performed with fifth instar nymphs of *Locusta migratoria*. Animals were purchased from a commercial breeder (HW-Terra; Herzogenaurach, Germany) and maintained at 24 °C; 55% humidity with a 12/12 h day/night cycle.

### Locust primary neuron culture

Primary neuron cultures were prepared as described previously [46–48]. In brief, two juvenile locust brains were dissected per primary culture. All brains of the same experiment were pooled and washed three times in Leibowitz 15 medium (L15; Gibco, Life Technologies, Darmstadt, Germany) supplemented with 1% Penicillin/Streptomycin (P/S; 10,000 units/ml penicillin and 10 mg/ml streptomycin, Sigma-Aldrich, Munich, Germany) and Amphotericin B (Ampho; Gibco, 250 µg/ml, ThermoFisher Scientific, Germany). Pooled brains were treated with Collagenase/Dispase (2 mg/ml; Sigma-Aldrich, Munich, Germany) for 30 min at



27 °C. Enzymatic digestion was stopped by three washes in Hanks balanced salt solution (Gibco, Life Technologies, Darmstadt, Germany). Brain cells were mechanically dissociated in 1 ml L15 by repeated pipetting. The dissociated neurons were briefly spun down with a table top centrifuge and the supernatant was discarded. The cell pellet was resuspended in 100 µl medium per cell culture. The cell suspension was equally distributed onto Concanavalin A-coated coverslips (ConA; Sigma-Aldrich, Munich, Germany). The coverslips (Ø 1 cm; Hartenstein, Würzburg, Germany) were coated for 1 h at room temperature, subsequently washed three times in PBS and placed into the centre of a culture dish (Ø 3 cm; Corning, New York, USA). Cells were let to settle down and attach to the coverslip for 2 h at room temperature before filling the dish with 1.9 ml L15 medium. Culture medium was further supplemented with 5% fetal bovine serum gold (FBSG; PAA Laboratories GmbH, Pasching, Austria) for the first four days. Cultures were maintained in humidified normal atmosphere at 27 °C if not stated otherwise. Culture medium was exchanged every other day.

### AChE inhibition and hypoxia treatment

To evaluate the effect of AChE inhibition on cell survival in normal culture conditions, cell culture medium was supplemented with either 10 µM neostigmine bromide (NSB; dissolved in H<sub>2</sub>O; Sigma-Aldrich, Munich, Germany) or 10 µM and 1 µM teritrem B (TRB, initially dissolved in methanol and further diluted in cell culture medium [MeOH final concentration < 0,001%]; Abcam, Cambridge, United Kingdom) for four days beginning at culture establishment. In order to evaluate the impact of AChE-inhibition on stressed neurons, cell cultures were exposed to hypoxic conditions for 36 h (0.3% O<sub>2</sub>; Hypoxia Incubator Chamber, STEMCELL™, Cologne, Germany). Cultures with and without supplemented AChE inhibitor were initially maintained for 5 days. On in vitro day 5, two cultures (AChE inhibitor-treated and untreated) were exposed to hypoxia, while one equivalent culture remained in normoxic conditions at the same temperature as the hypoxia-exposed cultures. Hypoxia-exposed cultures were reoxygenated for 12 h and all cultures were subsequently fixed in 4% paraformaldehyde (PFA).

### Cell viability assessment

Cell survival was assessed by DAPI nuclear staining. This method to distinguish physiologically intact from dead or dying neurons was validated by comparison with testing membrane integrity with the trypan blue exclusion assay [49] and TUNEL staining [this study]. Fixed cells were washed three times in PBS before washing twice with PBS/0.1% Triton-X-100 (PBST). Cultures were incubated for 30 min in DAPI (Sigma-Aldrich; Munich, Germany;

1:1000 in PBST) in the dark. Subsequently, coverslips were washed five times in PBS and once in DABCO (Roth, Karlsruhe, Germany) before mounting in DABCO. Experimental groups were evaluated with an epifluorescence microscope (Zeiss Axioskop; 40× objective, Oberkochen, Germany) equipped with a Spot CCD camera (InvisiTron, Puchheim, Germany). Two rows of non-overlapping photographs (~ 80 on average) covering the entire extension of the coverslips were taken from each cell culture for subsequent analysis. Live/Dead assessment was performed by manual counting of DAPI stained nuclei by an observer who was blinded with respect to the culture treatment. Cell counting was supported by using ImageJ Cell counter plug-in (Fiji ImageJ by NIH) as described elsewhere [46–48].

### Statistical analysis

Data of individual experiments were normalized to untreated control cultures with neurons derived from the same pool of locust brains, to evaluate the relative portion of surviving cells per culture. Data was analysed using RStudio (Version 1.2.1335 [50, 51]) employing pairwise permutation test (included in packages “coin” and “rcompanion” [52–54]). Data are represented in box plots including the median, upper and lower quartile. Whiskers represent 1.5× interquartile range. Circles show single data points. Benjamini–Hochberg correction was performed to avoid false positives resulting from multiple comparisons.

### Anti-cleaved caspase-3 immunostaining

Locust primary neuron cultures were stained for the presence of cleaved caspase-3, the activated form of caspase-3. Cultures were established and stressed by hypoxia as described above. For comparison of morphological alterations, apoptosis was additionally induced by exposing cultured locust neurons to UV light (10 h; TL-D 25 W G13, Philips Health Systems, Hamburg, Germany) or Mitomycin C (60 µg/ml, Sigma-Aldrich, Munich, Germany). After fixation in 4% PFA, cells were washed in PBS and subsequently permeabilized in PBST (0.1%). Coverslips were blocked in blocking solution (PBS/0.1% Triton; 5% normal goat serum; 0.25% bovine serum albumin) for 1 h before incubation with α-rabbit cleaved caspase-3 antibody (1:300 in blocking solution; Calbiochem, Merck, Darmstadt, Germany) at 4 °C over night. Subsequently, coverslips were washed in PBS before applying the secondary antibody (Cy2 goat-α-rabbit; 1:200 in blocking solution; Dianova, Hamburg, Germany) and DAPI (1:1000) for 2 h at room temperature. Cells were washed with PBS before mounting with PBS/Glycerin (1:1). Images of cleaved caspase-3 associated immunofluorescence

were taken with Leica TCS SP8 (40× magnification; Leica Microsystems, Wetzlar, Germany).

### Terminal deoxynucleotidyl transferase dUTP nick end labelling (TUNEL) staining

Locust primary neuronal cell cultures were prepared and stressed as described above. TUNEL stainings were performed using the Abcam In situ Direct DNA Fragmentation (TUNEL) Assay Kit (Abcam, Cambridge, United Kingdom) according to manufacturer's instructions. However, all staining steps were performed on cells attached to coverslips and volumes were adjusted to well sizes. Analysis of propidium iodide nuclear staining (488/623 wavelength) and fluorescein-labelled DNA fragments (488/520 wavelength) was performed with a Leica SP8 confocal microscope (Leica Microsystems, Wetzlar, Germany).

### Acetylcholinesterase-activity stainings in locust brain slices

NSB- and TRB-mediated interference with AChE activity was demonstrated on fixed brain sections of *L. migratoria* as originally described by Karnovsky and Roots [55] and modified for insect brain sections by Hoffmann and colleagues [56]. Briefly, dissected brains were fixed for 2 h in a mixture of 2.5% glutaraldehyde and 4% paraformaldehyde diluted in phosphate buffer, embedded in 5% agarose and sectioned horizontally (with respect to neuraxis) with a vibrating blade microtome (40 µm; VT 1000 S, Leica, Wetzlar, Germany). Brain slices were permeabilized with detergent, washed in Tris-Maleic buffer (TMB, pH 6) and one portion was incubated in NSB or TRB (10 µM, 1 µM and 0.1 µM respectively) diluted in TMB for 30 min. Control sections were incubated in TMB during that time. Subsequently, all but some sections, separated as negative control (no staining expected), were incubated for 45 min in freshly prepared AChE activity staining solution containing 10 mg acetylthiocholine iodide, 29.4 mg 0.1 M sodium citrate, 7.5 mg 30 mM CuSO<sub>4</sub>, and 1.6 mg 5 mM K<sub>3</sub>(Fe(CN)<sub>6</sub>) dissolved in 7.5 ml Tris-maleate buffer, with or without AChE inhibitor. After repeated washing in TMB brain sections were mounted on microscopy slides in DABCO and analysed by light microscopy.

### DNA isolation and DNA ladder

Locust primary neuronal cell cultures were prepared and stressed as described above. DNA was isolated following the protocol of Kasibathla and colleagues [57]. 1.5% Agarose gels were run at 50 V for 2 h. DNA was visualized by Roti®-GelStain (Roth, Karlsruhe, Germany) and documented with

an iBright CL1500 Imaging System (Thermo Fisher Scientific, Osterode am Harz, Germany).

### qRT-PCR analysis of in vivo *ace-1* expression

Intact juvenile locusts were exposed to hypoxic conditions (0.3% O<sub>2</sub>) for either 6.5 or 24 h while control animals were maintained in normoxic conditions for identical periods. For transcript expression analysis, brains were dissected either immediately after the end of the hypoxic period or after 1 h reoxygenation in normal atmosphere. Typically, five brains per treatment were pooled and RNA was extracted using Trizol (Sigma-Aldrich, Munich, Germany). Brain tissue was lysed in Trizol by TissueLyser LT (Qiagen, Hilden, Germany) aided by a 3 mm stainless steel bead. 200 µl chloroform (Labsolute, Th. Greyer, Renningen, Germany) were added and the samples were vigorously shaken for 15 s. Subsequently, lysed tissue samples were placed on ice for 15 min before centrifuging for 15 min at 12.000 × g at 4 °C. The RNA-containing translucent phase was carefully transferred to a fresh tube and precipitated with ice-cold 75% ethanol. Samples were incubated for at least 30 min at –20 °C before centrifuging for 10 min at 10.000 × g at 4 °C. The resulting RNA-containing pellet was washed three times in cold 75% ethanol before drying and elution in 30 µl ddH<sub>2</sub>O. RNA concentration was measured with NanoDrop™ (Thermo Scientific, Schwerte, Germany). Prior to cDNA synthesis RNA was subjected to DNase treatment using DNA-free™ DNA Removal Kit (Invitrogen, Schwerte, Germany; #AM1906) according to manufacturer's instructions. The same protocol was used to extract RNA from control animals that were continuously maintained in normoxic conditions.

cDNA was synthesized using LunaScript™ RT SuperMix Kit (New England BioLabs, Ipswich, MA, USA) according to the manufacturer's instructions. All reverse transcriptions were performed with 1 µg RNA as template.

qRT-PCR primers specific for locust *18 s rRNA* and *gapdh* were designed according to the corresponding sequences (*18 s rRNA* AF370793; *gapdh* JF915526). *Lm-ace* sequence of 560 bp was identified by aligning *Locusta migratoria manilensis* sequence (EU231603) and *Tribolium castaneum* (*ace-1* HQ260968; *ace-2* HQ260969) sequences against locust genome available on i5k platform (<https://i5k.nal.usda.gov/locusta-migratoria>). Alignments were performed using blastn with default settings, implemented on i5k platform. Sequence similarities were computed using Geneious Prime® (Version 2019.2.3) and ClustalW alignment tool (default settings applied). Computed *Lm-ace-1* sequence, alignments of reference sequences and sequence similarities are shown in Appendix Fig. 6, Table 3 and 4.

Prior to experimental data collection, all primers were tested for efficiency and housekeeping genes (HKG) were

**Table 1** qRT-PCR oligonucleotides used in this study

Gene	Sequence from 5'-3'	Accession no
<i>Lm-18S fwd</i>	CATGTCTCAGTACAAGCC GC	AF370793
<i>Lm-18S rev</i>	TCGGGACTCTGTTTGCAT GT	
<i>Lm-gapdh fwd</i>	GTCTGATGACAACAGTGC AT	JF915526
<i>Lm-gapdh rev</i>	GTCCATCACGCCACAAC TTC	
<i>Lm-ace fwd</i>	TTTGAAATGGCGGTGGTA GC	Computed sequence
<i>Lm-ace rev</i>	GTCGGAGGACTGCCT GTAC	

*Gapdh* primers were previously published in [48]

**Table 2** qRT-PCR program for amplification of *ace-1*, *18 s* rRNA and *gapdh* in locust brain cDNA samples

Step	Time [s]	Temperature [°C]	
Initial denaturation	180	95	
PCR reaction			
Denaturation	10	95	40×
Annealing	30	60	
Elongation	30	72	
Melting curve			
Denaturation	60	95	
Annealing	60	55	
Melting curve	10	55	0.5 °C per cycle up to 95 °C

further tested for stable expression in hypoxic samples (See Appendix Fig. 7 and Table 5). Primers used for qRT-PCR are summarized in Table 1.

qRT-PCRs were run using the MyiQ™ Single-ColorReal-Time PCR Detection System (Bio-Rad, Munich, Germany) in a 96-well plate with final PCR reaction volumes of 5 µl Luna® Universal qRT-PCR Master Mix (New England Bio-Labs, Ipswich, MA, USA), 0.1 µM forward and reverse primer and 10 ng cDNA (10 µl final reaction volume). Samples were run as triplicates and (–) RT controls were added for all measurements. Table 2 shows the program for cDNA amplification. Data was analysed using the Pfaffl method [58] and the geometric means of both *Lm-18S* and *Lm-gapdh* normalized values was calculated and plotted as bar plots in RStudio.

## Results

### Characterization of locust neuronal apoptosis

In order to characterize hypoxia-induced death of locust neurons as apoptotic, primary neuron cultures were subjected to cleaved-caspase-3 immunostaining, DNA labelling with DAPI and TUNEL stainings. First, we aimed to identify different stages of chromatin condensation in stressed neurons. Figure 2a displays a timeline (from left to right) of neuronal DNA condensation during apoptosis. Healthy cells display characteristic DAPI staining of intact euchromatin structures. During apoptosis, volumes of nuclei shrink and chromatin gets increasingly condensed until uniform DAPI labelling extends over the entire nucleus. In most cases, condensed nuclei persisted after cytomembranes disintegrated and the cytosol with all organelles was released into the culture medium. Only exceptionally nucleolysis and the generation of apoptotic bodies were observed (Fig. 2a, right). Additionally, we performed immunofluorescent stainings of cleaved-caspase-3 in hypoxia exposed neurons. Figure 2b shows representative stainings of an intact and a dead cell. The intact cell, recognizable by the typical patchy DAPI labelling pattern of its nucleus, lacks any cleaved-caspase-3 related immunoreactivity. Caspase-3 activity can be observed along parts of the nuclear envelope of the dead cell. Furthermore, nuclei which were in the process of apoptotic body formation displayed immunoreactivity in all nuclear fragments (Fig. 2c).

TUNEL stainings were conducted in order to visualize DNA double-strand breaks that typically appear during apoptotic DNA degradation. Figure 2d shows TUNEL positive staining in dead cells with highly compacted DAPI-labelled chromatin structure, while all intact cells with patchy DAPI-related fluorescence lacked the TUNEL related signal. Generally, neuron cultures not exposed to hypoxia displayed fewer cells with TUNEL positive nuclear staining in comparison with stressed cells (data not shown). DNA ladder formation as a sign for extensive internucleosomal DNA cleavage was not detected, when isolated DNA from stressed *in vitro* samples was separated by electrophoresis (Fig. 2e).

Besides hypoxia, primary cultured locust neurons were exposed to two additional stressors, that induced apoptosis in other studies. Locust neurons were either exposed to 10 h of UV light or to 60 µg/ml Mitomycin C (MMC) for 24 h. UV light was shown to induce DNA breaks followed by apoptotic death in a cell line derived from lepidopteran ovaries [59]. MMC is generally used in mouse embryonic fibroblast cultivation in order to disrupt DNA replication. Studies have

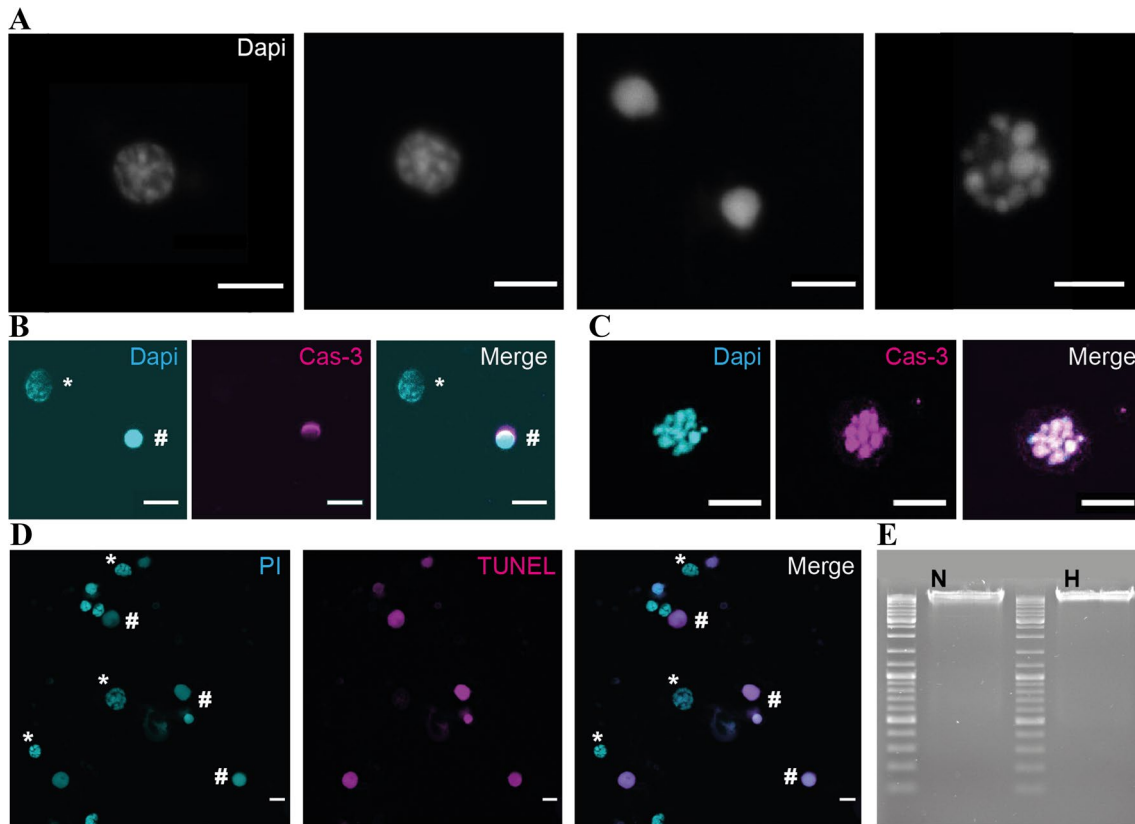


**Fig. 2** Characterization of locust neuronal apoptosis. **a** DAPI nuclear staining illustrates the process of DNA condensation in dying locust neurons. From left to right: Nucleus of intact cell. Condensation of chromatin structure, distinguishable by more tightly packed nuclear organization. Fully condensed DNA in two nuclei. Nucleolysis leads to formation of apoptotic bodies. Scale bars 5  $\mu\text{m}$ . **b** Nuclei of one intact (\*) and one dead (#) neuron with DAPI labelling,  $\alpha$ -cleaved caspase-3 immunofluorescence and merged signals. Cleaved caspase-3 activity is visible as a halo on the nuclear envelope of the dead cell. Scale bars 10  $\mu\text{m}$ . **c** DAPI labelling of a nucleus with

beginning nucleolysis.  $\alpha$ -cleaved caspase-3 immunofluorescence and merged signals that almost completely coincide. Scale bars 10  $\mu\text{m}$ . **d** DNA fragmentation of neurons visualized by TUNEL assay. Nuclei of intact (\*) and dead (#) neurons labelled with propidium iodide, TUNEL staining of DNA double strand breaks and merged signals. Only cells with condensed chromatin contain TUNEL staining. Scale bars 10  $\mu\text{m}$ . **e** After separation of DNA from hypoxia-exposed locust neurons on 1.5% agarose gel no DNA fragmentation (“DNA ladder”) is detectable. N=Normoxic sample, H=36 h hypoxia sample. 1 kb DNA ladder used as reference

shown that high concentrations of MMC can damage DNA and cause apoptosis in post-mitotic cells [60].

Both stressors induced equal cellular changes as hypoxia, including caspase-3 activation, nuclear condensation and DNA fragmentation in dying and dead cells’ nuclei visualized in TUNEL stainings (summarized in Suppl. Fig. S8). Also similar to hypoxia-induced apoptosis, DNA fragmentation leading to DNA ladder formation was not detectable.

### Increased expression of *ace-1* in hypoxia-exposed locust brains

A sequence with high (99.5%) similarity to *L. migratoria manilensis ace-1* was detected by blastn search in the poorly annotated genome of *L. migratoria migratoria* (Suppl. Fig. S6). Comparison of the identified *L. m. migratoria* consensus sequence with reported sequences

from *T. castaneum* revealed a higher similarity with *Tc-ace-1* (60.3% coverage) than with *Tc-ace-2* (46.7% coverage). Blast search using *Tc-ace-1* revealed high sequence similarity in the *L. m. migratoria* genome (73% coverage) in the same region that corresponded to the *L. m. manilensis* sequence. *Tc-ace-2* blast identified a corresponding sequence in the *L. m. migratoria* genome in a different region (76% coverage). These results suggest that the *L. migratoria ace* sequence we have been targeting is *ace-1*. Sequence similarities are summarized in Tables 3 and 4.

Juvenile locusts were exposed to either 6.5 or 24 h hypoxia (0.3%  $\text{O}_2$ ) before RNA isolation from dissected brains. qRT-PCR analysis, using both *Lm-18S rRNA* and *Lm-gapdh* as reference genes revealed a minor increase of average *ache* expression in animals exposed for 6.5 h to 1.19 ( $\pm 0.36$  STDV) fold of expression in untreated controls (Fig. 3a). Average *ace-1* expression levels increased to 1.66



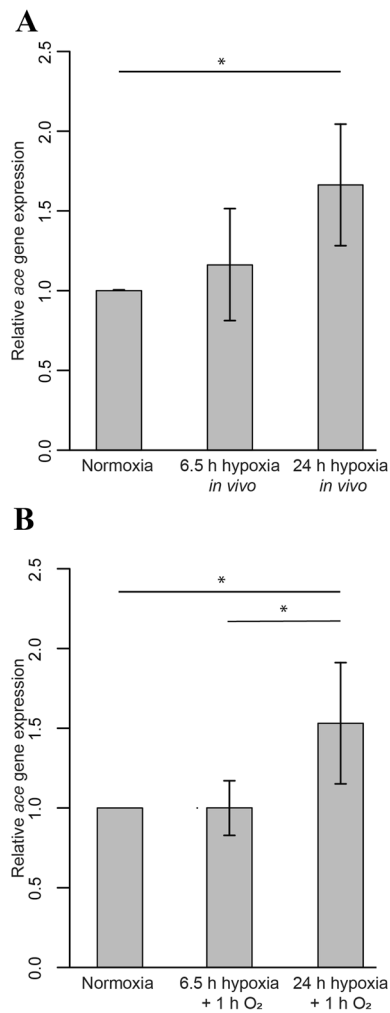


**Fig. 3** In vivo expression of *Lm-ace-1* transcript in hypoxia-exposed juvenile locusts. **a** Juvenile locusts were exposed to either 6.5 or 24 h hypoxia followed by immediate RNA isolation from dissected brains. qRT-PCR analysis shows minor insignificant changes after 6.5 h ( $1.19 \pm 0.36$  STDV) and significant ( $p=0.02$ ) moderate upregulation after 24 h ( $1.66 \pm 0.38$  STDV). **b** Juvenile locusts were exposed to either 6.5 or 24 h hypoxia followed by 1 h reoxygenation in normal atmosphere before RNA isolation from dissected brains. Average levels of *ace-1* transcript are unchanged ( $1.001 \pm 0.1$  STDV) after 6.5 h plus reoxygenation and moderately elevated ( $1.54 \pm 0.39$  STDV) after 24 h hypoxia plus reoxygenation in comparison with normoxic controls and 6.5 h exposed animals (both  $p=0.01$ ). **a, b** *18 s rRNA* and *gapdh* were used as internal controls. Geometric mean from  $n=6$  (except  $n=3$  for 6.5 h hypoxia plus reoxygenation in 3B) experiments was calculated and data plotted with RStudio. Statistics calculated with pairwise permutation test and Benjamini–Hochberg correction

( $\pm 0.38$  STDV) fold of control levels after 24 h exposure to hypoxia (significantly different with  $p=0.02$ ). To identify if *ace-1* transcription was hampered due to insufficient ATP as a result of hypoxic conditions, animals were exposed to both 6.5 and 24 h hypoxia followed by a 1 h reoxygenation period before RNA extraction. During the reoxygenation period locusts exposed to 6.5 h hypoxia reassumed upright

position and moved spontaneously. Animals exposed to 24 h hypoxia only performed twitches with their legs but did not reassume upright position. As shown in Fig. 3b, average *ace-1* expression levels remained unchanged after 6.5 h hypoxia plus reoxygenation ( $1.001 \pm 0.1$  STDV) and were slightly elevated after 24 h hypoxia plus reoxygenation ( $1.53 \pm 0.39$  STDV) compared to untreated control animals and 6.5 h exposed animals (both significantly different with  $p=0.01$ ). Therefore, the average of *ace-1* transcript was slightly reduced during the 1 h reoxygenation period (compare Figs. 3a and 3b).

### AChE inhibition increases the survival of insect neurons in vitro

As a first step, we confirmed that neostigmine bromide (NSB) and teritrem B (TRB) inhibit the hydrolysing activity of locust AChE. Fixed brain sections were incubated with acetylthiocholine (as part of a staining solution developed by Karnovsky and Roots [55]), which is converted into a dark precipitate by AChE. As shown in Fig. 4b, AChE-associated precipitate accumulated in various brain neuropils known to receive cholinergic innervation, including antennal lobes, central complex and mushroom body calyces. In contrast, brain sections that were not exposed to the staining solution remained entirely unlabelled (Fig. 4a). Similarly, AChE-generated precipitate was largely absent in brain sections that were co-exposed to staining solution and 10  $\mu$ M NSB (Fig. 4c1) or 10  $\mu$ M and 1  $\mu$ M TRB (Fig. 4d1, 2). Little precipitate was detected in antennal lobes, central complex and most other protocerebral neuropils, while slightly enhanced staining developed in the mushroom body calyces, which are known to receive profound cholinergic innervation. Nevertheless, largely reduced staining indicated that 10  $\mu$ M NSB and 1  $\mu$ M and 10  $\mu$ M TRB successfully suppressed most of the AChE-mediated conversion of the substrate. Stronger staining developed in the presence of 1  $\mu$ M and 0.1  $\mu$ M NSB (Fig. 4c2, 3) and 0.1  $\mu$ M TRB (Fig. 4d3) indicating weak or absent AChE inhibition at these concentrations. At 10  $\mu$ M and 1  $\mu$ M concentration TRB inhibited AChE activity more potently than NSB.

Initial experiments assessed the principal survival of primary neuron cultures from locust brains in the presence of the AChE inhibitor NSB. Primary neurons were cultured in full medium (with serum) supplemented with 10  $\mu$ M NSB (concentration was chosen according to histological experiments described above), starting immediately after culture establishment. After four days in vitro, cell survival was quantified on the basis of DAPI nuclear morphology and normalized to the respective untreated control cultures, which derived from the same pool of locust brains as the NSB-treated cultures. Comparison of non-treated control cultures with NSB-treated cultures revealed increased survival in the presence of the AChE inhibitor in all seven

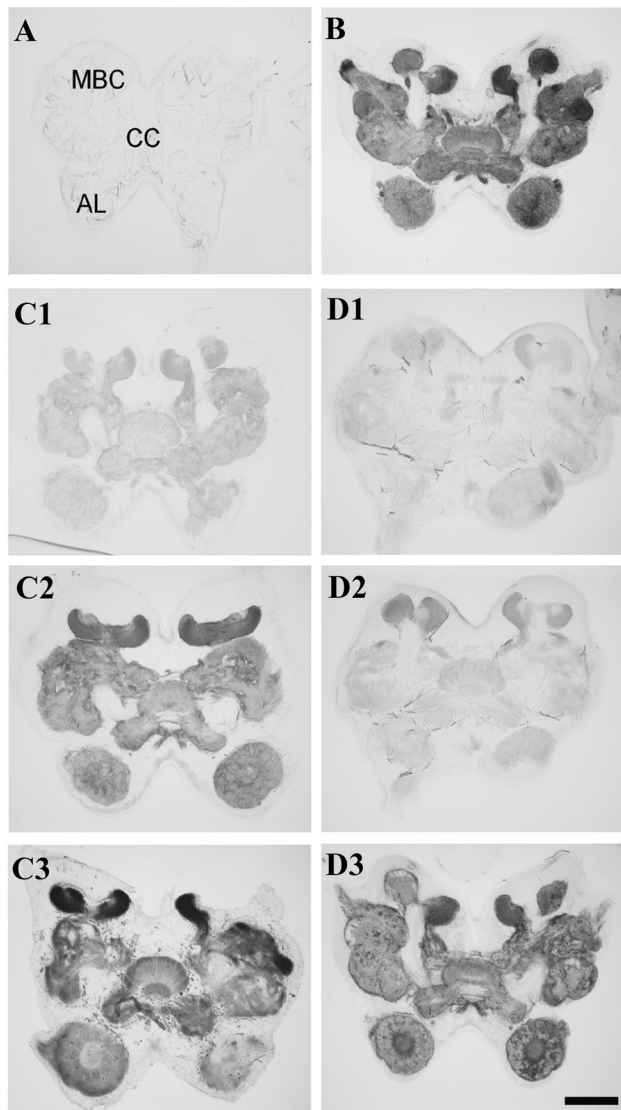


**Fig. 4** Acetylcholinesterase activity staining in locust brain slices. **a** Negative control incubated without substrate solution. Letters indicate position of neuropils that appear stained in B, C and D (AL antennal lobes, CC central complex, MBC mushroom body calyces). **b** Positive control incubated in substrate solution without AChE inhibitor. Strong AChE reaction product accumulates in various brain neuropils. C, D: Brain slices incubated for 45 min in substrate with different concentrations of NSB (C) and TRB (D). C1, D1: 10  $\mu$ M. C2, D2: 1  $\mu$ M. C3, D3: 0.1  $\mu$ M. Stainings indicate a concentration-dependent inhibition of AChE activity-generated staining by both AChE inhibitors. Scale bar 250  $\mu$ m valid for all photographs

experiments (Fig. 5a; 12 – 63% increase of surviving neurons; significantly different with  $p=0,02$ ). These results indicate that NSB supports the survival of locust primary neurons under normal culture conditions.

In order to evaluate whether inhibition of AChE alters neuronal survival under challenging physiological conditions, locust primary neuron cultures were subjected to hypoxia ( $O_2 < 0,3\%$ ) for 36 h. Data was normalized to the

respective control culture maintained in normoxic conditions, that derived from the same pool of locust brains as the respective experimental cultures. Hypoxia exposure reduced neuronal survival to 40 – 90% of survival in normoxic controls in all 12 experiments leading to a highly significant ( $p=0.0005$ ) loss of intact cells (Fig. 5b). Locust neurons that were maintained in medium supplemented with 10  $\mu$ M NSB were significantly less sensitive to hypoxia-induced apoptosis ( $p=0.003$ ). Within each experiment, relative survival in hypoxic NSB-treated cultures was higher than in the hypoxia-exposed cultures, derived from the same locust brains. In seven out of 12 experiments, survival in NSB-treated hypoxic cultures was even higher than in respective normoxic control cultures, although overall neuronal survival was not significantly different between these groups. These results indicate that the AChE inhibitor NSB interferes with hypoxia-induced apoptosis of locust primary brain neurons.

In order to confirm that the observed antiapoptotic effects of NSB resulted from its interaction with AChE, we exposed cultured locust neurons to another AChE inhibitor, TRB, with a different molecular structure and mode of AChE inhibition. Since 10  $\mu$ M and 1  $\mu$ M TRB inhibited AChE activity in locust brain sections, we used both concentrations in these experiments. TRB increased the survival of locust neurons under normal culture conditions (Fig. 5c). Compared to control cultures in normal medium, 1  $\mu$ M TRB increased cellular survival ( $p=0.03$ ) in five out of seven experiments (range of relative survival in all experiments: 98 – 130%, average: 111%). TRB in the concentration of 10  $\mu$ M increased cellular survival in all seven experiments (106 – 127%; average: 115%,  $p=0.004$ ). TRB also protected locust neurons from hypoxia-induced cell death (Fig. 5d). Compared to normoxic control cultures, hypoxia significantly reduced the average cell survival to 68% ( $p=0,001$ ). Treatment with 1  $\mu$ M and 10  $\mu$ M TRB increased the mean cell survival in hypoxia close to the level of survival in normoxic control cultures (105% and 99% respectively relative survival). Compared to hypoxia-exposed cultures, significantly more neurons survived in the presence of both concentrations of TRB (1  $\mu$ M:  $p=0.004$ , 10  $\mu$ M:  $p=0.007$ ), indicating that TRB interferes with hypoxia-induced death of primary locust brain neurons.

## Discussion

Apoptosis is involved in development, disease- and pathogen-induced cell death and tissue responses to challenging situations in most if not all animals. Prominent invertebrate model species *C. elegans* and *D. melanogaster* contain rather simple regulatory networks for apoptosis compared to mammalian species (Fig. 1). This led to the initial belief that the complexity of apoptotic mechanisms increased linearly from “simple” to “more complex” organisms. However,

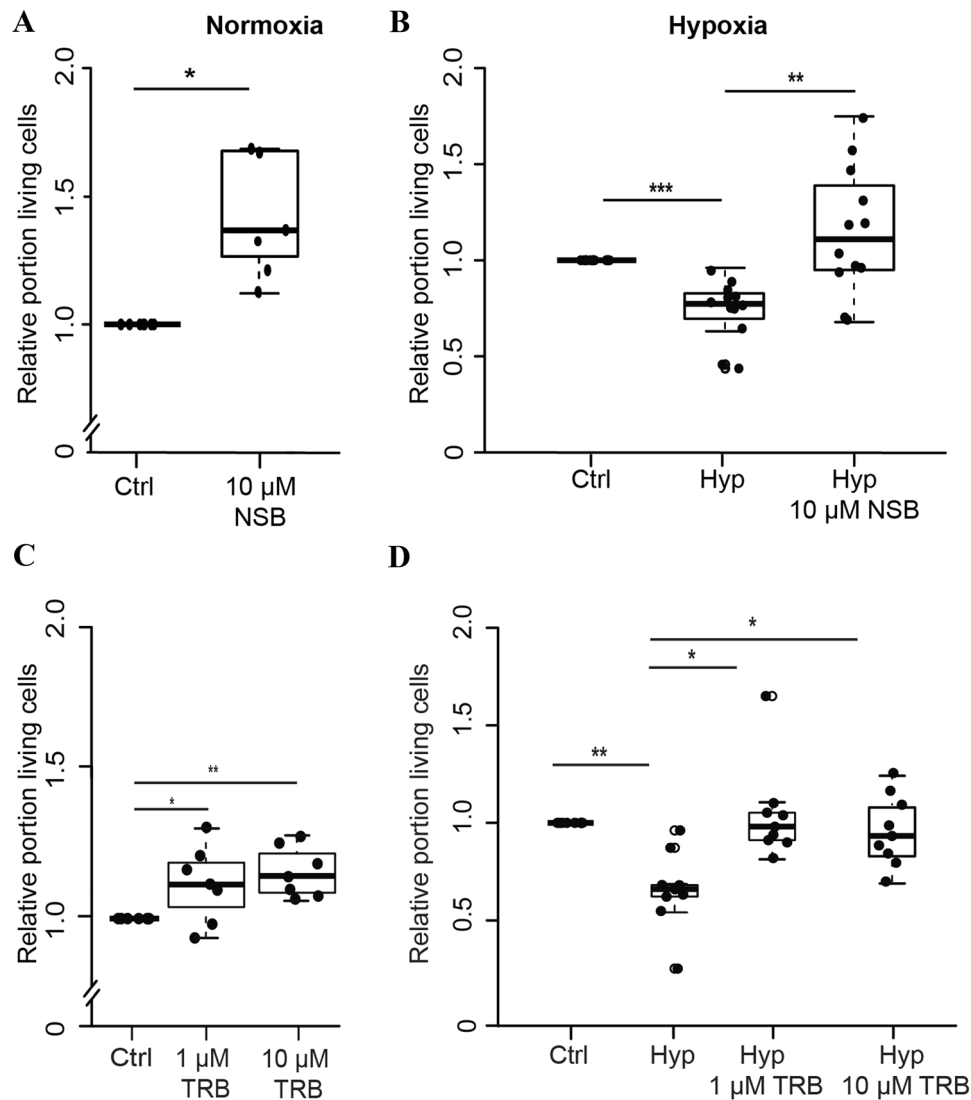


**Fig. 5** AChE inhibition increases neuronal survival in vitro. **a** Relative survival of locust neurons after 4 days in vitro. Inhibition of AChE with 10  $\mu\text{M}$  NSB significantly increased neuronal survival in normoxic control conditions.  $n=7$ ; 31,029 cells evaluated. **b** Relative survival of locust neurons after exposure to hypoxia ( $\text{O}_2 < 0.3\%$ ) for 36 h. Hypoxia-exposure reduced the median relative survival to 70% compared to control cultures that derived from the same pool of locust brains. Presence of 10  $\mu\text{M}$  NSB increased the survival of hypoxia-exposed neurons in each experiment. In some experiments, relative survival was even higher than in normoxic control cultures resulting in a median relative survival of 1.2 (compared to the controls in normoxic culture conditions). Cells were maintained in cul-

ture for five days before exposure to hypoxia.  $n=12$ ; 66,802 cells evaluated. **c** Effect of 1  $\mu\text{M}$  and 10  $\mu\text{M}$  TRB on locust neuronal survival in normoxic conditions. Treatment with either TRB concentration significantly increased cell survival in comparison to control.  $n=7$ ; 56,099 cells evaluated. **d** Relative survival of locust neurons exposed to 36 h hypoxia ( $\text{O}_2 < 0.3\%$ ). Hypoxia reduced the median cell survival to 60% in comparison to the control. Pretreatment with both 1  $\mu\text{M}$  and 10  $\mu\text{M}$  TRB rescued cells from hypoxia-induced apoptosis.  $n=9$ ; 95,907 cells evaluated. All statistics calculated with pairwise permutation test and Benjamini–Hochberg correction. \*  $p < 0.5$ , \*\*  $p < 0.01$ , \*\*\*  $p < 0.001$

apoptotic mechanisms in insects and other invertebrates that parallel the complex system of mammals have been identified. This suggests that the complex apoptotic system represents the ancient condition established in early metazoans and was subsequently simplified in some species including *C. elegans* and *D. melanogaster* [5, 8, 61]. In this respect, pro-apoptotic release of cytochrome c from

mitochondria as part of the endogenous apoptotic pathway has been demonstrated in mammals, sea urchins, planarians and insects, including the lepidopteran species *S. frugiperda* and *M. sexta* [18, 62–64] and few special cell types in *Drosophila* [20, 21]. Here, we describe another parallel between mammalian and insect apoptosis, namely the pro-apoptotic contribution of AChE to apoptosis of locust neurons. This

finding provides further support for the existence of a complex “mammalian-like” apoptotic regulatory network in the last common ancestors of invertebrates and vertebrates.

Studies on various cell types indicated that the pro-apoptotic function of AChE is a common phenomenon in mammalian species (review: [22]). Expression of AChE increases after apoptosis induction [36] and AChE enables the assembly and activity of the apoptosome. Cytosol-located AChE has been shown to associate with cytochrome c following its release from mitochondria. This interaction is required for Apaf-1 and caspase-9 recruitment, completing apoptosome formation and initiating caspase-3 activation [31, 35]. In addition, apoptotic cells accumulate AChE in their nuclei [28, 30, 35, 36] where it acts as a nuclear DNase with similar properties as caspase-activated deoxyribonuclease (CAD) and endonuclease G [32]. Although choline-hydrolyzing activity and non-enzymatic functions of AChE may be mediated by different domains of the AChE protein (the catalytic site and a peripheral anionic region [23]) both the reduction of AChE presence and pharmacological inhibition of its catalytic function interfered with apoptotic cell death in various cell types [23, 28, 29, 31–33]. The present study may suggest that the catalytic activity of AChE promotes apoptosis in locust neurons, since hypoxia-induced cell death was prevented by NSB and TRB, two AChE inhibitors with different molecular structure, both of which have been demonstrated to inhibit insect AChE activity ([65–68] and see below for more details). This suggests that functionality of AChE’s catalytic site is required for its pro-apoptotic role in locusts. Nonetheless, it cannot be fully excluded, that simultaneous non-catalytic interactions of locust AChE with other molecules might be altered in the presence of NSB and TRB as well.

As has been described for different cell types of various insect species, locust brain neurons also display typical characteristics of apoptotic cell death. Previous studies induced apoptosis in locust primary brain neurons by serum deprivation, H7 and hypoxia [46, 47]. Typical morphological hallmarks of apoptosis were detected in dying neurons. Most obviously and easy to quantify on the basis of fluorescent DNA labelling with DAPI [49], large and discontinuously labelled nuclei of intact cells became increasingly condensed and uniformly labelled. Chromatin condensation results from the loss of structural proteins in the nuclear matrix and represents an early event in apoptosis [69]. It typically takes place prior to DNA fragmentation by nucleases, which often leads to formation of apoptotic bodies [70, 71]. However, formation of apoptotic bodies by nucleolysis in final phases of apoptosis was only exceptionally observed in primary locust brain neurons. Instead, condensed nuclei persisted after cell membrane disintegration and loss of cytoplasm. Persistence of condensed nuclei following apoptotic cell death has previously been described in primary brain neurons of the beetle *Tribolium castaneum*

[72], Schneider cells and BG2 neuronal cells from *Drosophila melanogaster* (unpublished own observations) and developmental apoptosis of *Manduca sexta* labial glands and intersegmental muscles [73]. We have previously reported the accumulation of activated caspase-3 in the cytosol of dying locust brain neurons [46]. In the present study we also observed cleaved caspase-3 immunoreactivity in nuclei that were in the process of apoptotic condensation, suggesting that activated caspase-3 translocates to the nucleus of apoptotic cells. Involvement of caspase-3 in chromatin condensation of apoptotic HeLa, Sy5y and MCF-7 cells (neuroblastoma and breast cancer respectively) has previously been described [69, 74]. Additionally, recent publications suggest that caspase-3 translocation into the nucleus may be required for chromatin condensation [75, 76]. Though TUNEL stainings successfully marked DNA double-strand breaks in nuclei of dead locust neurons, visualization of extensive DNA fragmentation (described as “DNA ladder”) in agarose gels could not be detected, despite apoptosis induction by different stressors (hypoxia, MMC, UV light). This characteristic appearance of multimers of 180–200 bp DNA fragments results from internucleosomal DNA cleavage. Conventional methods of visualizing DNA fragments failed to demonstrate internucleosomal DNA fragmentation in a variety of cell types from both mammals [77–80] and insects [73, 81, 82]. In some of these studies, more sensitive methods based on end-labeling were sufficiently sensitive to detect DNA breakdown fragments [68, 71]. Several mechanisms that may prevent the detection of DNA ladder pattern have been suggested, including involvement of different types of nucleases, contribution of caspases and AChE to DNA degradation and persistent association of histone H1 with the internucleosomal linker. Failure to detect internucleosomal DNA fragmentation may also result from insufficient sensitivity of direct DNA fragment labelling, which could be improved by selective PCR amplification of blunt 5′ phosphorylated ends [83]. TUNEL-positive staining (labels 3′ blunt ends of DNA fragments) in the nuclei of dying and dead locust primary neurons may indicate the presence of 5′ blunt ends that could be amplified by this method.

The present study investigated a potential role of AChE in apoptotic cell death of locust neurons that parallels the pro-apoptotic function of AChE in vertebrates. While vertebrates contain a single *ache* gene, that is differently spliced into three variants, most insects express two *ace* genes (*ace-1* and *ace-2*) that code for proteins with respective ACh-hydrolysing synaptic function and non-synaptic roles related to growth, reproduction and development [38, 41–43]. *Ace-1* has been identified in the European locust *L. migratoria* by sequence similarity with Oriental locust *ace-1* (*L. migratoria manilensis*). The sequence and resulting protein from Oriental locust *ace-1* showed acetylcholine hydrolysing properties and was sensitive to insecticides



containing AChE inhibitors [43]. The sequence was more similar to *ace-1* from *T. castaneum*, which has been shown to mediate synaptic functions, while non-synaptic functions in this beetle were associated with *ace-2* [41]. A sequence with similarity to *Tc-ace-2* was identified at a different location in the locust genome, suggesting that locusts, as other insects, possess a second gene for AChE. Typically, *ace-2* is associated with non-synaptic functions in insects. While *ace-2* has not been studied for a potential function in insect apoptosis, *ace-1* seems to be critically involved in hypoxia-induced apoptosis of locust neurons. In order to assess, whether AChE expression changes with apoptosis-inducing stressful conditions, juvenile locusts were exposed to 6.5 or 24 h hypoxia. Our qRT-PCR data show that *Lm-ace-1* transcript increases moderately with prolonged hypoxia exposure. Since transcriptional activity might have been suppressed by the lack of ATP resulting from oxygen depletion, experiments were repeated with a reoxygenation period of 1 h in normal atmosphere between the end of hypoxia and the time of RNA isolation from brain tissues. Brains of reoxygenated animals contained slightly lower levels of *Lm-ace-1* transcript than animals that were not reoxygenated before RNA analysis. Nonetheless, our data indicate a hypoxia-dependent increase of *ace-1* expression. With reoxygenation, ATP production most probably increased, allowing the neurons to either undergo full apoptosis or recover if still possible. In the mammalian system, suppression of the presence or activity of AChE reduced, but did not fully prevent apoptosis [29, 30, 32, 35, 82]. Likewise, it seems unlikely that increased production of AChE is required for apoptosis in locust neurons, since apoptotic cells were also detected (though less frequently) in cultures supplemented with AChE inhibitors. However, promotion of apoptosome formation requires accumulation of AChE in the cytosol [31, 35] of mammalian cells. AChE is translated at the rough endoplasmic reticulum and should be targeted for export and/or association with the cell surface under normal conditions. It is currently unknown, whether a small portion of translated AChE is accidentally mislocated to the cytosol or whether a dedicated mechanism that redirects AChE to the cytosol [34] is at work here. Whether accidental mislocation or redirection to the cytosol increases with elevation of *AChE* transcript levels also remains to be demonstrated.

In this study we used two different AChE inhibitors, NSB and TRB, with different molecular structures, different binding sites and modes of interaction with AChE [84–86]. NSB is a carbamate inhibitor that covalently binds to a serine residue in the catalytic region of AChE. It has been employed in studies with several insects including cockroaches [68] and locusts [66]. A recent study demonstrated, that 100  $\mu\text{M}$ , 10  $\mu\text{M}$  and 1  $\mu\text{M}$  NSB inhibited  $\sim 95\%$ ,  $\sim 75\%$  and  $\sim 50\%$  of AChE activity in homogenates of larval lepidoptera respectively [67]. TRB, on the other hand, is a fungal mycotoxin whose AChE

inhibitory function was first characterized in a lepidopteran insect [65]. TRB establishes a very stable noncovalent binding with a larger portion of the AChE (including active site and entry of the gorge providing access to it) leading to profound conformational changes in AChE structure [84, 86]. Since 10  $\mu\text{M}$  NSB and 10  $\mu\text{M}$  and 1  $\mu\text{M}$  TRB effectively reduced AChE activity-related staining in brain sections of *L. migratoria* (Fig. 4), we selected these concentrations, to inhibit a large portion of AChE activity in our in vitro studies with primary cultured locust brain neurons. Even though some AChE inhibitors have been demonstrated to interact with other cellular targets (e.g. other esterases and neurotransmitter receptors; reviewed in [87]), the similar effects of two different molecules on apoptotic cell death of locust brain neurons demonstrated here are likely to emerge from their common function, the inhibition of AChE's enzymatic activity.

In order to assess a potential role of AChE in apoptotic cell death, an established in vitro approach [46, 88] with primary cultured locust brain neurons was adapted. The assay directly compares cellular survival between control and experimentally treated neuron cultures that derived from the same locust brains, minimizing variability between the treatment groups. The AChE inhibitors NSB and TRB increased the percentage of intact locust brain neurons during their cultivation for four days in normal culture conditions from 40–20% to 60–41%. Apart from the difference in the ratio of intact to dead neurons, no morphological changes between control and NSB- or TRB-treated cultures were observed. This suggested a rather specific interference of pharmacologically mediated AChE inhibition with ongoing apoptotic death in primary locust neuron cultures. In order to confirm this idea, apoptotic death was additionally stimulated by exposure of primary neuron cultures to hypoxia. Hypoxia exposure for 36 h reduced the median relative neuronal survival (compared to normoxic control cultures derived from the same locust brains) to approximately 70% (average), reproducing the efficient induction of apoptotic cell death seen in previous studies. Presence of NSB and TRB in hypoxia-treated cultures interfered with hypoxia-induced apoptosis and significantly increased neuron survival compared to hypoxia without inhibitor treatment. In fact, AChE inhibitor-treated hypoxia-exposed cultures reached the same level of neuron survival as the normoxic control cultures that derived from the same pool of brain cells. These results indicate that (in the absence of pharmacological inhibition) AChE promotes apoptosis in locust brain neurons. Whether the pro-apoptotic function of AChE is mediated through its esterase activity or other interactions with components of the apoptotic machinery cannot be decided at present state. Even though we demonstrated on brain sections that NSB and TRB are functional inhibitors of locust AChE enzymatic cleavage of choline-type substrates, locust AChE may contain other domains with distinct functions, similar to the peripheral site of vertebrate AChE. Since

cytochrome c release from mitochondria has been shown to promote apoptosis in insects [19, 63] an apoptotic role for AChE in the formation and functionality of the apoptosome (similar to vertebrates) seems quite possible. Alternatively, locust AChE may promote apoptosis through cleavage of nuclear DNA (as described above for mammalian cells). Several studies reported increased expression and translocation of AChE from cytosol into the nucleus. Nonetheless (as already mentioned above), it is currently unknown why AChE appears in the cytosol, although it is translated at the endoplasmic reticulum and designated for incorporation into the cytomembrane or export from the cell.

The migratory locust has been subject to various studies on pesticide resistance and hypoxia tolerance [43, 89]. Various pesticides target AChE in order to disrupt synaptic signalling by acetylcholine, a major transmitter in insect sensory systems and central nervous neuropils. The data presented in this study indicate, that in addition to its synaptic role, locust AChE mediates an important step in neuronal apoptosis. Contribution of AChE to apoptosis regulation is another, previously undescribed mechanism shared by mammalian and insect species. Together with other functional similarities mediated by homologous molecules (see Fig. 1) in mammals, insects and other invertebrates, this provides compelling evidence for the presence of a complex regulatory network already present at the basis of metazoa [8, 62, 90]. This finding enables comparative studies that exploit specific advances of certain species to unravel apoptotic mechanisms common to many animals including humans. Our knowledge on apoptosis essentially results from studies on classical model organisms *C. elegans* and *D. melanogaster*. However, regulation of apoptosis seems to be less complex here than typically seen in other insects and vertebrates. It becomes apparent, that the genetic repertoire of *C. elegans* and *D. melanogaster* diverged more profoundly from their last common ancestor with vertebrates than that of most other invertebrates and vertebrates [91]. Since cytochrome c release from mitochondria is not required for apoptosis in most *D. melanogaster* cell types a potential contribution of AChE to the formation of the apoptosome (as described for mammalian cells) cannot be extrapolated from locust neurons but requires experiments with this species. In any case, other insects like orthopteran (locusts and crickets) and lepidopteran (silkworms and others) species used in previous studies, may be better suited for comparative studies on the functions of AChE in apoptosis. Many degenerative diseases ultimately involve apoptotic cell death while cancer is promoted by inactivation of apoptosis. Knockdown or inactivation of AChE in normal cells decreased while induction of AChE in certain cancer cells increased their sensitivity to apoptotic stimuli [22, 24, 92]. Complete understanding of the apoptosis regulatory network will unravel new possibilities to interfere with dysregulated or disease-activated pathways. Some natural compounds [33] and synthetic molecules [23]

that interfere with AChE functions have already been demonstrated to prevent apoptotic cell death. Potential use of cell-protective drugs in degenerative diseases could be explored also with support of knowledge gained from insects and other invertebrate species. We believe, that the data presented here will not only be beneficial for the understanding of apoptosis, but will also open new possibilities in the field of neuroprotection and regeneration.

**Acknowledgements** Open Access funding provided by Projekt DEAL. We thank Martin C. Göpfert for financial support and scientific advice. We further thank Nina Hahn and Philip Hehlert for constructive discussions and methodological advice. Furthermore, we thank Silvia Gubert and Nicola Schwedhelm-Domeyer for technical assistance. We further thank the support of the Open Access Publication Funds of the Georg-August University Göttingen.

**Author contributions** All authors contributed to data collection. D. Knorr, N. Georges and R. Heinrich analyzed the data. The manuscript was written and edited by D. Knorr and R. Heinrich. D. Knorr and R. Heinrich designed and supervised the study. All authors read and approved the final manuscript.

**Funding** The project was funded by Deutsche Forschungsgemeinschaft (DFG; Project number: 398214842).

**Data Availability** Locust *ace-1* sequence was predicted by alignment of *Locusta migratoria manilensis ace-1* (Accession number: EU231603) with 99% coverage (e-value 0) and *Tribolium castaneum ace-1* (Accession number: HQ260968) with 73% coverage (e-value 4e-56) against locust genome available on i5k platform (<https://i5k.nal.usda.gov/locusta-migratoria>). All raw data can be accessed on request.

## Compliance with ethical standards

**Conflict of interest** All authors declare no conflicts concerning financial or commercial interests.

**Open Access** This article is licensed under a Creative Commons Attribution 4.0 International License, which permits use, sharing, adaptation, distribution and reproduction in any medium or format, as long as you give appropriate credit to the original author(s) and the source, provide a link to the Creative Commons licence, and indicate if changes were made. The images or other third party material in this article are included in the article's Creative Commons licence, unless indicated otherwise in a credit line to the material. If material is not included in the article's Creative Commons licence and your intended use is not permitted by statutory regulation or exceeds the permitted use, you will need to obtain permission directly from the copyright holder. To view a copy of this licence, visit <http://creativecommons.org/licenses/by/4.0/>.

## Appendix

### Lm-ace1 Sequence (560 bp)

```
TGCCCATTCG CAGTTTGATG TCATACATTC TGTGAA
TATG AAATAATAAC AACTGCAGGATCAGAAAGTGA
TGTCTGTTAT TTCGGAATAG ACGCCACATG TGTATA
```

TTCT TTA<sup>CT</sup>CCTCCTTTT<sup>G</sup>AAATG GCGGTGGTAG TACGACCACA AGACGCTGGTGTCCGAGGAG AAC  
 CGCTAGGGGCT GAACGGCCGT CCTGCCCGGC AGG GTGATCC TGGTGTTCGAT GCAGTACCGC GTCGCC  
 TGTTTCGGCGACTTCCCG GGCTCGGTGA TCTGGA TCGC TCGGCTTCCTCTTCTTCGAC ACGAGCGACG  
 ACCC GAACACGCAG CTGTCCGAGG ACTGCCTGT TGCCGGGCAA CGCGGGGCTC TTCGACCAGC TGA  
 ACATCAACGTG GTGGCGCCA AGCCGCGGCC GCG TGGCGCTGCAGTGGGTG CACGACAACA TCCACT  
 CAACGCC GCCGTCATGG TGTGGATCTTCGGCGGCG ACTT CGGCGGAAAC CCGCACAACG TGACGCTGT  
 GC TTCTACTCGG GCACGGCGAC GCTCGACGTG TCGGCGAGTCG GCGGGCGCCG.

**Table 3** Blast hits of *L. migratoria manilensis ace-1* and *T. castaneum ace* sequences on *L. migratoria* genome

	<i>L. migratoria manilensis</i> (EU231603)	<i>T. castaneum ace-1</i> (HQ260968)	<i>T. castaneum ace-2</i> (HQ260969)
Scaffold Hit	28,704	28,704	142,838
Coverage	99.50%	73%	75.70%
Sequence length	620 bp	386 bp	342 bp
Mismatches	3	104	67
Start (Sequence)	251.798	251.566	344.928
End (Sequence)	251.179	251.206	345.254
E Value	0	4E-56	1E-56

Blast was run on i5k platform

**Table 4** Coverage [%] of reference sequences to predicted *L. migratoria ace* sequence

	<i>L. migratoria manilensis ace-1</i>	<i>L. migratoria ace</i> Consensus sequence	<i>T. castaneum ace-1</i>	<i>T. castaneum ace-2</i>
<i>L. migratoria manilensis ace-1</i>		99.5	59.1	45.5
<i>L. migratoria ace</i>	99.5		60.3	46.7
<i>T. castaneum ace-1</i>	59.1	60.3		45.5
<i>T. castaneum ace-2</i>	45.5	46.7	45.5	

**Table 5** Ct values of locust housekeeping genes in normoxic and hypoxic conditions

Biological Replicates	Normoxia <i>Lm-18 s rRNA</i>		Hypoxia <i>Lm-18 s rRNA</i>		Normoxia <i>gapdh</i>		Hypoxia <i>gapdh</i>	
	Average Ct	ΔCt	Average Ct	ΔCt	Average Ct	ΔCt	Average Ct	ΔCt
1	9.08	0	9.07	0.02	18.95	0	19.51	-0.57
2	7.58	0	6.95	0.63	18.95	0	19.51	-0.57
3	7.30	0	7.39	-0.09	21.07	0	21.08	-0.01
4	6.41	0	7.10	-0.69	20.20	0	20.71	-0.51
5	6.78	0	6.77	0.01	20.18	0	20.16	0.03
6	6.78	0	6.77	0.01	19.67	0	19.95	-0.28
7	8.55	0	7.70	0.86	19.67	0	19.95	-0.28
8	6.76	0	6.59	0.16	20.69	0	20.06	0.63
9	6.97	0	6.99	-0.01	20.69	0	20.06	0.63
10	6.42	0	6.77	-0.35	20.20	0	20.20	0.00
11	6.99	0	6.79	0.20	19.67	0	20.42	-0.75
12	6.91	0	6.29	0.62	19.68	0	19.61	0.07
Average	7.21	0	7.10	0.12	19.97	0	20.10	-0.13
STDV	±0.82	±0	±0.72	±0.43	±7.28	±0	±7.31	±0.43

Expression of *Lm-gapdh* and *Lm-18 s rRNA* as housekeeping genes in hypoxic conditions

## References

1. Raff M (1998) Cell suicide for beginners. *Nature* 396:119–122. <https://doi.org/10.1038/24055>
2. Hengartner MO (2000) The biochemistry of apoptosis. 810–816
3. Lawen A (2003) Apoptosis—An introduction. *BioEssays* 25:888–896. <https://doi.org/10.1002/bies.10329>
4. Degterev A, Yuan J (2008) Expansion and evolution of cell death programmes. *Nat Rev Mol Cell Biol* 9:378–390. <https://doi.org/10.1038/nrm2393>
5. Green DR, Fitzgerald P (2016) Just So Stories about the Evolution of Apoptosis. *Curr Biol* 26:R620–R627. <https://doi.org/10.1016/j.cub.2016.05.023>
6. McLuskey K, Mottram JC (2015) Comparative structural analysis of the caspase family with other clan CD cysteine peptidases. *Biochem J* 466:219–232. <https://doi.org/10.1042/BJ20141324>
7. Galluzzi L, Kepp O, Trojel-Hansen C, Kroemer G (2012) Non-apoptotic functions of apoptosis-regulatory proteins. *EMBO Rep* 13:322–330. <https://doi.org/10.1038/embor.2012.19>
8. Zmasek CM, Godzik A (2013) Evolution of the animal apoptosis network. *Cold Spring Harb Perspect Biol*. <https://doi.org/10.1101/cshperspect.a008649>
9. Earnshaw WC, Martins LM, Kaufmann SH (1999) Mammalian caspases: Structure, Activation, Substrates, and functions during Apoptosis. *Annu Rev Biochem* 68:383–424
10. Kumar S (2007) Caspase function in programmed cell death. *Cell Death Differ* 14:32–43. <https://doi.org/10.1038/sj.cdd.4402060>
11. Bell RAV, Megeney LA (2017) Evolution of caspase-mediated cell death and differentiation: Twins separated at birth. *Cell Death Differ* 24:1359–1368. <https://doi.org/10.1038/cdd.2017.37>
12. Saelens X, Festjens N, Vande Walle L, Van Gurp M, Van Loo G, Vandenebeele P (2004) Toxic proteins released from mitochondria in cell death. *Oncogene* 23:2861–2874. <https://doi.org/10.1038/sj.onc.1207523>
13. Strasser A, Vaux DL (2018) Viewing BCL2 and cell death control from an evolutionary perspective. *Cell Death Differ* 25:13–20. <https://doi.org/10.1038/cdd.2017.145>
14. Sendoel A, Hengartner MO (2014) Apoptotic cell death under hypoxia. *Physiology* 29:168–176
15. Acehan D, Jiang X, Morgan DG, Heuser JE, Wang X, Akey CW (2002) Three-dimensional structure of the apoptosome: Implications for assembly, procaspase-9 binding, and activation. *Mol Cell* 9:423–432. [https://doi.org/10.1016/S1097-2765\(02\)00442-2](https://doi.org/10.1016/S1097-2765(02)00442-2)
16. Yuan S, Akey CW (2013) Apoptosome structure, assembly, and procaspase activation. *Structure* 21:501–515. <https://doi.org/10.1016/j.str.2013.02.024>
17. Liu KY, Yang H, Peng JX, Hong HZ (2012) Cytochrome c and insect cell apoptosis. *Insect Sci* 19:30–40
18. Huang J, Lv C, Hu M, Zhong G (2013) The Mitochondria-Mediate Apoptosis of Lepidopteran Cells Induced by Azadirachtin. *PLoS ONE* 8:1–15. <https://doi.org/10.1371/journal.pone.0058499>
19. Chen P, Hu YF, Wang L, Xiao WF, Bao XY, Pan C, Yi HS, Chen XY, Pan MH, Lu C (2015) Mitochondrial apoptotic pathway is activated by H<sub>2</sub>O<sub>2</sub>-mediated oxidative stress in BmN-SWU1 cells from *bombyx mori* ovary. *PLoS ONE* 10:1–14. <https://doi.org/10.1371/journal.pone.0134694>
20. Arama E, Bader M, Srivastava M, Bergmann A, Steller H (2006) The two *Drosophila* cytochrome C proteins can function in both respiration and caspase activation. *EMBO J* 25:232–243. <https://doi.org/10.1038/sj.emboj.7600920>
21. Mendes CS, Arama E, Brown S, Scherr H, Srivastava M, Bergmann A, Steller H, Mollereau B (2006) Cytochrome c-d regulates developmental apoptosis in the *Drosophila* retina. *EMBO Rep* 7:933–939. <https://doi.org/10.1038/sj.embor.7400773>
22. Zhang X-J, Greenberg DS (2012) Acetylcholinesterase Involvement in Apoptosis. *Front Mol Neurosci* 5:40
23. Mondal P, Gupta V, Das G, Pradhan K, Khan J, Gharai PK, Ghosh S (2018) Peptide-Based Acetylcholinesterase Inhibitor Crosses the Blood-Brain Barrier and Promotes Neuroprotection. *ACS Chem Neurosci* 9:2838–2848. <https://doi.org/10.1021/acschemneuro.8b00253>
24. Small DH, Michaelson S, Sberna G (1996) non-classical actions of cholinesterases: Role in cellular differentiation, tumorigenesis and Alzheimer's Disease. *Neurochem Int* 28:453–483
25. Grisaru D, Sternfeld M, Eldor A, Glick D, Soreq H (1999) Structural roles of acetylcholinesterase variants in biology and pathology. *Eur J Biochem* 264:672–686
26. Hicks D, John D, Makova NZ, Henderson Z, Nalivaeva NN, Turner AJ (2011) Membrane targeting, shedding and protein interactions of brain acetylcholinesterase. *J Neurochem* 116:742–746. <https://doi.org/10.1111/j.1471-4159.2010.07032.x>
27. Ye W, Gong X, Xie J, Wu J, Zhang X, Ouyang Q, Zhao X, Shi Y (2010) AChE deficiency or inhibition decreases apoptosis and p53 expression and protects renal function after ischemia/reperfusion. *Apoptosis* 15:474–487. <https://doi.org/10.1007/s10495-009-0438-3>
28. Zhang XJ, Yang L, Zhao Q, Caen JP, He HY, Jin QH, Guo LH, Alemany M, Zhang LY, Shi YF (2002) Induction of acetylcholinesterase expression during apoptosis in various cell types. *Cell Death Differ* 9:790–800. <https://doi.org/10.1038/sj.cdd.4401034>
29. Yang L, He HY, Zhang XJ (2002) Increased expression of intranuclear AChE involved in apoptosis of SK-N-SH cells. *Neurosci Res* 42:261–268. [https://doi.org/10.1016/S0168-0102\(02\)00005-6](https://doi.org/10.1016/S0168-0102(02)00005-6)
30. Jin QH, He HY, Shi YF, Lu H, Zhang XJ (2004) Overexpression of acetylcholinesterase inhibited cell proliferation and promoted apoptosis in NRK cells. *Acta Pharmacol Sin* 25:1013–1021
31. Park SE, Kim ND, Yoo YH (2004) Advances in Brief Acetylcholinesterase Plays a Pivotal Role in Apoptosome Formation. *Cancer Res* 64:2652–2655
32. Du A, Xie J, Guo K, Yang L, Wan Y, Ouyang Q, Zhang X, Niu X, Lu L, Wu J, Zhang X (2015) A novel role for synaptic acetylcholinesterase as an apoptotic deoxyribonuclease. *Cell Discov*. <https://doi.org/10.1038/celldisc.2015.2>
33. Zhaojie X, Gongmin D, Jiangren Y, Guo D, Zhu Y, Dengchao Y (2017) Multipotent AChE and BACE-1 inhibitors for the treatment of Alzheimer's disease: Design, synthesis and bio-analysis of 7-amino-1,4-dihydro-2H-isoquinolin-3-one derivatives. *Eur J Med Chem* 138:738–747. <https://doi.org/10.1016/j.ejmech.2017.07.006>
34. Hegde RS, Bernstein HD (2006) The surprising complexity of signal sequences. *Trends Biochem Sci* 31:563–571. <https://doi.org/10.1016/j.tibs.2006.08.004>
35. Park SE, Jeong SH, Yee S, Kim H, Soung YH, Ha NC, Kim D, Park J, Bae HR, Soo B, Lee HJ, Yoo YH (2008) Interactions of acetylcholinesterase with caveolin-1 and subsequently with cytochrome c are required for apoptosome formation. *Carcinogenesis* 29:729–737. <https://doi.org/10.1093/carcin/bgn036>
36. Xie J, Jiang H, Wan YH, Du AY, Guo KJ, Liu T, Ye WY, Niu X, Wu J, Dong XQ, Zhang XJ (2011) Induction of a 55 kDa acetylcholinesterase protein during apoptosis and its negative regulation by the Akt pathway. *J Mol Cell Biol* 3:250–259. <https://doi.org/10.1093/jmcb/mjq047>
37. Grubič Z, Komel R, Walker WF, Miranda AF (1995) Myoblast fusion and innervation with rat motor nerve alter distribution of acetylcholinesterase and its mRNA in cultures of human muscle. *Neuron* 14:317–327. [https://doi.org/10.1016/0896-6273\(95\)90288-0](https://doi.org/10.1016/0896-6273(95)90288-0)
38. Kim YH, Lee SH (2013) Which acetylcholinesterase functions as the main catalytic enzyme in the Class Insecta? *Insect Biochem Mol Biol* 43:47–53. <https://doi.org/10.1016/j.ibmb.2012.11.004>



39. Kim YH, Kwon DH, Ahn HM, Koh YH, Lee SH (2014) Induction of soluble AChE expression via alternative splicing by chemical stress in *Drosophila melanogaster*. *Insect Biochem Mol Biol* 48:75–82. <https://doi.org/10.1016/j.ibmb.2014.03.001>
40. Hall LM, Spierer P (1986) The Ace locus of *Drosophila melanogaster*: structural gene for acetylcholinesterase with an unusual 5' leader. *EMBO J* 5:2949–2954. <https://doi.org/10.1002/j.1460-2075.1986.tb04591.x>
41. Lu Y, Park Y, Gao X, Zhang X, Yao J, Pang YP, Jiang H, Zhu KY (2012) Cholinergic and non-cholinergic functions of two acetylcholinesterase genes revealed by gene-silencing in *Tribolium castaneum*. *Sci Rep* 2:1–7. <https://doi.org/10.1038/srep00288>
42. Revuelta L, Piulachs MD, Bellés X, Castañera P, Ortego F, Díaz-Ruiz JR, Hernández-Crespo P, Tenllado F (2009) RNAi of ace1 and ace2 in *Blattella germanica* reveals their differential contribution to acetylcholinesterase activity and sensitivity to insecticides. *Insect Biochem Mol Biol* 39:913–919. <https://doi.org/10.1016/j.ibmb.2009.11.001>
43. Zhou X, Xia Y (2009) Cloning of an acetylcholinesterase gene in *Locusta migratoria manilensis* related to organophosphate insecticide resistance. *Pestic Biochem Physiol* 93:77–84
44. Casida JE, Durkin KA (2013) Neuroactive Insecticides: Targets, Selectivity, Resistance, and Secondary Effects. *Annu Rev Entomol* 58:99–117. <https://doi.org/10.1146/annurev-ento-120811-153645>
45. Bicker G, Naujock M, Haase A (2004) Cellular expression patterns of acetylcholinesterase activity during grasshopper development. *Cell Tissue Res* 317:207–220. <https://doi.org/10.1007/s00441-004-0905-7>
46. Miljus N, Heibeck S, Jarrar M, Micke M, Ostrowski D, Ehrenreich H, Heinrich R (2014) Erythropoietin-mediated protection of insect brain neurons involves JAK and STAT but not PI3K transduction pathways. *Neuroscience* 258:218–227. <https://doi.org/10.1016/j.neuroscience.2013.11.020>
47. Ostrowski D, Ehrenreich H, Heinrich R (2011) Erythropoietin promotes survival and regeneration of insect neurons in vivo and in vitro. *Neuroscience* 188:95–108
48. Hahn N, Büschgens L, Schwedhelm-Domeyer N, Bank S, Geurten BRH, Neugebauer P, Massih B, Göpfert MC, Heinrich R (2019) The Orphan Cytokine Receptor CRLF3 Emerged With the Origin of the Nervous System and Is a Neuroprotective Erythropoietin Receptor in Locusts. *Front Mol Neurosci*. <https://doi.org/10.3389/fnmol.2019.00251>
49. Gocht D, Wagner S, Heinrich R (2009) Recognition, Presence, and Survival of Locust Central Nervous Glia In Situ and In Vitro. *Microsc Res Tech* 72:385–397. <https://doi.org/10.1002/jemt.20683>
50. Rs T (2015) RStudio: Integrated Development for R. RStudio Inc, Boston, MA
51. Core Team R (2019) An Introduction to dplR. *Ind Commer Train* 10:11–18. <https://doi.org/10.1108/eb003648>
52. Mangiafico SS (2019) Package ‘rcompanion’
53. Hothorn T, Hornik K, Van De Wiel MA, Zeileis A (2006) A lego system for conditional inference. *Am Stat* 60:257–263. <https://doi.org/10.1198/000313006X118430>
54. Zeileis A, Hornik K, Wiel MA, Hothorn T (2008) Implementing a class of permutation tests: The coin package. *J Stat Softw* 28:
55. Karnovsky M, Roots L (1969) A “direct-coloring” thiocholine method for cholinesterases. *J Histochem Cytochem* 12:219–221
56. Hoffmann K, Wirmer A, Kunst M, Gocht D, Heinrich R (2007) Muscarinic Excitation in Grasshopper Song Control Circuits Is Limited by Acetylcholinesterase Activity. *Zool Sci* 24:1028–1035. <https://doi.org/10.2108/zsj.24.1028>
57. Kasibhatla S, Amarante-Mendes GP, Finucane D, Brunner T, Bossy-Wetzell E, Green DR (2006) Analysis of DNA Fragmentation Using Agarose Gel Electrophoresis. *Cold Spring Harb Protoc*. <https://doi.org/10.1101/pdb.prot4429>
58. Pfaffl MW (2001) (2001) A new mathematical model for relative quantification in real-time RT–PCR. *Nucleic Acids Res* 29:2003–2007. <https://doi.org/10.1111/j.1365-2966.2012.21196.x>
59. Koval TM, Hart RW, Myser WC, Hink WF (1977) A comparison of survival and repair of uv-induced DNA damage in cultured insect versus mammalian cells. *Genetics* 87:513–518
60. Koval TM (1991) Recovery from exposure to DNA-damaging chemicals in radiation-resistant insect cells. *Mutat Res Lett* 262:219–225. [https://doi.org/10.1016/0165-7992\(91\)90087-K](https://doi.org/10.1016/0165-7992(91)90087-K)
61. Romero A, Novoa B, Figueras A (2015) The complexity of apoptotic cell death in mollusks: An update. *Fish Shellfish Immunol* 46:79–87. <https://doi.org/10.1016/j.fsi.2015.03.038>
62. Bender CE, Fitzgerald P, Tait SWG, Llambi F, McStay GP, Tupper DO, Pellettieri J, Alvarado AS, Salvesen GS, Green DR (2012) Mitochondrial pathway of apoptosis is ancestral in metazoans. *Proc Natl Acad Sci* 109:4904–4909. <https://doi.org/10.1073/pnas.1120680109>
63. Facey COB, Lockshin RA (2010) The execution phase of autophagy associated PCD during insect metamorphosis. *Apoptosis* 15:639–652
64. Shu B, Zhang J, Jiang Z, Cui G, Veeran S, Zhong G (2019) Harmine induced apoptosis in *Spodoptera frugiperda* S9 cells by activating the endogenous apoptotic pathways and inhibiting DNA topoisomerase I activity. *Pestic Biochem Physiol* 155:26–35
65. Dowd PF, Peng FC, Chen JW, Ling KH (1992) Toxicity and anticholinesterase activity of the fungal metabolites territrems to the corn earworm, *Helicoverpa zea*. *Entomol Exp Appl* 65:57–64. <https://doi.org/10.1111/j.1570-7458.1992.tb01627.x>
66. Benke D, Breer H (1990) Identification of an endogenous polypeptide modulating ligand binding sites of insect neuronal acetylcholine receptors. *Neurochem Int* 16:287–294. [https://doi.org/10.1016/0197-0186\(90\)90104-2](https://doi.org/10.1016/0197-0186(90)90104-2)
67. Zolfaghari M, Ghadamyari M, Sajedi RH (2019) Resistance mechanisms of a field population of diamond back moth, *Plutella xylostella* (Lepidoptera: Plutellidae) to current organophosphate pesticides. *J Crop Prot* 8:403–416
68. Harrow ID, Sattelle DB (1983) Acetylcholine Receptors on the Cell Body Membrane of Giant Interneuron 2 in the Cockroach, *Periplaneta Americana*. *J Exp Biol* 105:339–350
69. Robertson JD, Orrenius S, Zhivotovsky B (2000) Review: Nuclear events in apoptosis. *J Struct Biol* 129:346–358. <https://doi.org/10.1006/jsbi.2000.4254>
70. Howell DM, Martz E (1988) Nuclear disintegration induced by cytotoxic T lymphocytes. Evidence against damage to the nuclear envelope of the target cell. *J Immunol* 140:689–692
71. Allera C, Lazzarini G, Patrone E, Alberti I, Barboro P, Sanna P, Melchiori A, Parodi S, Balb C (1997) The condensation of chromatin in apoptotic thymocytes shows a specific structural change. *J Biol Chem* 272:10817–10822. <https://doi.org/10.1074/jbc.272.16.10817>
72. Hahn N, Knorr DY, Liebig J, Wüstefeld L, Peters K, Büscher M, Bucher G, Ehrenreich H, Heinrich R (2017) The Insect Ortholog of the Human Orphan Cytokine Receptor CRLF3 Is a Neuroprotective Erythropoietin Receptor. *Front Mol Neurosci* 10:1–11. <https://doi.org/10.3389/fnmol.2017.00223>
73. Zakeri ZF, Quagliano D, Latham T, Lockshin RA (1993) Delayed internucleosomal DNA fragmentation in programmed cell death. *FASEB J* 7:470–478
74. Jänicke RU, Sprengart ML, Wati MR, Porter AG (1998) Caspase-3 is required for DNA fragmentation and morphological changes associated with apoptosis. *J Biol Chem* 273:9357–9360. <https://doi.org/10.1074/jbc.273.16.9357>
75. Luo M, Lu Z, Sun H, Yuan K, Zhang Q, Meng S, Wang F, Guo H, Ju X, Liu Y, Ye T, Lu Z, Zhai Z (2010) Nuclear entry

- of active caspase-3 is facilitated by its p3-recognition-based specific cleavage activity. *Cell Res* 20:211–222. <https://doi.org/10.1038/cr.2010.9>
76. Prokhorova EA, Kopeina GS, Lavrik IN, Zhivotovsky B (2018) Apoptosis regulation by subcellular relocation of caspases. *Sci Rep* 8:1–11. <https://doi.org/10.1038/s41598-018-30652-x>
  77. Iglesias-Guimaraes V, Gil-Guñón E, Sánchez-Osuna M, Casanelles E, García-Belinchón M, Comella JX, Yuste VJ (2013) Chromatin collapse during caspase-dependent apoptotic cell death requires DNA fragmentation factor, 40-kDa subunit-/caspase-activated deoxyribonuclease- mediated 3'-OH single-strand DNA breaks. *J Biol Chem* 288:9200–9215. <https://doi.org/10.1074/jbc.M112.411371>
  78. Yamaguchi K, Uzzo R, Dulin N, Finke JH, Kolenko V (2004) Renal carcinoma cells undergo apoptosis without oligonucleosomal DNA fragmentation. *Biochem Biophys Res Commun* 318:710–713. <https://doi.org/10.1016/j.bbrc.2004.04.086>
  79. Yuste VJ, Bayascas JR, Llecha N, Sánchez-López I, Boix J, Comella JX (2001) The absence of oligonucleosomal DNA fragmentation during apoptosis of IMR-5 neuroblastoma cells. Disappearance of the caspase-activated DNase. *J Biol Chem* 276:22323–22331. <https://doi.org/10.1074/jbc.M100072200>
  80. Bortner CD, Oldenburg NBE, Cidlowski JA (1995) The role of DNA fragmentation in apoptosis. *Trends Cell Biol* 5:21–26. [https://doi.org/10.1016/S0962-8924\(00\)88932-1](https://doi.org/10.1016/S0962-8924(00)88932-1)
  81. Meneses-Acosta A, Mendona RZ, Merchant H, Covarrubias L, Ramírez OT (2001) Comparative characterization of cell death between Sf9 insect cells and hybridoma cultures. *Biotechnol Bioeng* 72:441–457. [https://doi.org/10.1002/1097-0290\(20000220\)72:4<441:AID-BIT1006>3.0.CO;2-3](https://doi.org/10.1002/1097-0290(20000220)72:4<441:AID-BIT1006>3.0.CO;2-3)
  82. Schwartz LM, Smith SW, Jones MEE, Osborne BA (1993) Do all programmed cell deaths occur via apoptosis? *Proc Natl Acad Sci U S A* 90:980–984. <https://doi.org/10.1073/pnas.90.3.980>
  83. Staley K, Blaschke AJ, Chun J (1997) Apoptotic DNA fragmentation is detected by a semiquantitative ligation-mediated PCR of blunt DNA ends. *Cell Death Differ* 4:66–75. <https://doi.org/10.1038/sj.cdd.4400207>
  84. Chen WL, Sheets JJ, Nolan RJ, Mattsson JL (1999) Human red blood cell acetylcholinesterase inhibition as the appropriate and conservative surrogate endpoint for establishing chlorpyrifos reference dose. *Regul Toxicol Pharmacol* 29:15–22. <https://doi.org/10.1006/rtph.1998.1256>
  85. Beri V, Wildman SA, Shiomi K, Al-Rashid ZF, Cheung J, Rosenberry TL (2013) The natural product dihydrotanshinone i provides a prototype for uncharged inhibitors that bind specifically to the acetylcholinesterase peripheral site with nanomolar affinity. *Biochemistry* 52:7486–7499. <https://doi.org/10.1021/bi401043w>
  86. Cheung J, Beri V, Shiomi K, Rosenberry TL (2014) Acetylcholinesterase complexes with the natural product inhibitors dihydrotanshinone I and territrem B: Binding site assignment from inhibitor competition and validation through crystal structure determination. *J Mol Neurosci* 53:506–510. <https://doi.org/10.1007/s12031-014-0261-3>
  87. Pope C, Karanth S, Liu J (2005) Pharmacology and toxicology of cholinesterase inhibitors: Uses and misuses of a common mechanism of action. *Environ Toxicol Pharmacol* 19:433–446. <https://doi.org/10.1016/j.etap.2004.12.048>
  88. Miljus N, Massih B, Weis M, Rison V, Bonnas C, Sillaber I, Ehrenreich H, Geurten B, Heinrich R (2017) Neuroprotection and endocytosis: erythropoietin receptors in insect nervous systems. *J Neurochem* 141:63–74. <https://doi.org/10.1111/jnc.13967>
  89. Ravn MV, Campbell JB, Gerber L, Jon F, Overgaard J (2019) Effects of anoxia on ATP, water, ion and pH balance in an insect. *Locusta migratoria*. <https://doi.org/10.1242/jeb.190850>
  90. Zmasek CM, Zhang Q, Ye Y, Godzik A (2007) Surprising complexity of the ancestral apoptosis network. *Genome Biol* 8:1–8. <https://doi.org/10.1186/gb-2007-8-10-r226>
  91. Raible F, Arendt D (2004) Metazoan Evolution: Some Animals Are More Equal than Others. *Curr Biol* 14:R106–R108. <https://doi.org/10.1016/j.cub.2004.01.015>
  92. Zhang J, Li D, Ge P, Yang M, Guo Y, Zhu KY, Ma E, Zhang J (2013) RNA interference revealed the roles of two carboxylesterase genes in insecticide detoxification in *Locusta migratoria*. *Chemosphere* 93:1207–1215. <https://doi.org/10.1016/j.chemosphere.2013.06.081>

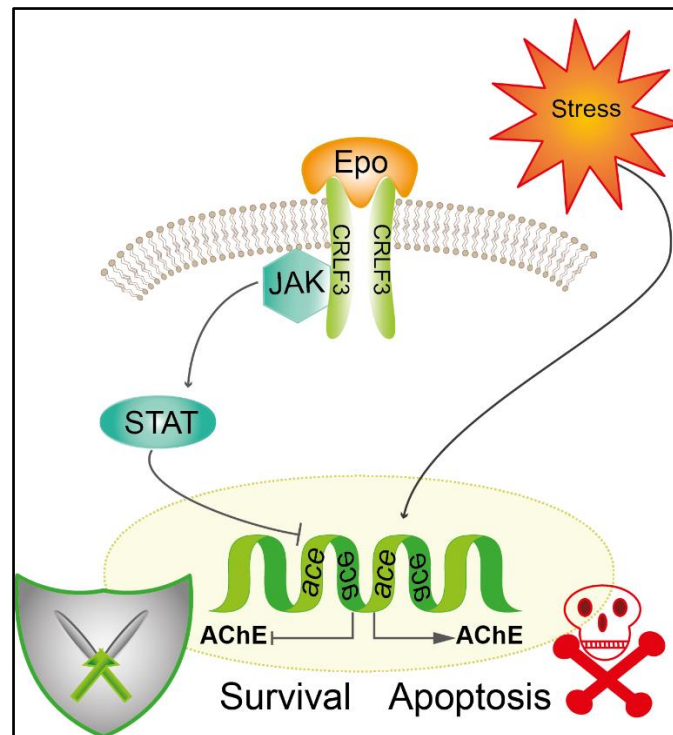
**Publisher's Note** Springer Nature remains neutral with regard to jurisdictional claims in published maps and institutional affiliations.

## Chapter 2

Protection of insect neurons by erythropoietin/CRLF3-mediated regulation of pro-apoptotic acetylcholinesterase

Debbra Y. Knorr, Kristin Schneider, Luca Büschgens, Jan Förster, Nadine S. Georges, Bart R.H. Geurten and Ralf Heinrich

- Under Review -

**Author contribution statement**

D.Y. Knorr, K. Schneider, L. Büschgens, J. Förster and N.S. Georges performed and analysed the experiments. B.R.H. Geurten generated and trained artificial intelligence for cell survival analysis. D.Y. Knorr and R. Heinrich designed and supervised the study. D.Y. Knorr and R. Heinrich wrote and edited the manuscript. All authors read and approved of the final version

<b>Figure 1</b>	<b>DYK</b> performed splice identification; <b>DYK</b> , KS and JF (supervised by <b>DYK</b> ) performed and analysed cell survival assay; NSG (supervised by <b>DYK</b> ) generated and analysed qPCR data
<b>Figure 2</b>	KS and JF (supervised by <b>DYK</b> ) performed and analysed cell survival assays
<b>Figure 3</b>	LB and NSG (supervised by <b>DYK</b> ) generated and analysed locust data; <b>DYK</b> generated and analysed tribolium data
<b>Figure 4</b>	LB (supervised by <b>DYK</b> ) generated and analysed locusts cell experiments; <b>DYK</b> performed tribolium experiments and analysed the data
<b>Figure 5</b>	KS and JF (supervised by <b>DYK</b> ) performed and analysed cell survival assay
<b>Figure 6</b>	<b>DYK</b> performed and analysed the experiment
<b>AI programing</b>	BRHG
<b>Experimental design</b>	RH and <b>DYK</b>
<b>Manuscript writhing</b>	RH and <b>DYK</b> , with contribution of all authors

## Protection of insect neurons by erythropoietin/CRLF3-mediated regulation of pro-apoptotic acetylcholinesterase

Debra Y. Knorr<sup>1</sup>, Kristin Schneider<sup>1</sup>, Luca Büschgens<sup>1</sup>, Jan Förster<sup>1</sup>, Nadine S. Georges<sup>1</sup>, Bart R.H. Geurten<sup>1</sup> and Ralf Heinrich<sup>1,\*</sup>

<sup>1</sup>Department of Cellular Neurobiology, Johann-Friedrich-Blumenbach-Institute for Zoology and Anthropology, Georg-August-University Göttingen, Göttingen, Germany

\* Corresponding author; E-Mail: rheinri1@gwdg.de

### Abstract

Cytokine receptor-like factor 3 (CRLF3) is a eumetazoan highly conserved but largely uncharacterized orphan cytokine receptor that shares structural similarity with vertebrate classical erythropoietin receptor (EpoR). CRLF3-mediated neuroprotection in insects can be stimulated with human erythropoietin and involves partly similar anti-apoptotic mechanisms as erythropoietin-mediated neuroprotection in mammals. To identify potential mechanisms of CRLF3-mediated neuroprotection we studied the expression and function of acetylcholinesterase which promotes apoptosis in different cell types, including mammalian neurons. We exposed primary brain neurons from the locust *Locusta migratoria* and the beetle *Tribolium castaneum* to apoptogenic stimuli and/or dsRNA to interfere with acetylcholinesterase gene expression and compared survival and/or acetylcholinesterase expression in the presence or absence of the CRLF3 ligand erythropoietin. Apoptogenic stimuli (hypoxia) increase the expression of both acetylcholinesterase-coding genes *ace-1* and *ace-2* associated with increased apoptotic cell death. Both *ace* genes give rise to single transcripts and hence single types of AChE-1 and AChE-2 in both normal and apoptogenic conditions. In contrast to elevated *ace* gene expression, pharmacological inhibition of acetylcholinesterases (completely) and RNAi-mediated knockdown of either *ace-1* or *ace-2* expression (partially) prevent hypoxia-induced apoptosis of primary brain neurons. Activation of CRLF3 with protective concentrations of Epo mediates neuroprotection by preventing the increased expression of pro-apoptotic acetylcholinesterase with larger impact on *ace-1* than on *ace-2*. Additionally, high concentrations of rhEpo that commonly (and seemingly paradoxically) cause death of insect and mammalian neurons induced *ace-1* expression and hence promoted apoptosis in locust and beetle neurons. Our study confirms the cell-intrinsic role of acetylcholinesterase as a major regulator of apoptotic death, that was previously described in mammalian neurons only. Moreover, we identify a mechanism (prevention of upregulation of pro-apoptotic acetylcholinesterase), by which CRLF3 activation mediates neuroprotection under apoptogenic conditions. Since both apoptosis and CRLF3 are conserved throughout the animal kingdom, the direct link between cytokine/CRLF3 activation and suppression of increased acetylcholinesterase expression underlying neuroprotection in insects may also be present in other cell types and other non-insect species.

### Key words:

Neuroprotection, CRLF3, erythropoietin, cytokine, acetylcholinesterase, AChE

## **Introduction**

Acetylcholinesterase (AChE) hydrolyses acetylcholine and terminates synaptic transmission at cholinergic synapses in vertebrates and invertebrates (Zhang *et al.*, 2002). AChE is expressed in tissues with and without cholinergic innervation and contributes to multiple processes including cellular adhesion, cell growth, cell differentiation, amyloid fiber assembly and apoptosis (Small, Michaelson and Sberna, 1996; Karczmar, 2010; Zhang and Greenberg, 2012; Rotundo, 2017). Altered presence and functions of AChE are associated with various degenerative diseases including Alzheimer's disease, Parkinson's disease and cancer in various tissues (Perry *et al.*, 2002; Hu, Gray and Brimijoin, 2003; Toiber *et al.*, 2008; Walczak-Nowicka and Herbet, 2021). Mammalian species express three major AChE splice variants from a single gene locus, that differ in their carboxy-terminal domains which determine localisation and interactions with other proteins (Grisaru *et al.*, 1999; Ye *et al.*, 2010; Hicks *et al.*, 2011; Zhang and Greenberg, 2012). Splice variants include the synaptic AChE (AChE-S), erythrocytic AChE (AChE-E) and the soluble read-through variant (AChE-R). Apoptogenic physiological stress enhances intracellular AChE levels in various mammalian tissues (including brain, retina, kidney, endothelial cells, bone, myoblasts) and cell lines (including PC12, neuroblastoma, HeLa cells) (reviewed by (Zhang and Greenberg, 2012; Campoy *et al.*, 2016). Increased levels of AChE sensitize cells to induce apoptosis upon exposure to pathogenic or physiologically challenging conditions (Jin *et al.*, 2004). Absence or catalytic inactivation of AChE have been correlated with reduced sensitivity to apoptogenic stimuli and reduced cell death in various cell types including neurons (Toiber *et al.*, 2008; Zhang *et al.*, 2013). (Toiber *et al.*, 2008; Zhang *et al.*, 2013). In mammalian organisms AChE expression is elevated under apoptogenic conditions and cytoplasm-located AChE interacts with caveolin-1, APAF-1 and cytochrome c in order to facilitate apoptosome formation (Park, Kim and Yoo, 2004; Park *et al.*, 2008; Zhang and Greenberg, 2012). Silencing of AChE inhibited apoptosome formation and increased cell survival (Zhang *et al.*, 2002a; Park, Kim and Yoo, 2004). Additionally, AChE can act as a DNase following nuclear translocation during apoptosis (Du *et al.*, 2015). However, overexpression of the enzyme is not invariably coupled with initiation of apoptosis, but rather sensitizes cells towards apoptotic stimuli (Jin *et al.*, 2004).

In contrast to mammals, most insects possess two distinct genes (*ace-1* and *ace-2*) coding for different AChE proteins (Hall and Spierer, 1986; Lu, Park, *et al.*, 2012; Kim and Lee, 2013). Depending on the species, either AChE-1 or AChE-2 mediates the canonical, synaptic functions of the enzyme (Revuelta *et al.*, 2009; Zhou and Xia, 2009; Lu, Park, *et al.*, 2012; Kim and Lee, 2013), while functions of the other protein remain largely uncharacterised (Revuelta *et al.*, 2009; He, Sun and Li, 2012; Lu, Pang, *et al.*, 2012; Lu, Park, *et al.*, 2012; Kim and Lee, 2013). Our previous studies identified a pro-apoptotic function of AChE in neurons of the migratory locust *Locusta migratoria* (Knorr *et al.*, 2020) that parallels the role of AChE mammalian apoptosis. We demonstrated that *Lm-ace-1* transcript levels increased under hypoxic conditions *in vivo* and that pharmacological inhibition of AChE prevented hypoxia-induced apoptotic death of locust primary neurons. This indicates a link between AChE-1 presence/activity and apoptotic cell death in insects (Knorr *et al.*, 2020). Since genetic information in locusts is scarce, sequence information is only available for *Lm-ace-1* but not for *Lm-ace-2*. This prevents the investigation of differential functions of *ace-1* and *ace-2* in apoptosis and other processes in locust species. The red flour beetle *Tribolium castaneum* expresses different *ace* transcripts and AChE proteins from two genes, with cholinergic functions accounted to *Tc-ace-1* and other, incompletely identified functions in developmental processes of *Tc-ace-2* (Lu, Pang, *et al.*, 2012; Lu, Park, *et al.*, 2012). Given that sequences for both *Tc-ace-1* and *Tc-ace-2* are available and protocols for *in vitro* studies with primary neurons were previously established, we decided to analyse the differential involvement of the two *ace* genes and AChE proteins in *T. castaneum* apoptosis.

Erythropoietin (Epo) is a helical cytokine generally known for its functions in vertebrate erythropoiesis, where it protects erythrocyte progenitor cells from apoptosis (Ma *et al.*, 2014; Samson *et al.*, 2020; Thompson *et al.*, 2020). Local production and cytoprotective functions of Epo have been discovered in various vertebrate tissues (Yilmaz *et al.*, 2004; Brines and Cerami, 2005; Sepodes *et al.*, 2006; Arcasoy, 2008; Noguchi, 2008; Ghezzi and Conklin, 2013). Epo-mediated cell protection typically relies on upregulation of anti-apoptotic proteins following phosphorylation of JAK associated with Epo receptors (reviewed in (Vittori *et al.*, 2021)). Nonetheless, a clear picture of Epo-mediated anti-apoptotic effects remains elusive. Both *L. migratoria* and *T. castaneum* express the phylogenetically conserved orphan cytokine receptor CRLF3 (cytokine receptor-like factor 3). CRLF3 belongs to group 1 of the prototypic class one cytokine receptors which also includes the classical erythropoietin receptor EpoR (Boulay, O'Shea and Paul, 2003; Liongue and Ward, 2007). Both receptors are expressed in various mammalian tissues including the nervous system. Erythropoietin signalling initiates neuroprotective processes in the mammalian nervous system (Sirén and Ehrenreich, 2001; Genc, Koroglu and Genc, 2004; Brines and Cerami, 2005; Ghezzi and Conklin, 2013) by activating homodimeric EpoR and/or alternative Epo receptors (Brines *et al.*, 2004; Leist *et al.*, 2004; Ostrowski and Heinrich, 2018). *EPO* and *EPOR* are widely but exclusively expressed in vertebrate species and therefore are absent in insects. Nonetheless, recombinant human Epo (rhEpo) protects locust and beetle neurons from toxin- and hypoxia-induced apoptosis by activating partially identical intracellular transduction pathways as in mammalian cells (Miljus *et al.*, 2014; Hahn *et al.*, 2017; Heinrich, Günther and Miljus, 2017a). CRLF3 was identified as the insect neuroprotective receptor for rhEpo and EV-3, a splice variant of human Epo with neuroprotective properties that cannot activate homodimeric EpoR (Bonnas *et al.*, 2017; Hahn *et al.*, 2017; Hahn, Büschgens, Schwedhelm-Domeyer, Bank, Bart R. H. Geurten, *et al.*, 2019). Signalling via an unknown Epo-like cytokine and CRLF3 seems to represent an ancient cell-protective system that secures neuron and other cells' survival and maintenance of tissue functionality under unfavourable physiological conditions.

Cell-protective concentrations of Epo vary between cell types, species and types of insult (Sinor and Greenberg, 2000; Ruscher *et al.*, 2002; Weber *et al.*, 2005; Heinrich, Günther and Miljus, 2017a). Optimum-type concentration-responses have been reported for mammalian and insect neurons, in which high Epo concentrations not only lack the protective effects but rather exert cytotoxic effects leading to increased cell death compared with untreated control cells (Siren *et al.*, 2001; Chong, Kang and Maiese, 2003; Weishaupt *et al.*, 2004; Ostrowski, Ehrenreich and Heinrich, 2011; Miller *et al.*, 2015; Hahn *et al.*, 2017). Reduced protective effects with Epo concentrations above the optimum have been explained by desensitization or downregulation of EpoR (Verdier *et al.*, 2000; Cohen *et al.*, 2004) and prevention of EpoR homo-dimerisation due to saturation of high-affinity binding sites of EpoR monomers (Kim *et al.*, 2017). An explanation for toxic effects of very high concentrations of Epo is currently lacking for EpoR, CRLF3 or other potential alternative Epo receptors.

In the present study on primary neuron cultures from *L. migratoria* and *T. castaneum* and whole *T. castaneum* pupae, we explore the differential expression of *Tc-ace-1* and *Tc-ace-2* under apoptogenic conditions (hypoxia) and their contribution to the progress of apoptosis. We link the previously reported neuroprotective effect of rhEpo-mediated CRLF3 activation in both insect species to reduced expression of pro-apoptotic AChE. While neuroprotective concentrations of rhEpo prevented overexpression of *ace-1* under apoptogenic conditions, toxic concentrations of rhEpo increased *ace-1* expression. Given the known pro-apoptotic functions of AChE in mammalian neurons (and other cells), Epo-mediated neuroprotection via EpoR and/or alternative Epo receptors may also rely on negative regulation of *ACHE* expression.

## Methods

Experiments were performed with *Tribolium castaneum* late pupae (San Bernadino wild type strain) kindly provided by the lab of Prof. Dr. Gregor Bucher and *Locusta migratoria* fifth instar nymphs obtained from a commercial breeder (HW-Terra, Herzogenaurach, Germany). Beetles were reared in plastic boxes filled with whole grain flour and yeast at 27°C, 40% humidity and 12/12 h day/night cycle. Locusts were kept at 24°C, 55% at 12/12 h day/night cycle.

### *Insect primary brain cell culture*

Primary neuron cultures were established as previously described (Miljus *et al.*, 2014; Hahn *et al.*, 2017; Hahn, Büschgens, Schwedhelm-Domeyer, Bank, Bart R. H. Geurten, *et al.*, 2019; Knorr *et al.*, 2020, 2021a). In brief, 20 tribolium or 2 locust brains per culture were dissected and collected in Leibowitz 15 medium (Gibco; Life Technologies, Darmstadt, Germany) supplemented with 1% penicillin/streptomycin and 1% amphotericin B (both Sigma-Aldrich, Munich, Germany) (from now referred to as L15 medium). Subsequently, brains were enzymatically digested in collagenase/dispase (2mg/ml, Sigma-Aldrich, Munich, Germany) for 45 min (*T. castaneum*) or 30 min (*L. migratoria*) at 27°C. Enzymatic reaction was stopped by repeated washing in Hanks' balanced salt solution and brains were mechanically dissociated by repeated pipetting in L15. The suspension of dissociated brain cells was seeded on Concanavalin A (Sigma-Aldrich, Munich, Germany) coated coverslips and let to rest for 2 h. Afterwards, culture dishes were filled with L15 supplemented with 5% fetal bovine serum gold (FBSG, PAA Laboratories GmbH, Pasching, Austria). Medium was replaced by L15 plus FBSG on day two and by L15 without serum on day four *in vitro*. Primary cell cultures were maintained at 27°C without CO<sub>2</sub> buffering.

### *Pharmacological treatment and hypoxia exposure of primary cell cultures*

Cell cultures were treated with 10 µM neostigmine bromide (NSB; Sigma-Aldrich, Munich, Germany), 10 µM territremin B (TRB; initially dissolved in methanol, further diluted in L15; Abcam, Cambridge, United Kingdom) or recombinant human Epo (33,3 ng/ml or 333 ng/ml for locust cultures and 0,8 ng/ml or 8 ng/ml for beetle neurons; NeoRecormon; Roche, Welwyn Garden City, United Kingdom). AChE inhibitors NSB and TRB were applied throughout the entire culturing period and replaced with each medium change. rhEpo was added to the medium on day 5 *in vitro*. 12 h after the onset of rhEpo treatment, cultures were exposed to hypoxia (<0,3% O<sub>2</sub>, Hypoxia Chamber; Stemcell, Cologne, Germany) for 36 h. Untreated control culture were maintained at normoxic conditions. Subsequently cell cultures were fixed and stained as described below. To compare effects of protective and deleterious concentrations of rhEpo, cultures were exposed to different concentrations of rhEpo for 48 h starting on day five *in vitro*.

### *RNA interference with ace-1 and ace-2 expression in T.castaneum neurons*

Double-stranded (ds) RNA fragments targeting *Tc-ace-1* or *Tc-ace-2* were designed and prepared as stated below. To reduce expression of respective protein, 10 ng/ml dsRNA targeting either *Tc-ace-1* or *Tc-ace-2* was added from the beginning of the experiment and renewed with each medium change.



Successful interference with protein expression by “soaking RNAi” was previously demonstrated in primary cultured *T. castaneum* neurons (Hahn *et al.*, 2017; Knorr *et al.*, 2021). Cells were exposed to hypoxia on day 5 for 36 h ( $O_2 < 0,3\%$ ) before being fixed and analyzed for cell survival.

### *Dapi staining and analysis of cell survival*

After treatments, cells were fixed in 4% paraformaldehyde (PFA) for 30 min. Cells were washed 3 times in phosphate-buffered saline (PBS) and twice in PBS/0,1% Triton-X-100 (PBST) for each 5 min. Subsequently nuclei were stained with Dapi (Sigma-Aldrich, Munich, Germany 1:1000 in PBST) for 30 min before being washed 5 times in PBS. Coverslips were transferred to microscopy slides, enclosed in DABCO (Roth, Karlsruhe, Germany) and sealed around the edges with nail polish.

Images of Dapi-stained nuclei were taken using an epifluorescence microscope (Zeiss Axioskop, Oberkochen, Germany) equipped with a spot CCD camera (Invisitron, Puchheim, Germany). From each cell culture, two rows of non-overlapping photographs were taken (for locust cultures ~80 images using 40x magnification; for *tribolium* cultures ~120 images using 63x magnification). Cell survival was assessed by the Dapi stained chromatin structure as described previously (Miljus *et al.*, 2014; Hahn *et al.*, 2017; Hahn, Büschgens, Schwedhelm-Domeyer, Bank, Bart R. H. Geurten, *et al.*, 2019; Knorr *et al.*, 2020, 2021a). Intact and dead/dying neurons were identified and counted automatically by an object recognition AI based on the Faster R-CNN (Ren *et al.*, 2015) net with Inception V2 (Ioffe and Szegedy, 2015). We re-trained a neuronal net that was previously trained and configured for the Oxford-III Pets dataset (Visual Geometry Group - University of Oxford, no date) and is available as part of the tensorflow model collection ([https://github.com/tensorflow/models/blob/master/research/object\\_detection/samples/configs/faster\\_r\\_cnn\\_inception\\_v2\\_pets.config](https://github.com/tensorflow/models/blob/master/research/object_detection/samples/configs/faster_r_cnn_inception_v2_pets.config), no date). Experts categorized living and dead cells for *Locusta* (3480 cells in 92 images) and *Tribolium* (3469 cells in 75 images). All routines for the AI cell counting routines were written in Python 3.5 (GDrake, 2009) utilizing numpy (Harris *et al.*, 2020), pandas (McKinney, 2011), and tensor flow (Abadi *et al.*, 2016) amongst others.

Cell survival in different treatment groups within one experiment was subsequently normalized towards the corresponding untreated control, set to 1.

### *dsRNA cloning and preparation*

Two non-overlapping fragments targeting either *Tc-ace-1* (HQ260968) or *Tc-ace-2* (HQ260969) were designed and cloned into the pCRII vector by TA cloning (TA cloning Kit, Invitrogen, Life Technologies, Darmstadt, Germany) (Fragment sequences are listed in Supplements). Vectors were transformed into XL-1 blue competent cells and grown on ampicillin-supplemented agar plates. Multiple clones were analyzed by colony PCR and sequencing for the proper insertion of the target fragments. Clones with the appropriate vector were grown and DNA was extracted using NucleoSpin Plasmid Kit (Macherey-Nagel, Düren, Germany).

For dsRNA preparation, plasmids were amplified by PCR using M13 fwd and M13 rev primers with a T7 RNA promoter sequence attached to the reverse primer. The PCR program and primer sequences are listed in tables 1 and 2. PCR products were separated on a 1% agarose gel and purified using the Macherey–Nagel NucleoSpin Gel and PCR Clean-up Kit (Macherey–Nagel, Düren, Germany) according to the manufacturer’s recommendations.



Purified DNA was subsequently in vitro transcribed by usage of the MEGAScript T7 transcription kit (Life Technologies, Darmstadt, Germany) following the manufacturer's instructions. The single-stranded RNA was washed three times in 70% EtOH before resuspension in injection buffer (1.4 mM NaCl, 0.07 mM Na<sub>2</sub>HPO<sub>4</sub>, 0.03 mM KH<sub>2</sub>PO<sub>4</sub>, 4 mM KCl). Single-stranded RNA was annealed to double strands (dsRNA) at 94°C for 5 min and cooled down to 20°C at a rate of 0,1°C per second. dsRNA concentrations were measured with a spectrophotometer (Nanodrop 1000, Thermo Fisher Scientific, Schwerte, Germany). dsRNA quality was assessed by agarose gel electrophoresis.

**Table 1:** Oligonucleotides used in this study. Primers for M13, M13-T7, *Lm ace-1*, *18srRNA* and *gapdh* were previously used (Hahn *et al.*, 2017; Knorr *et al.*, 2020). Lm= *L. migratoria*; Tc= *T. castaneum*. Oligonucleotides used for splice variant analysis of *Tc-ace-2* may potentially generate two amplicons.

	Sequence 5'-3'	Amplicon [bp]
<b>M13 fwd</b>	GTAAAACGACGGCCAGT	300
<b>M13-T7 rev</b>	TAATACGACTCATAGGCAGGAAACAGCTATGAC	
<b>Tc <i>ace-2</i>-E1-E3 fwd</b>	GCCAGAGACTTTCACAGCGA	1177 / 359
<b>Tc <i>ace-2</i>-E1-E3 rev</b>	CATCACGTTCCAACCGACTC	
<b>Tc <i>ace-2</i>-E2-E4 fwd</b>	CGGCTTCCTCTACTTGAGCA	731 / 588
<b>Tc <i>ace-2</i>-E2-E4 rev</b>	TCTGGTTCAAGTAGCCGTCG	
<b>Tc <i>ace-2</i>-E3-E5 fwd</b>	GAGTCGGTTGGAACGTGATG	345 / 192
<b>Tc <i>ace-2</i>-E3-E5 rev</b>	GCTGCAAATCTGGCAAAGGC	
<b>Tc <i>ace-2</i>-E4-E6 fwd</b>	CGACGGCTACTTGAACCAGA	424 / 266
<b>Tc <i>ace-2</i>-E4-E6 rev</b>	ATCGTTCCAAAACGCGCACG	
<b>Tc <i>ace-2</i>-E4-E7 rev</b>	TGCTCAAGTAGAGGAAGCCG	534 / 376
<b>Tc <i>ace-1</i> fwd</b>	AACTTCAGCAGCAAACGAGC	120
<b>Tc <i>ace-1</i> rev</b>	CTGTTCGACACCATCAGGAGG	
<b>Tc <i>ace-2</i> fwd</b>	ACAGCTGAGGTTTCAGGAAGC	116
<b>Tc <i>ace-2</i> rev</b>	GGGAAGTACTCGTAGCGCTC	
<b>Tc <i>rps3</i> fwd</b>	GGCGCTAAAGGGTGTGAAGT	150
<b>Tc <i>rps3</i> rev</b>	TGTCTTAGCAAGACGTGGCG	
<b>Tc <i>rps18</i> fwd</b>	CCTCAACAGGCAGAAGGACA	130
<b>Tc <i>rps18</i> rev</b>	CCTGTGGGCCCTGATTTTCT	
<b>Lm <i>ace-1</i> fwd</b>	TTTGAAATGGCGGTGGTAGC	120
<b>Lm <i>ace-1</i> rev</b>	GTCGGAGGACTGCCTGTAC	
<b>Lm <i>18s rRNA</i> fwd</b>	CATGTCTCAGTACAAGCCGC	106
<b>Lm <i>18s rRNA</i> rev</b>	TCGGGACTCTGTTTGCATGT	
<b>Lm <i>gapdh</i> fwd</b>	GTCTGATGACAACAGTGCAT	110
<b>Lm <i>gapdh</i> rev</b>	GTCCATCACGCCACAACCTTC	

**Table 2:** PCR program for dsRNA template amplification

Step	Temperature [°C]	Time [s]	Cycle
<b>Initial denaturation</b>	98	180	
<b>Denaturation</b>	98	30	x30
<b>Annealing</b>	60	30	
<b>Elongation</b>	72	30	
<b>Final elongation</b>	72	300	

*RNA isolation and cDNA synthesis*

RNA of cell cultures and brains was isolated using Trizole (Thermo Fisher Scientific, Schwerte, Germany) as described previously (Knorr *et al.*, 2020, 2021a). For tissue specimen 15 brains of late *T. castaneum* pupae were extracted and collected in RNALater (Sigma-Aldrich, Munich, Germany). In the case of cell culture specimen, 5 cultures of each treatment group were prepared as described above. Cells were scraped in medium and cell suspension was centrifuged at 21.000 x g for 5 min. Medium was discarded and the cell pellet was washed in PBS once before RNA isolation.

In brief, 1 ml Trizole was added per sample and samples were homogenized using a tissue lyser (Qiagen, Hilden, Germany) at 50 Hz for 3 min (stainless steel beads were used in case of tissue samples). Subsequently 200 µl chloroform (Labsolute, Th. Geyer, Renningen, Germany) was added and the mixture was returned into the tissue lyser for 20 s. Samples were centrifuged at 12.000 x g for 15 min at 4°C and the translucent, RNA-containing phase was carefully transferred to a fresh Eppendorf tube and mixed with 1 ml ice cold 70% EtOH. Tissue samples were incubated for at least 30 min at -20°C. Cell culture samples were incubated overnight. The precipitated RNA was centrifuged at 10.000 x g for 15 min at 4°C and the RNA pellet was washed three times in ice cold 70% EtOH. RNA pellets were air dried and resuspended in 6 – 30 µl ddH<sub>2</sub>O. RNA concentrations were measured with a spectrophotometer (Nanodrop 1000, Thermo Fisher Scientific, Schwerte, Germany).

Complementary DNA (cDNA) was synthesized using the NEB LunaScript RT SuperMix Kit (New England BioLabs, Ipswich, MA, USA) according to the manufacturer's instructions.

*Ace splice variant analysis*

In order to identify if *Tribolium* performed alternative splicing on *ace-2*, exon spanning primers, skipping one exon, were designed (see table 1). Primers were set into the middle of each exon and reverse transcription PCR (RT-PCR) from brain cDNA was run. RNA and cDNA were prepared as described above. RT-PCR Program can be seen in table 3. RT-PCRs were performed using GoTaq Green Master Mix (Promega, Madison, USA) according to the manufacturer's instructions. Expected amplicon sizes in case of alternative splicing can be seen in table 1.

**Table 3:** RT-PCR program for *Tc ace-2* splice variant analysis.

Step	Temperature [°C]	Time [s]	Cycle
<b>Initial denaturation</b>	98	180	
<b>Denaturation</b>	98	30	x30
<b>Annealing</b>	61	30	
<b>Elongation</b>	72	30	
<b>Final elongation</b>	72	300	

*qPCR analysis for Tc-ace-1 and Tc-ace-2 expression in vitro and in vivo*

In order to evaluate if either *Tc-ace-1* or *Tc-ace-2* are differentially expressed in neurons of *T. castaneum* pupae during physiological stress qPCR analyses were performed.

*T. castaneum* pupae were exposed to hypoxia for either 24 or 36 h. Control animals remained in normoxic conditions. 15 brains were extracted and collected in RNALater. RNA isolation and cDNA synthesis were performed as described above. For cell culture experiments cells of different treatment conditions (normoxia, hypoxia, rhEpo) were collected and prepared as described above.

qPCR analysis was run using primers for amplification of *T. castaneum ace-1* and *ace-2* and *L. migratoria ace-1* (EU231603). *Rps18* and *rps3* (TC014405 and TC008261) were run as controls for beetle neurons, while *18s rRna* and *gapdh* (AF370793 and JF915526) were used for qPCR analysis of locust neurons. Prior to experimental qPCR runs, all primers for housekeeping genes were tested for efficiency and stability in hypoxic conditions. Primer sequences are listed in table 1.

qPCRs were run using the MyiQ™ Single-ColorReal-Time PCR Detection System (Bio-Rad, Munich, Germany) in a sealed 96-well plate. Final PCR reactions contained 5 µl Luna Universal qRT-PCR Master Mix (New England Bio- Labs, Ipswich, MA, USA), 0,1 µM forward and reverse primers and 10 ng cDNA resulting in a final reaction volume of 10 µl. All samples were run as triplicates and (-) RT and water controls were always included. The PCR amplification protocol is displayed in table 4.

**Table 4:** qPCR program employed for gene expression studies.

	Step	Temperature [°C]	Time [s]	
	<b>Initial denaturation</b>	95	180	
<b>PCR reaction</b>	<b>Denaturation</b>	95	10	x40
	<b>Annealing</b>	61	30	
	<b>Elongation</b>	72	30	
<b>Melting curve</b>	<b>Denaturation</b>	95	60	0.5 °C per cycle up to 95 °C
	<b>Annealing</b>	55	60	
	<b>Melting curve</b>	55	10	

Data was analyzed using the Pfaffl method (Pfaffl, 2001) and geometric means of both housekeeping genes were calculated and normalized towards the control group for both species.

#### *Statistical analysis and data plotting*

All statistical calculations were performed with RStudio (Version 1.2.1335). Pairwise permutation tests contained in the R packages “coin” and “rcompanion” were employed and combined with Benjamini-Hochberg corrections for multiple comparisons (Zeileis *et al.*, 2008; Mangiafico, 2019). Normalized relative survival data are plotted as box plots, depicting the median cell survival, upper and lower quartile and whiskers representing 1,5x interquartile ranges. Dots represent data points from individual experiments. qPCR results are shown as bar plots of geometric mean calculations of single experimental data. Standard deviations were calculated with Excel (Microsoft).

## Results

### Involvement of *ace* in *T. castaneum* apoptosis

Before studying the role of AChE in the neuronal apoptosis of *T. castaneum* we explored the possibility of multiple splice variants from the two *ace* genes. While *ace-1* includes only two exons making alternative transcripts rather unlikely, *ace-2* consists of seven exons carrying the potential for multiple different splice variants (Fig. 1A). We designed primers spanning central regions of various pairs of *ace-2* exons (indicated in Fig. 1A) in order to detect potential splice variants in the present transcripts. Transcripts were analysed in brains of untreated pupae and brains of pupae after 24 h exposure to hypoxia (<0,3% O<sub>2</sub>). RT-PCR analysis revealed no alternative splicing products of *ace-2*, neither in normoxic control nor in hypoxia-treated pupae (Fig 1B). All detected PCR products included the exon that was interspersed between the two exons targeted by the primers. Hence, all PCR products were clearly larger than expected if the sandwiched exon was spliced out (size of potential PCR product from alternate transcript indicated by yellow boxes in Fig. 1B). The results are in line with the existence of only one transcript that includes all seven exons in normal and hypoxia-challenged *T. castaneum* brains.

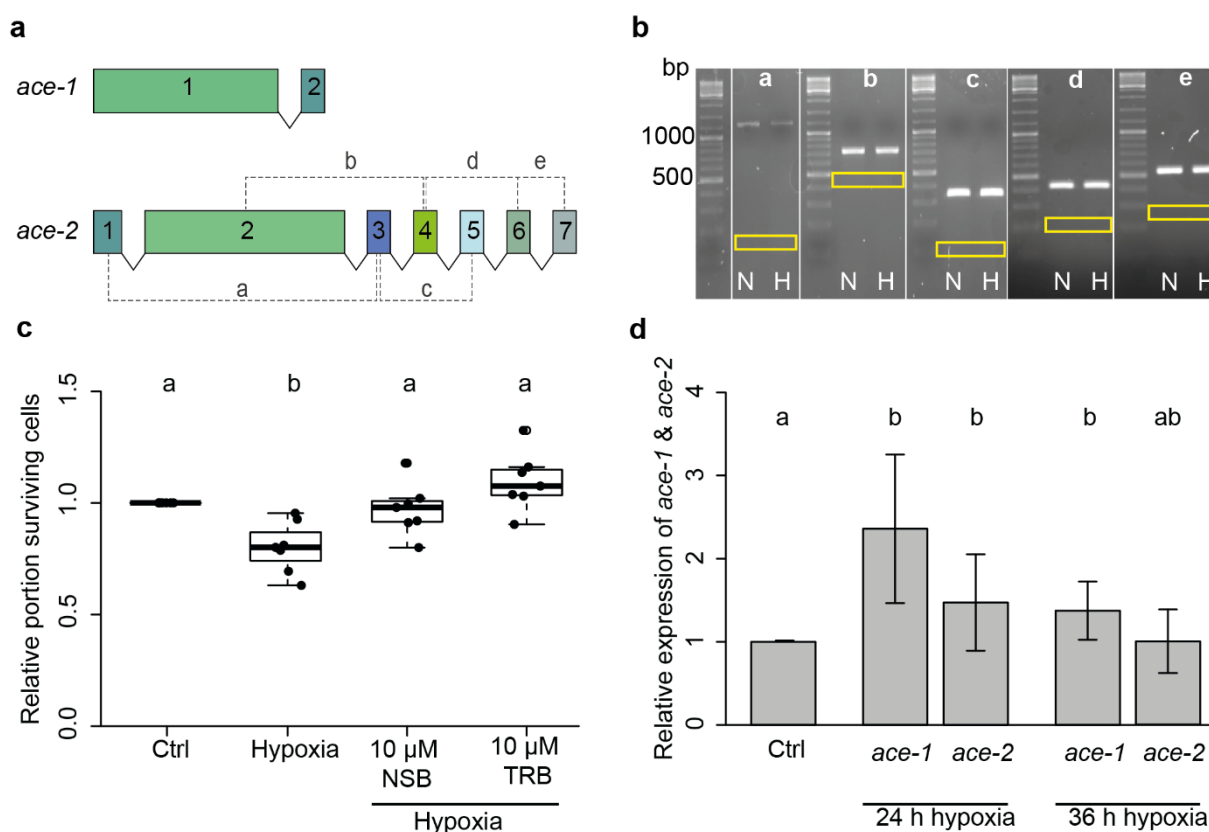


**Fig 1** AChE/*ace* in *Tribolium castaneum* neurons. **A:** Schematic representation of *T. castaneum* *Tc-ace-1* and *Tc-ace-2* genes. Exons are represented as boxes with sizes corresponding to exon length. Introns are represented as lines that do not depict intron length. For splice variant identification exon spanning primers were designed depicted by dashed lines. **B:** RT-PCR analysis for splice variant identification in brains of untreated pupae (N=normoxia) and pupae after 24 h hypoxia-exposure (<0,3% O<sub>2</sub>) (H=hypoxia). Yellow boxes show the expected band size if the sandwiched exon was spliced out. Letters above panels correspond to primer pairs depicted in **A**. **C:** Survival of *T. castaneum* primary neurons exposed to hypoxia (<0,3% O<sub>2</sub>; 36 h) and AChE inhibitors NSB or TRB (10 μM). Hypoxia significantly reduces cell survival. Inhibition of AChE with either NSB or TRB completely prevent hypoxia-induced apoptosis. n=7, 73.118 cells analyzed. Statistics with pairwise permutation test and Benjamini-Hochberg correction. Significant differences (p<0,05) are depicted by differing letters. **D:** qPCR analysis of *Tc-ace-1* and *Tc-ace-2* transcript expression in *T. castaneum* brains after hypoxia-exposure. 24 h hypoxia significantly increases transcript levels of both *Tc-ace-1* and *Tc-ace-2*. After 36 h hypoxia only *Tc-ace-1* transcript levels remain significantly elevated compared to normoxic control animals. n=3, *rps3* and *rps18* were used as housekeeping genes. Statistics with pairwise permutation test and Benjamini-Hochberg correction for multiple comparison. Significant differences (p<0,05) are depicted by differing letters

We previously demonstrated that pharmacological inhibition of AChE rescues primary cultured locust neurons from hypoxia-induced apoptosis (Knorr *et al.*, 2020). Following a similar protocol, primary neuron cultures from *T. castaneum* were exposed to hypoxic conditions (<0,3% O<sub>2</sub>) for 36 h. Hypoxia-exposure reduced the median relative survival of cultured neurons (0,8) in comparison to normoxic control cultures (normalized to 1,0; Fig. 1C). Hypoxia-induced cell death was completely prevented in the presence of 10 μM of the two AChE inhibitors neostigmine bromide (NSB; median relative survival 0,98) and territrein B (TRB; median relative survival 1,1). Neuron survival in hypoxia was significantly increased by both AChE inhibitors compared to untreated hypoxic cultures reaching the same level as the normoxic control cultures.

Expression of *Tc-ace-1* and *Tc-ace-2* under apoptogenic conditions was studied by qPCR in brains of *T. castaneum* following hypoxia-exposure (<0,3% oxygen) of pupae for 24 and 36 hours. 24 h hypoxia significantly increases transcript levels of both *Tc-ace-1* (2,36 fold ± 0,8 Stdv) and *ace-2* (1,47 fold ± 0,6 Stdv) compared to brains of control animals in normoxic atmosphere (Fig. 1D). Prolonging the hypoxic period to 36 h reduced high expression levels detected after 24 h. While *Tc-ace-1* expression remained significantly elevated (1,37 fold ± 0,3 Stdv), *Tc-ace-2* transcript levels were no longer different from controls kept under normoxic conditions (1,02 fold ± 0,4 Stdv). The results presented in figures 1C and 1D indicate a pro-apoptotic involvement of both *T. castaneum ace* genes in hypoxia-induced neuronal apoptosis.

In order to assess the individual contributions of *Tc-ace-1* and *Tc-ace-2* to hypoxia-induced apoptosis in *T. castaneum* we inhibited the production of the respective AChE proteins by RNA interference in primary cultured brain neurons before subjecting them to hypoxia (<0,3% O<sub>2</sub>; 36 h). Neuron survival was compared between normoxic control cultures, hypoxia-exposed cultures and hypoxia-exposed

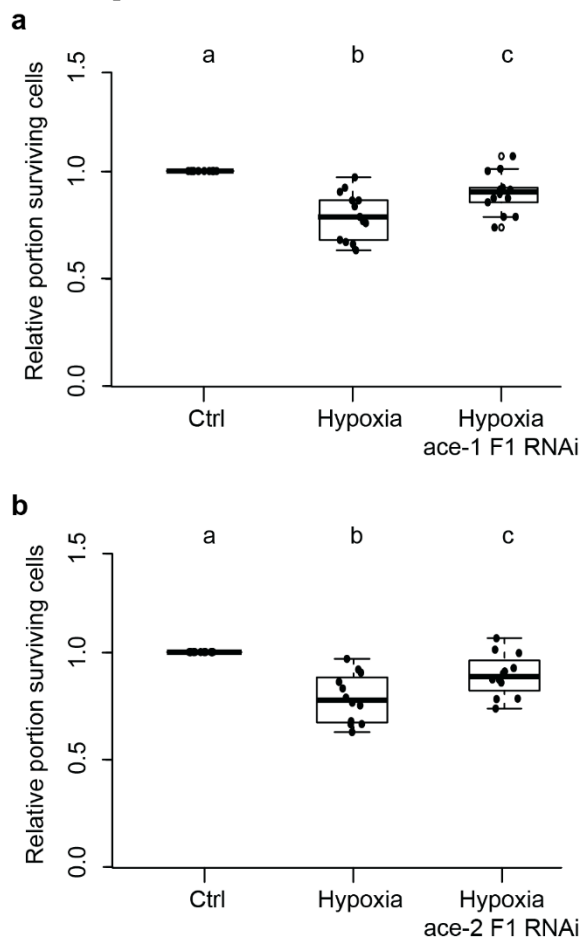


**Fig 2** Survival of hypoxia-exposed *T. castaneum* primary neurons after RNAi-mediated knock down of *ace-1* and *ace-2* expression. Primary cell cultures were maintained for 5 days *in vitro* with addition of dsRNA before being exposed to hypoxia (<0,3% O<sub>2</sub>) for 36 h. **A**, **B**: Hypoxia significantly decreased neuron survival in comparison to untreated control cultures. **A**: Knockdown of *ace-1* using fragment 1 significantly increased relative survival of hypoxia-exposed primary neurons. Cell survival is yet significantly lower in comparison to normoxic controls. n= 8, 156.006 cells analyzed. **B**: Knockdown of *ace-2* with fragment 1 partially rescues neurons from hypoxia-induced apoptosis. However, relative cell survival is still significantly lower in comparison to normoxic control cultures. n= 12, 145.894 cells analyzed. Statistics with pairwise permutation test and Benjamini-Hochberg correction for multiple comparisons. Significant differences (p<0,05) are indicated by different letters

cultures after dsRNA-mediated knockdown of either *Tc-ace-1* or *Tc-ace-2* expression. For each *ace* gene two dsRNA fragments that target non-overlapping regions of the respective transcript, were designed and knockdown was induced by soaking RNAi as described previously (Hahn *et al.*, 2017; Knorr *et al.*, 2020). Figure 2 depicts data from experiments with the respective fragment 1 to knock down *Tc-ace-1* and *Tc-ace-2* expression (Data from experiments with fragment 2 are provided in the supplement (Fig. 5 supporting information)).

Hypoxia significantly reduced relative neuron survival compared with normoxic control cultures in both experimental series (Fig. 2A: median relative survival 0,80; Fig. 2B: median relative survival 0,78). Knock down of *Tc-ace-1* with fragment 1 significantly increased relative neuron survival in hypoxia-exposed cultures (median relative survival 0.97), however without reaching survival levels in normoxic control cultures (Fig. 2A). Knock down of *Tc-ace-1* expression with fragment 2 elevated median relative neuron survival in hypoxia-exposed cultures from 0,77 to 0,82 (not significant, Fig. 5 A supporting information). RNAi-mediated suppression of *Tc-ace-2* expression with fragment 1 significantly increased neuron survival in hypoxia-exposed cultures (median relative survival 0.89) (Fig 2B). Similar results were obtained after knock down of *Tc-ace-2* expression with fragment 2 which increased median neuron survival in hypoxia from 0,84 to 0,94 (Fig. 5 B; supporting information). However, interference with *Tc-ace-2* expression with either fragment was not sufficient to increase cell survival in hypoxia to the levels of normoxic cultures. In summary, dsRNA-mediated interference with *Tc-ace-1* and *Tc-ace-2* expression for five days prior to hypoxia-exposure partially rescues *T. castaneum* primary neurons from hypoxia-induced apoptosis.

#### *rhEpo prevents hypoxia-induced apoptosis and elevated ace expression*

Previous studies reported anti-apoptotic effects of rhEpo on locust and beetle neurons (Miljus *et al.*, 2014; Hahn *et al.*, 2017) whereas AChE was associated with pro-apoptotic activity ((Knorr *et al.*, 2020); this study). In order to evaluate a potential convergence of these pro- and anti-apoptotic pathways we combined rhEpo and AChE-inhibitor treatment of hypoxia-exposed neurons and studied potential regulatory effects of rhEpo on *ace* expression in both *L. migratoria* and *T. castaneum* primary neuron cultures.

Hypoxia-induced apoptosis of locust neurons was completely prevented by 33,3 ng/ml rhEpo, 10  $\mu$ M NSB and combined treatment with rhEpo and NSB (Fig. 3A). Relative neuron survival was statistically similar in rhEpo-, NSB- and rhEpo/NSB-treated cultures indicating no additive effects of the beneficial compounds following combined application. The same hypoxic treatment (<0,3% O<sub>2</sub>; 36 h) that caused apoptotic death of primary cultured locust neurons elevated the expression of *ace-1* transcript (1,47 fold  $\pm$  0,3 Stdv) compared to normoxic control cultures (Fig. 3B). *Lm-ace-1* expression was normalized to *18s rRNA* and *gapdh* which were not affected by hypoxia-exposure. Elevated *ace-1* expression was prevented by neuroprotective concentration of rhEpo, indicating a link of Epo-mediated neuroprotection with the suppression of pro-apoptotic AChE expression during apoptogenic stress (Fig. 3B). Since sequence information about *L. migratoria ace-2* is not available, expression of *Lm-ace-2* could not be analysed.

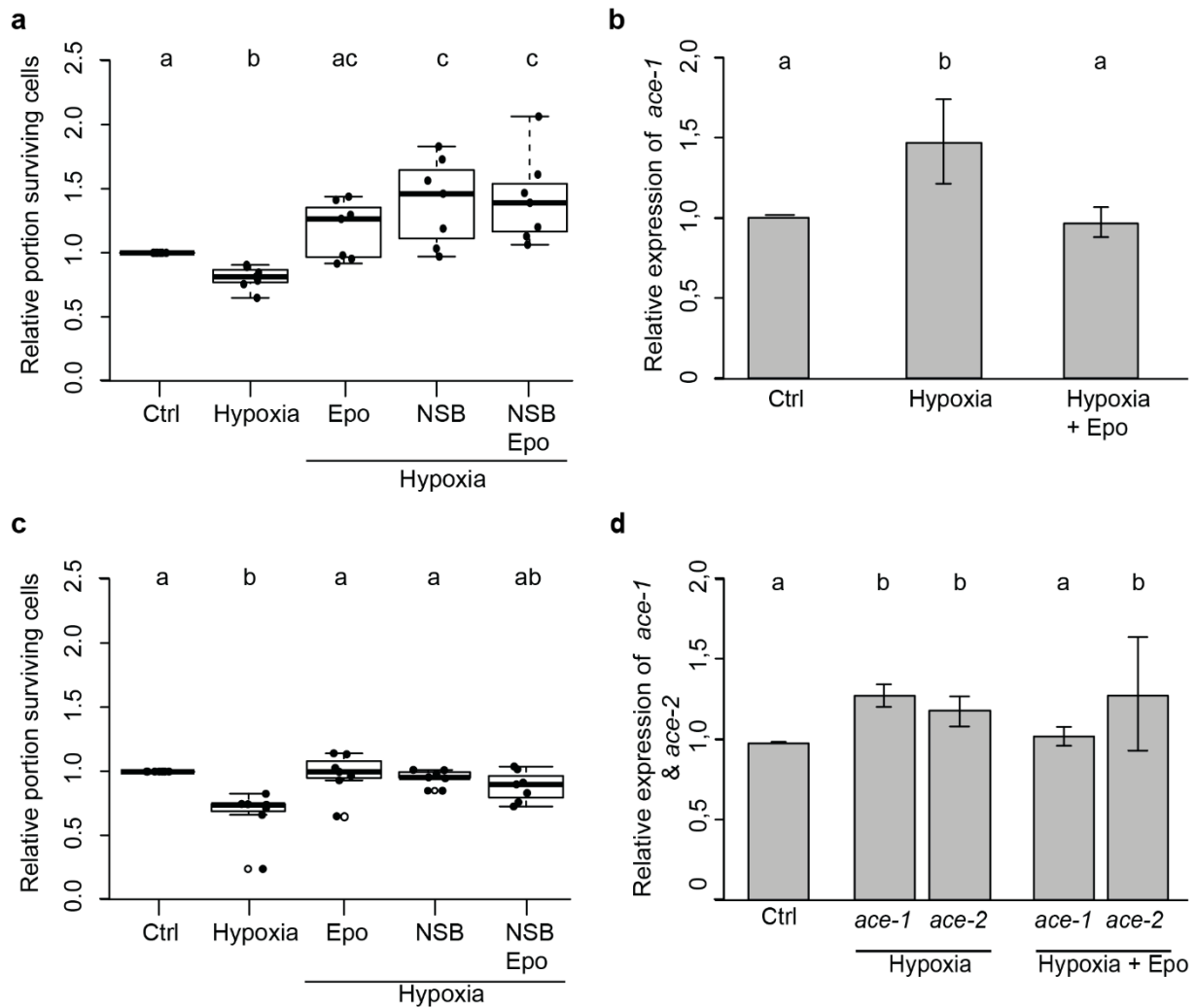


**Fig 3** rhEpo-mediated regulation of neuron survival and *ace* expression in hypoxia-exposed primary cultures. **A,B:** Experiments with *L. migratoria* primary neuron cultures. Cultures were exposed to hypoxic conditions (<0,3% O<sub>2</sub> for 36 h) and treated with 10 μM NSB (entire in vitro period) or/and 33,3 ng/ml rhEpo (starting 12 h before start of hypoxic period). **A:** Relative survival of primary neurons normalized to untreated normoxic controls. Hypoxia significantly decreased neuron survival. rhEpo, NSB and rhEpo/NSB prevent hypoxia-induced cell death and increase survival at least to the level of normoxic controls. n=7, 56.845 cells analyzed. **B:** qPCR analysis of *Lm-ace-1* expression in primary neuron cultures. Hypoxia increases *ace-1* expression (1,47 ± 0,3 Stdv). Hypoxia-induced increase of *Lm-ace-1* transcript levels is prevented by rhEpo (0,96 ± 0,1 Stdv). n=4. **C,D:** Experiments with *T. castaneum* primary neuron cultures. Cultures were exposed to hypoxic conditions (<0,3% O<sub>2</sub> for 36 h) and treated with 10 μM NSB (entire in vitro period) or/and 0,8 ng/ml rhEpo (starting 12 h before start of hypoxic period). **C:** Relative survival of primary neurons normalized to untreated normoxic controls. Hypoxia significantly decreased neuron survival. rhEpo and NSB prevent hypoxia-induced cell death and increase survival to the level of normoxic controls. Combined treatment with rhEpo/NSB increases neuron survival in hypoxia-exposed cultures without reaching significance level. n=7, 112.114 cells analyzed. **D:** qPCR analysis of *Tc-ace-1* and *Tc-ace-2* expression in *T. castaneum* primary neuron cultures. Hypoxia increases expression of both *Tc-ace-1* (1,2 ± 0,2 Stdv) and *Tc-ace-2* (1,33 ± 0,3 Stdv). rhEpo inhibited the hypoxia-induced overexpression of *Tc-ace-1* (1,05 ± 0,2 Stdv) but not of *Tc-ace-2* (1,2 ± 0,1 Stdv). n=3. Statistics with pairwise permutation test and Benjamini-Hochberg correction. Significances are indicated by letters, with different letters depicting significant differences (p<0,05)

In primary neuron cultures of *T. castaneum* hypoxia-induced apoptosis was prevented by 0,8 ng/ml rhEpo and by 10 μM NSB (Fig. 3C). Combined treatment with the same concentrations of rhEpo and NSB also increased relative neuron survival in hypoxia-exposed cultures (from 0,81 to 0,96 median relative survival) to the level of normoxic control cultures, but this increase did not reach significance level. Hypoxia (<0,3% O<sub>2</sub>; 36 h) increased the expression of *Tc-ace-1* (1,2 fold ± 0,2 Stdv) and *ace-2* (1,33 fold ± 0,3 Stdv) transcripts in *T. castaneum* neurons (Fig. 3D). *Tc-ace* gene expression was normalized to *rps3* and *rps18* whose abundance remained stable during the hypoxic period. Treatment

of hypoxia-exposed cultures with neuroprotective concentration of rhEpo prevented the increase of *Tc-ace-1* expression (1,05 fold  $\pm$  0,2 Stdv compared with normoxic control cultures) but not the increase of *Tc-ace-2* expression (1,2  $\pm$  0,1 Stdv) (Fig. 3D). Thus, while hypoxia induces apoptosis and elevated expression of *Tc-ace-1* and *Tc-ace-2* in *T. castaneum* neurons, Epo-mediated neuroprotection correlates with suppressed *ace-1* expression, suggesting that elevated *Tc-ace-2* transcript levels alone are not sufficient to drive apoptosis.

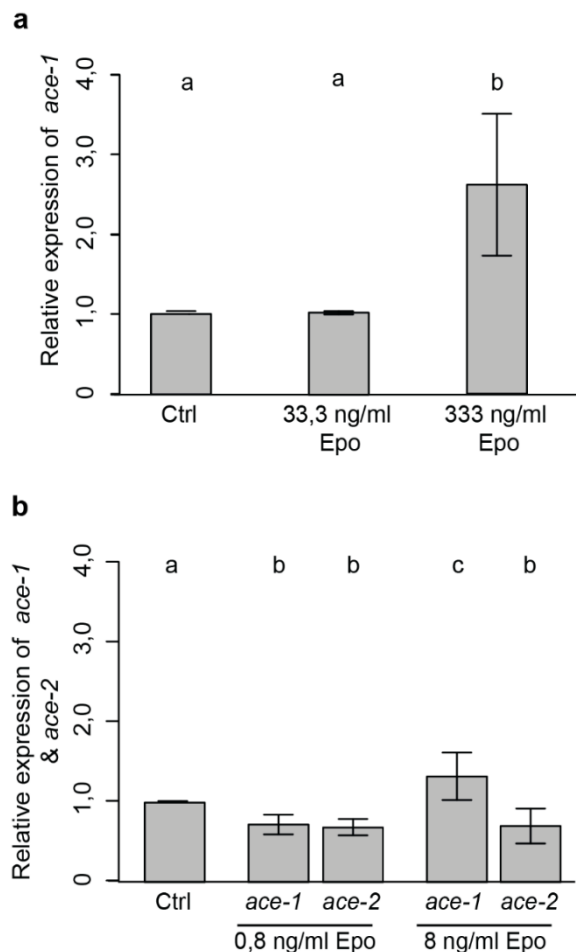


**Fig 4** rhEpo-mediated regulation of *ace* expression in *L. migratoria* and *T. castaneum* neurons. Primary neuron cultures were depleted of serum on day 3 *in vitro* and exposed to protective and toxic concentrations of rhEpo for 48 h starting on day 5 *in vitro*. **A:** *L. migratoria*: 33,3 ng/ml Epo (= protective concentration) has no impact on *Lm-ace-1* transcript levels. 333 ng/ml rhEpo (= toxic concentration) significantly increases *ace-1* expression to 2,3 fold ( $\pm$  0,8 Stdv) compared with untreated controls.  $n=4$ . **B:** *T. castaneum*: 0,8 ng/ml rhEpo (= protective concentration) decrease *Tc-ace-1* and *Tc-ace-2* transcript levels to 0,71 fold ( $\pm$  0,1 Stdv) and 0,69 fold ( $\pm$  0,1 Stdv) respectively. 8 ng/ml rhEpo (= toxic concentration) increased *Tc-ace-1* transcript levels (1,33 fold  $\pm$  0,3 Stdv) but reduced *Tc-ace-2* transcript levels (0,71 fold  $\pm$  0,2 Stdv) in comparison to untreated controls.  $n=3$ . Statistics with pairwise permutation test and Benjamini-Hochberg correction. Significant differences ( $p < 0,05$ ) are indicated by differing letters

Previous studies reported optimum-type dose-response curves for Epo-mediated protection of mammalian and insect neurons (Siren *et al.*, 2001; Weishaupt *et al.*, 2004; Ostrowski, Ehrenreich and Heinrich, 2011; Miller *et al.*, 2015; Hahn *et al.*, 2017). So far, no mechanistic explanation for toxic effects of high Epo concentrations mediated via homodimeric EpoR or alternative Epo receptors has been provided. In this context, we compared *ace* expression in *L. migratoria* and *T. castaneum* primary neuron cultures following exposure to previously established neuroprotective and toxic concentrations of rhEpo. Serum was removed from culture media after three days *in vitro* as a mild apoptogenic stimulus before neurons were stimulated with rhEpo for 48 h starting on day five *in vitro*. Stimulation



of locust neurons with neuroprotective concentrations of rhEpo (33,3 ng/ml) had no impact on *Lm-ace-1* expression while toxic concentrations of rhEpo (333 ng/ml) significantly increased *ace-1* transcript levels (2,3 fold  $\pm$  0,8 Stdv) compared to untreated controls (Fig. 4A). *Lm-ace-1* expression was normalized to *18s rRNA* and *gapdh* that were not affected by rhEpo. In *T. castaneum* neurons neuroprotective concentrations of rhEpo (0,8 ng/ml) reduced the expression of both *Tc-ace-1* (0,72 fold  $\pm$  0,1 Stdv) and *Tc-ace-2* (0,69 fold  $\pm$  0,1 Stdv) compared with untreated control cultures (Fig. 4B). Toxic concentrations of rhEpo (8 ng/ml) affected the expression of the two *ace* genes differentially, leading to increased *Tc-ace-1* (1,33 fold  $\pm$ 0,3 Stdv) and decreased *Tc-ace-2* (0,71 fold  $\pm$ 0,2 Stdv) transcript levels compared with untreated controls (Fig. 4B). *Tc-ace* gene expression was normalized to *rps3* and *rps18* whose abundance was not altered by rhEpo stimulation. Thus, toxic concentrations of rhEpo elevate the expression of pro-apoptotic *ace-1* in both locust and beetle neurons.

## **Discussion**

AChE is an important regulator and executor of apoptosis in mammalian cells and altered presence of AChE is associated with various degenerative diseases and cancer (Perry *et al.*, 2002; Hu, Gray and Brimijoin, 2003; Gilboa-geffen *et al.*, 2007; Toiber *et al.*, 2008; Abdel-Aal *et al.*, 2021). A pro-apoptotic function of AChE, that parallels its role in mammals, was recently reported in the migratory locust *L. migratoria* (Knorr *et al.*, 2020). Due to incomplete genomic information in this species only one (*ace-1*) of typically two genes coding for AChE in insects has so far been identified. Hence, we extended our studies to the beetle *T. castaneum* in which expression and function of both *Tc-ace-1* and *Tc-ace-2* could be differentially studied. Previous studies suggested that Tc-AChE-1 is predominantly responsible for ACh hydrolysis at cholinergic synapses while *Tc-ace-2* is involved in developmental processes (Lu, Park, *et al.*, 2012).

In regard to AChE isoforms by alternative splicing and alternative promotor selection in vertebrates (Meshorer *et al.*, 2004; Rotundo, 2017) and reports about multiple and partly stress-induced AChE-2 splice variants in *Drosophila melanogaster* (Kim and Lee, 2013; Kim *et al.*, 2014) we explored the possibility of alternatively spliced *T. castaneum ace-1* and *ace-2*. *Tc-ace-1* includes two exons. Since exon 2 contains no start codon, only one gene product is expected from this locus. *Tc-ace-2* contains seven exons providing the possibility for multiple alternatively spliced transcripts. qPCR-based analysis of pupal brains with various pairs of exon-spanning primers detected single transcripts of respective sizes that were expected in the absence of splicing. Detected transcripts were identical in brains of untreated pupae and pupae that were exposed to hypoxia for 24 h. These results suggest a single transcript from the *Tc-ace-2* locus under both normal and physiologically challenging conditions. Since cyclorrhaphan flies possess only one gene for AChE (a paralogue to *ace-2* of other insects) the previously reported alternative splicing of *ace-2* in *D. melanogaster* may be required to generate different types of AChE that perform both synaptic and extrasynaptic functions (Kim and Lee, 2013).

Survival of unchallenged and hypoxia-exposed primary neurons from *L. migratoria* increased with pharmacological inhibition of AChE (Knorr *et al.*, 2020). This indicated a pro-apoptotic role for AChE in this species that parallels AChE functions in vertebrates. Hypoxia-challenged neurons of *T. castaneum* were also rescued from apoptotic cell death by AChE inhibition (this study), suggesting the general presence of AChE-mediated pro-apoptotic functions in insect neurons and probably other cell types. In contrast to unselective pharmacological inhibition of both AChE-1 and AChE-2 by two different inhibitors (NSB and TRB), which completely prevented hypoxia-induced cell death, RNAi-mediated knockdown of either *Tc-ace-1* or *Tc-ace-2* expression rescued hypoxia-exposed neurons only partially (Fig. 2; Fig. 5 supporting information). Incapability of full rescue may be related to incomplete clearance of AChE proteins, partial functional compensation by the other AChE type or direct contribution of AChE types to some but not all apoptotic mechanisms. Double knockdown of both *Tc-ace-1* and *Tc-ace-2* expression had no apparent effect on the survival of primary brain neurons in normal cultures and (unexpectedly) did not rescue neurons from hypoxia-induced apoptosis (see Fig. 6 supporting information). Both AChE types contain conserved sequence motifs for functional esterase catalytic domains but Tc-AChE-2 may be catalytically less efficient than Tc-AChE-1 because of a narrowed entry region to the esterase region (Lu, Pang, *et al.*, 2012). Nevertheless, reduced levels of either Tc-AChE-1 or Tc-AChE-2 significantly interfered with hypoxia-induced cell death, indicating their involvement in cellular mechanisms that promote apoptosis.

Previous studies detected enhanced expression of *Lm-ace-1* transcript in brains of hypoxia-exposed locusts (Knorr *et al.*, 2020) and *in vitro* experiments with primary brain neurons (this study) confirmed upregulation of *Lm-ace-1* transcripts under apoptogenic conditions. In contrast to *L. migratoria*, sequences of both *ace* genes are available for *T. castaneum*, allowing studies of the differential

expression of *Tc-ace-1* and *Tc-ace-2* in this species. Transcript levels of both *ace* genes were elevated in the brains of hypoxia-exposed *T. castaneum* pupae, with more pronounced and more persistently enhanced expression of *Tc-ace-1* compared to *Tc-ace-2* (Fig.1D). Similarly, enhanced expression of both *Tc-ace-1* and *Tc-ace-2* was also detected in primary brain neurons exposed to 36 h of hypoxia, representing a strong apoptogenic stimulus (Fig. 3C, D). Upregulation of *ACHE* expression under apoptogenic conditions has frequently been reported in mammalian cells and tissues. Here, AChE-S, predominantly involved in synaptic ACh hydrolysis, was typically involved (Toiber *et al.*, 2008; Xie *et al.*, 2011; Du *et al.*, 2015). *Tc-ace-1* is the predominant AChE associated with synaptic functions in *T. castaneum* while *Tc-ace-2* participates in rather diffusely characterized developmental processes (Lu, Pang, *et al.*, 2012; Lu, Park, *et al.*, 2012). Our results suggest that synaptic *Tc-ace-1* seems to play a more important role for the induction and execution of apoptosis than *Tc-ace-2*, since its expression is induced by hypoxia and toxic concentrations of rhEpo (discussed below). Locust and beetle brains and primary brain neurons express basal levels of AChE that may largely differ between cholinergic neurons and neurons that signal via the release of other transmitters. While the presence of these basal AChE levels does not invariantly induce apoptosis, increased *ACHE* expression stimulated by hypoxia or some other apoptogenic stimuli increases the vulnerability of the cells towards physiological insults. Similar to mammalian cells (Jin *et al.*, 2004), above-normal levels of AChE seem to determine the sensitivity of an insect neuron to initiate apoptosis under unfavourable conditions.

Having demonstrated an important regulatory function of AChE in apoptosis of locust and beetle neurons ((Knorr *et al.*, 2020); this study) we explored the possibility that CRLF3-mediated neuroprotection relies on interference with pro-apoptotic functions of AChE. CRLF3 is a phylogenetically (from Cnidaria to humans) conserved cytokine receptor, whose endogenous ligand could not be identified in any species. Based on sequence comparison, CRLF3 is a class I cytokine receptor that shares similarities (e.g. initiates transduction via Janus kinase and STAT signalling) with vertebrate receptors for prolactin, growth hormone, thrombopoietin, and Epo (Boulay, O'Shea and Paul, 2003; Liongue and Ward, 2007). Epo/CRLF3 interaction initiates antiapoptotic mechanisms in locust and beetle neurons (Hahn *et al.*, 2017; Hahn, Büschgens, Schwedhelm-Domeyer, Bank, Bart R. H. Geurten, *et al.*, 2019) that share a number of similar characteristics with Epo-mediated protection of mammalian neurons and other non-hematopoietic cell types (reviews: (Genc, Koroglu and Genc, 2004; Leist *et al.*, 2004). Remarkably, insect CRLF3 is activated by both rhEpo and Epo-like ligands that elicit protection of mammalian neurons without activation of EpoR. One of these ligands is the human Epo splice variant EV-3, that neither activates homodimeric EpoR nor the heteromeric EpoR/ $\beta$ -common receptor, which have been implicated in mammalian cell protection (Bonnas *et al.*, 2017; Miljus *et al.*, 2017). Since insects do not express Epo, EV-3, EpoR,  $\beta$  common receptor or any other identified mammalian Epo receptor, we can apply rhEpo to selectively activate CRLF3 on insect neurons in our experiments. The endogenous insect CRLF3 ligand is an unidentified cytokine that, like Epo in vertebrates, serves as hormonal signal in circulation and as a local paracrine signal in the nervous system and other tissues (Knorr *et al.*, 2021). Cytokines regulate responses to exogenous and endogenous insults, repair and restoration of tissue homeostasis in both invertebrates and vertebrates (Beschin *et al.*, 2001; Liongue and Ward, 2007).

A recent study demonstrated that cell-free locust hemolymph mediates CRLF3-dependent protection of both locust and beetle neurons, indicating the presence of a conserved ligand for CRLF3 in the circulating fluid (Knorr *et al.*, 2021). Protective concentrations of rhEpo prevented both hypoxia-induced apoptosis and hypoxia-induced upregulation of pro-apoptotic *ace-1* expression in *L. migratoria* and *T. castaneum* primary neurons (Fig. 3). The neuroprotective effects of rhEpo and pharmacological inhibition of AChE with NSB were similar and combined treatment with both substances had no detectable synergistic additive effect on neuron survival in hypoxia. Together with the previous observation that the inhibitor of translation anisomycin prevented Epo-mediated neuroprotection of

primary locust neurons (Heinrich, Günther and Miljus, 2017a), these results indicate that activation of CRLF3 by Epo or another unknown cytokine prevents the elevated expression of AChE-1 under apoptogenic conditions and hence suppresses the induction and/or execution of apoptotic cell death. Our experiments with neuroprotective and toxic concentrations of rhEpo (for detailed discussion see below) confirm that apoptogenic stimuli induce elevated *ace-1* expression and initiation of protective pathways keep *ace-1* expression on basal or even lower levels. A direct regulation of AChE expression by Epo signalling has been demonstrated in mammalian erythrocyte progenitor cells that express classical EpoR (Xu *et al.*, 2018). Epo-stimulated transduction pathways included activation of the transcription factor GATA-1 which induced *ACHE* transcription and production of erythrocytic AChE-E. In erythrocyte progenitor cells, expression of AChE-E was essential for survival and maturation (Xu *et al.*, 2018). Epo has previously been described to activate GATA-binding transcription factors that regulate transcription of target genes in various cell types (Ogilvie *et al.*, 2000; Zhao *et al.*, 2006; Obara *et al.*, 2008; Rogers *et al.*, 2008; Jun *et al.*, 2013). GATA transcription factors are evolutionary conserved and have been associated with innate immune responses (Uvell and Engström, 2007). Whether they provide the link between CRLF3 activation and apoptosis-suppressing restriction of *ace* transcription in insect neurons has to be demonstrated in future studies.

Cell-protective concentrations of Epo and EV-3 depend on cell type, species, physiological condition of the cell and the type of insult in both mammals and insects (Sinor and Greenberg, 2000; Ruscher *et al.*, 2002; Weber *et al.*, 2005; Hahn *et al.*, 2017; Heinrich, Günther and Miljus, 2017a). Maximal Epo-mediated protection of primary brain neurons is achieved with 33,3 ng/ml (compares to ~4U/ml) in *L. migratoria* and 0,8 ng/ml (compares to ~0,1 U/ml) in *T. castaneum* (Heinrich, Günther and Miljus, 2017a). Instead of reaching a state of saturation, higher than optimum concentrations of Epo elicit toxic effects (in particular: Epo concentrations that protect locust neurons will kill beetle neurons). Optimum-type concentration dependence of protection including toxic effects of high concentrations has been reported in mammalian and insect neurons (Siren *et al.*, 2001; Chong, Kang and Maiese, 2003; Weishaupt *et al.*, 2004; Ostrowski, Ehrenreich and Heinrich, 2011; Miller *et al.*, 2015; Hahn *et al.*, 2017). While saturation of neuroprotective effects with increasing concentration of Epo has been associated with desensitization or downregulation of Epo receptors or prevention of ligand-induced receptor dimerization (Verdier *et al.*, 2000; Cohen *et al.*, 2004; Kim *et al.*, 2017), the switch from protective via less protective to toxic effects of further elevated concentrations of Epo could not be explained. Previous studies identified 333 ng/ml (*L. migratoria*) and 8 ng/ml (*T. castaneum*) as toxic Epo concentrations that reduced the survival of primary brain neurons to ~80% compared to untreated control cultures, while species-specific optimal neuroprotective concentrations of Epo increased survival to ~110-120 % (Heinrich, Günther and Miljus, 2017a). In the present study, toxic concentrations of Epo increased *ace-1* transcripts in both species while respective neuroprotective concentrations caused no alteration (*L. migratoria*) or even reduced (*T. castaneum*) *ace* expression (Fig. 4). In contrast to *Tc-ace-1*, expression of *Tc-ace-2* in beetle neurons is not stimulated by toxic Epo concentrations, indicating a specific regulatory effect on the expression of only one of the two *ace* genes. The data from both species studied suggest that proapoptotic *ace-1* is differentially regulated by low to optimal neuroprotective concentrations and higher toxic concentrations of Epo. How insect neurons distinguish neuroprotective from toxic concentrations of CRLF3 ligand is currently unknown. Moreover, protective concentrations seem to depend on the physiological state and other signals converging on a locust brain neuron since identical dilutions of hemolymph (which contains the endogenous CRLF3 ligand) switched from toxic to protective effects if pre-treatment with serum was omitted (Knorr *et al.*, 2021).

The data presented in this manuscript clearly identify AChE as a major driver of apoptosis in insect neurons. Apoptogenic stimuli (hypoxia, toxic concentrations of CRLF3 ligand) increase *ace* expression and induce cell death. Activation of CRLF3 (either by Epo or endogenous cytokine ligand) mediates

neuroprotection by preventing the increased expression of pro-apoptotic AChE with larger impact on *ace-1* than on *ace-2*. Studies on primary brain neurons from two insect species (*L. migratoria* and *T. castaneum*) belonging to different taxonomic groups (Orthoptera and Coleoptera) led to similar results, suggesting that the observed mechanisms may be representative for insects. Since both apoptosis and CRLF3 are conserved throughout the animal kingdom, the processes observed in insect neurons may also be present in other cell types and other non-insect species. Altogether, this manuscript allows the connection between vertebrate and insect Epo-mediated mechanisms and is, to our knowledge, the first report of a connection between AChE and Epo in apoptotic mechanisms. Given that most of the results collected in insects on Epo functions could be replicated in mammalian cells and vice versa, it is likely that a similar mechanism is involved in mammalian Epo-mediated cell protection.

## Chapter 2

### References

- Abadi, M. et al. (2016) 'TensorFlow: Large-Scale Machine Learning on Heterogeneous Distributed Systems'. Available at: <http://arxiv.org/abs/1603.04467>.
- Abdel-Aal, R. et al. (2021) 'Celecoxib effect on rivastigmine anti-Alzheimer activity against aluminum chloride-induced neurobehavioral deficits as a rat model of Alzheimer's disease; novel perspectives for an old drug', *Journal of Medical and Life Science*, 0(0), pp. 44–82. doi: 10.21608/jmals.2021.210630.
- Arcasoy, M. O. (2008) 'The non-haematopoietic biological effects of erythropoietin', *British Journal of Haematology*. John Wiley & Sons, Ltd, 141(1), pp. 14–31. doi: 10.1111/j.1365-2141.2008.07014.x.
- Beschin, A. et al. (2001) 'On the existence of cytokines in invertebrates', *Cellular and Molecular Life Sciences*, 58(5–6), pp. 801–814. doi: 10.1007/PL00000901.
- Bonnas, C. et al. (2017) 'EV-3, an endogenous human erythropoietin isoform with distinct functional relevance', *Scientific Reports*, 7(3684), pp. 1–15. doi: 10.1038/s41598-017-03167-0.
- Boulay, J. L., O'Shea, J. J. and Paul, W. E. (2003) 'Molecular phylogeny within type I cytokines and their cognate receptors', *Immunity*. Cell Press, pp. 159–163. doi: 10.1016/S1074-7613(03)00211-5.
- Brines, M. et al. (2004) 'Erythropoietin mediates tissue protection through an erythropoietin and common b -subunit heteroreceptor', *PNAS*, 101(41).
- Brines, M. and Cerami, A. (2005) 'Emerging biological roles for erythropoietin in the nervous system', *Nature Reviews Neuroscience*. Nature Publishing Group, pp. 484–494. doi: 10.1038/nrn1687.
- Campoy, F. J. et al. (2016) 'Cholinergic system and cell proliferation', *Chemico-Biological Interactions*. Elsevier Ltd, 259, pp. 257–265. doi: 10.1016/j.cbi.2016.04.014.
- Chong, Z. Z., Kang, J. Q. and Maiese, K. (2003) 'Erythropoietin fosters both intrinsic and extrinsic neuronal protection through modulation of microglia, Akt1, Bad, and caspase-mediated pathways', *British Journal of Pharmacology*, 138(6), pp. 1107–1118. doi: 10.1038/sj.bjp.0705161
- Cohen, J. et al. (2004) 'Protein tyrosine phosphatase 1B participates in the down-regulation of erythropoietin receptor signalling', *Biochemical Journal*, 377(2), pp. 517–524. doi: 10.1042/BJ20031420.
- Du, A. et al. (2015) 'A novel role for synaptic acetylcholinesterase as an apoptotic deoxyribonuclease', *Cell Discovery*. Nature Publishing Groups, 1. doi: 10.1038/celldisc.2015.2.
- GDrake, F. V. R. (2009) *Python 3 Reference Manual*, Scotts Valley, CA: CreateSpace. Available at: <http://citebay.com/how-to-cite/python/> (Accessed: 1 March 2022).
- Genc, S., Koroglu, T. F. and Genc, K. (2004) 'Erythropoietin and the nervous system', *Brain Research*, 1000(1–2), pp. 19–31. doi: 10.1016/j.brainres.2003.12.037.
- Ghezzi, P. and Conklin, D. (2013) 'Tissue-protective cytokines: Structure and evolution', *Methods in Molecular Biology*. Humana Press Inc., 982, pp. 43–58. doi: 10.1007/978-1-62703-308-4\_3.
- Gilboa-geffen, A. et al. (2007) 'The thymic theme of acetylcholinesterase splice variants in myasthenia gravis', *Blood*, 109(10), pp. 4383–4392. doi: 10.1182/blood-2006-07-033373.The.
- Grisaru, D. et al. (1999) 'Structural roles of acetylcholinesterase variants in biology and pathology', *European Journal of Biochemistry*, pp. 672–686. doi: 10.1046/j.1432-1327.1999.00693.x.
- Hahn, N. et al. (2017) 'The Insect Ortholog of the Human Orphan Cytokine Receptor CRLF3 Is a Neuroprotective Erythropoietin Receptor', *Front. Mol. Neurosci.*, 10(July), pp. 1–11. doi: 10.3389/fnmol.2017.00223.
- Hahn, N. et al. (2019) 'The Orphan Cytokine Receptor CRLF3 Emerged With the Origin of the Nervous System and Is a Neuroprotective Erythropoietin Receptor in Locusts', *Frontiers in Molecular Neuroscience*, 12. doi: 10.3389/fnmol.2019.00251.
- Hall, L. M. and Spierer, P. (1986) 'The Ace locus of *Drosophila melanogaster*: structural gene for acetylcholinesterase with an unusual 5' leader.', *The EMBO Journal*, 5(11), pp. 2949–2954. doi: 10.1002/j.1460-2075.1986.tb04591.x.
- Harris, C. R. et al. (2020) 'Array programming with NumPy', *Nature*. Springer US, 585(7825), pp. 357–362. doi: 10.1038/s41586-020-2649-2.
- He, G., Sun, Y. and Li, F. (2012) 'Rna interference of two acetylcholinesterase genes in *Plutella xylostella* reveals their different functions', *Archives of Insect Biochemistry and Physiology*, 79(2), pp. 75–86. doi: 10.1002/arch.21007.

- Heinrich, R., Günther, V. and Miljus, N. (2017) 'Erythropoietin-Mediated Neuroprotection in Insects Suggests a Prevertebrate Evolution of Erythropoietin-Like Signaling', in *Vitamins and Hormones*. Academic Press Inc., pp. 181–196. doi: 10.1016/bs.vh.2017.02.004.
- Hicks, D. et al. (2011) 'Membrane targeting, shedding and protein interactions of brain acetylcholinesterase', *Journal of Neurochemistry*, 116(5), pp. 742–746. doi: 10.1111/j.1471-4159.2010.07032.x.
- [https://github.com/tensorflow/models/blob/master/research/object\\_detection/samples/configs/faster\\_rcnn\\_inception\\_v2\\_pets.config](https://github.com/tensorflow/models/blob/master/research/object_detection/samples/configs/faster_rcnn_inception_v2_pets.config) (no date).
- Hu, W., Gray, N. W. and Brimijoin, S. (2003) 'Amyloid-beta increases acetylcholinesterase expression in neuroblastoma cells by reducing enzyme degradation', pp. 470–478. doi: 10.1046/j.1471-4159.2003.01855.x.
- Ioffe, S. and Szegedy, C. (2015) 'Batch Normalization: Accelerating Deep Network Training by Reducing Internal Covariate Shift', *PMLR*, pp. 448–456. doi: 10.1080/17512786.2015.1058180.
- Jin, Q. H. et al. (2004) 'Overexpression of acetylcholinesterase inhibited cell proliferation and promoted apoptosis in NRK cells', *Acta Pharmacologica Sinica*, 25(8), pp. 1013–1021.
- Jun, J. H. et al. (2013) 'Erythropoietin prevents hypoxia-induced GATA-4 ubiquitination via phosphorylation of serine 105 of GATA-4', *Biological and Pharmaceutical Bulletin*, 36(7), pp. 1126–1133. doi: 10.1248/bpb.b13-00100.
- Karczmar, A. G. (2010) 'Cholinesterases (ChEs) and the cholinergic system in ontogenesis and phylogenesis, and non-classical roles of cholinesterases-A review', *Chemico-Biological Interactions*. Elsevier Ireland Ltd, 187(1–3), pp. 34–43. doi: 10.1016/j.cbi.2010.03.009.
- Kim, A. et al. (2017) 'Functional Selectivity in Cytokine Signaling Revealed Through a Pathogenic EPO Mutation', *Cell*, 168(6), pp. 1053–1064. doi: 10.1016/j.cell.2017.02.026.Functional.
- Kim, Y. H. et al. (2014) 'Induction of soluble AChE expression via alternative splicing by chemical stress in *Drosophila melanogaster*.' , *Insect biochemistry and molecular biology*, 48, pp. 75–82. doi: 10.1016/j.ibmb.2014.03.001.
- Kim, Y. H. and Lee, S. H. (2013) 'Which acetylcholinesterase functions as the main catalytic enzyme in the Class Insecta?', *Insect biochemistry and molecular biology*, 43(1), pp. 47–53. doi: 10.1016/j.ibmb.2012.11.004.
- Knorr, D. Y. et al. (2020) 'Acetylcholinesterase promotes apoptosis in insect neurons', *Apoptosis*. Springer US, 25(0123456789), pp. 730–746. doi: 10.1007/s10495-020-01630-4.
- Knorr, D. Y. et al. (2021) 'Locust Hemolymph Conveys Erythropoietin-Like Cytoprotection via Activation of the Cytokine Receptor CRLF3', *Frontiers in Physiology*. Frontiers Media S.A., 12. doi: 10.3389/fphys.2021.648245.
- Leist, M. et al. (2004) 'Derivatives of Erythropoietin That Are Tissue Protective But Not Erythropoietic', 305(July), pp. 239–243.
- Liongue, C. and Ward, A. C. (2007) 'Evolution of Class I cytokine receptors', *BMC Evolutionary Biology*, 7. doi: 10.1186/1471-2148-7-120.
- Lu, Y., Park, Y., et al. (2012) 'Cholinergic and non-cholinergic functions of two acetylcholinesterase genes revealed by gene-silencing in *Tribolium castaneum*', *Scientific Reports*, 2, pp. 1–7. doi: 10.1038/srep00288.
- Lu, Y., Pang, Y.-P., et al. (2012) 'Genome organization, phylogenies, expression patterns, and three-dimensional protein models of two acetylcholinesterase genes from the red flour beetle.', *PloS one*. Public Library of Science, 7(2), p. e32288. doi: 10.1371/journal.pone.0032288.
- Ma, R. et al. (2014) 'JAK2/STAT5/Bcl-xL signalling is essential for erythropoietin-mediated protection against apoptosis induced in PC12 cells by the amyloid  $\beta$ -peptide A $\beta$ 25-35', *British Journal of Pharmacology*. John Wiley and Sons Inc., 171(13), pp. 3234–3245. doi: 10.1111/bph.12672.
- Mangiafico, S. S. (2019) 'Package "rcompanion"', (September 2016).
- McKinney, W. (2011) 'pandas: a Foundational Python Library for Data Analysis', *Python for high performance and scientific computing*, 14(9), pp. 1–9. doi: 10.1002/mmce.20381.
- Meshorer, E. et al. (2004) 'Combinatorial complexity of 5' alternative acetylcholinesterase transcripts and protein products', *Journal of Biological Chemistry*, 279(28), pp. 29740–29751. doi: 10.1074/jbc.M402752200.
- Miljus, N. et al. (2014) 'Erythropoietin-mediated protection of insect brain neurons involves JAK and STAT but not PI3K transduction pathways', *Neuroscience*. IBRO, 258, pp. 218–227. doi: 10.1016/j.neuroscience.2013.11.020.



## Chapter 2

- Miljus, N. et al. (2017) 'Neuroprotection and endocytosis: erythropoietin receptors in insect nervous systems', *Journal of neurochemistry*, 141, pp. 63–74. doi: 10.1111/jnc.13967.
- Miller, J. L. et al. (2015) 'Discovery and characterization of nonpeptidyl agonists of the tissue-protective erythropoietin receptors', *Molecular Pharmacology*. American Society for Pharmacology and Experimental Therapy, 88(2), pp. 357–367. doi: 10.1124/mol.115.098400.
- Noguchi, C. T. (2008) 'Where the Epo cells are', *Blood*, 111(10), pp. 4836–4837. doi: 10.1182/blood-2008-02-135988.
- Obara, N. et al. (2008) 'Repression via the GATA box is essential for tissue-specific erythropoietin gene expression', *Blood*, 111(10), pp. 5223–5232. doi: 10.1182/blood-2007-10-115857.
- Ogilvie, M. et al. (2000) 'Erythropoietin stimulates proliferation and interferes with differentiation of myoblasts', *Journal of Biological Chemistry*. *J Biol Chem*, 275(50), pp. 39754–39761. doi: 10.1074/jbc.M004999200.
- Ostrowski, D., Ehrenreich, H. and Heinrich, R. (2011) 'Erythropoietin promotes survival and regeneration of insect neurons in vivo and in vitro', *Neuroscience*, pp. 95–108. doi: 10.1016/j.neuroscience.2011.05.018.
- Ostrowski, D. and Heinrich, R. (2018) 'Alternative Erythropoietin Receptors in the Nervous System'. doi: 10.3390/jcm7020024.
- Park, S. E. et al. (2008) 'Interactions of acetylcholinesterase with caveolin-1 and subsequently with cytochrome c are required for apoptosome formation', 29(4), pp. 729–737. doi: 10.1093/carcin/bgn036.
- Park, S. E., Kim, N. D. and Yoo, Y. H. (2004) 'Advances in Brief Acetylcholinesterase Plays a Pivotal Role in Apoptosome Formation', *Cancer Res*, 64, pp. 2652–2655.
- Perry, C. et al. (2002) 'Complex regulation of acetylcholinesterase gene expression in human brain tumors', *Oncogene*, 21(55), pp. 8428–8441. doi: 10.1038/sj.onc.1205945.
- Pfaffl, M. W. (2001) 'A new mathematical model for relative quantification in real-time RT-PCR', *Nucleic Acids Research*, 29(9), pp. 2003–2007. doi: 10.1111/j.1365-2966.2012.21196.x.
- Ren, S. et al. (2015) 'Faster R-CNN: Towards Real-Time Object Detection with Region Proposal Networks', *Advances in neural information processing systems*, (28). doi: 10.4324/9780080519340-12.
- Revuelta, L. et al. (2009) 'RNAi of ace1 and ace2 in *Blattella germanica* reveals their differential contribution to acetylcholinesterase activity and sensitivity to insecticides', *Insect Biochemistry and Molecular Biology*, 39(12), pp. 913–919. doi: 10.1016/j.ibmb.2009.11.001.
- Rogers, H. M. et al. (2008) 'Hypoxia alters progression of the erythroid program', *Exp Hematol.*, 36(1). doi: 10.1016/j.exphem.2007.08.014.
- Rotundo, R. L. (2017) 'Biogenesis, assembly and trafficking of acetylcholinesterase', *Journal of Neurochemistry*, 142(Suppl 2), pp. 52–58. doi: 10.1111/jnc.13982.
- Ruscher, K. et al. (2002) 'Erythropoietin is a paracrine mediator of ischemic tolerance in the brain: Evidence from an in vitro model', *Journal of Neuroscience*, 22(23), pp. 10291–10301. doi: 10.1523/jneurosci.22-23-10291.2002.
- Samson, F. P. et al. (2020) 'Dual Switch Mechanism of Erythropoietin as an Antiapoptotic and Pro-Angiogenic Determinant in the Retina', *ACS Omega*. American Chemical Society, 5(33), pp. 21113–21126. doi: 10.1021/acsomega.0c02763.
- Sepodes, B. et al. (2006) 'Recombinant human erythropoietin protects the liver from hepatic ischemia-reperfusion injury in the rat', *Transplant International*. John Wiley & Sons, Ltd, 19(11), pp. 919–926. doi: 10.1111/J.1432-2277.2006.00366.X.
- Sinor, A. D. and Greenberg, D. A. (2000) 'Erythropoietin protects cultured cortical neurons, but not astroglia, from hypoxia and AMPA toxicity', *Neuroscience Letters*, 290(3), pp. 213–215. doi: 10.1016/S0304-3940(00)01361-6.
- Siren, A.-L. et al. (2001) 'Erythropoietin prevents neuronal apoptosis after cerebral ischemia and metabolic stress', *Proceedings of the National Academy of Sciences*, 98(7), pp. 4044–4049. doi: 10.1073/pnas.051606598.
- Sirén, A. L. and Ehrenreich, H. (2001) 'Erythropoietin - A novel concept for neuroprotection', *European Archives of Psychiatry and Clinical Neuroscience*, 251(4), pp. 179–184. doi: 10.1007/s004060170038.
- Small, D. H., Michaelson, S. and Sberna, G. (1996) 'non-classical actions of cholinesterases: Role in cellular differentiation, tumorigenesis and Alzheimer's Disease', *Neurochem. Int.*, 28(5), pp. 453–483.

- Thompson, A. M. et al. (2020) 'Erythropoietin modulates striatal antioxidant signalling to reduce neurodegeneration in a toxicant model of Parkinson's disease', *Molecular and Cellular Neuroscience*. Academic Press Inc., 109, p. 103554. doi: 10.1016/j.mcn.2020.103554.
- Toiber, D. et al. (2008) 'N-acetylcholinesterase-induced apoptosis in alzheimer's disease', *PLoS ONE*, 3(9). doi: 10.1371/journal.pone.0003108.
- Uvell, H. and Engström, Y. (2007) 'A multilayered defense against infection: combinatorial control of insect immune genes', *Trends in Genetics*, 23(7), pp. 342–349. doi: 10.1016/j.tig.2007.05.003.
- Verdier, F. et al. (2000) 'Proteasomes regulate the duration of erythropoietin receptor activation by controlling down-regulation of cell surface receptors', *Journal of Biological Chemistry*, 275(24), pp. 18375–18381. doi: 10.1074/jbc.275.24.18375.
- Visual Geometry Group - University of Oxford (no date). Available at: <https://www.robots.ox.ac.uk/~vgg/data/pets/> (Accessed: 1 March 2022).
- Vittori, D. C. et al. (2021) 'Erythropoietin and derivatives: Potential beneficial effects on the brain', *Journal of Neurochemistry*. John Wiley and Sons Inc, pp. 1032–1057. doi: 10.1111/jnc.15475.
- Walczak-Nowicka, L. J. and Herbet, M. (2021) 'Acetylcholinesterase inhibitors in the treatment of neurodegenerative diseases and the role of acetylcholinesterase in their pathogenesis', *International Journal of Molecular Sciences*, 22(17). doi: 10.3390/ijms22179290.
- Weber, A. et al. (2005) 'Neuronal damage after moderate hypoxia and erythropoietin', *Neurobiology of Disease*, 20(2), pp. 594–600. doi: 10.1016/j.nbd.2005.04.016.
- Weishaupt, J. H. et al. (2004) 'Effect of erythropoietin axotomy-induced apoptosis in rat retinal ganglion cells', *Investigative Ophthalmology and Visual Science*. The Association for Research in Vision and Ophthalmology, 45(5), pp. 1514–1522. doi: 10.1167/iovs.03-1039.
- Xie, J. et al. (2011) 'Induction of a 55 kDa acetylcholinesterase protein during apoptosis and its negative regulation by the Akt pathway', *Journal of Molecular Cell Biology*, 3(4), pp. 250–259. doi: 10.1093/jmcb/mjq047.
- Xu, M. L. et al. (2018) 'Erythropoietin regulates the expression of dimeric form of acetylcholinesterase during differentiation of erythroblast', *JOURNAL OF NEUROCHEMISTRY*, 146(November), pp. 390–402. doi: 10.1111/jnc.14448.
- Ye, W. et al. (2010) 'AChE deficiency or inhibition decreases apoptosis and p53 expression and protects renal function after ischemia/reperfusion', *Apoptosis*, 15(4), pp. 474–487. doi: 10.1007/s10495-009-0438-3.
- Yilmaz, S. et al. (2004) 'The protective effect of erythropoietin on ischaemia/reperfusion injury of liver', *HPB*. Elsevier, 6(3), pp. 169–173. doi: 10.1080/13651820410026077.
- Zeileis, A. et al. (2008) 'Implementing a class of permutation tests: The coin package', *Journal of Statistical Software*, 28(8). Available at: <http://epub.wu.ac.at/4004/%5Cnpapers3://publication/uuid/BF1BBE55-2A35-44D0-96DA-FCCC209A5334>.
- Zhang, Jianqin et al. (2013) 'RNA interference revealed the roles of two carboxylesterase genes in insecticide detoxification in *Locusta migratoria*', *Chemosphere*, 93(6), pp. 1207–1215. doi: 10.1016/j.chemosphere.2013.06.081.
- Zhang, X.-J. and Greenberg, D. S. (2012) 'Acetylcholinesterase Involvement in Apoptosis', *Frontiers in Molecular Neuroscience*. doi: 10.3389/fnmol.2012.00040.
- Zhang, X. J. et al. (2002) 'Induction of acetylcholinesterase expression during apoptosis in various cell types', *Cell Death and Differentiation*, 9(8), pp. 790–800. doi: 10.1038/sj.cdd.4401034.
- Zhao, W. et al. (2006) 'Erythropoietin stimulates phosphorylation and activation of GATA-1 via the PI3-kinase/AKT signaling pathway', *Blood*, 107(3), pp. 907–915. doi: 10.1182/blood-2005-06-2516.
- Zhou, X. and Xia, Y. (2009) 'Cloning of an acetylcholinesterase gene in *Locusta migratoria manilensis* related to organophosphate insecticide resistance', *Pesticide Biochemistry and Physiology*, pp. 77–84. doi: 10.1016/j.pestbp.2008.11.007.



CCGCCACCTCCGACGTCATCGTCGCCTCCATGCAATATCGCGTGGGGGCGTTTCGGCTTCCTCTACTTGAGCA  
 AGTACTTCCCTCGCGGCAGTGAGGAGGCGCCCGGTAACATGGGCATGTGGGACCAAGCCCTGGCCATCCGC  
 TGGATCAAGGAGAACGCGGGCGGCCTTTGGGGGCGACCCAGACCTCATCACGCTGTTTGGGGAGTCGGCTG  
 GAGGCGGCTCCGTCAGCATCCTGCTCCTGAGTCCGGTTACTAAAGGCCTGGCCAGGAGGGGGATTCTGCAG  
 TCGGGGACTATGAACGCCCCTTGGAGTTACATGTCTGGGGGAGAGGGCGCCGCAAATCGGGAAGGTCCTGG  
 TGGAGGACTGCGGGTGCAACGCTCTCCTTGTGGAGACGAGGCCGCATGAGGTCATTGATTGCATGAGGGCG  
 GTGGAGGCCAAGACGATTTGCTGCAACAGTGAATTCGTATTCGGGGATTTTGGGCTTCCCCTCAACGCC  
 TACGGTTGATGGCGTCTTCATGCCAAGCATCCCATGGATATGCTGGCGGAAGGGGATTACGAGGATATGG  
 AGATCCTGGTCGGGAGTAACCAAGATGAAGGCACTTACTTCTTACTTTACGATTTTATCGATTTCTTCGAAA  
 AGGATGGCCCTAGCTTCTCCAACGAGACAAATACCACGACATTATCGATACGATATTCAAAAATATGAGT  
 CGGTTGGAACGTGATGCCATAGTATTTCACTATACTGATTGGGAGCACGTCAACGACGGCTACTTGAACCA  
 GAAAATGGTGGGCGACGTCGTCGGAGATTATTTTTTTCATTTGTCCAACCAACGATTTTCGCCGAGCTGGCAG  
 CAGAGCGCGAATGAAAGTCTACTATTATTTTTTACACACACAGGACAAGCACGTCGTTGTGGGGCGAATGG  
 ATGGGGGTGATGCACGGGGATGAGATAGAATACGTGTTTGGCCATCCTTTGAACATGTCGTTGCAGTTTAA  
 CTC AAGGGAACGGGAACCTCAGTCTGAAGATAATGCAAGCCTTTGCCAGATTTGCAGCAACGGGGAAACCA  
 GTGACAGACGACGTGAATTGGCCATTGTACATAAAAAGACCAACCGCAGTATTTTCATCTCAACGCCGACAA  
 AAACGGCATCGGCAAAGGTCCTCGAGCGACAGCGTGC GCGTTTTGGAACGATTTCTGCCAAGCTTCGGG  
 ATAACCCAGGTAAATTCAATCGTTGCAGTCTGCATCATTA

## Fragment 1:

GTCTTACC GGGATTCCCTTCGCCAAGCCGCCCATCGAACAGCTGAGGTT CAGGAAGCCC GTGCCATCGATCC  
 CTGGCACGGCACCTTAGATGCCACCAAGCTGCCAACTCGTGCTACCAGGAGCGCTACGAGTACTTCCCCGGC  
 TTTGAGGGCGAGGAGATGTGGAACCCCAACACGAACATCTCCGAGGACTGCCTCTACCTCAACATCTGGGTGC  
 CCCAGCGCTTGCGCATCCGGCACACGGCGAGAAG

## Fragment 2:

CCTCCATGCAATATCGCGTGGGGGCGTTTCGGCTTCCTCTACTTGAGCAAGTACTTCCCTCGCGGCAGTGAGGAG  
 GCGCCCGGTAACATGGGCATGTGGGACCAAGCCCTGGCCATCCGCTGGATCAAGGAGAACGCGGCGGCCTTTG  
 GGGGCGACCCAGACCTCATCACGCTGTTTGGGGAGTCGGCTGGAGGCGGCTCCGTCAGCATCCTGCTCCTGAG  
 TCCGGTTACTAAAGGCCTGGCCAGGAGGGGGATTTC

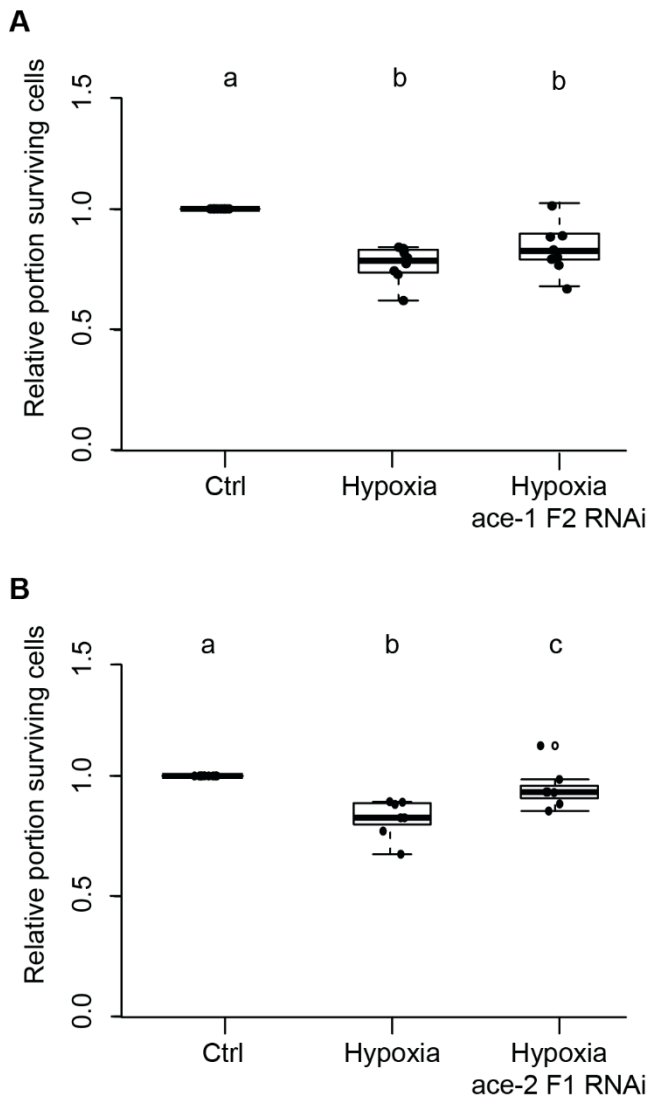


**Fig 5** RNAi mediated knock down of *Tc-ace-1* and *Tc ace-2* in *T.castaneum* primary cell cultures. **A:** Knock down using *Tc ace-1* Fragment 2 (F2) did not rescue cells from hypoxia-induced apoptosis. n=8, 93.919 cells analyzed. **B:** Knock down of *Tc ace-2* using Fragment 2 (F2) significantly increased cell survival of hypoxia-challenged neurons in comparison to sole hypoxia exposure. Cell survival is however yet significantly reduced in comparison to control cultures. n=7, 83.710 cells analyzed. Pairwise permutation test with Benjamini-Hochberg correction for multiple comparison. Significances ( $p < 0,05$ ) are shown by differing letters

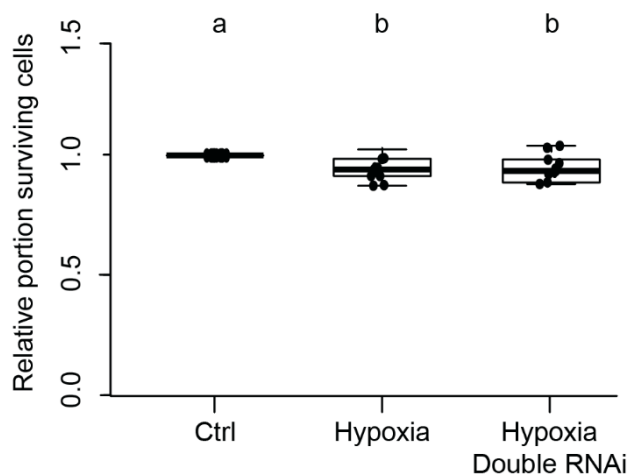


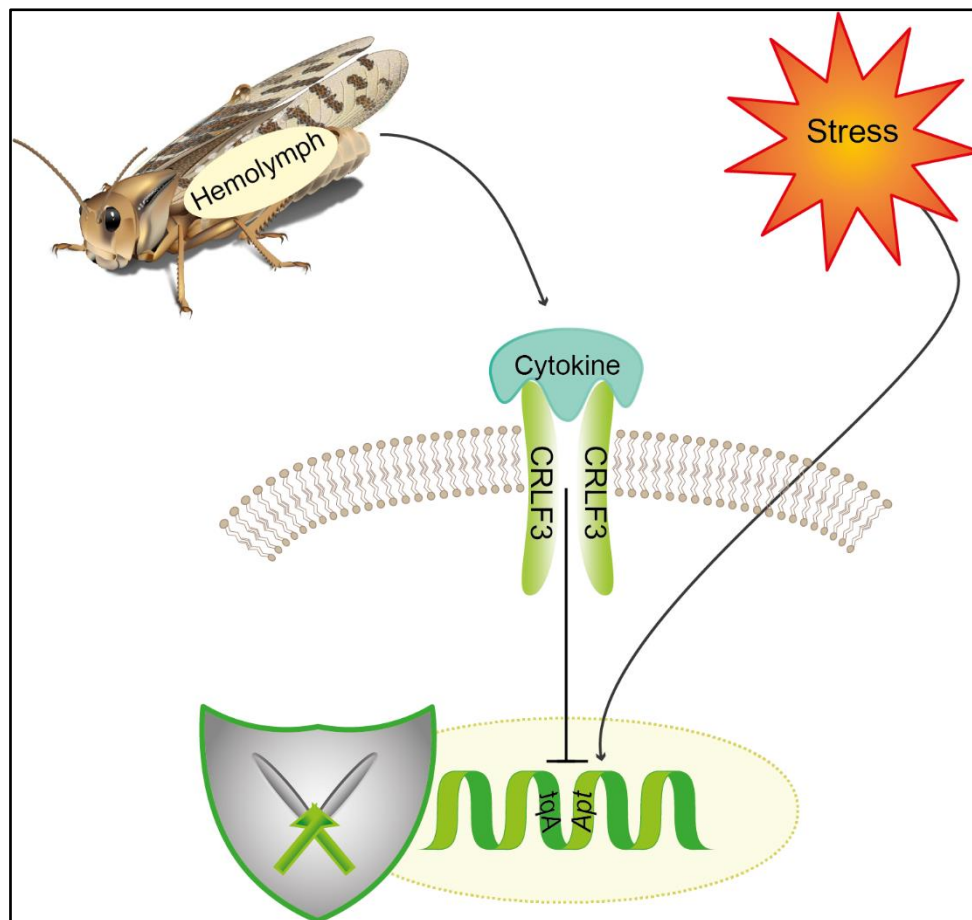
**Fig 6** Double knockdown of both *Tc ace-1* and *Tc ace-2* was not able to rescue *T. castaneum* primary neurons from hypoxia induced apoptosis. n=10; 248.868 cells analyzed. Pairwise permutation test with Benjamini-Hochberg correction for multiple comparison. Significant differences ( $p < 0,05$ ) are shown by differing letters

## Chapter 3

Locust Hemolymph Conveys Erythropoietin-Like Cytoprotection via Activation of the Cytokine Receptor CRLF3

Debbra Y. Knorr , Denise Hartung , Kristin Schneider , Luzia Hintz , Hanna S. Pies and Ralf Heinrich

- Published in *Frontiers of Invertebrate Physiology*-



All authors contributed to experimental data. D.Y. Knorr, D. Hartung, K. Schneider and L. Hintz analysed the data. D.Y. Knorr and R. Heinrich designed and supervised the study. D.Y. Knorr and R. Heinrich wrote and edited the manuscript. All authors read and approved of the manuscript.

**Author contribution statement**

<b>Figure 1</b>	<b>DYK</b> performed and analysed the experiments
<b>Figure 2</b>	DH (supervised by <b>DYK</b> ) performed and analysed cell survival assays
<b>Figure 3</b>	DH and KS (supervised by <b>DYK</b> ) performed and analysed the experiments
<b>Figure 4</b>	LH (supervised by <b>DYK</b> ) and <b>DYK</b> generated and analysed the data
<b>Figure 5</b>	<b>DYK</b> performed and analysed cell survival assays
<b>Hemocyte cell culture establishment</b>	HSP (supervised by <b>DYK</b> )
<b>Experimental design</b>	RH and <b>DYK</b>
<b>Manuscript writhing</b>	RH and <b>DYK</b> , with contribution of all authors



# Locust Hemolymph Conveys Erythropoietin-Like Cytoprotection via Activation of the Cytokine Receptor CRLF3

Debra Y. Knorr, Denise Hartung, Kristin Schneider, Luzia Hintz, Hanna S. Pies and Ralf Heinrich\*

Department of Cellular Neurobiology, Johann-Friedrich-Blumenbach Institute for Zoology and Anthropology, Georg-August-University Göttingen, Göttingen, Germany

## OPEN ACCESS

### Edited by:

Robert Huber,  
Bowling Green State University,  
United States

### Reviewed by:

Peter Bräunig,  
RWTH Aachen University, Germany  
Marcela Barbosa Figueiredo,  
Swansea University, United Kingdom

### \*Correspondence:

Ralf Heinrich  
rheinri1@gwdg.de

### Specialty section:

This article was submitted to  
Invertebrate Physiology,  
a section of the journal  
Frontiers in Physiology

**Received:** 31 December 2020

**Accepted:** 15 March 2021

**Published:** 09 April 2021

### Citation:

Knorr DY, Hartung D, Schneider K,  
Hintz L, Pies HS and  
Heinrich R (2021) Locust Hemolymph  
Conveys Erythropoietin-Like  
Cytoprotection via Activation of the  
Cytokine Receptor CRLF3.  
Front. Physiol. 12:648245.  
doi: 10.3389/fphys.2021.648245

The cytokine receptor-like factor 3 (CRLF3) is an evolutionary conserved class 1 cytokine receptor present in all major eumetazoan groups. Endogenous CRLF3 ligands have not been identified and the physiological responses mediated by mammalian CRLF3 are poorly characterized. Insect CRLF3 is activated by erythropoietin (Epo) and several related molecules that protect mammalian neurons from stress-induced apoptosis. However, insects neither express Epo nor “classical” Epo receptor. Cell-protective effects of insect hemolymph have been described for several species. In this study, we explored the possibility that the endogenous CRLF3 ligand is contained in locust hemolymph. PCR analyses confirmed expression of *crf3*-transcripts in neurons and hemocytes of *Locusta migratoria* and *Tribolium castaneum*. Survival of locust hemocytes in primary cultures was significantly increased by supplementation of culture medium with locust hemolymph serum. Locust primary neuron cultures were also protected by locust hemolymph, though preceding exposure to fetal bovine serum changed the hemolymph dose-dependency of neuroprotection. Direct comparison of 10% hemolymph serum with recombinant human Epo in its optimal neuroprotective concentration revealed equivalent anti-apoptotic effects on hypoxia-exposed locust neurons. The same concentration of locust hemolymph serum also protected hypoxia-exposed *T. castaneum* neurons. This indicates that the neuroprotective factor in locust hemolymph is sufficiently conserved in insects to allow activation of neuroprotective receptors in different species. Locust hemolymph-induced neuroprotection in both *L. migratoria* and *T. castaneum* was abolished after RNAi-mediated suppression of *crf3*-expression. In summary, we report the presence of a conserved endogenous cytokine in locust hemolymph that activates CRLF3 and connected anti-apoptotic processes in hemocytes and neurons. Identification and characterization of the CRLF3 ligand will promote knowledge about cytokine evolution and may unravel cell-protective agents with potential clinical application.

**Keywords:** cytokine receptor-like factor 3, hemolymph, cytokine, cytoprotection, neuroprotection, hemocytes, neurons, insect



## INTRODUCTION

Insect hemolymph contains multiple cell types, suspended in a protein-rich liquid plasma, that circulates through the body cavity of the organism (reviewed by Douglas and Siva-Jothy, 2013; Hillyer and Pass, 2020). Propelled through an open circulatory system by a contractile dorsal vessel and accessory pulsatile organs, hemolymph directly contacts most insect tissues. However, metabolic exchange with the central nervous system is restricted and regulated by the “hemolymph-brain-barrier,” consisting of surface glia interconnected by septate junctions (reviewed by Weiler et al., 2017). Hemolymph and hemocyte functions are largely similar to those of vertebrate blood, including transport of metabolites and hormones, maintaining homeostasis (pH, osmolarity, water balance, and ion composition), sealing of wounds, and serving immune functions among others. In contrast to the mammalian acquired immunity involving specific antibodies and memory cells, insects rely on innate immune functions to neutralize various kinds of pathogens (Lavine and Strand, 2002; Siva-Jothy et al., 2005; Strand, 2008). Immune responses in mammals and insects are balanced by cytokines that either promote or dampen defensive cellular reactions. Hemolymph proteins involved in immune functions and adaptation to environmental challenges are synthesized and released into the circulation by the fat body, midgut, endocrine glands such as *corpora allata* or the *corpora cardiaca*, neurosecretory cells, hemocytes, and other organs (Arrese and Soulages, 2010; Oda et al., 2010; Roma et al., 2010; Hoshizaki, 2013; Kodrik et al., 2015).

Several hemolymph proteins directly interfere with invading pathogens (anti-microbial peptides; reviewed by Yi et al., 2014; Wu et al., 2018) or activate hemocytes to neutralize pathogens by various mechanisms (plasmacyte spreading peptides, growth blocking peptides, and paralytic peptides; Strand, 2008; Duressa et al., 2015). Other hemolymph proteins initiate physiological adaptations of insect tissues, supporting cell survival and functionality in challenging conditions. Previous publications have reported protective and anti-apoptotic effects of insect hemolymph on various cell types. Studies with *Bombyx mori* hemolymph demonstrated beneficial effects on lepidopteran cells and various rodent and human cell lines (Rhee and Park, 2000; Rhee et al., 2002; Park et al., 2003; Kim et al., 2004; Yu et al., 2013). A group of approximately 30 proteins (named 30K protein family due to their molecular sizes around 30 kDa) was identified to promote cell survival, with individual proteins contributing some portion of the protective effects (Kim et al., 2001, 2003, 2004; Rhee et al., 2002; Park et al., 2003; Zhong et al., 2005; Yu et al., 2013; Pakkianathan et al., 2015). Protective effects of these 30K proteins seem to be mediated (at least to a large extent) by adhesion to cellular membranes rather than by activation of a particular receptor. In addition to lepidopteran species, beneficial effects of hemolymph on the survival and neurite regeneration of insect neurons have been

reported in locusts and cockroaches (Howes et al., 1991; Kirchhof and Bicker, 1992).

Cytokines are involved in responses to exogenous and endogenous insults, repair and restoration of tissue homeostasis in both invertebrates and vertebrates (Beschlin et al., 2001; Liongue and Ward, 2007). Various insect cytokines and cytokine-like factors have been identified (e.g., growth blocking peptide, spätzle, unpaired, vago, insect chemotactic peptide, stress responsive peptide, and dielid) to activate specific cytokine receptors (e.g., domeless, toll, and growth blocking peptide receptor) or interact with cell surface carbohydrate patterns (Zanetta et al., 1996; Welchman et al., 2009; Ghezzi and Conklin, 2013; Kingsolver et al., 2013; Tsuzuki et al., 2014; Lamiable et al., 2016). Though cytokines typically share little sequence similarities between animal groups (Liongue and Ward, 2007), some invertebrate cytokines can activate mammalian cytokine receptors, e.g., sponge-derived cytokines activate thrombopoietin receptor and/or erythropoietin (Epo) receptor (Watari et al., 2019). Particular cytokines often activate different receptors, receptors may be activated by multiple cytokine ligands and cytokine receptor diversity is increased by formation of homo- and heteromeric receptor complexes with different stoichiometry of subunits (Liongue et al., 2016). The flexible or loose match between cytokines and cytokine receptors within and across species appears to be a common characteristic of cytokine signaling that may result from a common evolutionary origin (Huising et al., 2006).

We have recently reported the expression of the cytokine receptor, cytokine receptor-like factor 3 (CRLF3), in hemocytes of *Locusta migratoria* (Hahn et al., 2019). CRLF3 is an orphan class I cytokine receptor that shares similarities with vertebrate receptors for prolactin, growth hormone, thrombopoietin, and Epo (Boulay et al., 2003; Liongue and Ward, 2007). While most class I cytokine receptors are exclusively present in vertebrates, CRLF3 is highly conserved throughout eumetazoan species ranging from cnidarians to humans (Hahn et al., 2019). Despite the absence of Epo or recognized Epo receptors in insects, recombinant human Epo (rhEpo) protects cultured insect neurons from apoptotic cell death (Miljus et al., 2014; Hahn et al., 2017; Heinrich et al., 2017) and promotes regeneration of neurites *in vitro* and *in vivo* (Ostrowski et al., 2011). CRLF3 was identified as the neuroprotective receptor activated by rhEpo in the orthopteran *L. migratoria* and the coleopteran *Tribolium castaneum* (Hahn et al., 2017, 2019). Similar to Epo-mediated neuroprotection in vertebrates (Brines and Cerami, 2005; Zhang et al., 2014; Ostrowski and Heinrich, 2018), anti-apoptotic effects in insect neurons are mediated by janus kinase/signal transducer and activator of transcription (JAK/STAT) transduction (Miljus et al., 2014). Activation of insect CRLF3 by human Epo and several other molecules that mimic its neuroprotective functions in mammals indicates structural similarities between the ligand-binding domains of mammalian tissue-protective Epo receptors and insect CRLF3. Nonetheless, CRLF3 is still considered as an orphan receptor since its endogenous ligand has not been identified in any organism expressing the receptor. Expression of CRLF3 in insect brains, muscle, and hemocytes (Hahn et al., 2019) parallels the

**Abbreviations:** Epo, Erythropoietin; rhEpo, Recombinant human Epo; HL, Hemolymph; dHL, Denatured hemolymph.

multi-tissue-expression of its mammalian orthologues (Yang et al., 2009) and suggests both local tissue-specific and systemic functions. The endogenous ligand must be present in both the nervous system and the hemolymph, suggesting its production on both sides of the hemolymph-brain-barrier. The ligand, like Epo in mammals, might activate CRLF3 in various tissues to mediate general cell protection.

In the present study, we investigated the cytoprotective potential of locust hemolymph by using the previously described protective effects of rhEpo as comparison. We show expression of *crfl3* in brain and hemocytes of *L. migratoria* and *T. castaneum*. *In vitro* experiments on primary cell cultures reveal dose-dependent anti-apoptotic effects of cell-free *L. migratoria* hemolymph on locust hemocytes and neurons. Locust hemolymph also protected *T. castaneum* neurons. Neuroprotection in both locust and beetle neurons was mediated by CRLF3 and was similar to previously reported rhEpo protection. These results indicate the presence of a conserved CRLF3 ligand in insect hemolymph that initiates protective mechanisms in different cell types.

## MATERIALS AND METHODS

Studies were performed with the migratory locust *L. migratoria* and the red flour beetle *Tribolium castaneum*. Locusts were purchased from a commercial breeder (HW-Terra; Herzogenaurach, Germany) and maintained at 24°C; 55% humidity with a 12/12 h day/night cycle. *T. castaneum* were maintained on full grain flour and yeast in plastic boxes at 27°C and 40% humidity.

### Hemolymph Extraction From Locusts

Adult locusts were cooled at 4°C for 10 min. Cold-anesthetized animals were fixed dorsal side down on clay without injuring the animal. Seven-hundred microliter ice cold anticoagulation solution (ACS; 98 mM NaOH, 186 mM NaCl, 17 mM Na<sub>2</sub>EDTA, 41 mM citric acid, pH 4.5) was slowly injected into the lower abdomen. After incubating for 1 min, a small incision was made at the injection site and the hemolymph (~1 ml) was extracted with a Pasteur pipette. Collected hemolymph (HL) and ACS mix was transferred to an Eppendorf tube containing 500 µl ice cold ACS. The mixture was centrifuged at 500 x g for 5 min. The cell-free serum was transferred to a fresh Eppendorf tube. HL of different animals (up to 100) was pooled and sterile filtered (0.20 µm syringe filter; Merck, Darmstadt, Germany) twice to ensure sterility and to avoid conglomerates in the sample.

In order to separate proteins of HL samples from ACS, the HL/ACS mixture was purified by molecular weight cut off (MWCO) filters (Cut off 5,000 Da; Corning, New York, United States). HL/ACS was transferred into sterile (sterilized through 24 h UV-light exposure) MWCO filters and centrifuged at 4000 x g for up to 3 h until samples were highly concentrated. To ensure full ACS elimination from samples, concentrated HL was diluted 1:5 in phosphate-buffered saline (PBS) and respun

in MWCO filters. This procedure was repeated four times. Samples of HL/ACS extract, MWCO filter flow through and purified HL containing hemolymph proteins were analyzed by 10% sodium dodecyl sulfate–polyacrylamide gel electrophoresis (SDS-PAGE) electrophoresis. Filter flow through contained no significant amounts of protein (data not shown) indicating little loss of proteins during the purification and buffer exchange procedure. Purified HL was aliquoted á 100 µl and stored at –20°C until further usage as experimental supplement to cell culture medium.

### Heat Denaturation of HL

To evaluate if cell protective effects of HL were due to a protein or a peptide, HL was subjected to heat denaturation. Eppendorf cups containing 1 ml HL were immersed in a temperature-controlled water bath at either 63 or 103°C (to compensate for isolation by the Eppendorf cup) for 10 min. Denatured HL (dHL) was centrifuged for 10 min at 1000 x g in order to spin down precipitated proteins. Supernatant was transferred to a fresh tube and cooled on ice. dHL was stored at –20°C until further usage.

### Hemocyte Culture

Adult locusts were cold-anesthetized for 10 min at 4°C. Cell culture plates (Ø 3 cm; Corning, New York, United States) were equipped with 1 cm coverslips (Hartenstein, Würzburg, Germany). Coverslips were coated with Concanavalin A (Sigma-Aldrich, Munich, Germany) for 1 h and subsequently washed three times with PBS. Each experiment contained hemocytes of only one animal that were allocated to differently treated cultures.

Hemolymph was collected from cooled locusts and hemocytes were separated from serum by centrifugation as described above. Serum was discarded and the cell pellet was resuspended in 1 ml sterile ACS. Cell suspension was centrifuged for 5 min. Supernatant was discarded and hemocytes were resuspended in 1 ml basal Grace insect medium (Gibco, Life Technologies, Darmstadt, Germany) +5% penicillin/streptomycin (P/S; 10,000 units/ml penicillin and 10 mg/ml streptomycin, Sigma-Aldrich, Munich, Germany) +5% Amphotericin B (AmphoB; Gibco, 250 µg/ml, ThermoFisher Scientific, Osterode am Harz, Germany). Cells were centrifuged and supernatant was discarded. The cell pellet was resuspended in 1 ml Grace + P/S + AmphoB and 10 µl of cell suspension was used for cell counting with a Neubauer Improved counting chamber (0.1 mm depth; Marienfeld Superior, Lauda-Königshofen, Germany). Cell suspension was centrifuged one last time and resuspended in fresh medium. 25,000 cells per coverslip were seeded. Cells were let to settle and attach to the coverslip for 2 h before dishes were filled with 500 µl cell culture medium. Cultures were maintained at 27°C in normal atmosphere. First medium change was performed the next day, subsequently medium was exchanged every 2nd day.

### Treatment of Hemocyte Cultures

Hemocyte cultures were established as described above. Right after establishment, hemocyte cultures were maintained in

either basal Grace insect medium, 100% HL, 50% HL mixed with Grace medium or in Grace medium supplemented with 33.3 ng/ml recombinant human Epo (rhEpo/Epo). Cells were maintained for 7 days (respective culture medium was renewed on *in vitro* day 1, 3, and 5), fixed in 4% paraformaldehyde and prepared for cell survival analysis (see below).

## Locust and Beetle Neuron Culture

Primary neuron cultures were established from 5th instar locust nymphs (previously described by Miljus et al., 2014; Hahn et al., 2019; Knorr et al., 2020) or late beetle pupae (previously described by Hahn et al., 2017). In brief, two locust brains or 20 beetle brains per culture were dissected. Brains were washed three times in Leibowitz 15 medium (L15; Gibco, Life Technologies, Darmstadt, Germany) and supplemented with 1% P/S and 1% AmphoB. L15 with antibiotics lacking any additional additives will be referred to as “basal L15 medium” throughout the manuscript. Insect brains were then transferred to an enzyme mix containing Collagenase/Dispase (2 mg/ml; Sigma-Aldrich, Munich, Germany) for 30 min (locust) or 45 min (beetle) at 27°C. Digestion was stopped by washing the brains three times in Hanks balanced salt solution (Gibco, Life Technologies, Darmstadt, Germany). Subsequently, brains were mechanically dissociated by repeated pipetting until no chunks of tissue remained. Dissociated neurons were centrifuged down, washed once with medium, and centrifuged again. Cells were resuspended in 100 µl/coverlip cell culture medium and plated on Concanavalin A coated 1 cm coverslips. Cells were let to rest for 2 h and dishes were subsequently filled up with medium supplemented with 5% fetal bovine serum gold (FBSG/FBS; PAA Laboratories GmbH, Pasching, Austria), a natural serum with individual ingredients first separated and then recomposed in a defined composition. All experiments were performed with the same Lot of FBS. Cells were maintained at 27°C in normal atmosphere and medium was changed every other day.

## Dose-Dependent HL Effect on Neuronal Survival

To determine potential effects of HL on locust *in vitro* neuronal survival, HL was mixed in different proportions with culture medium. Four primary neuron cultures per experiment were established as described above and kept at 27°C throughout the experiment. Neuron cultures were physiologically challenged to different degrees in three variations of the experimental protocol.

## Cell Survival in Unchallenged Conditions

All neuron cultures were initially cultured in basal L15 medium with 5% FBSG supplementation for 2 days, to support their transition to *in vitro* conditions. After this initial period, cultures were exposed for 3 days to basal L15 medium without FBSG (control) or culture medium with either 10, 25, or 50% HL supplementation. After 5 days *in vitro*, neurons were fixed and prepared for survival analysis.

## Cell Survival Without Initial FBSG Treatment

Neuron cultures were maintained in basal L15 medium for 2 days. Subsequently cells were treated with basal L15 medium (control) or either 10, 25, or 50% HL in L15 for another 3 days before fixation and analysis.

## Cell Survival in Hypoxia

Cultures were established as described above and maintained in medium supplemented with 5% FBSG for 4 days. On *in vitro* day 5, cultures were treated with basal L15 medium (hypoxia control) or either 50, 25, 10% HL or 33.3 ng/ml Epo diluted in L15 medium before being exposed to hypoxia 12 h later. One additional culture in basal L15 medium remained in standard atmospheric conditions (normoxia control). Neurons were maintained in hypoxic conditions ( $O_2 < 0.3\%$ ; Hypoxia Incubator Chamber, STEMCELL™, Cologne, Germany) for 36 h. Subsequently cells were fixed and prepared for survival analysis.

Experiments with neuron cultures from *T. castaneum* were performed in a similar way; however, six differently treated cultures were compared in each experiment. On day 5 *in vitro* (12 h before being exposed to hypoxia for 36 h), three cultures were treated with either 0.25, 1, or 10% locust HL diluted in basal L15 medium. A fourth culture was treated with 3.33 ng/ml Epo. Normoxic and hypoxic control cultures in basal L15 medium were run for comparison with treated cultures as described above.

## Involvement of CRLF3 in HL-Mediated Neuroprotection

To analyze if neuroprotective effects of HL were mediated by CRLF3, soaking RNAi was performed on primary neuron cultures to knockdown either locust or beetle *crlf3* expression. Soaking RNAi was established previously for both species used in this study (Hahn et al., 2017, 2019). In the original publications, we validated the specificity of the knockdown by targeting two non-overlapping fragments of locust *Lm-crlf3* and beetle *Tc-crlf3* with different dsRNA molecules. In this study, *Lm-crlf3* Fragment 1 and *Tc-crlf3* Fragment 2 from the previous studies were used. Four cultures of either locust or beetle neurons were established as described above. One culture was treated with dsRNA (10 ng/µl) targeting *crlf3* immediately after culture establishment. FBSG was removed from cell culture media on day 4. On day 5, two cultures, one untreated and one dsRNA-treated, were exposed to 10% HL diluted in basal L15 medium. Twelve hours later, the treated cultures and one untreated culture (hypoxia control) were exposed to hypoxia ( $O_2 < 0.3\%$ ) for 36 h. One additional neuron culture was kept in normoxic conditions (normoxia control) for the same time. Cells were subsequently fixed and analyzed for cell survival.

## Effects of Heat-Denatured HL on Neuron Survival

To evaluate if cell-protective effects were retained after heat denaturation of HL, neuron cultures were established,



maintained, and exposed to hypoxia as described above. Five cultures were established and maintained in basal L15 medium supplemented with 5% FBSG for 4 days *in vitro*. Four cultures were treated with basal L15 medium (hypoxia control) or basal medium supplemented with either 10% HL, 10% dHL after exposure to 60°C or 10% dHL after exposure to 100°C, respectively, on day 5, 12 h before onset of hypoxia ( $O_2 < 0.3\%$ ) for 36 h. One additional neuron culture was kept in normoxic conditions (normoxia control) for the same time. Cells were subsequently fixed and prepared for cell survival analysis.

## Cell Survival Assessment

Both hemocyte and neuron survival was analyzed as described previously (Miljus et al., 2014; Hahn et al., 2017, 2019). After fixation, coverslips with attached cells were washed (5 min per step) three times in PBS followed by two wash steps in PBS/0.1% Triton-X-100 (PBST). Cells were stained with Dapi (1:1000 in PBST; Sigma-Aldrich; Munich, Germany) for 30 min in the dark. Subsequently, coverslips were washed five times in PBS before mounting on microscopy slides in DABCO (Roth, Karlsruhe, Germany).

Coverslips were imaged with an epifluorescence microscope (Zeiss Axioskop; Oberkochen, Germany; 40x objective was used for locust neurons or hemocytes, 63x oil objective was used for tribolium neurons) equipped with a Spot CCD camera (Invisitron, Puchheim, Germany). Non-overlapping series of photographs passing the center of the coverslip to the left and the right were taken from all cultures (~80 pictures per locust culture and ~120 pictures per tribolium culture). Cells were manually scored as intact or dead/dying on the basis of Dapi-fluorescence pattern reflecting nuclear chromatin structure. The scorer was blinded with respect to the culture treatment during counting. Cell counting was supported by ImageJ Cell counter plug-in (Fiji ImageJ by NIH) as described elsewhere (Miljus et al., 2014; Hahn et al., 2019; Knorr et al., 2020).

## Statistical Analysis

Ratios of the numbers of intact and dead/dying cells of individual cultures were normalized to the respective untreated control cultures of the same experiment, providing the relative portion of surviving cells within the experiment. Data were analyzed using R studio Version 1.2.1335 (RStudio Team, 2015; R Core Team, 2019) employing pairwise permutation test included in packages “coin” and “rcompanion” (Hothorn et al., 2006, 2008; Mangiafico, 2019). Data are presented in box plots displaying the upper and lower quartiles and the medians. Whiskers represent 1.5x interquartile range. Single data points are shown by circles. Benjamini-Hochberg correction was applied to avoid false positives resulting from multiple comparisons.

## SDS-PAGE

To visualize the protein composition of HL, SDS-PAGE analysis was performed. Protein concentrations were measured by Bradford assay (Bradford solution; PanReac AppliChem,

Darmstadt, Germany). For all samples, 50 µg protein was denatured at 75°C for 10 min in 2X Lämmli buffer (Sigma-Aldrich, Munich, Germany). Ten percent acrylamide (Sigma-Aldrich, Munich, Germany) gels were cast and samples were run in the Bio-Rad™ Mini Protean System (Bio-Rad™, Feldkirchen, Germany) for 30 min at 70 V followed by 60 min at 120 V. PageRuler Plus Prestained Protein ladder (Thermo Fisher Scientific, Osterode am Harz) was used as size reference. Gels were stained in InstantBlue™ Coomassie Protein Stain (Abcam, Cambridge, United Kingdom) over night and imaged using the iBright CL1500 Imaging System (Thermo Fisher Scientific, Osterode am Harz, Germany). SDS-PAGEs were run as controls for HL purification and for heat denatured HL to validate protein denaturation.

## RT-PCR

Locust and *T. castaneum* brains and locust hemocytes were extracted and collected as described above. *T. castaneum* hemocytes were collected from pupae by puncturing their lower abdomen. Forty punctured pupae were transferred to 0.5 ml Eppendorf cups with small holes in their bottom. This cup was then placed into a larger 1.5 ml Eppendorf cup containing 10 µl ACS. This composition was centrifuged for 10 min at 12,000 x g in order to collect the hemolymph in the bigger cup. Hemolymph diluted in ACS was then centrifuged at 5000 x g for 10 min to spin down hemocytes. Serum was discarded and hemocytes were subjected to RNA isolation. RNA from all cell types studied was isolated by a modified Trizole (Sigma-Aldrich, Munich, Germany) protocol (described by Knorr et al., 2020). In brief, tissue was disrupted in Trizole reagent, aided by the Tissue Lyser LT (Qiagen, Hilden, Germany) and a 3 mm stainless steel bead. Two-hundred microliter chloroform (Labsolute, Th. Geyer, Renningen, Germany) was added and samples were incubated for 15 min on ice. Samples were subsequently centrifuged for 15 min at 12,000 x g at 4°C. The resulting translucent phase was transferred to a fresh Eppendorf cup and mixed with ice cold 75% EtOH. Samples were then incubated at -20°C for at least 1 h before centrifuging for 10 min at 10,000 x g. RNA pellets were washed three times in 75% ice cold EtOH before airdrying. RNA concentrations were measured using NanoDrop 1,000 (Thermo Scientific, Schwerte, Germany). One microgram RNA was transcribed into cDNA using the LunaScript™ RT SuperMix Kit (New England BioLabs, Ipswich, MA, United States) according to the manufacturer's instructions.

Reverse transcription polymerase chain reactions (RT-PCRs) were run for amplification of both tribolium and locust *crlf3*. Locust 18S rRNA and tribolium  $\alpha$ -tubulin were amplified as housekeeping genes (primer sequences listed in **Table 1**; *Lm-crlf3* was previously published in Hahn et al., 2019, *Lm-18s* was published in Knorr et al., 2020, and *Tc-crlf3* was published in Hahn et al., 2017). (-)RT controls were always run together with genes of interest. RT-PCR (program in **Table 2**) was run with GoTaq Green Master Mix (Promega, Germany) in a final reaction volume of 25 µl.

**TABLE 1** | Oligonucleotides used in this study.

Gene	Sequence 5' – 3' FWD	Sequence 5' – 3' REV	Accession no
<i>Lm-crlf3</i>	GGAACCCAGTCACTCTGCGAG	CGAATATTACCCAGGCTGGAG	MN245516
<i>Lm-18s</i>	CATGTCTCAGTACAAGCCGC	TCGGGACTCTGTTTGCATGT	AF370793
<i>Tc-crlf3</i>	CGATTGTTATGTGGGCGCAGAGAC	GAGTCAGTATTGATACGTGTAACA	LOC661093
<i>Tc-<math>\alpha</math>-tubulin</i>	CGCCAATAACTACGCCAGAG	CGAACGAGTGGAAAATCAAGAA	LOC656649

**TABLE 2** | PCR program for amplification of *Tribolium castaneum* and *Locusta migratoria crlf3*.

Step	Time (s)	Temperature (°C)	
Initial denaturing	3 min	95	
Denaturing	30	95	
Annealing	30	61	30 x
Elongation	30	72	
Final elongation	5 min	72	

PCR products were run on 1% agarose gels containing Roti®-GelStain (Roth, Karlsruhe, Germany) for 45 min at 75 V. Gels were imaged using the iBright CL1500 Imaging System, (Thermo Fisher Scientific, Osterode am Harz, Germany).

## RESULTS

### Locust Hemolymph Promotes Survival of Hemocytes in Primary Culture

We aimed to study the potential anti-apoptotic effects of locust hemolymph. As a first step, we investigated effects on hemocytes, the cells that naturally are directly exposed to signals that circulate within the hemolymph serum. Hemocyte cultures from *L. migratoria* contained cells with heterogeneous appearance (Figure 1C), many of which could be identified as granulocytes and plasmatocytes. Dapi stainings of hemocytes revealed variable morphologies of nuclei (Figure 1D). Intact and dead/dying hemocytes could be distinguished by chromatin condensation visualized by DNA-associated Dapi fluorescence, as described previously for insect neurons and other cells. CRLF3 has previously been identified as a neuroprotective receptor in *L. migratoria* and *T. castaneum*. RT-PCR analysis revealed expression of *Tc-crlf3* in both brain cells and hemocytes (Figure 1A). Both lanes contained amplicons of expected size (527 bp) which were absent in (–)RT controls. Similarly, *Lm-crlf3* transcripts were detected in both brain tissue and hemocytes of *L. migratoria* (Figure 1B) indicated by amplicons of expected sizes (323 bp). PCR-products related to *crlf3* and *18s rRNA* were absent in (–)RT controls.

We then evaluated the effect of locust hemolymph on hemocyte survival in standard culturing conditions. Locust hemocyte cultures were prepared and maintained for 7 days *in vitro* either in basal Grace medium, pure cell-free locust hemolymph, 50% locust hemolymph diluted in Grace medium or medium supplemented with 33.3 ng/ml Epo. Treatment with either hemolymph concentration significantly increased cell survival in comparison to control cultures ( $p < 0.05$ , respectively; Figure 1E). Both 100 and 50% hemolymph increased the

relative survival to a relative median of 1.4 and 1.2, respectively. Epo did not alter cell survival in comparison to either control or treatment groups.

### Effects of Locust Hemolymph on the Survival of Locust Neurons in Primary Culture

Hemolymph and hemocyte cultures contain a heterologous mix of different cell types that rapidly change their physiological properties in response to pathogens and injury (reviewed in Hillyer and Pass, 2020). Since both hemocytes and brain neurons express CRLF3, we selected the well-characterized neuron culture system for further studies. In a first series of experiments, locust primary brain cell cultures were initially maintained in culture medium supplemented with 5% FBS for 2 days, followed by another 3 days with differing treatments. As expected (and previously reported by Ostrowski et al., 2011), 5% FBS significantly increased neuron survival compared to cultures in basal L15 medium ( $p < 0.05$ ; Median 1.5; Figure 2A). Treatment with HL evoked a dose-dependent effect on relative survival. Fifty percent HL significantly decreased neuron survival in comparison to control cultures ( $p < 0.01$ ) to a median of 0.49. Treatment with 25% HL also decreased cell survival ( $p < 0.05$ ; Median: 0.59), while supplementation of medium with 10% HL did not significantly change cell survival and rather suggested weak promotion of cellular survival (Median 1.02).

Transition of neurons from intact brains into dissociated culture conditions represents a major physiological challenge since it involves disruption of neurites and adjustment to a new environment. FBS supports these adjustments but may initiate prolonged physiological mechanisms that outlast the period of its presence in the culture medium. In a second series of experiments, primary neuron cultures were initially maintained in FBS-free culture medium for 2 days before being exposed to different concentrations of HL for another 3 days. Omitting FBS reduced the total number of surviving neurons in basal L15 medium to less than 5%, compared to ~30% intact neurons in cultures that received FBS treatment during the first 2 days *in vitro*. Exposure of FBS-free cultures to 50, 25, and 10% HL significantly increased relative neuron survival compared to control cultures maintained in basal L15 culture medium ( $p < 0.01$  for all HL concentrations tested; Figure 2B). Medians of relative survival were 7.88 for 50% HL, 7.98 for 25% HL, and 5.57 for 10% HL. Although there was a tendency for weaker neuroprotection in culture medium supplemented with 10% HL (compared to 25 and 50% HL), relative survival of neurons was not significantly different between HL concentrations applied.

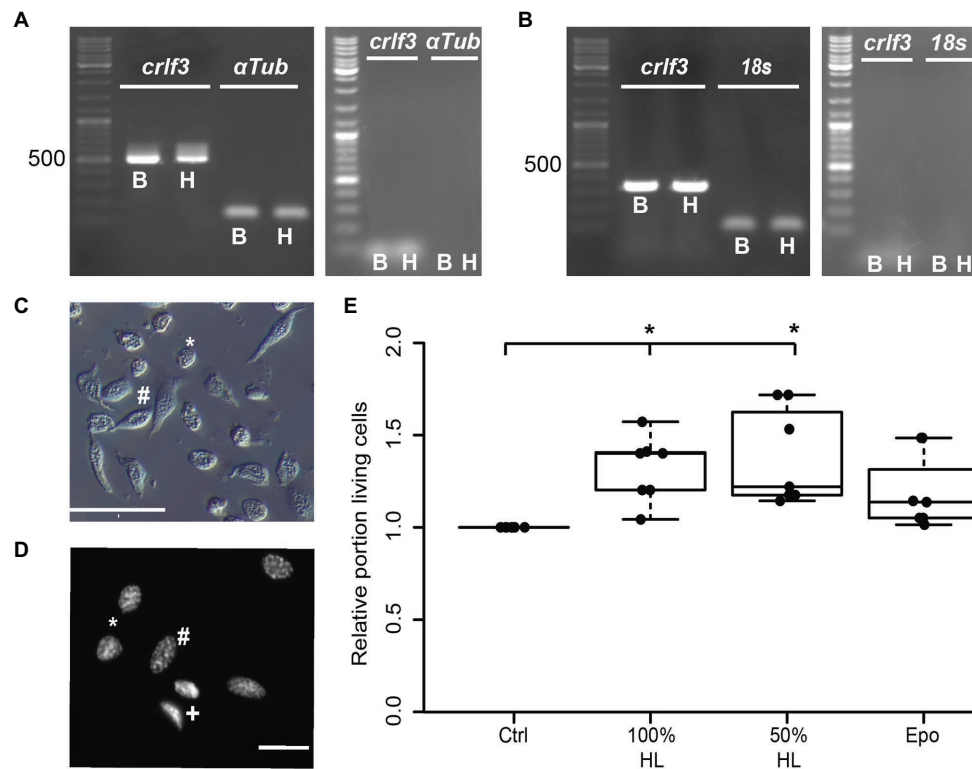
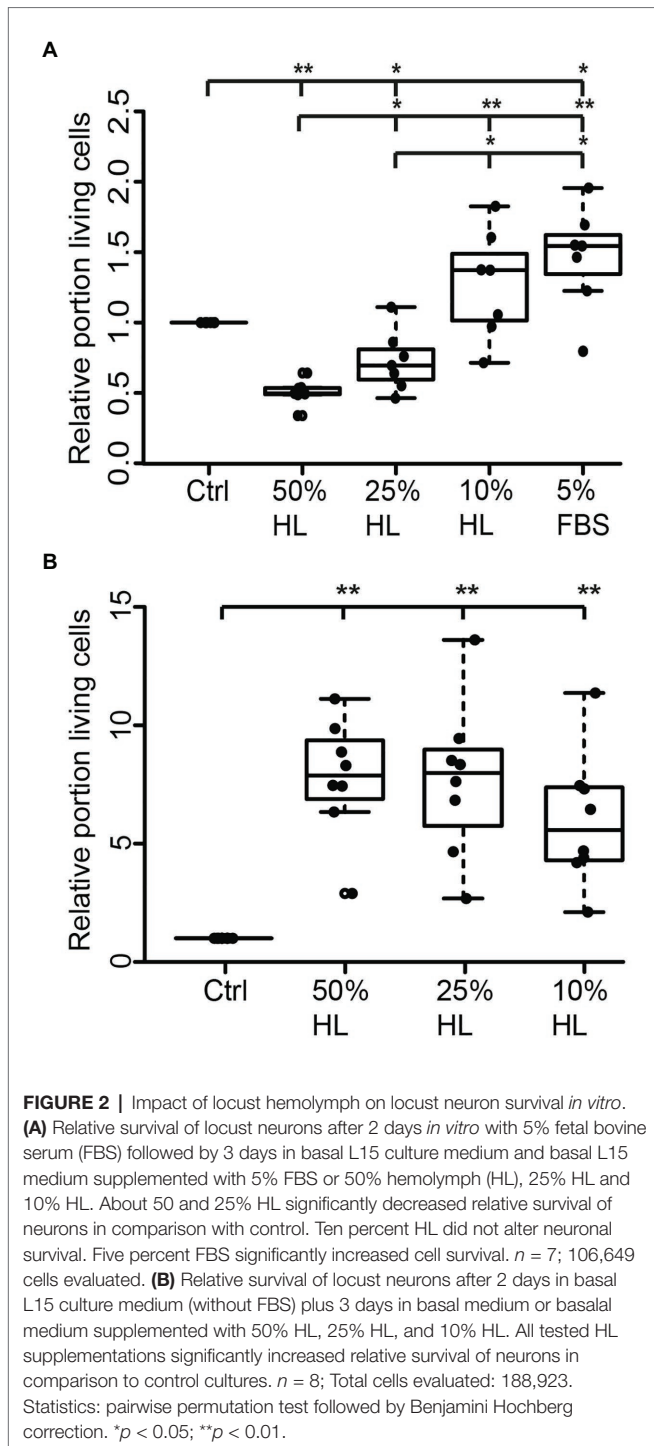


**FIGURE 1 |** Characterization of hemocyte cultures. **(A)** Reverse transcription polymerase chain reaction (RT-PCR) analysis demonstrates *Tc-crlf3* expression in *T. castaneum* brain tissue (B) and hemocytes (H). The PCR product has the expected size of 527 bp for *crlf3* amplification.  $\alpha$ -Tubulin ( $\alpha$ Tub) was used as control with a predicted amplicon of 128 bp. (–)RT controls were negative (see right gel panel). **(B)** RT-PCR reveals *Lm-crlf3* transcript in *L. migratoria* brain (B) and hemocytes (H). Both samples show clear bands for *Lm-crlf3* at the expected size of 323 bp. *18s rRNA* was amplified as control and generates bands at 135 bp as expected. No gDNA was detected in (–)RT controls (see right panel). **(C)** Locust hemocyte cultures after 7 days *in vitro* contain cells of diverse morphologies. Main hemocyte populations were identified as granulocytes (\*) and plasmatocytes (#). Scale bar 50  $\mu$ m. **(D)** Dapi-labeled nuclei of locust hemocytes. Intact cells display patchy staining reflecting normal chromatin structure (\*, #). Dead/dying cells show uniform nuclear staining (+) indicative of DNA degradation and nuclear condensation. Nuclear morphology allows for characterization of the cell type (#plasmatocyte, \*granulocyte). Scale bar 10  $\mu$ m. **(E)** Hemolymph promotes survival of locust hemocytes after 7 days *in vitro*. Both 100% hemolymph and 50% hemolymph diluted in Grace culture medium significantly increase hemocyte survival in comparison to cultures with basal Grace medium. About 33.3 ng/ml erythropoietin (Epo) had no significant effect on hemocyte survival. Statistics were calculated with pairwise permutation test followed by Benjamini Hochberg correction.  $n = 7$ ; Cells evaluated: 154,983. \* $p < 0.05$ .

## Hemolymph Suppresses Hypoxia-Induced Apoptosis in Primary Locust Brain Neurons *via* CRLF3 Activation

In order to evaluate if HL factors interfere with apoptotic processes, we exposed locust primary neurons to hypoxia ( $O_2 < 0.3\%$  for 36 h), which was previously demonstrated to initiate apoptotic cell death (Miljus et al., 2014; Knorr et al., 2020). Based on the results from experiments with FBS-free culture medium (Figure 2B), 50% HL and 25% HL were initially selected for these experiments. As shown in Figure 3A, hypoxia significantly decreased the relative proportion of intact neurons compared with normoxic control cultures ( $p < 0.05$ ). Hypoxia-induced cell death was not prevented by supplementation of culture medium with 25% HL and 50% HL. Fifty percent HL rather further decreased neuronal survival ( $p < 0.01$  to control). However, 25% HL was clearly less deleterious for hypoxia-exposed neurons than 50% HL ( $p < 0.05$ –50% HL) and median relative survival was between normoxic and hypoxic controls (Figure 3A).

Given that the previous experiments suggested a dose-dependent effect of HL treatment toward better survival with lower HL concentrations, the experiments were repeated with 10% HL supplementation. For comparison, additional cultures were treated with 33.3 ng/ml Epo, which was previously shown to prevent hypoxia-induced apoptosis (Miljus et al., 2014; Heinrich et al., 2017; Hahn et al., 2019). Hypoxia significantly decreased cell survival in comparison to normoxic controls in basal L15 culture medium ( $p < 0.05$ ; Figure 3B). Treatment with both Epo and 10% HL rescued cells from hypoxia-induced apoptosis ( $p < 0.05$  in both cases) even leading to slightly (though not statistically significant) increased relative neuron survival compared with normoxic control (Medians: Epo 1.03 and 10% HL 1.2). Hence, 10% HL was at least as effective in suppressing hypoxia-induced apoptosis as Epo in its optimal dosage. In order to determine whether HL, like Epo (Hahn et al., 2017, 2019), mediates neuroprotection *via* activation of CRLF3, *Lm-crlf3* expression was knocked down by soaking RNAi. RNAi was achieved by addition of 10 ng/ $\mu$ l dsRNA to



the culture medium during the initial 5 days *in vitro*. On day 5, one untreated and the dsRNA-supplemented culture were treated with 10% HL. Together with another untreated neuron culture in basal L15 medium, these cultures were exposed to hypoxic conditions ( $O_2 < 0.3\%$  for 36 h) 12 h later. Hypoxia significantly decreased the proportion of intact neurons in comparison to the normoxic control culture ( $p < 0.01$ ; **Figure 3D**). Treatment with 10% HL prevented hypoxia-induced

cell death and significantly increased cell survival ( $p < 0.01$  to hypoxic control group) to similar levels as in unchallenged normoxic cultures. RNAi targeting *Lm-crlf3* expression abolished the protective effect of HL. Knockdown of *crlf3* expression reduced relative neuron survival compared to hypoxia-exposed HL-treated cultures ( $p < 0.01$ ; Median 0.82 vs. 1.1) and normoxic control cultures ( $p < 0.05$ ). There was no difference in survival compared to the hypoxic control cultures.

### Effects of Heat-Denatured Hemolymph on Locust Neuronal Survival

Assuming that the protective factor contained in locust HL is a peptide or protein, we aimed to gain a rough estimate about its size. In order to do so, we denatured HL at 60 and 100°C before testing its protective effects on hypoxia-exposed neurons. It is expected that larger and more complex proteins are more sensitive to heat-denaturation than smaller proteins (meaning they will be eliminated in HL cooked at 60°C). Following heat-denaturation and removal of precipitated proteins by centrifugation, 50  $\mu$ g protein from untreated HL, HL denatured at 60°C and HL denatured at 100°C were separated on a 10% SDS-PAGE (**Figure 4A**). Both untreated and 60°C dHL contained a large portion of proteins in size ranges of  $\geq 55$  kDa and showed minor differences of labeling patterns between samples. In contrast, HL denatured at 100°C lacked the larger sized proteins. Increased labeling intensity of smaller-sized proteins (most obvious between  $\sim 30$  and  $\sim 50$  kDa) can be noted in HL denatured at 100°C. This effect might be due to the lack of high molecular weight proteins in the sample. In order to determine the neuroprotective functions of heat-denatured HL, locust primary neuron cultures were treated with untreated and heat-denatured HL after 5 days *in vitro*, starting 12 h before hypoxia-exposure for 36 h. Hypoxia significantly decreased cell survival in comparison to untreated normoxic control cultures ( $p < 0.01$ ; Median relative survival 0.67; **Figure 4B**). Both 10% HL (Median of relative survival 1.13) and 10% HL denatured at 60°C (Median of relative survival 1.07) significantly rescued cells from hypoxia-induced apoptosis (both  $p < 0.05$  compared with hypoxia control). Relative neuron survival in cultures supplemented with 10% HL denatured at 100°C (Median 0.81) was neither different from normoxic nor from hypoxic control cultures.

### Locust Hemolymph Protects Beetle Neurons via CRLF3 Activation

Since both *L. migratoria* and *T. castaneum* neurons express CRLF3 that is activated by Epo, we wondered whether the endogenous ligand present in locust hemolymph may also protect beetle neurons. *Tribolium castaneum* primary neuronal cell cultures were established and maintained for 5 days before treatments were initiated. Twelve hours prior to hypoxia exposure ( $O_2 < 0.3\%$  for 36 h), neuron cultures were supplemented with either 10, 1, or 0.25% of locust HL or 3.33 ng/ml Epo. As shown in **Figure 5A**, hypoxia decreased the relative proportion of intact neurons in comparison to normoxic control cultures ( $p < 0.05$ ; Median 0.76). Ten percent locust HL (Median relative



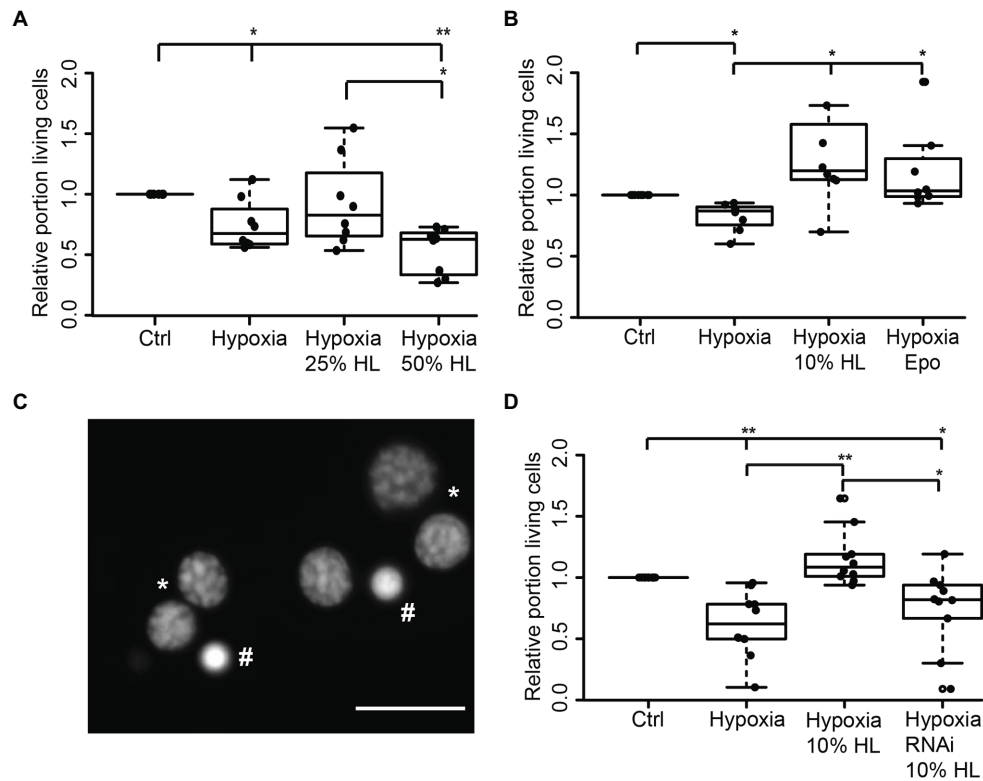


**FIGURE 3** | Impact of locust hemolymph on survival of hypoxia-exposed locust neurons *in vitro*. **(A)** Relative survival of hypoxia-exposed ( $O_2 < 0.3\%$  for 36 h) primary neurons. Exposure to hypoxia decreased relative survival of neurons in comparison to normoxic control ( $p < 0.05$ ). Twenty-five percent HL did not alter cell survival to either the control nor to the hypoxia group, while treatment with 50% HL significantly decreased cell survival to control cultures and cultures treated with 25% HL ( $p < 0.01$  and  $p < 0.05$ , respectively).  $n = 8$ ; 180,563 cells evaluated. **(B)** Hypoxia-induced cell death ( $p < 0.05$  compared with normoxic control) is prevented by 10% HL supplementation ( $p < 0.05$  compared with hypoxic control; no difference to normoxic control). Similarly, 33.3 ng/ml Epo increases relative survival in hypoxic conditions to normoxic control levels.  $n = 8$ ; 152,703 cells evaluated. **(C)** Survival of neurons was evaluated on the basis of fluorescent DNA labeling with Dapi. Intact neurons display patchy chromatin labeling (\*) while dead/dying cells show uniform staining of condensed chromatin (#). Scale bar 10  $\mu\text{m}$ . **(D)** Locust hemolymph protects neurons from hypoxia-induced apoptosis by activation of cytokine receptor-like factor 3 (CRLF3). Hypoxia significantly ( $p < 0.01$ ) decreased relative survival of neurons compared to normoxic control. Hypoxia-induced cell death was prevented by addition of 10% HL to cell culture medium ( $p < 0.01$  compared to hypoxic control). RNAi-mediated knockdown of *crlf3* expression abolished cell protective effects of locust HL on hypoxia-exposed neurons. Relative survival in RNAi- and HL-treated hypoxia-exposed neuron cultures was not different from hypoxic controls and significantly reduced compared with 10% HL-treated hypoxia-exposed cultures ( $p < 0.05$ ).  $n = 10$ ; Cells evaluated: 143,587. Statistics: pairwise permutation test followed by Benjamini Hochberg correction. \* $p < 0.05$ ; \*\* $p < 0.01$ .

survival 1.10) and 1% locust HL (Median relative survival 1.04) significantly increased neuron survival to the level seen in normoxic control cultures ( $p < 0.05$  compared with hypoxic control). Treatment with 0.25% locust HL could not significantly protect *T. castaneum* neurons from hypoxia-induced apoptosis. As expected from previous studies (Hahn et al., 2017), Epo protected beetle neurons from hypoxia-induced apoptosis ( $p < 0.05$ ).

We further tested if the neuroprotective effect elicited by locust HL on tribolium neurons was also CRLF3 dependent. *Tc-crlf3* was knocked down by means of soaking RNAi and cells were subsequently treated with 10% locust HL. Hypoxia again significantly reduced cell survival in comparison to untreated controls ( $p < 0.01$ ; Median 0.89; **Figure 5B**). Treatment with 10% locust HL (Median relative survival 1.28) rescued beetle neurons from hypoxia-induced apoptosis ( $p < 0.05$  compared with hypoxic control). The protective effect of locust

HL was absent, when *Tc-crlf3* expression in tribolium neurons was suppressed for 5 days prior to the hypoxia challenge (Median relative survival 0.73,  $p < 0.05$  compared to HL-treated hypoxia-exposed cultures). Relative neuron survival of CRLF3-depleted cultures was not different from hypoxic control cultures.

## DISCUSSION

The physiological functions of insect hemolymph have been studied in various species and its beneficial effects on cell survival were already noticed in early *in vitro* studies with various cell types (Day and Grace, 1954). Numerous studies have indicated that hemolymph is highly reactive to the physiological state of the insect. The impact of physiological stressors is reflected in the changing molecular and cellular composition of it (Hillyer and Christensen, 2002).

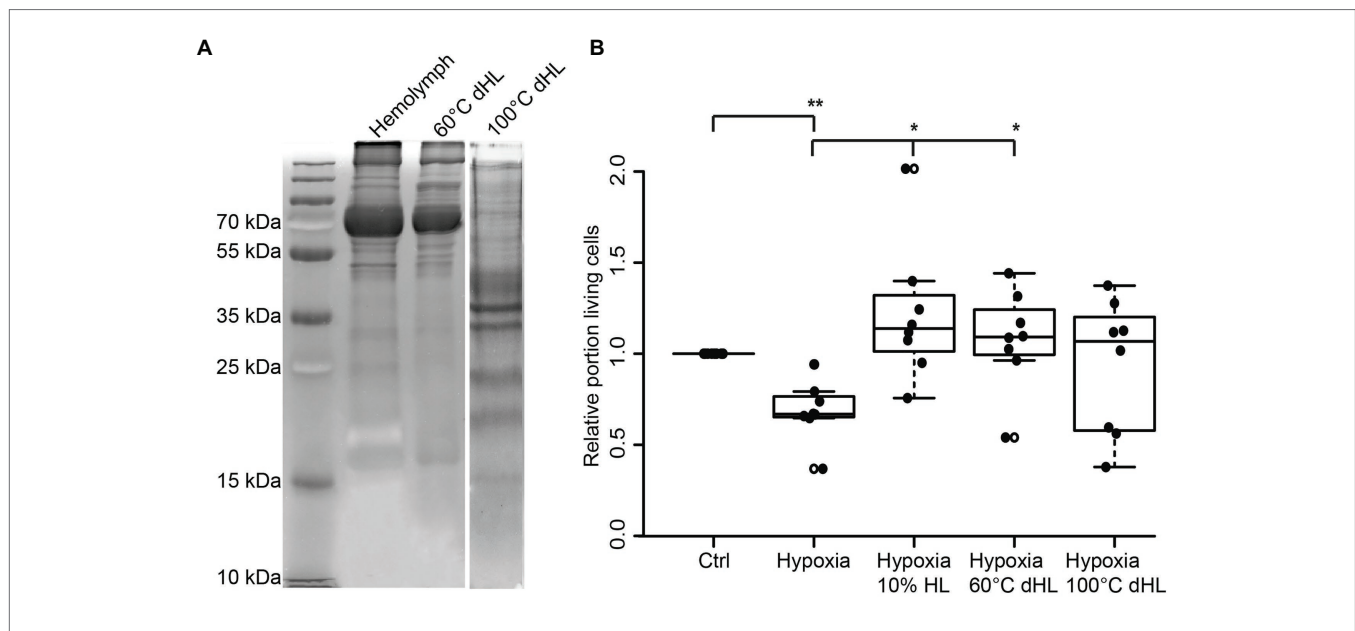


**FIGURE 4 |** Effects of heat-denatured locust hemolymph (dHL) on relative survival of hypoxia-exposed locust neurons *in vitro*. **(A)** Ten percent sodium dodecyl sulfate–polyacrylamide gel electrophoresis (SDS PAGE) was loaded with 50  $\mu$ g protein of HL, HL denatured at 60°C and HL denatured at 100°C. HL denatured at 60°C shows similar patterns of separated proteins compared to control HL. In contrast, larger proteins ( $\geq 50$  kDa) are absent in HL denatured at 100°C. Intense staining of proteins between 30 and 50 kDa (including two clear bands at around 35 kDa) might result from higher concentrations of smaller proteins in the applied sample (50  $\mu$ g total protein) due to previous removal of heat-denatured proteins. Hundred degrees Celsius dHL proteins show no intense protein bands above 35/40 kDa. **(B)** Locust neurons were treated with either basal L15 medium, 10% HL, 10% 60°C dHL, or 100°C dHL during hypoxia-exposure. Hypoxia significantly decreased relative neuron survival compared to normoxic control. Hypoxia-induced apoptosis was prevented by 10% HL and 10% HL denatured at 60°C. Neuron survival in cultures supplemented with HL denatured at 100°C was not significantly different to normoxic control or hypoxic control cultures.  $n = 8$ ; Total cells evaluated: 160,595. Pairwise permutation test with Benjamini Hochberg correction. \* $p < 0.05$ ; \*\* $p < 0.01$ .

Exposure of insects to pathogens or other stressors increased the abundance of a variety of hemolymph proteins, like antimicrobial peptides, prophenol oxidase, apolipoprotein, vago, unpaired3, growth blocking peptides, transferrin, and hexamerin (Wang et al., 2007; Welchman et al., 2009; Kingsolver et al., 2013) among others. Principal origin of most humoral defense factors is the fat body. Besides functions in insect metabolism (reviewed in Arrese and Soulages, 2010), it regulates the release and uptake of proteins into and from the serum (Lavine and Strand, 2002; Roma et al., 2010; Hoshizaki, 2013; Duressa et al., 2014). Humoral factors are also produced and secreted from midgut, hemocytes, prothoracic gland, and neurosecretory cells within the *corpore allata*, *corpore cardiaca*, the anterior sympathetic system, ventral ganglia, and various sites along peripheral nerves (Reynolds, 2013; Kodrik et al., 2015). Cytokines and cytokine-like proteins are among these circulating proteins, regulating innate immune responses and adaptive reactions to various stress factors (Beschinn et al., 1999, 2001).

Cytokines and their receptors play major roles in immune and stress responses, cell activation, proliferation, maturation, and differentiation in both vertebrates and invertebrates (Shields et al., 1995; Beschinn et al., 2001). Apart from some general structural features, cytokines typically share little sequence similarities within and between animal groups (Boulay et al., 2003; Liongue and Ward, 2007). The diversity of cytokines and cytokine receptors identified today most likely date back to ancient molecules in common ancestors of vertebrates and

invertebrates (Huisling et al., 2006; Liongue and Ward, 2007). CRLF3 is one example for an evolutionarily ancient cytokine receptor, which may be regarded as the prototype for class 1 cytokine receptors (Liongue and Ward, 2007). CRLF3 is highly conserved across eumetazoan species, implying an essential role for the organism (Liongue and Ward, 2007; Hahn et al., 2019). Insect CRLF3, activated by human Epo, initiates anti-apoptotic mechanisms in insect neurons even though insects lack genes for Epo and the classical Epo receptor (Hahn et al., 2017, 2019). Epo mediates anti-apoptotic effects in various mammalian cells (including neurons and erythrocytes) *via* the classical homodimeric Epo receptor and additional tissue-protective alternative Epo receptors (reviewed by Ostrowski and Heinrich, 2018). Several molecules that mimic the cell-protective but not the erythropoietic effects of Epo in vertebrate tissues have been identified (Wrighton et al., 1996; Middleton et al., 1999; Johnson and Jolliffe, 2000; Brines et al., 2008; Ueba et al., 2010; Wu et al., 2013; Bonnas et al., 2017). Some of these, including the natural Epo splice variant EV-3 and several small peptides with little or no sequence similarity to Epo also protect insect neurons from apoptotic cell death (Miljus et al., 2014; Hahn et al., 2017; own unpublished results). Whether vertebrate CRLF3 may also serve as a tissue-protective receptor for Epo is presently not known.

Given that insects do not express Epo or any known vertebrate Epo receptors, we gained interest in the identification of the endogenous ligand of insect CRLF3. We first confirmed that

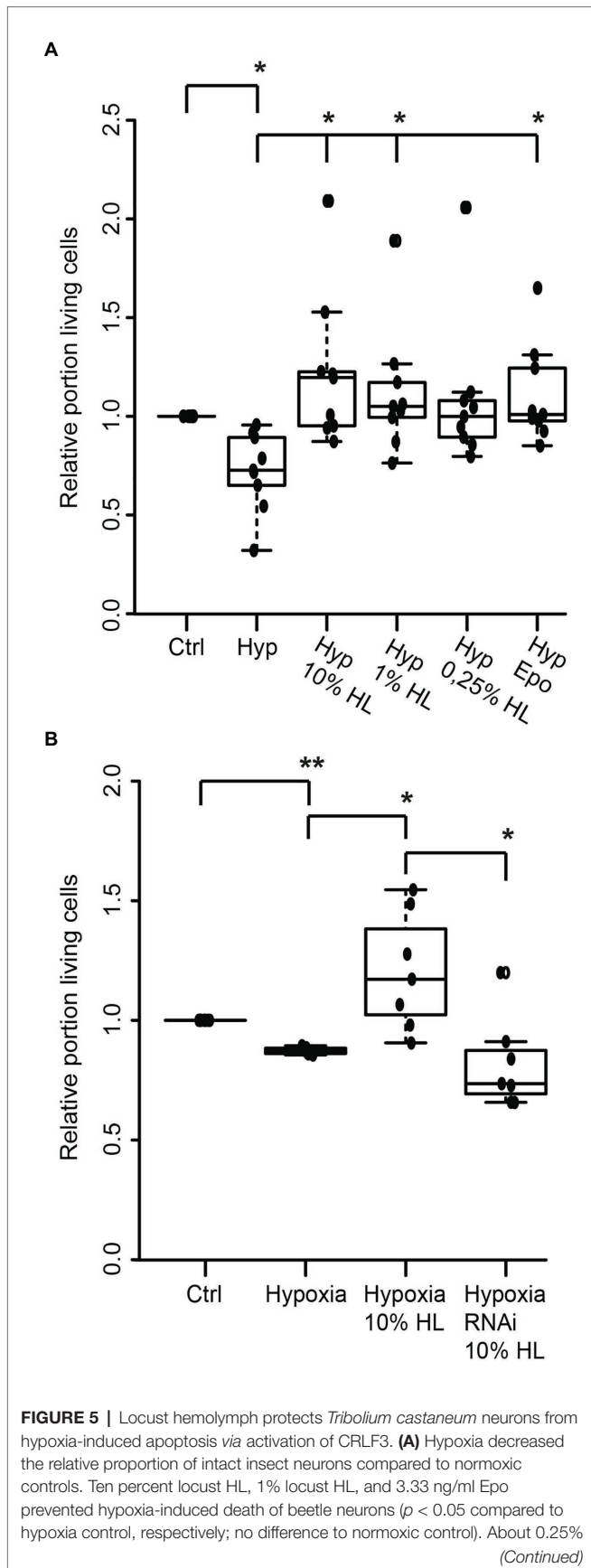


**FIGURE 5 |** locust HL did not significantly alter cell survival compared to normoxic control and to hypoxic control cultures.  $n = 9$ , total cells evaluated: 185,970. **(B)** *T. castaneum* neurons were maintained for 5 days in standard culture conditions with one culture being exposed to dsRNA targeting *Tc-crlf3*. Hypoxia significantly decreased relative neuron survival in comparison to the normoxic control. The protective effect of 10% locust HL ( $p < 0.05$  compared to hypoxic control) was absent after RNAi-mediated depletion of CRLF3 ( $p < 0.05$ ). Relative survival of CRLF3-depleted neurons treated with locust HL was not different from hypoxia-exposed controls without the protective HL supplementation.  $n = 7$ ; Cells evaluated: 163,740. Statistics: pairwise permutation test with Benjamini Hochberg correction. \* $p < 0.05$ ; \*\* $p < 0.01$ .

*crlf3* is expressed in brain and hemocytes of both *L. migratoria* and *T. castaneum*. For both species, PCR amplified fragments of identical size in brain and hemocytes (**Figures 1A,B**) were confirmed. Next, we exposed primary cultured locust hemocytes for 7 days to rhEpo and cell-free hemolymph collected from different locusts. Supplementation of cultures with pure hemolymph and 50% hemolymph significantly increased cell survival in comparison to serum-free cultures. Epo supplementation only showed a tendency toward support of hemocyte survival which did not reach significance level ( $p = 0.06$ ; **Figure 1E**). Previous studies on insect (Hahn et al., 2017; Heinrich et al., 2017) and mammalian neurons (Siren et al., 2001; Chong et al., 2003; Weishaupt et al., 2004) demonstrated that Epo elicits neuroprotective effects in an optimum-type curve with both lower and higher concentrations of Epo being less effective. We treated locust hemocytes with 33.3 ng/ml rhEpo, which was determined as the optimal concentration to suppress hypoxia-induced apoptosis in locust primary neuron cultures. It seems that a multiplicity of factors determines the optimal concentration of Epo, within them: species (hypoxia-challenged neurons of *T. castaneum* are best protected by 3.33 ng/ml rhEpo), physiological condition (hemolymph impact on survival of challenged and unchallenged locust neurons discussed below), type of challenge, and cell type. We have not studied the effects of different rhEpo concentrations on primary cultured locust hemocytes. Nonetheless, we predict hemocyte protection to occur with appropriate Epo dosage. However, hemolymph clearly protected primary cultured hemocytes, indicating the presence of protective molecules in hemolymph serum.

Representing the major site of immune defense and the medium that distributes signals and metabolites to all organs, hemolymph is a highly responsive “fluid tissue.” With respect to the surrounding circumstances, both the molecular composition of the serum and the physiological state of various hemocyte types will be altered (Wang et al., 2007; Altincicek et al., 2008; Duressa et al., 2015). In order to reduce this extensive variability, we studied the protective functions of hemolymph serum with well-established protocols of primary neuron cultures from two different species, *L. migratoria* and *T. castaneum*. These were previously utilized to demonstrate the neuroprotective functions of CRLF3 following its activation with rhEpo. However, the hemolymph serum used in our studies was numerously extracted from different locusts (each time pooled from up to 100 individuals received from a commercial breeder) and its molecular composition, including

the presence of cell-protective agents, likely varied between these batches. Variability of the cell-protective HL effects described in this study may partly result from pre-exposure of HL-donor animals to stressful conditions (transport, infections, extreme crowding, and others). Keeping locusts under optimal conditions for several days and/or exposing them to a defined stressor before HL extraction may result in a more uniform composition of HL protein content.

We hypothesized that the yet unknown CRLF3 ligand might be an ancestral cytokine with similarity to Epo that acts in a similar, cytoprotective way as Epo does. We demonstrated that locust hemolymph increased the survival of primary-cultured locust neurons in a dose-dependent manner (**Figure 2**). Compared to serum-free culture medium, addition of locust hemolymph significantly increased neuronal survival with 50 and 25% supplementation showing higher median survival compared to 10% hemolymph. Serum deprivation, containing growth factors and cytokines that support cellular survival in dissociated cultures, has been used as an apoptosis-inducing stressor in various *in vitro* studies with both vertebrate and invertebrate cells (Macleod et al., 2001; Siren et al., 2001; Charles et al., 2005). Though serum-free culturing of adult and embryonic locust neurons has previously been achieved (Kirchhof and Bicker, 1992; Sukiban et al., 2014), only a small portion of brain neurons survive the dissociation process during culture establishment in our study (which involves the disruption of all neurites) without FBS supplementation. The FBS used in our studies has a defined composition of natural components (nevertheless small variations may not fully be excluded) and originated from the same Lot. To increase the number of intact neurons in locust brain cultures, we typically apply FBS during the first day *in vitro*. While promoting neuron survival, FBS is detrimental for locust brain glia (Ostrowski et al., 2011) leading to increasingly pure neuronal cultures during the initial culture period. Since serum has been shown to induce long-lasting effects in cultured neurons, we withdraw FBS from the culture medium 24 h before experimental treatment with hemolymph or Epo.

Serum withdrawal induced cell death in locust and beetle primary neuron cultures while Epo (if applied in appropriate dosage) fully restored the beneficial effects on neuronal survival (Ostrowski et al., 2011; Hahn et al., 2017). Withdrawal of FBS after 2 days significantly decreased neuronal survival during the following 3 days *in vitro* compared to cultures maintained with FBS. This indicates protective effects of FBS throughout prolonged presence in the medium (**Figure 2A**). In contrast to its effects on neurons that were not supported by additional FBS, hemolymph exposure after 2 days of FBS treatment revealed dose-dependent negative effects (**Figure 2B**). In this case, higher hemolymph concentrations acted deleterious on neuronal cell survival, while 10% HL showed a trend toward neuroprotection. Moreover, neurons that were initially cultured with FBS and subsequently subjected to hypoxia were best protected by 10% hemolymph. Twenty-five percent hemolymph only weakly (but not significantly) improved survival and 50% hemolymph rather seemed to aggravate hypoxia-induced neuronal death (**Figure 3**). Together, these results indicate

long-lasting effects of FBS that promote neuronal survival beyond its presence in the culture medium. To explain the differing impact of hemolymph on cultured neurons that were exposed to FBS and hypoxia, one has to assume long-lasting changes in the neurons' physiological state that were induced by different stressful conditions (such as injury during dissociation, presence/absence of serum and other supporting factors, and hypoxia). Depending on their state and the type of challenge, cells may require different amounts and types of protective factors for their survival (Dinarello, 2007). Hence, as observed in our present study, a particular dose of hemolymph (reflecting a certain concentration of ligands) may be beneficial for locust neurons in one situation and deleterious in the other. Studies on *T. castaneum* revealed optimum-type protective effects of different rhEpo concentrations, with high concentrations not only being non-protective but deleterious for neuron survival (Hahn et al., 2017). This indicates that overactivation of CRLF3 and/or its downstream transduction processes has negative impacts on neuron survival. Similarly, protective effects and efficacy of different concentrations of Epo have been shown to vary in murine astrocytes exposed to different inducers of cell death (Diaz et al., 2005) and rat brain neurons after exposure to mild hypoxic periods (Sanchez et al., 2009).

In a previous study with locust primary neuron cultures, *crlf3*-expression was suppressed by soaking RNAi (Hahn et al., 2019). Efficient uptake of dsRNA from extracellular space into insect cells has been associated with two types of cell-surface receptors and clathrin-dependent endocytosis in *Drosophila* (Ulvila et al., 2006). In locusts, supplementation of culture medium with two different dsRNA fragments (non-overlapping targets of *crlf3* mRNA) abolished Epo-mediated protection of hypoxia-exposed neurons completely. This indicated that Epo initiates anti-apoptotic mechanisms by binding to CRLF3 (Hahn et al., 2019). After confirming that 10% hemolymph acted equally protective as 33.3 ng/ml rhEpo on hypoxia-exposed locust neurons (**Figure 2B**), we selected one dsRNA fragment to knockdown *crlf3*-expression by RNAi. dsRNA-incubation prior to hypoxia exposure abolished the anti-apoptotic effect of 10% hemolymph on locust neurons. This finding suggests that locust hemolymph contains a ligand that activates CRLF3 and its downstream anti-apoptotic pathways (**Figure 2D**).

Given the high similarity of *crlf3* between *L. migratoria* and *T. castaneum* and the fact that both *Lm*-CRLF3 and *Tc*-CRLF3 mediate neuroprotection upon stimulation with rhEpo (Hahn et al., 2017, 2019), we studied the protective effects of locust hemolymph on beetle neurons. *T. castaneum* neurons were protected from hypoxia-induced apoptosis by 10 and 1% locust hemolymph and the protective effect was clearly mediated by *Tc*-CRLF3 (**Figure 5**). The protective effect was similar to 3.33 ng/ml rhEpo, which was previously determined as the most protective concentration for *T. castaneum* neurons (Hahn et al., 2017). The most protective Epo concentration for tribolium neurons is only a tenth of the most protective concentration for locust neurons (33.3 ng/ml). In contrast, 10% locust hemolymph protected both locust and beetle neurons to the same degree as the (different) optimal Epo concentrations of both species. One may speculate that the endogenous ligand



in locust hemolymph binds to *Lm*-CRLF3 and *Tc*-CRLF3 with similar affinity, whereas rhEpo has a higher affinity to *Tc*-CRLF3. This might result from slight structural differences of the locust receptor to the human and beetle receptor. Amino acid sequences of *Lm*-CRLF3 and *Tc*-CRLF3 share 35% similarity, whereas locust and human CRLF3 display 29% similarity (Hahn et al., 2017, 2019). High conservation and multi-tissue expression of CRLF3 among eumetazoan species suggests an important role for CRLF3-mediated functions in these organisms. The endogenous ligand that circulates within locust hemolymph seems to be conserved among insects and may also be present in species outside the insect clade.

Lepidopteran 30K proteins were shown to retain their protective functions following exposure to 60°C but lost their beneficial effects when exposed to higher temperatures (Kim et al., 2001). A later study described thermostability of 30K proteins up to 70–80°C (Pakkianathan et al., 2015). Heat denaturation disrupts the secondary and tertiary structure of proteins which typically results in the precipitation of denatured proteins from the solvent (Michnik and Drzazga, 2010). Larger and more complex proteins are typically denatured at lower temperatures and are less likely to reassume their native structure during subsequent cooling. Heating locust hemolymph to 60°C had no impact on its anti-apoptotic effects. Heating hemolymph to 100°C resulted in no significant difference in cell viability compared to sole hypoxia exposure, however, the protective activity was retained to some extent (Figure 4). Heating the serum to 100°C removed proteins of ≥50 kDa suggesting that the protective CRLF3 ligand is smaller than this size. Biological activity of a 14 kDa protein Thrombocortin from sponge was gradually abolished by extending the duration of its exposure to 98°C (Watari et al., 2019), leaving the possibility that longer periods of exposure to 100°C might abolish protective effects of locust hemolymph.

This study indicates the presence of a conserved cytokine in insect hemolymph, activating the phylogenetically conserved CRLF3, whose endogenous ligand has not been identified in any species. Human Epo, its splice variant EV-3 and various small peptides that mimic neuroprotective effects of Epo on mammalian cells all activate insect CRLF3 to initiate anti-apoptotic mechanisms. This suggests some structural similarity

between Epo-like ligands and the endogenous CRLF3 ligand present in locust hemolymph. Whether mammalian CRLF3, like insect CRLF3, initiates cell-protective intracellular processes upon Epo binding is currently not known. CRLF3 expression in various insect and mammalian tissues suggests a conserved function in adaptive responses to physiological challenges similar to Epo signaling in mammals. Molecular identification of the insect CRLF3 ligand may lead to the discovery of mammalian orthologues and opportunities to activate beneficial CRLF3 functions for medical treatment.

## DATA AVAILABILITY STATEMENT

The raw data supporting the conclusions of this article will be made available by the authors, without undue reservation.

## AUTHOR CONTRIBUTIONS

DK and RH designed and supervised the study, and wrote and edited the manuscript. DK, DH, KS, LH, and HP performed the experiments. DK, DH, KS, and LH analyzed the data. All authors contributed to the article and approved the submitted version.

## FUNDING

The study was supported by the Deutsche Forschungsgemeinschaft (DFG; project number: 398214842).

## ACKNOWLEDGMENTS

We thank Nicola Schwedhelm-Domeyer, Stephanie Pauls, and Silvia Gubert for technical assistance, and Elke Küster for *Tribolium castaneum* breeding and stock keeping. We also thank Nina Hahn for constructive scientific advice and Martin C. Göpfert for generous financial support.

## REFERENCES

- Altincicek, B., Knorr, E., and Vilcinskis, A. (2008). Beetle immunity: identification of immune-inducible genes from the model insect *Tribolium castaneum*. *Dev. Comp. Immunol.* 32, 585–595. doi: 10.1016/j.dci.2007.09.005
- Arrese, E. L., and Soulages, J. L. (2010). Insect fat body: energy, metabolism, and regulation. *Annu. Rev. Entomol.* 55, 207–225. doi: 10.1146/annurev-ento-112408-085356
- Beschin, A., Bilej, M., Brys, L., Torreele, E., Lucas, R., Magez, S., et al. (1999). Convergent evolution of cytokines. *Nature* 400, 627–628. doi: 10.1038/23164
- Beschin, A., Bilej, M., Torreele, E., and De Baetselier, P. (2001). On the existence of cytokines in invertebrates. *Cell. Mol. Life Sci.* 58, 801–814. doi: 10.1007/PL00000901
- Bonnas, C., Wüstefeld, L., Winkler, D., Kronstein-wiedemann, R., Dere, E., Specht, K., et al. (2017). EV-3, an endogenous human erythropoietin isoform with distinct functional relevance. *Sci. Rep.* 7:3684. doi: 10.1038/s41598-017-03167-0
- Boulay, J. L., O'Shea, J. J., and Paul, W. E. (2003). Molecular phylogeny within type I cytokines and their cognate receptors. *Immunity* 19, 159–163. doi: 10.1016/S1074-7613(03)00211-5
- Brines, M., and Cerami, A. (2005). Emerging biological roles for erythropoietin in the nervous system. *Nat. Rev. Neurosci.* 6, 484–494. doi: 10.1038/nrn1687
- Brines, M., Patel, N. S. A., Villa, P., Brines, C., Mennini, T., De Paola, M., et al. (2008). Nonerythropoietic, tissue-protective peptides derived from the tertiary structure of erythropoietin. *Proc. Natl. Acad. Sci. U. S. A.* 105, 10925–10930. doi: 10.1073/pnas.0805594105
- Charles, I., Khalyfa, A., Kumar, D. M., Krishnamoorthy, R. R., Roque, R. S., Cooper, N., et al. (2005). Serum deprivation induces apoptotic cell death of transformed rat retinal ganglion cells via mitochondrial signaling pathways. *Investig. Ophthalmol. Vis. Sci.* 46, 1330–1338. doi: 10.1167/iovs.04-0363
- Chong, Z. Z., Kang, J. Q., and Maiese, K. (2003). Erythropoietin fosters both intrinsic and extrinsic neuronal protection through modulation of microglia, Akt1, bad, and caspase-mediated pathways. *Br. J. Pharmacol.* 138, 1107–1118. doi: 10.1038/sj.bjp.0705161

- Day, M. F., and Grace, T. D. C. (1954). Culture of insect tissues. *Annu. Rev. Entomol.* 173, 504–505. doi: 10.1038/173504a0
- Diaz, Z., Assaraf, M. I., Miller, W. H. Jr., and Schipper, H. M. (2005). Astroglial cytoprotection by erythropoietin pre-conditioning: implications for ischemic and degenerative CNS disorders. *J. Neurochem.* 93, 392–402. doi: 10.1111/j.1471-4159.2005.03038.x
- Dinarello, C. A. (2007). Historical insights into cytokines. *Eur. J. Immunol.* 37(Suppl. 1), S34–S45. doi: 10.1002/eji.200737772
- Douglas, A. E., and Siva-Jothy, M. T. (2013). “Circulatory system, blood and the immunessystem” in *The insects, structure and function*. ed. R. F. Chapman (Cambridge, UK: Cambridge University Press), 107–131.
- Duressa, T. F., Vanlaer, R., and Huybrechts, R. (2014). Locust cellular defense against infections: sites of pathogen clearance and hemocyte proliferation. *Dev. Comp. Immunol.* 48, 244–253. doi: 10.1016/j.dci.2014.09.005
- Duressa, T. F., Vanlaer, R., and Huybrechts, R. (2015). Identification and functional characterization of a novel locust peptide belonging to the family of insect growth blocking peptides. *Peptides* 74, 23–32. doi: 10.1016/j.peptides.2015.09.011
- Ghezzi, P., and Conklin, D. (2013). Tissue-protective cytokines: structure and evolution. *Methods Mol. Biol.* 982, 43–58. doi: 10.1007/978-1-62703-308-4\_3
- Hahn, N., Büschgens, L., Schwedhelm-Domeyer, N., Bank, S., Geurten, B. R. H., Neugebauer, P., et al. (2019). The orphan cytokine receptor CRLF3 emerged with the origin of the nervous system and is a neuroprotective erythropoietin receptor in locusts. *Front. Mol. Neurosci.* 12:251. doi: 10.3389/fnmol.2019.00251
- Hahn, N., Knorr, D. Y., Liebig, J., Wüstefeld, L., Peters, K., Büscher, M., et al. (2017). The insect ortholog of the human orphan cytokine receptor CRLF3 is a neuroprotective erythropoietin receptor. *Front. Mol. Neurosci.* 10:223. doi: 10.3389/fnmol.2017.00223
- Heinrich, R., Günther, V., and Miljus, N. (2017). Erythropoietin-mediated neuroprotection in insects suggests a prevertebrate evolution of erythropoietin-like signaling. *Vitam. Horm.* 105, 181–196. doi: 10.1016/bs.vh.2017.02.004
- Hillyer, J. F., and Christensen, B. M. (2002). Characterization of hemocytes from the yellow fever mosquito, *Aedes aegypti*. *Histochem. Cell Biol.* 117, 431–440. doi: 10.1007/s00418-002-0408-0
- Hillyer, J. F., and Pass, G. (2020). The insect circulatory system: structure, function, and evolution. *Annu. Rev. Entomol.* 65, 121–143. doi: 10.1146/annurev-ento-011019-025003
- Hoshizaki, D. K. (2013). “Fat body” in *The insects: Structure and function*. ed. R. F. Chapman (Cambridge, UK: Cambridge University Press), 5.
- Hothorn, T., Hornik, K., Van De Wiel, M. A., and Zeileis, A. (2006). A lego system for conditional inference. *Am. Stat.* 60, 257–263. doi: 10.1198/000313006X118430
- Hothorn, T., Hornik, K., Van De Wiel, M. A., and Zeileis, A. (2008). Implementing a class of permutation tests: the coin package. *J. Stat. Softw.* 28, 1–23. doi: 10.18637/jss.v028.i08
- Howes, E. A., Cheek, T. R., and Smith, P. J. (1991). Long-term growth in vitro of isolated, fully differentiated neurones from the central nervous system of an adult insect. *J. Exp. Biol.* 156, 591–605.
- Huising, M. O., Kruiswijk, C. P., and Flik, G. (2006). Phylogeny and evolution of class-I helical cytokines. *J. Endocrinol.* 189, 1–25. doi: 10.1677/joe.1.06591
- Johnson, D. L., and Jolliffe, L. K. (2000). Erythropoietin mimetic peptides and the future. *Nephrol. Dial. Transplant.* 15, 1274–1277. doi: 10.1093/ndt/15.9.1274
- Kim, E. J., Park, H. J., and Park, T. H. (2003). Inhibition of apoptosis by recombinant 30K protein originating from silkworm hemolymph. *Biochem. Biophys. Res. Commun.* 308, 523–528. doi: 10.1016/S0006-291X(03)01425-6
- Kim, E. J., Rhee, W. J., and Park, T. H. (2001). Isolation and characterization of an apoptosis-inhibiting component from the hemolymph of *Bombyx mori*. *Biochem. Biophys. Res. Commun.* 285, 224–228. doi: 10.1006/bbrc.2001.5148
- Kim, E. J., Rhee, W. J., and Park, T. H. (2004). Inhibition of apoptosis by a *Bombyx mori* gene. *Biotechnol. Prog.* 20, 324–329. doi: 10.1021/bp034130y
- Kingsolver, M. B., Huang, Z., and Hardy, R. W. (2013). Insect antiviral innate immunity: pathways, effectors, and connections. *J. Mol. Biol.* 425, 4921–4936. doi: 10.1016/j.jmb.2013.10.006
- Kirchhof, B., and Bicker, G. (1992). Growth properties of larval and adult locust neurons in primary cell culture. *J. Comp. Neurol.* 323, 411–422. doi: 10.1002/cne.903230308
- Knorr, D. Y., Georges, N. S., Pauls, S., and Heinrich, R. (2020). Acetylcholinesterase promotes apoptosis in insect neurons. *Apoptosis* 25, 730–746. doi: 10.1007/s10495-020-01630-4
- Kodrik, D., Bednářová, A., Zemanová, M., and Krishnan, N. (2015). Hormonal regulation of response to oxidative stress in insects—an update. *Int. J. Mol. Sci.* 16, 25788–25816. doi: 10.3390/ijms161025788
- Lamiable, O., Kellenberger, C., Kemp, C., Troxler, L., Pelte, N., Boutros, M., et al. (2016). Cytokine dielid and a viral homologous suppress the IMD pathway in drosophila. *Proc. Natl. Acad. Sci. U. S. A.* 113, 698–703. doi: 10.1073/pnas.1516122113
- Lavine, M. D., and Strand, M. R. (2002). Insect hemocytes and their role in immunity. *Insect Biochem. Mol. Biol.* 32, 1295–1309. doi: 10.1016/S0965-1748(02)00092-9
- Liongue, C., Sertori, R., and Ward, A. C. (2016). Evolution of cytokine receptor signaling. *J. Immunol.* 197, 11–18. doi: 10.4049/jimmunol.1600372
- Liongue, C., and Ward, A. C. (2007). Evolution of class I cytokine receptors. *BMC Evol. Biol.* 7:120. doi: 10.1186/1471-2148-7-120
- Macleod, M. R., Allsopp, T. E., McLuckie, J., and Kelly, J. S. (2001). Serum withdrawal causes apoptosis in SHSY 5Y cells. *Brain Res.* 889, 308–315. doi: 10.1016/S0006-8993(00)03173-5
- Mangiafico, S. (2019). Package “Rcompanion,” no. September 2016.
- Michnik, A., and Drzazga, Z. (2010). Thermal denaturation of mixtures of human serum proteins: DSC study. *J. Therm. Anal. Calorim.* 101, 513–518. doi: 10.1007/s10973-010-0826-5
- Middleton, S. A., Barbone, F. P., Johnson, D. L., Thurmond, R. L., You, Y., McMahon, F. J., et al. (1999). Shared and unique determinants of the erythropoietin (EPO) receptor are important for binding EPO and EPO mimetic peptide. *J. Biol. Chem.* 274, 14163–14169. doi: 10.1074/jbc.274.20.14163
- Miljus, N., Heibeck, S., Jarrar, M., Micke, M., Ostrowski, D., Ehrenreich, H., et al. (2014). Erythropoietin-mediated protection of insect brain neurons involves JAK and STAT but not PI3K transduction pathways. *Neuroscience* 258, 218–227. doi: 10.1016/j.neuroscience.2013.11.020
- Oda, Y., Matsumoto, H., Kurakake, M., Ochiai, M., Ohnishi, A., and Hayakawa, Y. (2010). Adaptor protein is essential for insect cytokine signaling in hemocytes. *Proc. Natl. Acad. Sci. U. S. A.* 107, 15862–15867. doi: 10.1073/pnas.1003785107
- Ostrowski, D., Ehrenreich, H., and Heinrich, R. (2011). Erythropoietin promotes survival and regeneration of insect neurons in vivo and in vitro. *Neuroscience* 188, 95–108. doi: 10.1016/j.neuroscience.2011.05.018
- Ostrowski, D., and Heinrich, R. (2018). Alternative erythropoietin receptors in the nervous system. *J. Clin. Med.* 7:24. doi: 10.3390/jcm7020024
- Pakkianathan, B. C., Singh, N. K., and König, S. (2015). Antiapoptotic activity of 30 kDa lipoproteins family from fat body tissue of silkworm, *Bombyx mori*. *Insect Sci.* 22, 629–638. doi: 10.1111/1744-7917.12119
- Park, H. J., Kim, E. J., Koo, T. Y., and Park, T. H. (2003). Purification of recombinant 30K protein produced in *Escherichia coli* and its anti-apoptotic effect in mammalian and insect cell systems. *Enzym. Microb. Technol.* 33, 466–471. doi: 10.1016/S0141-0229(03)00149-2
- R Core Team (2019). An introduction to dplR. *Ind. Commer. Train.* 10, 11–18.
- Reynolds, S. (2013). “Endocrine system” in *The insects: structure and function*. 5th Edn. eds. S. J. Simpson and A. E. Douglas (Cambridge, UK: Cambridge University Press), 674–707.
- Rhee, W. J., Kim, E. J., and Park, T. H. (2002). Silkworm hemolymph as a potent inhibitor of apoptosis in Sf9 cells. *Biochem. Biophys. Res. Commun.* 295, 779–783. doi: 10.1016/S0006-291X(02)00746-5
- Rhee, W. J., and Park, T. H. (2000). Silkworm hemolymph inhibits baculovirus-induced insect cell apoptosis. *Biochem. Biophys. Res. Commun.* 271, 186–190. doi: 10.1006/bbrc.2000.2592
- Roma, G. C., Bueno, O. C., and Camargo-Mathias, M. I. (2010). Morphophysiological analysis of the insect fat body: a review. *Micron* 41, 395–401. doi: 10.1016/j.micron.2009.12.007
- RStudio Team (2015). RStudio: integrated development for R. Boston, MA: RStudio Inc.
- Sanchez, P. E., Fares, R. P., Risso, J. J., Bonnet, C., Bouvard, S., Morales, A., et al. (2009). Optimal neuroprotection by erythropoietin requires elevated expression of its receptor in neurons. *Proc. Natl. Acad. Sci. U. S. A.* 106, 9848–9853. doi: 10.1073/pnas.0901840106
- Shields, D. C., Harmon, D. L., Nunez, F., and Whitehead, A. S. (1995). The evolution of haematopoietic cytokine/receptor complexes. *Cytokine* 7, 679–688. doi: 10.1006/cyto.1995.0080
- Siren, A.-L., Fratelli, M., Brines, M., Goemans, C., Casagrande, S., Lewczuk, P., et al. (2001). Erythropoietin prevents neuronal apoptosis after cerebral ischemia and metabolic stress. *Proc. Natl. Acad. Sci.* 98, 4044–4049. doi: 10.1073/pnas.051606598

- Siva-Jothy, M. T., Moret, Y., and Rolff, J. (2005). Insect immunity: an evolutionary ecology perspective. *Adv. Insect Phys.* 32, 1–48. doi: 10.1016/S0065-2806(05)32001-7
- Strand, M. R. (2008). The insect cellular immune response. *Insect Sci.* 15, 1–14. doi: 10.1111/j.1744-7917.2008.00183.x
- Sukiban, J., Bräunig, P., Mey, J., and Bui-Göbbels, K. (2014). Retinoic acid as a survival factor in neuronal development of the grasshopper, *Locusta migratoria*. *Cell Tissue Res.* 358, 303–312. doi: 10.1007/s00441-014-1957-y
- Tsuzuki, S., Matsumoto, H., Furihata, S., Ryuda, M., Tanaka, H., Sung, E. J., et al. (2014). Switching between humoral and cellular immune responses in drosophila is guided by the cytokine GBP. *Nat. Commun.* 5, 4628–4628. doi: 10.1038/ncomms5628
- Ueba, H., Brines, M., Yamin, M., Umemoto, T., Ako, J., Momomura, S. I., et al. (2010). Cardioprotection by a nonerythropoietic, tissue-protective peptide mimicking the 3D structure of erythropoietin. *Proc. Natl. Acad. Sci.* 107, 14357–14362. doi: 10.1073/pnas.1003019107
- Uvila, J., Parikka, M., Kleino, A., Sormunen, R., Ezekowitz, R. A., Kocks, C., et al. (2006). Double-stranded RNA is internalized by scavenger receptor-mediated endocytosis in drosophila S2 cells. *J. Biol. Chem.* 281, 14370–14375. doi: 10.1074/jbc.M513868200
- Wang, C., Cao, Y., Wang, Z., Yin, Y., Peng, G., Li, Z., et al. (2007). Differentially-expressed glycoproteins in locusta migratoria hemolymph infected with metarhizium anisopliae. *J. Invertebr. Pathol.* 96, 230–236. doi: 10.1016/j.jip.2007.05.012
- Watari, H., Nakajima, H., Atsumi, W., Nakamura, T., Nanya, T., Ise, Y., et al. (2019). A novel sponge-derived protein thrombocortin is a new agonist for thrombopoietin receptor. *Comp. Biochem. Physiol. C Toxicol. Pharmacol.* 221, 82–88. doi: 10.1016/j.cbpc.2019.04.003
- Weiler, A., Volkenhoff, A., Hertenstein, H., and Schirmeier, S. (2017). Metabolite transport across the mammalian and insect brain diffusion barriers. *Neurobiol. Dis.* 107, 15–31. doi: 10.1016/j.nbd.2017.02.008
- Weishaupt, J. H., Rohde, G., Pölking, E., Siren, A. L., Ehrenreich, H., and Bähr, M. (2004). Effect of erythropoietin axotomy-induced apoptosis in rat retinal ganglion cells. *Investig. Ophthalmol. Vis. Sci.* 45, 1514–1522. doi: 10.1167/iovs.03-1039
- Welchman, D. P., Aksoy, S., Jiggins, F., and Lemaitre, B. (2009). Insect immunity: from pattern recognition to symbiont-mediated host defense. *Cell Host Microbe* 6, 107–114. doi: 10.1016/j.chom.2009.07.008
- Wrighton, N. C., Farrell, F. X., Chang, R., Kashyap, A. K., Barbone, F. P., Mulcahy, L. S., et al. (1996). Small peptides as potent mimetics of the protein hormone erythropoietin. *Science* 273, 458–463. doi: 10.1126/science.273.5274.458
- Wu, Q., Patočka, J., and Kuča, K. (2018). Insect antimicrobial peptides, a mini review. *Toxins* 10:461. doi: 10.3390/toxins10110461
- Wu, Y., Zhang, J., Liu, F., Yang, C., Zhang, Y., Liu, A., et al. (2013). Protective effects of HBSP on ischemia reperfusion and cyclosporine a induced renal injury. *Clin. Exp. Immunol.* 2013:758159. doi: 10.1155/2013/758159
- Yang, F., Xu, Y. P., Li, J., Duan, S. S., Fu, Y. J., Zhang, Y., et al. (2009). Cloning and characterization of a novel intracellular protein P48.2 that negatively regulates cell cycle progression. *Int. J. Biochem. Cell Biol.* 41, 2240–2250. doi: 10.1016/j.biocel.2009.04.022
- Yi, H. Y., Chowdhury, M., Huang, Y. D., and Yu, X. Q. (2014). Insect antimicrobial peptides and their applications. *Appl. Microbiol. Biotechnol.* 98, 5807–5822. doi: 10.1007/s00253-014-5792-6
- Yu, W., Li, Q., Yao, Y., Quan, Y., and Zhang, Y. (2013). Two novel 30K proteins overexpressed in baculovirus system and their antiapoptotic effect in insect and mammalian cells. *Int. J. Genomics* 2013:323592. doi: 10.1155/2013/323592
- Zanetta, J. P., Scior, T., Wantyghem, J., Wermuth, C., Aubery, M., Strecker, G., et al. (1996). Lectin activities of cytokines and growth factors: function and implications for pathology. *Histol. Histopathol.* 11, 1101–1108.
- Zhang, Y., Wang, L., Dey, S., Alnaeeli, M., Suresh, S., Rogers, H., et al. (2014). Erythropoietin action in stress response, tissue maintenance and metabolism. *Int. J. Mol. Sci.* 15, 10296–10333. doi: 10.3390/ijms150610296
- Zhong, B. X., Li, J. K., Lin, J. R., Liang, J. S., Su, S. K., Xu, H. S., et al. (2005). Possible effect of 30K proteins in embryonic development of silkworm *Bombyx mori*. *Acta Biochim. Biophys. Sin.* 37, 355–361. doi: 10.1111/j.1745-7270.2005.00044.x

**Conflict of Interest:** The authors declare that the research was conducted in the absence of any commercial or financial relationships that could be construed as a potential conflict of interest.

Copyright © 2021 Knorr, Hartung, Schneider, Hintz, Pies and Heinrich. This is an open-access article distributed under the terms of the Creative Commons Attribution License (CC BY). The use, distribution or reproduction in other forums is permitted, provided the original author(s) and the copyright owner(s) are credited and that the original publication in this journal is cited, in accordance with accepted academic practice. No use, distribution or reproduction is permitted which does not comply with these terms.

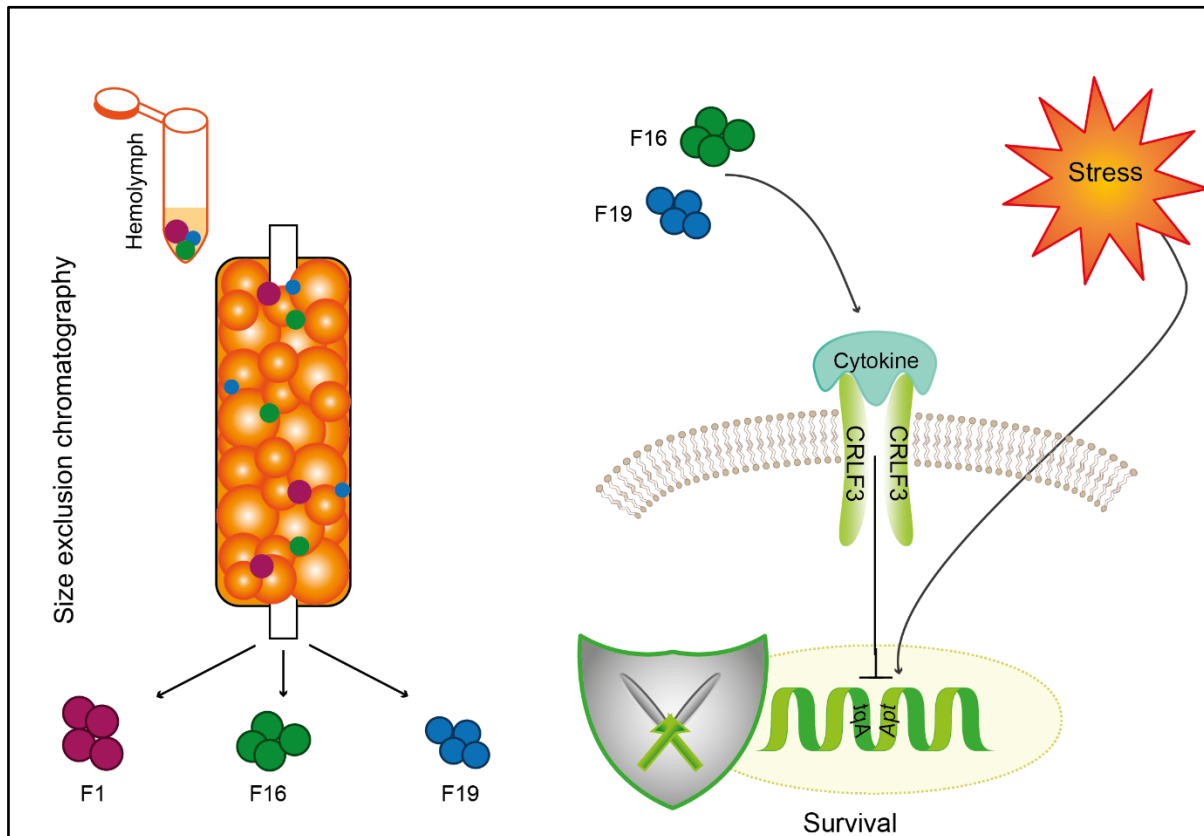
## Chapter 3.1

Follow up to:

### Locust Hemolymph Conveys Erythropoietin-Like Cytoprotection via Activation of the Cytokine Receptor CRLF3

-Preliminary data-

Potential authors: Debra Y. Knorr, Sonja Pribicevic, Denise Hartung, Hendrik Liekefeld and Ralf Heinrich



D. Y. Knorr, D. Hartung, H. Liekefeld and S. Pribicevic performed experiments and analysed the data. D. Y. Knorr and R. Heinrich designed and supervised the study.

#### Author contribution statement

<b>Figure 1</b>	<b>DYK</b> and <b>DH</b> (supervised by <b>DYK</b> ) performed and analysed the experiments
<b>Figure 2</b>	<b>DYK</b> , <b>DH</b> and <b>HL</b> (supervised by <b>DYK</b> ) performed and analysed the experiments
<b>Table 1</b>	<b>DYK</b> identified potential candidate proteins and performed vector cloning
<b>Size exclusion chromatography</b>	SP
<b>Recombinant protein expression</b>	SP



**Follow up to:**  
**Locust Hemolymph Conveys Erythropoietin-Like Cytoprotection via Activation of the Cytokine Receptor CRLF3**

Following our publication on the neuroprotective functions of locust hemolymph (HL), we proceeded our studies to identify endogenous ligands for insect CRLF3. Insect HL is a highly responsive fluid, which reacts rapidly to foreign particles including pathogens and environmental changes by innate immune responses (Hillyer and Christensen, 2002; C. Wang *et al.*, 2007; Welchman *et al.*, 2009; Kingsolver, Huang and Hardy, 2013). Since Erythropoietin (Epo) is upregulated under various types of physiological stress in vertebrates (Li *et al.*, 2020) we first studied whether the cell-protective CRLF3 ligand accumulated in the hemolymph and altered its anti-apoptotic potency in cell survival assays. We exposed adult locusts to hypoxic conditions ( $O_2 < 0,3\%$ ) for 24 h before extracting their HL as described in Chapter 3. HL of untreated locusts was collected for comparison. Primary neuronal cell cultures from juvenile locusts were prepared as described previously and treated with different concentrations of stressed HL (HL Str) before exposure to hypoxia. Control cultures were treated with 10% HL known to suppress hypoxia-induced apoptosis from previous experiments. Interestingly, HL Str concentrations above 0,3% abolished all cells from the respective cultures. Whether cultured neurons died or just escaped from microscopic analysis by detaching from the cover slips during exposure to  $\geq 0,3\%$  HL Str was not determined. However, as displayed in Figure 3.1-1A lower concentrations of HL Str left sufficiently high numbers of cells for analysis and indicated potent neuroprotective effects. As expected from previous experiments, exposure to hypoxia for 36 h significantly reduced the survival of locust primary neurons (median relative survival 0,69 compared to 1 in untreated control). Treatment with both 10% HL and 0,1% HL Str rescued cells from hypoxia-induced apoptosis (HL 1,37; HL Str 1,64 median relative survival). 0,1% HL Str increased cell survival significantly beyond control cultures. It is to be noted that variances between individual experiments were high, indicating even lower standardization of stressed samples compared to control HL. Nonetheless, HL Str elicited similar or even stronger neuroprotective effects than HL at hundred times lower concentration, indicating an upregulation of the endogenous CRLF3 ligand in the hemolymph of the donor locusts. Assuming that hemolymph levels of the CRLF3 ligand might have been enriched during hypoxia to 100 times of normal locusts, toxic effects of higher HL Str concentrations ( $\geq 0,3\%$ ) match the toxic effects of high concentrations of rhEpo on locust and mammalian neurons (Siren *et al.*, 2001; Chong, Kang and Maiese, 2003; Weishaupt *et al.*, 2004; Bonnas *et al.*, 2017; Hahn *et al.*, 2017; Heinrich, Günther and Miljus, 2017). Previous studies have identified hemolymph-contained cytokines and other hormonal factors differentially expressed by physiological insults in insects (C. Wang *et al.*, 2007; Altincicek, Knorr and Vilcinskis, 2008; Kodrik *et al.*, 2015). Besides the previously published similarities (Knorr *et al.*, 2021), this data adds to the similarities between Epo-mediated cell protection in mammals and “CRLF3-ligand”-mediated mechanisms in insects.

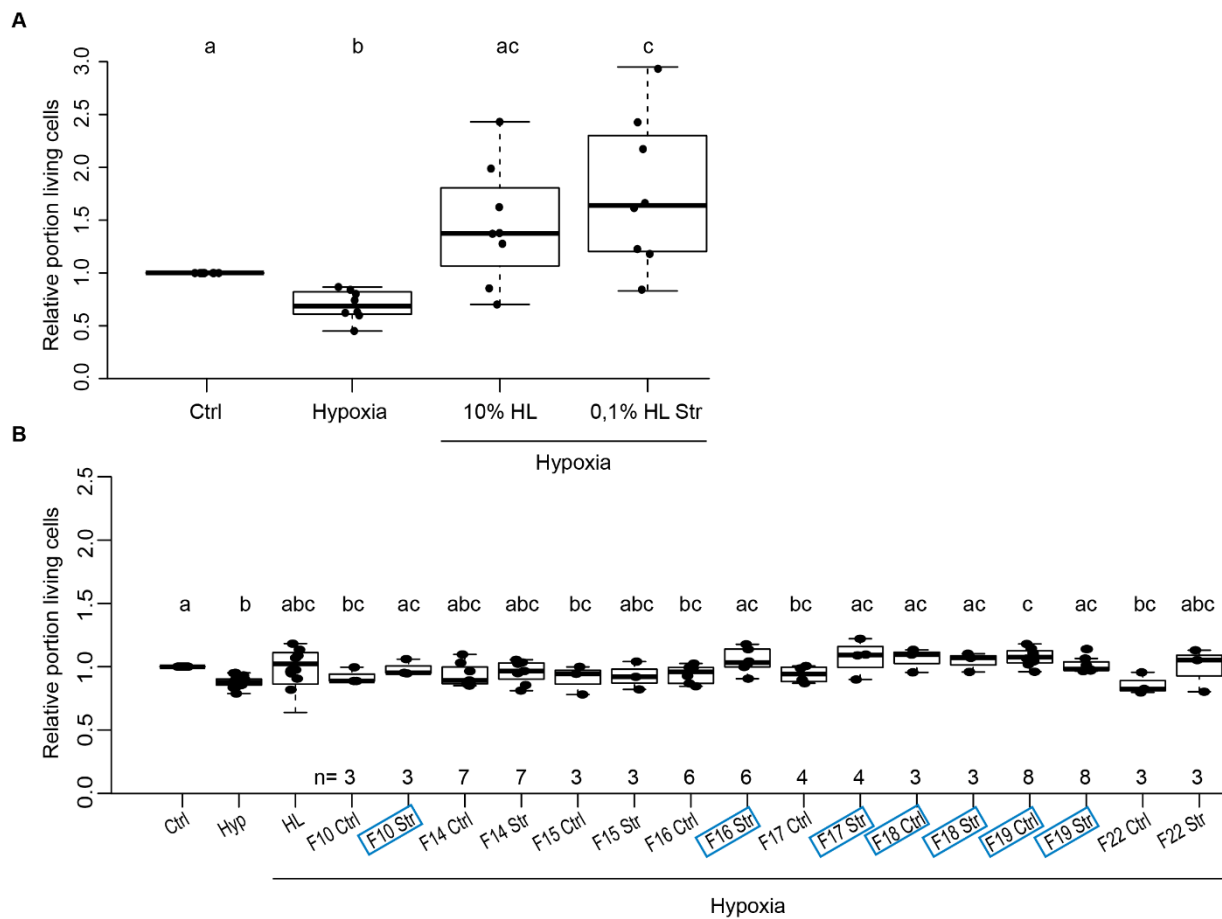


**Figure 3.1-1:** Locust primary neuron cultures are protected from hypoxia-induced apoptosis by locust hemolymph (HL). Cell cultures were maintained for 4 days before being treated with different HL samples. 12 h post treatment, cells were exposed to hypoxic conditions ( $O_2 < 0,3\%$ ) for 36 h before fixation and analysis of cell survival. **A:** 0,1% stressed HL samples (HL Str) protect hypoxia-exposed neurons at least as effectively as 10% HL.  $n=8$ , 52.231 cells analysed in total. **B:** Locust HL was fractionated into samples containing proteins with similar size and complexity by size exclusion chromatography. All Fractions (F) containing proteins below 50 kDa were tested in survival assays. Graph only depicts fractions with  $n \geq 3$ . Fractions from both control and stressed HL were prepared and tested against each other. Blue frames highlight fractions that significantly protected neurons from hypoxia-induced apoptosis.  $n$  (along the x-axis) represents numbers of experiments with the respective fractions. Statistics with pairwise permutation test and Benjamini-Hochberg correction for multiple comparison. Significant differences ( $p < 0.05$ ) are indicated by differing letters.

Insect hemolymph is regarded as a fluid tissue with heterogenous cell types (hemocytes) whose composition may rapidly change in response to various challenges originating from altered internal state or impact by exogenous factors (Hillyer and Christensen, 2002; C. Wang *et al.*, 2007; Welchman *et al.*, 2009; Kingsolver, Huang and Hardy, 2013). Moreover, circulating hemocytes and stationary secretory cells in various tissues release complex blends of chemical signals to monitor and regulate the physiological state of the insect. In order to reduce the complexity of dissolved chemical signals, we performed size exclusion chromatography (SEC) of locust HL in cooperation with Dr. Sonja Pribicevic (Max Planck Institute for Biophysical Chemistry, Dep. for Neurobiology). SEC allows for the separation of proteins within a sample by their size and complexity, resulting in eluted samples that contain proteins with similar topology (Barth and Boyes, 1990). Based on our results from previous studies with denatured HL samples, we selected fractions containing proteins below 50 kDa for further studies. By testing separate fractions from both HL and HL Str, we aimed to narrow the spectrum of potential candidate ligands to a particular size range and identify same-size HL fractions from normal and stressed locusts that differ in their neuroprotective effects. Locust primary cell cultures were treated with either the control or stressed fraction before hypoxia exposure. HL fractions were applied in concentrations estimated from their protein content in the respective HL fraction in relation to the protein content of 10% total (unfractionated) hemolymph, whose neuroprotective potency was previously demonstrated (Fig. 3.1-1A and Knorr *et al.*, 2021). Eleven different HL fractions were tested for neuroprotective effects on primary locust neurons. Figure 3.1-1B depicts data collected for fractions that were tested at

least three times (n varies between 3 – 8) in independent experiments. Hypoxia significantly decreased cell survival as expected from previous studies (median cell survival 0,88). 10% HL increased the survival of hypoxia-exposed neurons to the level of untreated controls (median 1,02), however without reaching significant difference compared to the hypoxia-exposed cultures. The HL sample used for these experiments was newly extracted, which could explain the lower neuroprotective effects of 10% HL in comparison with previous experiments. Fractionated HL samples influenced neuron survival in different ways, ranging from no effect (Fraction 14 [F14] both; Fraction 15 Str [F15 Str]; Fraction 22 Str [F22 str]) to toxic effects (F10 Ctrl; F15 Ctrl; F16 Ctrl; F17 Ctrl; F22 Ctrl). The fractions highlighted in Figure 3.1-1B elicited neuroprotective effects on hypoxia-exposed neurons (F10 Str; F16 Str; F17 Str; F18 both; F19 both). While the repetition numbers for most of the neuroprotective fractions was low, we were able to reach 6 and 8 repetitions for F16 and F19 respectively (individually displayed in Fig 3.1-2A and B). Strikingly, neuroprotective effects of HL fraction F16 differed between F16 extracted from HL of normal animals (median relative survival 0,95) and F16 HL extracted from hypoxia-challenged locusts (median relative survival 1,03; significantly different from hypoxia-exposed cultures). In the case of cell cultures treated with control and stressed F19 HL samples, both fractions elicited significant cytoprotective effects on hypoxia-exposed cells (1,08 and 0,98 median cell survival respectively). This further underlines the dynamic changes occurring in the composition of HL in physiological stressful conditions. Furthermore, it is important to point out that the concentrations used for these experiments were extrapolated but might not have been optimal. In light of our previous studies on concentration-dependant cytoprotective effects of HL, neuroprotective properties follow an optimum-type concentration dependency with too low or too high concentrations being ineffective and very high concentrations mediating toxic effects.

In order to verify that the neuroprotective factors contained in HL fractions F16 Str and F19 mediated their effects via activation of CRLF3, we knocked down CRLF3 expression in primary locust & beetle neurons by soaking RNAi as previously described. It is important to note, that fractions used for this experimental series originated from a new batch of locust HL samples that most likely contained slightly altered composition of solutes compared to the samples used in previous experiments. As shown in Figure 3.1-2C hypoxia significantly decreased locust neuron survival (median survival 0,79) and treatment with F16 Str rescued cells from hypoxia-induced apoptosis (1,1 median survival). Knockdown of CRLF3 abolished the neuroprotective effects of F16 Str treatments (0,87). Hemolymph fraction F19 also protected neurons from hypoxia-induced apoptosis (median survival 1,05), but this effect was not significant though a clear tendency was observed. This protective tendency was absent after knockdown of CRLF3. Survival of hypoxia-exposed F19-treated neurons with reduced CRLF3 expression was as low as in hypoxic control cultures (median relative survival 0,77). In light of the data presented here, it seems likely that both locust HL fractions, F16 Str and F19, contain a CRLF3-activating ligand.

Since locust hemolymph also protected *T. castaneum* neurons via activation of CRLF3 we repeated experiments with locust F16 Str and F19 with beetle neurons. Unfortunately, these experiments provided no statistically significant and hence no conclusive results (Fig. 3.1-2D). A major problem in this experimental series was the lack of significant apoptosis induction by hypoxia-exposure. Nonetheless, some tendencies were observed. Given that no prior experiments with fractions were performed with *T. castaneum* neurons, locust HL was included as internal control for neuroprotection. HL treatment increased survival in comparison to pure hypoxia exposure (median relative survival 0,99 and 0,89 respectively). Treatment with F16 Str also increased cell survival to control level (median survival 1,01). Knock down of CRLF3 slightly reduced cell survival of F16 Str-treated hypoxia-exposed neurons (0,95). F19 only shows slight protective effects with knock down of CRLF3 not altering survival levels (median relative survival 0,97 and 0,97 respectively).

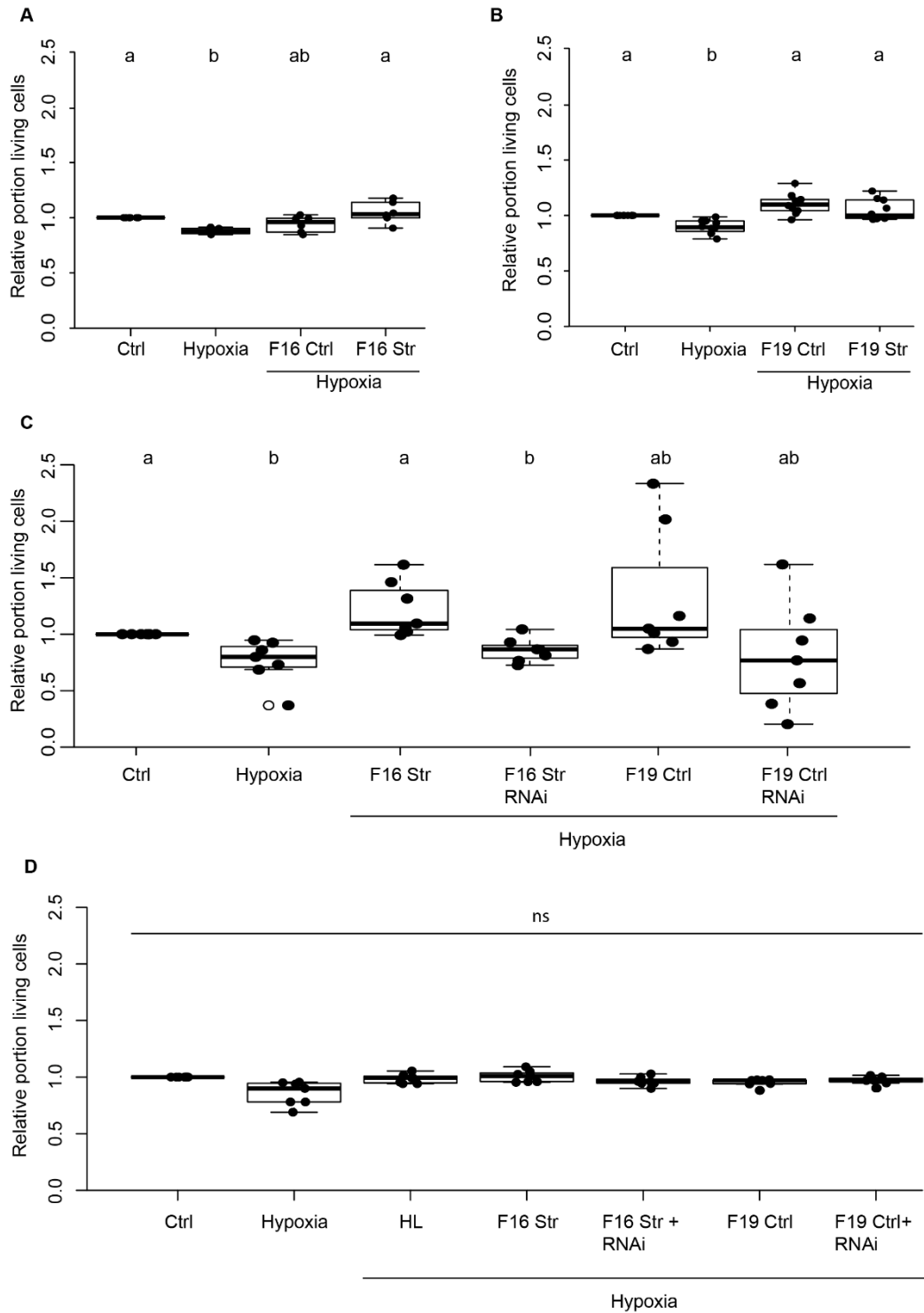


**Figure 3.1-2:** *Locusta migratoria* HL fractions 16 from stressed (Str) and 19 from both control (Ctrl) and Str pools protect locust primary neuron cultures from hypoxia-induced apoptosis. **A:** F16 Str rescues neurons from hypoxia-induced apoptosis while F16 Ctrl only evokes a minor increase of intact neurons.  $n=6$ ; 45.698 cells analysed. **B:** Both Ctrl and Str F19 HL samples protect neurons from hypoxia-induced apoptosis.  $n=7$ ; 50.396 cells analysed. **C:** RNAi-mediated knockdown of CRLF3 in locust neuron cultures prevents the neuroprotective effects of F16 Str. F19 Ctrl mediated a slight but insignificant increase of survival compared to hypoxia-exposed neuron cultures that was reduced after knockdown of CRLF3  $n=7$ ; 80.765 cells analysed. **D:** *T. castaneum* neurons do not show any statistically relevant changes in cell survival when treated with *L. migratoria* HL, F16 Str and F19. Hypoxia evoked an unusually small (not significant) impact on neuron survival. Pre-treatment with HL and F16 seems to rescue cells from hypoxia-induced apoptosis. Knock down of CRLF3 together with F16 treatment slightly reduces cell survival in comparison to sole F16 treatment. F19 treatment does not influence cell survival of hypoxia-exposed beetle neurons.  $n=7$ , 131.396 cells analysed. Statistics with pairwise permutation test and Benjamini-Hochberg correction for multiple comparison. Significant differences between treatment groups are represented by differing letters.

Based on the experiments described above, we hypothesized that the endogenous CRLF3 ligand is an intermediate-size protein, which is upregulated and released in physiologically stressful conditions, potentially to protect locust tissues from stress-induced apoptosis. In order to finalize our hunt for the endogenous, neuroprotective CRLF3 ligand we followed an approach based on ligand fishing by cofloatation assay. We cloned the sequence of locust *CRLF3* (MN245516), previously published in Hahn *et al.* (Hahn *et al.*, 2019), into an pET28a+ expression vector for recombinant expression by Gibson cloning (NEBuilder HiFi DNA Assembly Cloning Kit; New England Biolabs, #E5520). Vector map for the generated expression vector can be found in Supplementary Fig 1 and Fig. 2. Experiments comprising receptor expression and cofloatation assay were performed by Dr. Sonja Pribicevic (Dept. Neurobiology, MPI for Biophysical Chemistry, Göttingen). The basic principle of the cofloatation assay is the integration of the receptor into a artificial liposome, by which it becomes stable and immobile (Jong *et al.*, 2005). Liposome gradients were incubated with either complete *L. migratoria* hemolymph, F16 Str or F19 samples. No ligand could be extracted by receptor binding from either of the applied samples. Failure of this approach might be related to unfunctional ligand-binding regions of improperly membrane-inserted CRLF3 or due to low ligand concentrations within the applied samples.

In another approach to identify the CRLF3 ligand we analysed protective hemolymph fractions by mass spectrometry. We build a database including the *Tribolium castaneum* proteome (*T. castaneum* neurons are protected by locust HL (Knorr *et al.*, 2021)), *Bombyx mori* 30K Proteins (the ligand in question might belong to the same family; see (Knorr *et al.*, 2021)) and all known *L. migratoria* proteins (a full proteome is unfortunately not available). We prepared samples for analysis comprising the neuroprotective fractions F16 Str and F19, the cytotoxic fraction F10 Ctrl and the non-effective fraction F22 Str as controls. We expected to identify hemolymph proteins by their presence in protective fractions and their absence (or reduced levels) in non-protective samples. Results of the mass spectrometry analysis are summarized in Supplementary sub-chapter “Mass spectrometry data”. No matches with any of the *B. mori* 30K proteins were detected. This was not very surprising since cytokines generally share low sequence similarities between organisms (Huisling, Kruiswijk and Flik, 2006; Liongue, Sertori and Ward, 2016). However, it became apparent, that there were some proteins which were only present within the protective fractions but not in the internal control fractions. Table 3.1-1 depicts promising candidate proteins identified by mass spectrometry. Most of these proteins have been reported to elicit immune responses, however the functions of locust Basic 19kDA serum protein, tribolium larval serum protein and locust juvenile binding hormone are poorly characterized (Kanost *et al.*, 1988; Braun and Wyatt, 1996; Reichhart, Gubb and Leclerc, 2011; Wang *et al.*, 2013; Chen *et al.*, 2020; Han *et al.*, 2020).

**Table 3.1-1:** Candidate CRLF3 ligands identified by mass spectrometry and oligonucleotides used for sequence amplification and Gibson cloning.

Organism	Gene	Primer 5'-3'	Gibson Cloning Primer
<i>Lm</i>	Basic 19 kDA serum protein LMIB19KP	GAAGCTGGTGGTGGCT	ATGGGTTCGCGGATCCGTTATGAAGCTGGTG
		GCAG	GTGGCTG
<i>Lm</i>	Basic 19 kDA serum protein LMIB19KP	CTAAGCAGCAACTGCGT	CTTGTCGACGGAGCTCGACTAAGCAGCAAC
		TGTC	TGCGTTGT
<i>Tc</i>	Larval serum protein KQ971363	GAGATTCCTTTTGGTAG	ATGGGTTCGCGGATCCGTTATGAGATTCCTTT
		CTGCC	TGGTAGCTGC
<i>Tc</i>	Larval serum protein KQ971363	TTAGTAGTGGTAGTAGT	CTTGTCGACGGAGCTCGATTAGTAGTGGTA
		CTTG	GTAGTCTTGCTCT
<i>Lm</i>	Serpins 7 MT005549	GGCAACTGAAAAACA	ATGGGTTCGCGGATCCGTTATGGCAACTGAA
		GAAG	AAAACAGAAGC
<i>Lm</i>	Serpins 7 MT005549	CTAATTACAATTTGGAA	CTTGTCGACGGAGCTCGACTAATTACAATTT
		TAC	GGAATACAGATGCGC
<i>Lm</i>	Serpins 5 MT005547	GCTGTACGAGGGCGCG	ATGGGTTCGCGGATCCGTTATGCTGTACGAG
		ACGG	GGCGC
<i>Lm</i>	Serpins 5 MT005547	TATTGCGGAGGCCTTTG	CTTGTCGACGGAGCTCGACTATTGCGGAGG
		TGG	CCTTTGTG
<i>Lm</i>	Immulectin MK250966	GCAGGTGCTACTGCTAC	ATGGGTTCGCGGATCCGTTATGCAGGTGCTA
		TGA	CTGCTACTG

Organism	Gene	Primer 5'-3'	Gibson Cloning Primer
		CTAGGGCAGGATCTCGC AG	CTTGTCGACGGAGCTCGACTAGGGCAGGAT CTCGCAGA
<i>Lm</i>	GNBP3 JF915525	GCGCGCGTCGCCGCTGC TAG TACAGTGCCCACACTTT TAC	ATGGGTTCGCGGATCCGTTATGCGCGCGTCC CC CTTGTCGACGGAGCTCGACTACAGTGCCCA CACTTTTACA
<i>Lm</i>	Juvenile binding hormone U74469	GCAACTTGCTGCTGCTT CTG TGGTAGATGGTGACGG GCTC	ATGGGTTCGCGGATCCGTTAUGGCGGCCUC UGCAACUUGCUGCUGCUUCUG CTTGTCGACGGAGCTCGAGACCCGGTGGTA GATGGTGACGGGCTC
<i>Tc</i>	Uncharact. Protein KQ971310	GAACAGAATTCAGTGG AAATCGAG TCATGACCTGTGTTTTT TCC	ATGGGTTCGCGGATCCGTTATGAACAGAATT CAGTGGAAATCGA CTTGTCGACGGAGCTCGATCATGACCTGTG TTTTTTCCT

To overcome the unsuccessful ligand fishing approach using whole HL fractions, we cloned the sequences for the candidate ligands seen in table 3.1-1 into a pET28a+ expression vector by Gibson cloning. Primers used for this approach can be seen in table 3.1-1. Together with Dr. Sonja Pribicevic we are currently recombinantly expressing these candidates. We will subsequently proceed with the previously mentioned cofloatation approach using recombinantly expressed locust CRLF3. This approach allows us to directly test potential candidates at appropriate concentrations for the assay.

Even though we have not yet identified the endogenous insect CRLF3 ligand, we can make a well based approximation of its nature. Our data points towards an intermediate-size cytokine, which is positively regulated by physiological stress and released into the hemolymph of *L. migratoria*. We know, that the locust cell-protective ligand is sufficiently conserved to activate both locust and beetle CRLF3 and mediate neuroprotection in both insects. Searching for cytokines and cytokine receptors by sequence comparison is problematic resulting from generally low sequence conservation between different organisms and functional assays are complicated by low selectivity of particular cytokines for their receptors (Huisling, Kruiswijk and Flik, 2006; Liongue, Sertori and Ward, 2016). Moreover, the main organism which is used in our studies, the migratory locust, does not have a fully annotated genome or proteome, making sequence searches and comparisons challenging. Nonetheless, many cytokines, especially those related to immune responses, have been described in invertebrates (Beschin *et al.*, 2001; Ottaviani, Malagoli and Franchini, 2004). There is mounting evidence, that cytokine signalling evolved early in animal evolution and has been adapted and expanded to face varying physiological insults and life circumstances in different taxa (Liongue, Sertori and Ward, 2016). It is likely, that the ligand in question might be immune-related, given the evidence that it is differentially regulated in harmful conditions. Similar to vertebrate Epo, it seems to be upregulated to maintain functionality of cells and tissues under challenging conditions (Li *et al.*, 2020). Identification of the endogenous CRLF3 ligand will not only help us understand the modes of neuroprotective actions elicited by the receptor, but also play a great role in understanding the evolution of neuroprotective cytokine signalling.

## **References**

- Altincicek, B., Knorr, E. and Vilcinskis, A. (2008) 'Beetle immunity: Identification of immune-inducible genes from the model insect *Tribolium castaneum*', *Developmental and Comparative Immunology*, pp. 585–595. doi: 10.1016/j.dci.2007.09.005.
- Barth, H. G. and Boyes, B. E. (1990) 'Size Exclusion Chromatography', *Analytical Chemistry*, 62(12), pp. 268–303. doi: 10.1021/ac00211a020.
- Beschin, A. et al. (2001) 'On the existence of cytokines in invertebrates', *Cellular and Molecular Life Sciences*, 58(5–6), pp. 801–814. doi: 10.1007/PL00000901.
- Bonnas, C. et al. (2017) 'EV-3 , an endogenous human erythropoietin isoform with distinct functional relevance', *Scientific Reports*, 7(3684), pp. 1–15. doi: 10.1038/s41598-017-03167-0.
- Braun, R. P. and Wyatt, G. R. (1996) 'Sequence of the hexameric juvenile hormone-binding protein from the hemolymph of *Locusta migratoria*', *Journal of Biological Chemistry*. © 1996 ASBMB. Currently published by Elsevier Inc; originally published by American Society for Biochemistry and Molecular Biology., 271(49), pp. 31756–31762. doi: 10.1074/jbc.271.49.31756.
- Chen, J. et al. (2020) 'Serpin7 controls egg diapause of migratory locust (*Locusta migratoria*) by regulating polyphenol oxidase', *FEBS Open Bio*, 10(5), pp. 707–717. doi: 10.1002/2211-5463.12825.
- Chong, Z. Z., Kang, J. Q. and Maiese, K. (2003) 'Erythropoietin fosters both intrinsic and extrinsic neuronal protection through modulation of microglia, Akt1, Bad, and caspase-mediated pathways', *British Journal of Pharmacology*, 138(6), pp. 1107–1118. doi: 10.1038/sj.bjp.0705161.
- Hahn, N. et al. (2017) 'The Insect Ortholog of the Human Orphan Cytokine Receptor CRLF3 Is a Neuroprotective Erythropoietin Receptor', *Front. Mol. Neurosci.*, 10(July), pp. 1–11. doi: 10.3389/fnmol.2017.00223.
- Hahn, N. et al. (2019) 'The Orphan Cytokine Receptor CRLF3 Emerged With the Origin of the Nervous System and Is a Neuroprotective Erythropoietin Receptor in Locusts', *Frontiers in Molecular Neuroscience*. Frontiers Media S.A., 12. doi: 10.3389/fnmol.2019.00251.
- Han, P. et al. (2020) '20-Hydroxyecdysone enhances Immulectin-1 mediated immune response against entomogenous fungus in *Locusta migratoria*', *Pest Management Science*, 76(1), pp. 304–313. doi: 10.1002/ps.5515.
- Heinrich, R., Günther, V. and Miljus, N. (2017) 'Erythropoietin-Mediated Neuroprotection in Insects Suggests a Prevertebrate Evolution of Erythropoietin-Like Signaling', in *Vitamins and Hormones*. Academic Press Inc., pp. 181–196. doi: 10.1016/bs.vh.2017.02.004.
- Hillyer, J. F. and Christensen, B. M. (2002) 'Characterization of hemocytes from the yellow fever mosquito , *Aedes aegypti*', pp. 431–440. doi: 10.1007/s00418-002-0408-0.
- Huising, M. O., Kruiswijk, C. P. and Flik, G. (2006) 'Phylogeny and evolution of class-I helical cytokines', *Journal of Endocrinology*, 189(1), pp. 1–25. doi: 10.1677/joe.1.06591.
- Jong, L. A. A. De et al. (2005) 'Receptor – ligand binding assays : Technologies and Applications', 829, pp. 1–25. doi: 10.1016/j.jchromb.2005.10.002.
- Kanost, M. R. et al. (1988) 'Gene structure, cDNA sequence, and developmental regulation of a low molecular weight hemolymph protein from *Locusta migratoria*', *Archives of Insect Biochemistry and Physiology*, 8(4), pp. 203–217. doi: 10.1002/arch.940080402.
- Kingsolver, M. B., Huang, Z. and Hardy, R. W. (2013) 'Insect antiviral innate immunity: Pathways, effectors, and connections', *Journal of Molecular Biology*. Elsevier Ltd, 425(24), pp. 4921–4936. doi: 10.1016/j.jmb.2013.10.006.
- Knorr, D. Y. et al. (2021) 'Locust Hemolymph Conveys Erythropoietin-Like Cytoprotection via Activation of the Cytokine Receptor CRLF3', *Frontiers in Physiology*, 12(April). doi: 10.3389/fphys.2021.648245.
- Kodrík, D. et al. (2015) 'Hormonal regulation of response to oxidative stress in insects—an update', *International Journal of Molecular Sciences*. MDPI AG, pp. 25788–25817. doi: 10.3390/ijms161025788.
- Li, J. et al. (2020) 'HIF-1 $\alpha$  attenuates neuronal apoptosis by upregulating EPO expression following cerebral ischemia-reperfusion injury in a rat MCAO model', *International Journal of Molecular Medicine*, 45(4), pp. 1027–1036. doi: 10.3892/ijmm.2020.4480.
- Liongue, C., Sertori, R. and Ward, A. C. (2016) 'Evolution of Cytokine Receptor Signaling', *The Journal of Immunology*, 197(1), pp. 11–18. doi: 10.4049/jimmunol.1600372.
- Ottaviani, E., Malagoli, D. and Franchini, A. (2004) 'Invertebrate humoral factors: cytokines as mediators of cell survival.', *Progress in molecular and subcellular biology*, 34, pp. 1–25. doi: 10.1007/978-3-642-18670-7\_1.

- Reichhart, J. M., Gubb, D. and Leclerc, V. (2011) *The Drosophila serpins: Multiple functions in immunity and morphogenesis*. 1st edn, *Methods in Enzymology*. 1st edn. Elsevier Inc. doi: 10.1016/B978-0-12-386471-0.00011-0.
- Siren, A.-L. et al. (2001) 'Erythropoietin prevents neuronal apoptosis after cerebral ischemia and metabolic stress', *Proceedings of the National Academy of Sciences*, 98(7), pp. 4044–4049. doi: 10.1073/pnas.051606598.
- Wang, C. et al. (2007) 'Differentially-expressed glycoproteins in *Locusta migratoria* hemolymph infected with *Metarhizium anisopliae*', *Journal of Invertebrate Pathology*, 96(3), pp. 230–236. doi: 10.1016/j.jip.2007.05.012.
- Wang, Y. et al. (2013) 'Altered Immunity in Crowded Locust Reduced Fungal (*Metarhizium anisopliae*) Pathogenesis', *PLoS Pathogens*, 9(1). doi: 10.1371/journal.ppat.1003102.
- Weishaupt, J. H. et al. (2004) 'Effect of erythropoietin axotomy-induced apoptosis in rat retinal ganglion cells', *Investigative Ophthalmology and Visual Science. The Association for Research in Vision and Ophthalmology*, 45(5), pp. 1514–1522. doi: 10.1167/iovs.03-1039.
- Welchman, D. P. et al. (2009) 'Insect Immunity: From Pattern Recognition to Symbiont-Mediated Host Defense', in *Cell Host and Microbe*. Cell Press, pp. 107–114. doi: 10.1016/j.chom.2009.07.008.

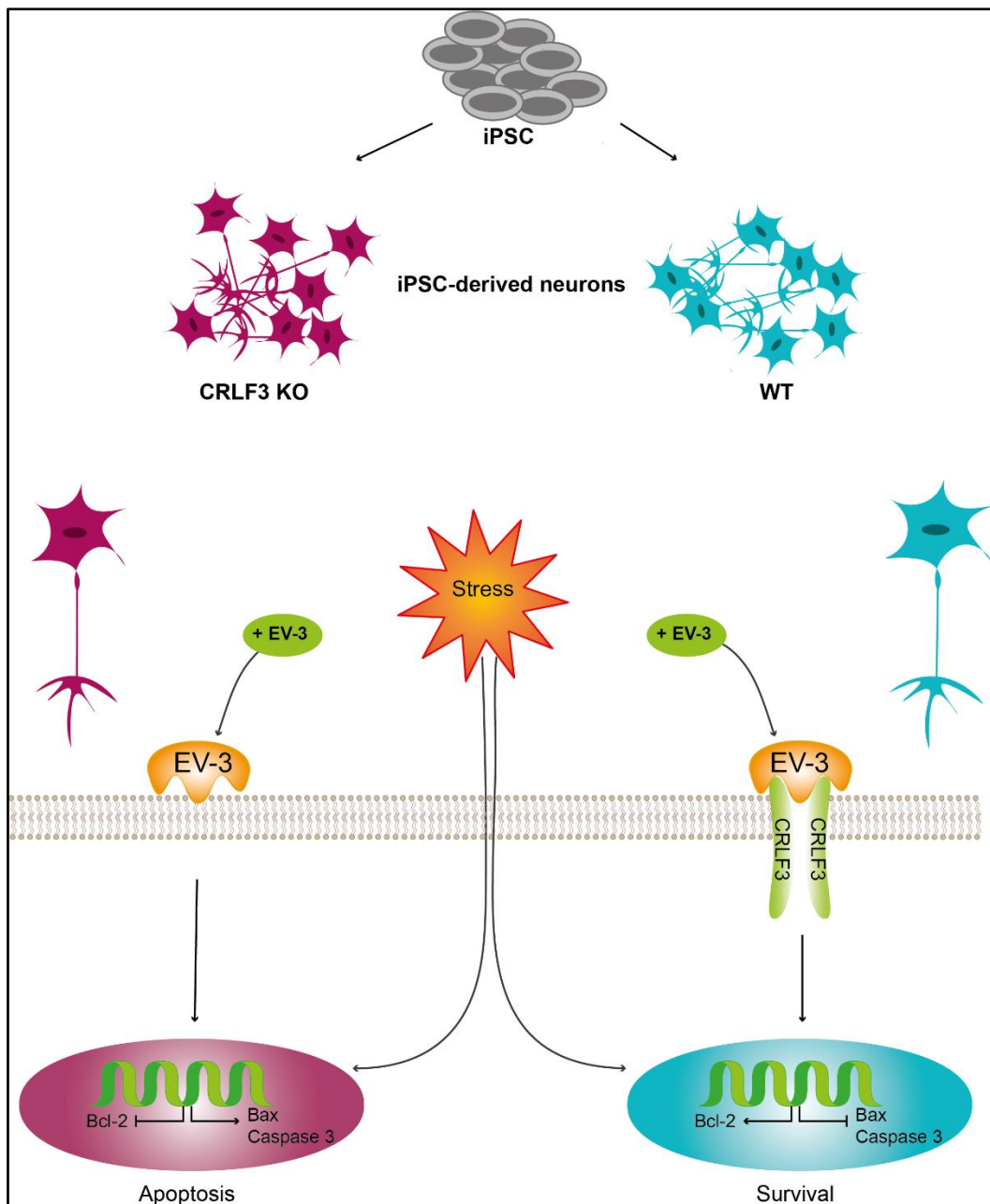


## Chapter 4

Human CRLF3 is a neuroprotective EV-3 (Epo) receptor

Debra Y. Knorr, Ignacio Rodriguez Polo, Hanna S. Pies, Nicola Schwedhelm-Domeyer, Stephanie Pauls, Rüdiger Behr and Ralf Heinrich

- Submitted -



D. Y. Knorr, I. Rordriguez Polo, H. S. Pies, N. Schwedhelm-Domeyer and S. Pauls collected the data. D. Y. Knorr, I. Rordriguez Polo and H. S. Pies, analysed the experiments. D. Y. Knorr, I. Rordriguez Polo, R. Behr and R. Heinrich designed the study. D. Y. Knorr and R. Heinrich wrote and edited the manuscript. All authors read and approved of the final manuscript.

**Author contribution statement**

<b>Figure 1</b>	IRP performed vector cloning, nucleofection and single cell sorting of mutated lines; <b>DYK</b> analysed and characterized mutated lines
<b>Figure 2</b>	<b>DYK</b> and HSP (supervised by <b>DYK</b> ) performed and imaged the stainings
<b>Figure 3</b>	<b>DYK</b> performed and analysed the experiments
<b>Figure 4</b>	<b>DYK</b> performed and analysed the experiments
<b>Supp. Figure 2</b>	<b>DYK</b> analysed differentiation efficiency
<b>Supp. Figure 3</b>	HSP (supervised by <b>DYK</b> ) performed and imaged the stainings
<b>Supp. Figure 4</b>	<b>DYK</b> and HSP (supervised by <b>DYK</b> ) performed and analysed the experiments
<b>Supp. Figure 5</b>	<b>DYK</b> performed and analysed the experiments
<b>Experimental design</b>	<b>DYK</b> , IRP, RB and RH
<b>Manuscript writhing</b>	<b>DYK</b> and RH with contribution of all authors

## **Title**

Human CRLF3 is a neuroprotective EV-3 (Epo) receptor

## **Authors**

Debra Y. Knorr<sup>1</sup>, Ignacio Rodriguez Polo<sup>2,3,4</sup>, Hanna S. Pies<sup>1</sup>, Nicola Schwedhelm-Domeyer<sup>1</sup>, Stephanie Pauls<sup>1</sup>, Rüdiger Behr<sup>3,4</sup>, and Ralf Heinrich<sup>1,\*</sup>

## **Affiliations**

<sup>1</sup> Johann-Friedrich-Blumenbach Institute for Zoology and Anthropology, Georg-August University Göttingen

<sup>2</sup> Göttingen Center for Molecular Biosciences, Department of Developmental Biology, Georg-August University Göttingen

<sup>3</sup> Research Platform Degenerative Diseases, German Primate Center – Leibniz Institute for Primate Research, Göttingen, Germany

<sup>4</sup> German Center for Cardiovascular Research (DZHK), Partner Site Göttingen, Göttingen, Germany

\* Materials and Corresponding author; rheinri1@gwdg.de

## **Author contributions**

DYK, IRP, RB and RH designed and supervised the study. DYK, IPR, HSP, SP, NSD performed experiments. DYK, IRP and HSP analysed the data. DYK, IRP and RH wrote the manuscript. All authors read and approved of the manuscript.

## **Acknowledgements**

We thank Stoyan Petkov for help with neuronal differentiation protocols and intellectual input and Martin C. Göpfert for financial support. We furthermore thank Epomedics for providing EV-3. This work was supported by the Deutsche Forschungsgemeinschaft (DFG; Project number: 398214842 and 499371712).

**Abstract**

The orphan cytokine receptor like factor 3 (CRLF3) has only recently been implied in mammalian disease and insect neuroprotection. While specific functions and characterization for the receptor are elusive, experimental evidence point toward a crucial role in cell homeostasis. Erythropoietin (Epo), first described within the vertebrate hematopoietic system, is widely accepted as a cytoprotective cytokine. While erythropoietic mechanisms of Epo administration are well understood, cytoprotective mechanisms remain widely unknown. A major limitation for studying Epo-mediated neuroprotection is the absence of an Epo-responsive receptor. In the presented study, we aimed to unravel the importance of CRLF3 in Epo-mediated neuroprotection in humans. We generated *CRLF3* knock-out iPSC lines and differentiated them towards the neuronal lineage. We treated the output neuron-like cells with the naturally occurring human Epo splice variant EV-3 to avoid activation of the classical Epo receptor. Our data demonstrates the crucial involvement of CRLF3 in EV-3 mediated neuroprotection of human neuron-like cells. In the absence of functional CRLF3 protein, no neuroprotective effects of EV-3 treatment could be observed. The data presented here is the first evidence that CRLF3 is an EV-3 (and by this Epo) responsive receptor in humans, with its activation resulting in neuroprotection of human neuron-like cells.

## **Introduction**

The helical cytokine erythropoietin (Epo) is a major kidney-derived hormonal regulator of vertebrate hematopoiesis, protecting erythroid progenitor cells from apoptosis (Jelkmann and Metzen, 1996; Constantinescu, Ghaffari and Lodish, 1999; Lundby and Olsen, 2011). Local expression and release of Epo has been described for various tissues including brain, liver and lung and numerous studies reported its cytoprotective and regenerative functions in these and other tissues (reviewed in (Ghezzi and Brines, 2004; Chateauvieux *et al.*, 2011; Zhang *et al.*, 2014). With respect to the nervous system, Epo is crucial for normal brain development, acts neuroprotectively after hypoxic/ischemic and other toxic insults and promotes regeneration after axonal damage (Morishita *et al.*, 1996; Yu *et al.*, 2002; Genc, Koroglu and Genc, 2004; Kretz *et al.*, 2005). Beneficial functions also included enhanced cognitive performance and memory functions in healthy humans and patients affected by schizophrenia and mood disorders (Miskowiak, O'Sullivan and Harmer, 2007; Miskowiak *et al.*, 2008, 2016; Kästner *et al.*, 2012). Clinical studies explored the potential of Epo to interfere with cell loss in neurodegenerative diseases including Alzheimer's disease, Parkinson's disease and amyotrophic lateral sclerosis (Maiese, Chong and Shang, 2008; Chong *et al.*, 2013; Rey *et al.*, 2019). A drawback of prolonged and/or high dose Epo administration is the overproduction of erythrocytes leading to increased risk of thrombosis, stimulation of cancerogenic cell proliferation and tumor vascularization all resulting from activation of homodimeric classical EpoR (Hardee *et al.*, 2006; Ehrenreich *et al.*, 2009; Pedroso *et al.*, 2012; Cao, 2013). Studies with Epo-mimetics (some with partial sequence similarity, others with rather unrelated structure compared to full Epo) have demonstrated neuroprotective and regenerative effects without activation of homodimeric EpoR (Leist *et al.*, 2004; Brines *et al.*, 2008; Ueba *et al.*, 2010; Wu *et al.*, 2013). Some of these may activate a heteroreceptor consisting of EpoR and  $\beta$  common receptor (synonym CD131), which mediates neuroprotection in some but not all brain regions (Brines *et al.*, 2004; Nadam *et al.*, 2007; Pascal E. Sanchez *et al.*, 2009; Chamorro *et al.*, 2013; Miller *et al.*, 2015; Ding *et al.*, 2017). The naturally occurring Epo splice variant EV-3, characterized by the lack of exon 3, mediates neuroprotection independent of both homodimeric and heteromeric EpoR suggesting that additional alternative neuroprotective receptors for Epo-like signals exist in the mammalian brain (Bonnas *et al.*, 2017; Ostrowski and Heinrich, 2018).

Studies on insects demonstrated that both, human recombinant Epo and EV-3 increased the survival of hypoxia- or toxin-challenged cells by activation of cytokine receptor-like factor 3 (CRLF3) (Miljus *et al.*, 2014, 2017; Hahn *et al.*, 2017; Hahn, Büschgens, Schwedhelm-Domeyer, Bank, Bart R. H. Geurten, *et al.*, 2019) suggesting that CRLF3 might be a general neuro- or tissue-protective receptor for Epo-like cytokines across species. CRLF3 is a cytokine receptor that belongs to group 1 of cytokine type I receptors, together with classical EpoR, thrombopoietin receptor, prolactin receptor and growth hormone receptor (Boulay, O'Shea and Paul, 2003; Liongue and Ward, 2007; Hahn, Büschgens, Schwedhelm-Domeyer, Bank, Bart R. H. Geurten, *et al.*, 2019). CRLF3 is highly conserved and present in all major eumetazoan taxa including cnidarians, various invertebrates and vertebrates including humans. Nonetheless, CRLF3 remains poorly characterized and is listed as an orphan cytokine receptor since no endogenous CRLF3 ligand has so far been identified in any species (insects do not possess orthologs of Epo). Human CRLF3 is expressed in most tissues including the nervous system and contains the characteristic cytokine receptor motif (WSXWS), a single-pass transmembrane region and a Janus kinase docking site (Boulay, O'Shea and Paul, 2003; Hahn *et al.*, 2017). Without revealing underlying mechanisms, CRLF3 has been associated with the regulation of proliferation, differentiation and cell survival (Hashimoto *et al.*, 2012; Wegscheid *et al.*, 2021). Increased CRLF3 levels have been detected in tumours and various tumour cell lines (Dang *et al.*, 2006; Yang *et al.*, 2009) and sequence alterations have been linked to amyotrophic lateral sclerosis (ALS) (Cirulli *et al.*, 2015), autism spectrum disorders (Wegscheid *et al.*, 2021) and sensitivity to *Leishmania* infections (Castellucci *et al.*, 2021).

In light of highly conserved *CRLF3* orthologues in insects and mammals, we hypothesized that Epo also mediates cell-protective functions via activation of CRLF3 in human neurons. To study whether

Epo/CRLF3-signalling protects human neurons from stress-induced apoptosis we established survival assays with human induced pluripotent stem cell- derived neurons.

Induced pluripotent stem cells (iPSC), that can give rise to various cell types upon exposure to appropriate differentiation protocols, harbour great potential for biomedical research and disease modelling (Rodriguez-Polo *et al.*, 2019; Stauske *et al.*, 2020; Doss and Sachinidis, 2019; Wiegand and Banerjee, 2019). We generated *CRLF3* knock out (KO) iPSC lines along with isogenic control lines (Ig-Ctrl) from two independent human iPSC lines by means of a Piggy-Bac-CRISPR-Cas9 system and differentiated them into neuron-like cells. Apoptosis was induced through “chemical hypoxia” by addition of rotenone, an inhibitor of complex I of the mitochondrial electron transport chain. CRLF3 was stimulated with the natural human Epo splice variant EV-3 to prevent coactivation of homodimeric EpoR or EpoR/  $\beta$ cR (Bonnas *et al.*, 2017). We demonstrate that EV-3 protects WT and Ig-Ctrl iPSC-derived neurons from rotenone-induced apoptosis. In contrast, *CRLF3*-KO neurons were not protected, indicating that CRLF3 serves as neuroprotective receptor for EV-3 in human neurons. The results of our study deorphanize human CRLF3 by identifying EV-3 (and most likely also Epo) as a natural ligand. Moreover, we show that EV-3/CRLF3 signalling mediates protection of human cells indicating that CRLF3 can be selectively targeted by Epo-like ligands to counteract neurodegenerative diseases without simultaneously promoting inappropriate erythropoiesis and tumor growth.

## **Methods**

Experiments were conducted with two human iPSC lines. iPSC were generated from commercially available human fibroblasts originating from a female and a male patient (referred to from now as iPSC#1 and iPSC#2 respectively; Lonza CC-2511, lot 0000490824 [iPSC#1], and lot 0000545147 [iPSC#]). Reprogramming was performed according to Okita et al. (Okita *et al.*, 2011). iPSC characterization was described in Stauske et al. (Stauske, Rodriguez Polo, *et al.*, 2020). Human iPSC were maintained at 37°C, 5% CO<sub>2</sub> in Universal primate pluripotent stem cell medium (UPPS medium), and cell splitting was performed using Versene solution (Thermo Fisher Scientific; #15040066) according to Stauske et al. (Stauske, Rodriguez Polo, *et al.*, 2020). iPSC were cultured on Geltrex-coated 6 cm or 12- well dishes (Thermo Fisher; A1413202). For all molecular analysis described below, cells (both iPSC and iPSC-derived neurons) were washed twice in Phosphate buffered saline (PBS) before being scraped (Cell scraper, Sarstedt; #833945040) and collected in an 1,5 ml Eppendorf tube. Cell suspensions were centrifuged at 12.000 x g for 2 min. PBS was removed and cell pellets snap-frozen in liquid nitrogen. Samples were stored at -80°C until further analysis.

### ***Establishment and characterization of transgenic lines***

The KO lines were generated according to Rodríguez-Polo et al. (Rodríguez-Polo *et al.*, 2021), following a constitutive Cas9-gRNA expression strategy. In brief, cells were nucleofected with a piggyBac-CRISPR-Cas9-GFP vector carrying a guide RNA (gRNA) specifically targeting *CRLF3* (see Table 1) and a second vector carrying Transposase-dtTomato, (Pac-PB-Tomato) (Debowski *et al.*, 2015). In parallel, a different subset of cells was transfected with an empty piggyBac-CRISPR-Cas9 (no gRNA) construct in order to generate isogenic control (Ig-Ctrl) lines. After transfection the GFP positive (Cas9-GFP-gRNA positive) population was sorted by Fluorescence assisted cell sorting (FACS; Sony Flow Cytometry FACS SH800S). The presence of INDEL mutations in the polyclonal population was evaluated using PCR (Primer sequences see Table 1) in combination with T7 endonuclease I assay and Sanger sequencing. For the generation of the *CRLF3* KO monoclonal lines, polyclonal populations were single-cell sorted into a 96-well plate, expanded and genotyped. Presence of the transgene was evaluated by GFP expression using a Zeiss Observer Fluorescent microscope (Carl Zeiss, #4001584). Successful introduction of loss-of-function mutations was evaluated in the monoclonal lines amplifying the targeted locus by PCR, subcloning the product in pCRII vector (TA cloning kit; Thermo Fisher Scientific # K207020), transforming the vector into competent *E.coli*, and sequencing by Sanger (20 bacterial clones per cell line analysed). Subsequent sequence analysis revealed allele-specific variations in each one of the iPSC clones. Additionally, protein depletion from mutated iPSC and iPSC-neurons was confirmed by Western blot (see below).

### ***Genomic DNA extraction and PCR***

Genomic DNA (gDNA) was extracted using DNeasy Blood & Tissue Kit (Qiagen; #69504) according to the manufacturer's instructions. The gRNA target site was amplified using specific primers as stated below (Table 1). PCR was run using GoTaq Green Master Mix (Promega; #M7122) and PCR program was set as shown in Table 2. PCR products were loaded on a 1% agarose gel and run for 30 min at 100 V before extracting DNA fragments using Macherey–Nagel NucleoSpin Gel and PCR Clean-up Kit (Macherey–Nagel; #740609.50). The isolated DNA fragments were subsequently either sent for sequencing using specific PCR primers (for Polyclonal approach; Sequencing facility Microsynth AG, Göttingen, Germany) or cloned into a pCRII vector for allele characterization (for clonal expansion).

**Table 5:** Oligonucleotides

Application	Gene	Oligonucleotide 5'-3'	Tm	Accession number
gRNA	CRLF3-guide 1 fwd	CACCGAAAGGCCTCGCACATTCAGT		ENSP00000318804.6
gRNA	CRLF3-guide 1 rev	AAACACTGAATGTGCGAGGCCTTTC		
PCR	CRLF3-Guide1-fwd	CCCTGGGCTTTCTGCTTTGC	61°C	
PCR	CRLF3-Guide1-rev	ACCACGCATGGTCTGAAAACC		
qPCR	CRLF3 fwd	CAACGTTGGGGTCTATGTGC	61°C	
qPCR	CRLF3 rev	CGCCCACCAAGTACAGATAGA		
qPCR	Bax-fwd	CGAGTGGCAGCTGACATGTT	61°C	ENST00000293288.12
qPCR	Bax-rev	TCCAGCCCATGATGGTTCTG		
qPCR	Caspase 3-fwd	GGAGGCCGACTTCTTGTATG	61°C	ENST00000308394.9
qPCR	Caspase 3-rev	TGCCACCTTTCGGTTAACCC		
qPCR	BCL-2-fwd	CGTTATCCTGGATCCAGGTG	61°C	ENST00000398117.1
qPCR	BCL-2-rev	GTGTGTGGAGAGCGTCAAC		
qPCR	bActin-fwd	GCGAGAAGATGACCCAGATC	61°C	ENST00000674681.1
qPCR	bActin-rev	GGGCATACCCCTCGTAGATG		

**Table 6:** PCR program for *CRLF3* amplification

Step	Temperature [°C]	Time [sec]	Cycle
Initial denaturation	95	180	
Denaturation	95	30	
Annealing	61	30	x30
Elongation	72	30	
Final elongation	72	300	

### Transformation

pCRII vectors carrying PCR products of single-cell clones were transformed into XL1-blue competent cells (Agilent; #200249). 500 ng plasmid were carefully mixed with 100  $\mu$ l of competent cells and let to rest on ice for 30 min. Subsequently, cells received a heat shock at 42°C for 40 sec before 900  $\mu$ l super optimal broth (SOB) (Roth; #AE27.1) without antibiotics was added. Cell suspension was transferred into a bacterial incubator for 1 h at 37°C, 225 rpm. Afterwards, cell suspension was centrifuged at 3000 x g for 2 min, supernatant was removed, and cells were resuspended in 100 ml SOB medium before being dispersed on LB agar plates + ampicillin (Sigma-Aldrich; #L2897). Plates were let to rest at room temperature (RT) for 10 min before being transferred to 37°C.



*Western blot*

Cell pellets were lysed in protein lysis buffer (150mM NaCl; 20mM Tris.HCl pH 7.5; 1mM EDTA; 1% Triton-X-100) + Protease inhibitor (Thermo Fisher Scientific; #78429) by vigorous shaking in a tissue lyser (Qiagen; #85300) for 3 min at 50 Hz. Subsequently, the lysates were transferred onto ice and incubated for 30 min. Cell lysate was centrifuged at 10.000 x g for 10 min at 4°C and the protein containing supernatant was transferred to a fresh Eppendorf tube. Protein concentration was measured by Bradford assay (PanReac AppliChem; #A6932,0500). For all Western blots run in this study 50 µg protein was denatured in 2X Lämmli buffer (Sigma-Aldrich; #S3401) at 95°C for 5 min. 10% SDS-Pages were run for 30 min at 70 V and 1 h at 120 V. For size reference, PageRuler Plus Prestained Protein ladder (Thermo Fisher Scientific; #26619) was loaded together with samples. The separated protein was transferred onto nitrocellulose membranes (Roth; #9200.1) in a wet blot approach for 1,5 h at 180 mA. Membranes were incubated in Ponceau S (Sigma-Aldrich; #P3504) in order to check for sufficient and successful protein transfer before being blocked in 5% Milk/ PBS-0,1% Tween-20 (PBST) for 30 min at room temperature (Milk Roth; #T145; Tween-20 PanReac AppliChem; #A7564). Membranes were probed for CRLF3 (see antibody list for dilutions in table 3) either at RT for 2 h or overnight at 4°C. Subsequently, membranes were washed 3 times in PBST before incubation in  $\alpha$ -HRP solution for 30 min at RT. Membranes were imaged by incubation in Pierce ECL Western blotting substrate (Thermo Fisher Scientific; #32209) using iBright CL1500 Imaging System (Thermo Fisher Scientific; #A44114). Subsequently, membranes were stripped in 0,5 M NaOH for 3 min, washed 3 times in PBS before being blocked again. Membranes were incubated in  $\alpha$ Tubulin (see table 3) for 1 h at RT before incubation with the secondary  $\alpha$ -HRP antibody and imaging. Quantification of protein band intensities was performed using ImageJ. Band intensities were normalized to the corresponding  $\alpha$ Tubulin band intensity of each sample and then towards control samples within treatment groups. Data is shown as bar plots representing the average band intensities measured together with the calculated standard deviation and single data points.

*Transgenic iPSC characterization*

To confirm pluripotency of the newly generated transgenic lines (namely CRLF3 KO and corresponding Ig Ctrl of iPSC#1 and #2) we stained for pluripotency markers NANOG and OCT4A (see antibody list in table 3). iPSC were grown on 2 cm glass coverslips (Menzel-Gläser, #CB00200RA1) and fixed when confluent in 4% Paraformaldehyde (PFA) for 30 min. Coverslips were subsequently washed 3x in PBS before being blocked in 0,5 % bovine serum albumin (BSA; Thermo Fisher Scientific, #15260037) either for 30 min at RT or longer at 4°C. Cells were washed again 3 times in PBS and subsequently incubated with primary antibody according to table 3 at 4°C overnight. Coverslips were washed 3 times in PBS before incubation with the corresponding secondary antibody (table 3) at 37°C for 1 h. Cells were washed three times in PBS and once in water before mounting in Fluoromount-G (Thermo Fisher Scientific, #00-4958-02). Images were taken with a Zeiss Observer Fluorescent microscope.

To show that differentiation capacities of transgenic lines remain intact after transgenesis we performed spontaneous differentiation assays, by embryoid body formation (EB), according to Rodriguez-Polo *et al.*, (Rodriguez-Polo *et al.*, 2019). In brief, iPSC colonies were detached with 200 U/ml Collagenase Type IV for 10 min at 37°C, scraped off and transferred to uncoated bacterial dishes. EBs were maintained in Iscoves medium (Thermo Fisher Scientific, # 12440053) at 37°C and the medium changed every second day.

After 8 days EB were transferred onto Geltrex-coated 6-well plates equipped with 2 cm coverslips for spontaneous differentiation and further maintained in Iscove's Medium. Cells were fixed between day 18 and 20. Stainings were performed as described above. Spontaneously differentiated cells were stained for Smooth muscle actin (SMA) and  $\alpha$ -Fetoprotein according to table 3.

**Table 7:** Antibodies used

Antibody	Company	Host	Dilution	Application
CRLF3	Santa Cruz; #sc-398388	mouse	1:500	IF / Western blot
$\alpha$ Tubulin	Sigma-Aldrich; T9026	mouse	1:5000	Western blot
Nanog	Cell Signaling, #D73G4	rabbit	1:400	IF
OCT4A	Cell Signaling, #C53G3	rabbit	1:1600	IF
SMA	Sigma-Aldrich, #A2547	mouse	1:100	IF
$\alpha$ Fetoprotein	Dako, #A0008	rabbit	1:100	IF
Neurofilament 200	Sigma-Aldrich; #N4142	rabbit	1:400	IF
$\beta$ -III-tubulin/AF 594	Santa Cruz; #sc-80005 AF594	mouse	1:50	IF / FACS
Phantom dye red 780	Proteintech; #PD00002	/	1:1000	FACS
Alexa Fluor 555	Thermo Fisher; #A32727	mouse	1:1000	IF
Alexa Fluor 594	Thermo Fisher; #A32732	rabbit	1:1000	IF
Alexa Fluor 633	Thermo Fisher; #A21070	rabbit	1:1000	IF
HRP	Sigma-Aldrich; #A4416	mouse	1:10000	Western blot

### Neuronal differentiation and survival-assay establishment

iPSC were differentiated as described previously (Qi *et al.*, 2017)(Qi *et al.*, 2017) with slight modifications of the original protocol. iPSC were split on 12-well plates and maintained in UPPS until reaching confluency of 60-80%. Medium was changed every 2<sup>nd</sup> to 3<sup>rd</sup> day. For the first 7 days of differentiation, cells were maintained in induction medium consisting of DMEM/F12 (Thermo Fisher Scientific; #11320033), 10% Knock out serum (KOS; Thermo Fisher Scientific; # 10828028), 1% Non-essential amino acids (NEAA, Thermo Fisher Scientific; # 11140050), 200  $\mu$ M L-Ascorbic Acid (L-AA, Sigma-Aldrich; # A92902-100G), 2  $\mu$ M SB431542 (Peprotech; # 3014193), 3  $\mu$ M Chir99021 (Sigma-Aldrich, # SML1046) and 1,5  $\mu$ M dorsomorphin (Peprotech, # 8666430). Cells were split onto fresh Geltrex-coated plates on day 6. Neuron splitting was performed following incubation in 0,25% Trypsin/EDTA (Thermo Fisher Scientific; # 25200056) for 3 min at 37°C. Cells were scraped and carefully resuspended before collection in a 5 ml falcon containing 5 ml DMEM/FBS. Cell suspension was centrifuged for 5 min at 200 x g. The supernatant was discarded, cells were resuspended in Induction medium + 0,001 %  $\beta$ -mercaptoethanol (Thermo Fisher Scientific; #21985023) and seeded onto 6-well plates. Medium was changed the next day to neuralization medium containing DMEM/F12, 200  $\mu$ M L-AA, 1% NEAA, 1X N2 supplement (Thermo Fisher Scientific; # 17502048), 1X B27 supplement (Thermo Fisher Scientific; #17504044), 10 ng/ml bFGF (Peprotech; #100-18B) and 10 ng/ml EGF (Peprotech; #AF-100-15). Cells were fed with neuralization medium for one week before switching to neuronal differentiation medium I, consisting of DMEM/F12, 200  $\mu$ M L-AA, 1% NEAA, 1X N2 supplement, 1X B27 supplement, 300 ng/ml cAMP (Peprotech; #6099240). For the final 7 days of neural differentiation, cells were maintained in neural differentiation medium II containing DMEM/F12, 200  $\mu$ M L-AA, 1% NEAA, 1X N2 supplement, 1X B27 supplement, 300 ng/ml cAMP, 10 ng/ml BDNF (Peprotech; #450-02) and 10 ng/ml NT-3 (Peprotech; #AF450-03). During the differentiation process, cells were split once on Poly-L-Lysin/ Laminin-coated plates when reaching 100% confluency. For each experiment 4 6-well plates were first coated in 1  $\mu$ g/ml Poly-L-Lysin (Sigma-Aldrich; #P5899) for 30 min at 37°C. Subsequently, plates were washed 3x with PBS before being coated with 2  $\mu$ g/ml Laminin (Sigma-Aldrich; #11243217001) for at least 8 h at RT in the dark. Before cells were seeded, plates were washed twice in PBS. Cell splitting was performed as described above. Differentiations were regularly monitored for differentiation progress using an inverted light microscope (Carl Zeiss; #4001648). A graphical overview of the differentiation process is presented in Supplementary figure 1. Characterization of the emerging iPSC-derived neurons was performed by immunofluorescent stainings for  $\beta$ -III-tubulin, Neurofilament and CRLF3 as described above (table 3).

*Establishment of survival assay*

Different concentrations of rotenone as a pro-apoptotic stressor and EV-3 as an anti-apoptotic protectant were tested. For final experiments rotenone (Sigma-Aldrich; #R8875; dissolved in DMSO at stock concentration of 1,3 M) concentrations of 800 nM (for iPSC#1) and 1  $\mu$ M (for iPSC#2) were applied for 18 h after treating cells with either 41,5 ng/ml (iPSC#1) or 33,3 ng/ml (iPSC#2) EV-3 (IBA GmbH, Göttingen, Germany) for 12 h. For each experiment one well of differentiations were treated with 0,006% DMSO as rotenone solvent control. After treatment periods, iPSC-derived neurons were prepared for FACS analysis as stated below.

*FACS sample preparation and analysis*

To collect samples for FACS analysis cell cultures were incubated in 0,25% Trypsin/EDTA for 3 min at 37°C before stopping the reaction with DMEM/FBS. Cells were scraped and resuspended by gentle pipetting before being transferred to falcon tubes. 2 ml DMEM/FBS were added and samples were centrifuged at 800 x g for 5 min. Samples were subsequently washed twice in PBS, with centrifugation steps between washing steps. In order to have samples for all treatment groups and to set FACS gates, only a subset of the cells were stained for further analysis. Table 4 shows the different treatment conditions and staining procedures employed for this protocol. Samples designated for live/dead analysis were stained in Phantom dye Red 780 (Proteintech; #PD00002) for 30 min at 4°C according to the antibody list in table 3. Samples were subsequently diluted with 2 ml PBS + 0,1 % FBS and centrifuged at 800 x g for 5 min. Samples were washed one more time in PBS/FBS before being blocked alongside with unstained samples for at least 1 h at 4°C in PBS/0,5% BSA. 2 ml PBS were added and samples were centrifuged before a second PBS washing step. Subsequently, samples stained for  $\beta$ -III-tubulin as neuronal marker were incubated with antibody according to table 3 overnight at 4°C. Samples that did not receive staining solution remained in blocking buffer. The next day 2 ml PBS were added to all falcons and the samples were centrifuged. After a second PBS washing step, cells were resuspended in FACS buffer (Containing PBS + 0,5% BSA + 2 mM EDTA) and strained through a 40  $\mu$ m cell strainer (Sarstedt; #833945040) into FACS tubes (Fisher Scientific; #10579511). Samples were kept on ice until analysis with Sony cell sorter SH800S.

**Table 8:** FACS samples prepared for survival assays

Treatment	FACS sample
Control	Neg. control
	Phantom dye
	$\beta$ -III-tubulin
	$\beta$ -III/Phantom dye
Rotenone	Phantom dye
	$\beta$ -III/Phantom dye
EV-3 + rotenone	$\beta$ -III/Phantom dye

FACS gates were set according to the forward and sideward scatter measured in the main gate for single-cell analysis. Gates for the selection of  $\beta$ -III-tubulin-positive cells were set according to the unstained control samples. Phantom dye gates for live and dead cells were set according to the unstressed population. For all samples 100.000 cells were measured. Only  $\beta$ -III-tubulin positive cells (i.e., neuron-like cells) were analysed for their survival according to Phantom dye staining. A representation of the gating strategy can be seen in Supplementary Figure 2.

FACS data is presented as boxplots showing the median cell survival, upper and lower quartile and whiskers representing 1,5 x interquartile ranges. Single data points are shown as circles within the boxplot. Cell survival data was normalized to the corresponding untreated control, which was set to 1.

#### *CRLF3 immunostaining of iPSC-derived neurons*

iPSC-derived neurons were grown on glass coverslips and fixed on day 30 of differentiation. Cell staining was performed as described above using primary antibodies for Neurofilament 200 and CRLF3 (See antibody list table 3) and Dapi (1:1000 in H<sub>2</sub>O; Sigma Aldrich; #D9564) as nuclear marker. Images were taken using Leica SP8 confocal microscope (Leica Microsystems). Images were further processed using ImageJ.

#### **Statistical analysis**

Statistical analyses of all experiments conducted in this study was performed using R Studio (Team, 2015; R Core Team, 2019) and pairwise permutation test (two-tailed) within the packages coin and rcompanion (Zeileis *et al.*, 2008; Mangiafico, 2019). In order to avoid false-positive results due to multiple comparisons, Benjamini Hochberg correction was included in all statistical calculations. Significant differences are shown by differing letters (e.g. a is significantly different to b but not to ab). All data presented was collected from independent experiments. Only experiments with a minimum of 5 % survival loss in rotenone treated cultures were included into final analysis.

## Results

### Characterization of CRISPR-generated cell lines

In order to generate *CRLF3* deficient cell lines, two independent human iPSC lines (#1 and #2, female and male respectively) were transfected with a plasmid coding for the piggyBac transposase, and a piggyBac vector containing Cas9-GFP and gRNAs to target exon 3 of the gene (see Fig 1A). Fig 1 shows a representation of the mutation characterizations performed. Only cell lines showing two types of mutation (corresponding to alleles A and B) were considered for further analysis. Both generated KO lines contained frameshift-inducing mutations at the scaffold site resulting in termination of protein translation due to premature stop codons. Expression of *CRLF3* protein in the generated cell lines was analysed by Western blots. Both clonal KO lines generated from iPSC#1 and iPSC#2 entirely lack *CRLF3* protein (**Fig 1 C**). In contrast, *CRLF3*-related immunoreactivity of the expected size of 55 kDa was detected as single bands of WT and Ig-Ctrl cells.  $\alpha$ Tubulin was probed as loading control and detected at the expected size in all cell lines. The newly generated clonal lines all express GFP homogeneously, allowing to monitor cross-contaminations with other cell lines (see Fig 1 D). Both Ig-Ctrl and KO cells from iPSC#1 and #2 were characterized for their pluripotent state (see Supp Fig. 3). All four lines retained the capacity for spontaneous differentiation into all three germ layers (Supp Fig 3 A) and exhibited staining for core pluripotency markers (Supp Fig 3 B).

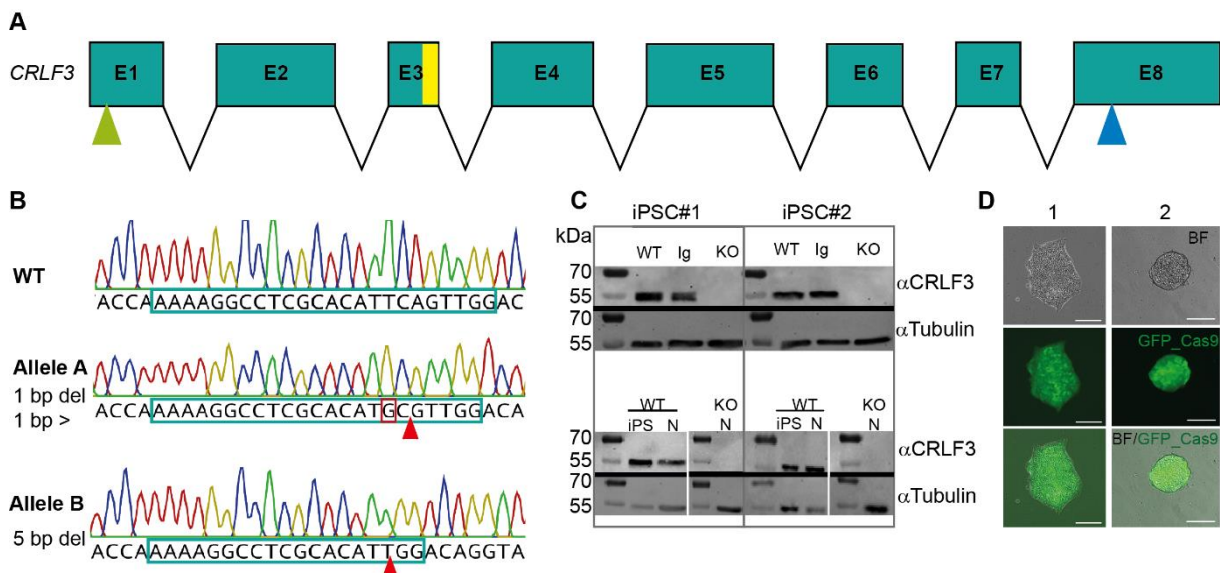


**Figure 5:** Characterization of CRISPR-induced *CRLF3* mutation in human iPSC lines. **A:** Schematic overview of *CRLF3* gene. Exons are represented as boxes, with sizes corresponding to exon length. Introns are represented as arrows and do not depict intron length. Yellow bar in exon 3 (E3) shows mutation site. Green and blue arrows mark start and stop codon of the coding sequence respectively. **B:** Chromatograms illustrating mutations in alleles A and B of iPSC#X line. Top: WT sequence, with gDNA scaffold marked by framed portion of the nucleotide sequence. Middle: Allele A of the mutated line, which is characterized by one deleted base pair (marked with arrow) and a base pair exchange (marked by red box). Bottom: Allele B of the same iPSC line lacking a row of 5 deleted base pairs. Both mutations induce frameshifts that generate premature stop codons. **C:** Western blot analysis of Ig-Ctrl and mutated iPSC lines and differentiated neurons. Top: Protein lysates of iPSC#1 and #2 probed for *CRLF3* and  $\alpha$ Tubulin. WT and Ig-Ctrl lysates show bands for *CRLF3* protein, while the mutated lines (marked with KO) do not.  $\alpha$ Tubulin probed as loading control appears for all lines. Bottom: Western blot analysis of differentiated neurons originating from WT or *CRLF3* mutated cells of both lines. While WT lysates show bands for *CRLF3*, no protein was detected in KO cells.  $\alpha$ Tubulin bands are present. **D:** Transfected iPSC colonies express EGFP as reporter gene. Both lines show homogeneous eGFP expression within iPSC colonies consisting of more than 100 cells. Scale bar: 50  $\mu$ M.

### EV-3 induces CRLF3-mediated protection of human iPSC-derived neurons

EpoR, but not  $\beta$ cR, is expressed in iPSC-derived neurons used in this study (data not shown). Instead of Epo, which activates both classical EpoR and alternative tissue-protective receptors, we used the human natural Epo splice variant EV-3. EV-3 is unable to activate classical EpoR, stimulates anti-apoptotic mechanisms in mammalian neurons (via alternative Epo receptors) and has been demonstrated to mediate protection of insect neurons via binding to CRLF3 (Bonnas *et al.*, 2017; Hahn *et al.*, 2017; Heinrich, Günther and Miljus, 2017). Before starting with main experiments, we established protocols for apoptosis induction with rotenone and EV-3-mediated cell protection by testing different concentrations and exposure periods separately for both lines (Supp Fig 5 shows results of these experiments). Best combinations for apoptosis induction and neuroprotection differed between the two lines and led to the following protocols for subsequent survival assays: iPSC#1-derived neurons were exposed to 41,5 ng/ml EV-3 starting 12 h before exposure to 800 nM rotenone for 18 h. iPSC#2-derived neurons were exposed to 33,3 ng/ml EV-3 starting 12 h before exposure to 1  $\mu$ M rotenone. In these preliminary experiments EV-3 protected neurons from both iPSC lines during rotenone-induced chemical hypoxia indicating that alternative Epo receptors activate the protective intracellular pathways.

For core experiments WT, Ig-Ctrl and CRLF3 KO cells from both lines were differentiated for 30 days and subsequently treated with EV-3 according to our previous findings (41,5 ng/ml iPSC#1 / 33,3 ng/ml iPSC#2) EV-3. After 12 h 800 nM (iPSC#1) or 1  $\mu$ M (iPSC#2) rotenone was added for 18 h before samples were collected for FACS analysis. 100.000 cells per sample were measured in five repetitions for each cell line. Of these, only  $\beta$ -III-tubulin immunopositive cells were included in the quantitative analysis to circumvent variations resulting from divergent differentiation efficiencies (differentiation efficiencies are displayed in Supp. Fig 3). Neuron-specific  $\beta$ -III-tubulin staining of iPSC-derived neurons at day 30 of differentiation labelled extensive axonal networks of all lines (Fig 2).

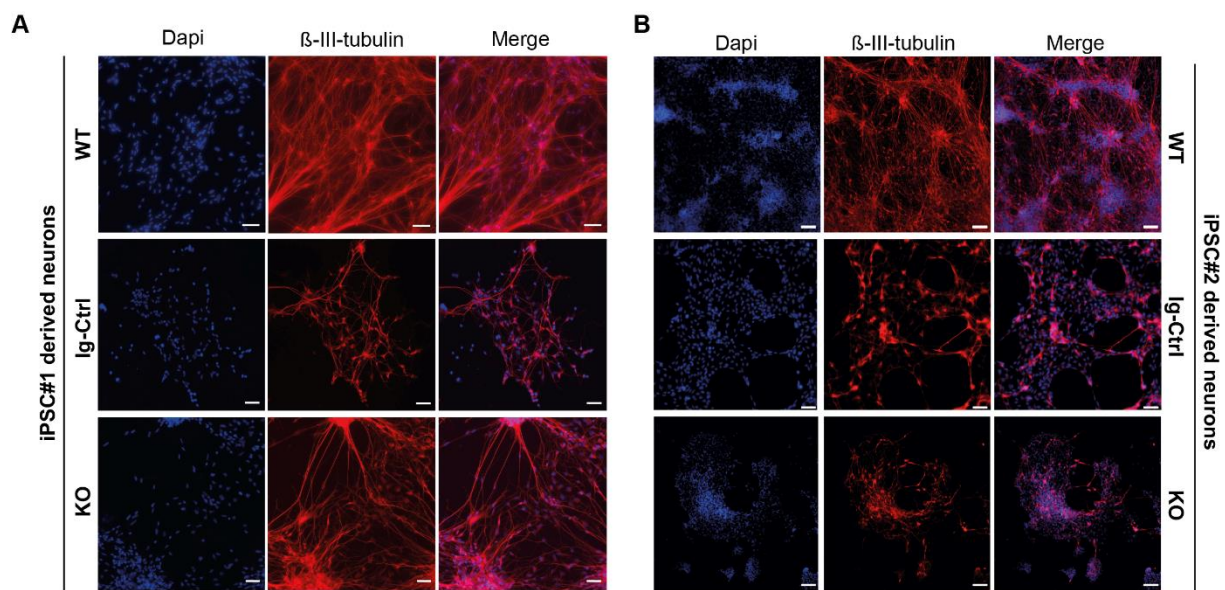


**Figure 2:**  $\beta$ -III-tubulin stainings of iPSC-derived neurons. **A:** Cells derived from iPSC#1. **B:** iPSC#2-derived neurons. All generated cell lines contain extensive axonal networks and anatomical cell-cell contacts. Scale bar 100  $\mu$ m.



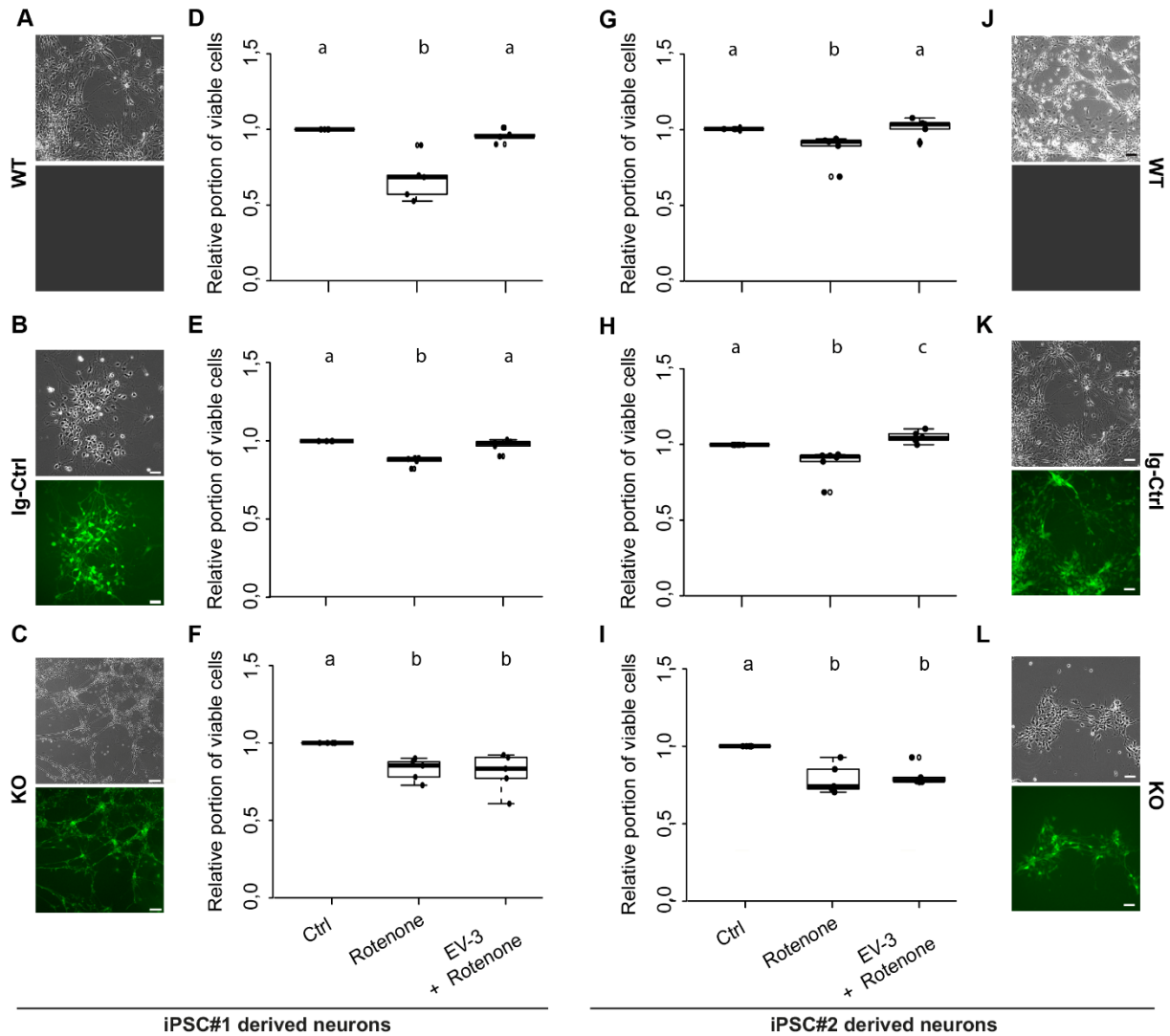


**Figure 3:** EV-3-mediated protection of rotenone-exposed iPSC-derived neurons (left: iPSC#1; right: iPSC#2). Horizontal panels depict data and images from WT (A), isogenic controls (Ig-Ctrl) (B) and *CRLF3*-mutated (KO) (C) iPSC-derived neurons. **A, B, C, J, K, L:** Brightfield and fluorescent images of iPSC-derived neurons. Ig-Ctrl (B) and KO (C) cells display GFP fluorescence, indicating Cas9-GFP fuse transcript. **D, E, F, G, H, I:** Relative survival of iPSC-derived neurons. Cells were prepared for FACS analysis by live/dead and  $\beta$ -III-tubulin staining. **D, E, F:** Data collected for neuron-like cells originating from iPSC#1. 18 h exposure to 800 nM rotenone reduced the survival of WT (D), Ig-Ctrl (E) and KO (F) neurons significantly when normalized and compared to survival in respective untreated control cultures. Rotenone-induced cell death was prevented by EV-3 (41,5 ng/ml) in WT and Ig-Ctrl neurons but not in *CRLF3*- KO neurons. Numbers of analyzed neurons: WT 313.250, Ig-Ctrl 292.996, KO 129.191. **G, H, I:** Relative survival of iPSC-derived neurons originating from iPSC#2. Cells were prepared for FACS analysis by live/dead and  $\beta$ -III-tubulin staining. 18 h exposure to 1  $\mu$ M rotenone reduced the survival of WT (D), Ig-Ctrl (E) and KO (F) neurons significantly when normalized and compared to survival in respective untreated control cultures. Rotenone-induced cell death was prevented by EV-3 (33,3 ng/ml) in WT and Ig-Ctrl neurons but not in *CRLF3*- KO neurons. Treatment of Ig-Ctrl neurons to EV-3 significantly increased cell survival in comparison to control cells. Numbers of analyzed neurons: WT 234.135, Ig-Ctrl 298.864, KO 279.976. Statistics with pairwise permutation test and Benjamini-Hochberg correction for multiple comparison. Significant differences ( $p < 0,05$ ) are indicated by differing letters.

Exposure to 800 nM rotenone reduced survival of WT, Ig-Ctrl and *CRLF3*-mutated iPSC#1-derived neurons (Fig 3 D, E, F). WT neurons were particularly sensitive to rotenone treatment (median relative survival 0,68) compared to Ig-Ctrl (0,88) and KO (0,87) neurons. The deleterious effect of rotenone was completely prevented by EV-3 (41,5 ng/ml) in WT and Ig-Ctrl neurons (median relative survival 0,96 and 0,99). In contrast, EV-3 had no protective effect on *CRLF3* KO neurons (median relative survival 0,83) since cell survival was not different from rotenone-treated cultures (median relative survival 0,87).

Given that rotenone solutions are prepared in DMSO, control experiments with 0,006 % DMSO (represents the final concentration during treatments with 1  $\mu$ M rotenone) had no impact on the survival of WT and Ig-Ctrl neurons compared to untreated cultures (median relative survival 0,99 and 1,02).



Survival of *CRLF3* KO was slightly, yet significantly, decreased (median relative survival 0,96). However, the toxic effect of DMSO in these cells was not as severe as in rotenone exposed cultures (median relative survival 0,87).

iPSC-derived neurons originating from iPSC#2 show similar results in survival assays as cells originating from iPSC#1 (Figure 3 G, H, I). Exposure to 1  $\mu$ M rotenone, significantly decreased survival of WT, Ig-Ctrl and *CRLF3* KO neurons in comparison to untreated control cells (median survival 0,90, 0,92, 0,74 respectively). Treatment of WT and Ig-Ctrl cells with 33,3 ng/ml EV-3 rescued iPSC-derived neurons from rotenone-induced apoptosis, with cell survival of Ig-Ctrl cells being significantly increased to or beyond survival of untreated control cells (median survival 0,97 for WT and 1,04 for Ig-Ctrl cells). Treatment of *CRLF3* KO cells with EV-3 did not increase cell survival in comparison to sole rotenone exposure (0,78 median cell survival). Neurons derived from iPSC#2 reacted more strongly to DMSO treatment than iPSC#1 cells (see Supp. Fig. 6).

### CRLF3 protein levels in apoptogenic and rescue conditions

Potential treatment-related alterations of CRLF3 protein levels in WT and Ig-Ctrl iPSC-derived neurons were analysed by Western blots. Samples from control and pharmacologically treated cultures of the same experiment were simultaneously analysed on the same gel and blot. Both antibodies labelled single bands at the expected molecular size ( $\sim$ 55 kDa for both proteins) in each sample.

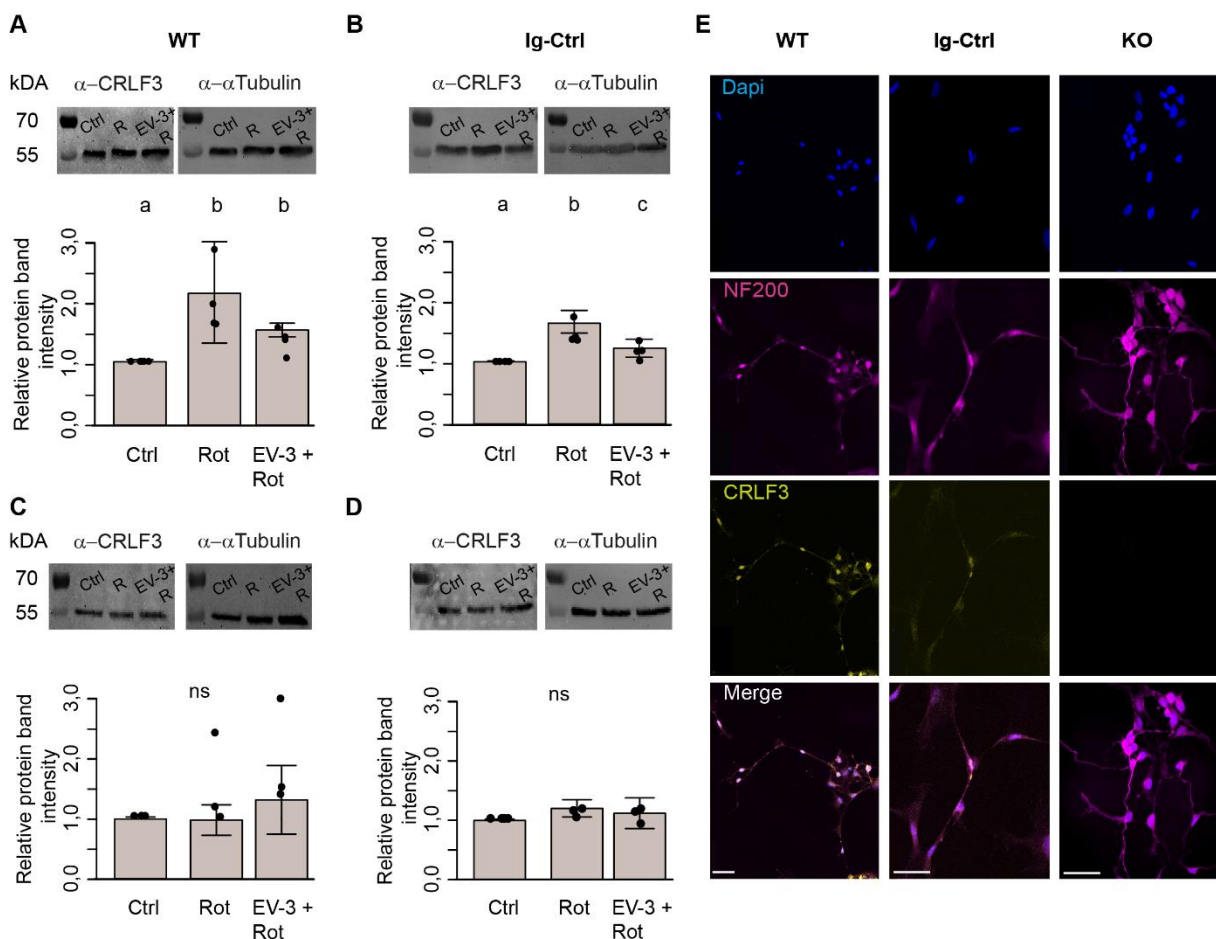


**Figure 4:** Presence of CRLF3 in iPSC-derived neurons. Treatment with EV-3 and/or rotenone for 12 + 18 h started on day 30 of the differentiation protocol. Immediately after treatment, samples were collected. **A, B:** Protein immunoblots of iPSC#1-derived WT (A) and Ig-Ctrl (B) neurons labelled with anti-CRLF3 (left) and anti- $\alpha$ Tubulin (right) as loading control. Both antibodies labelled single bands of the expected molecular size (both  $\sim$ 55 kDa) in each sample. Rotenone (800 nM) increased CRLF3 protein levels in WT and Ig-Ctrl neurons. Co-treatment with EV-3 (41,5 ng/ml) reduced rotenone-induced CRLF3 accumulation insignificantly in WT and significantly in Ig-Ctrl neurons.  $n = 4$ . **C, D:** Protein immunoblots of iPSC#2-derived

## Chapter 4

WT (A) and Ig-Ctrl (B) neurons labelled with anti-CRLF3 (left) and anti- $\alpha$ Tubulin (right) as loading control. Both antibodies labelled single bands of the expected molecular size. Neither rotenone (1  $\mu$ M) alone nor its combination with EV-3 (33,3 ng/ml) altered CRLF3 protein levels significantly. n= 3. Statistics: pairwise permutation test with Benjamini-Hochberg correction for multiple comparison. Significant differences ( $p < 0,05$ ) are indicated by differing letters. **E:** Immunofluorescent labeling of neurofilament 200 (NF200; neuronal/axonal marker) and CRLF3 in all iPSC#2-derived neurons. Nuclei were labelled with Dapi. CRLF3 immunoreactivity in WT and Ig-Ctrl covers entire neurons with extensive labelling in the soma. No CRLF3 immunoreactivity is detected in KO cells. Scale bars 100  $\mu$ M.

Exposure to rotenone increased CRLF3 levels in iPSC#1 WT ( $2,1 \pm 0,7$  fold) and Ig-Ctrl neurons ( $1,6 \pm 0,2$  fold) compared to untreated controls (Fig. 4 A,B). Rotenone-induced accumulation of CRLF3 was reduced by co-treatment with EV-3 in WT ( $1,5 \pm 0,1$  STDV, not significant compared to rotenone-only treatment) and Ig-Ctrl neurons ( $1,2 \pm 0,1$  STDV, significantly different from rotenone-only exposure). In contrast, CRLF3 levels were not affected by rotenone  $\pm$  EV-3 exposure of WT and Ig-Ctrl neuron-like cells originating from iPSC#2 (Fig 4 C,D). In order to determine the localization of CRLF3 iPSC#1-derived neurons, we labelled differentiated WT, Ig-Ctrl and *CRLF3* KO cells with Dapi and antibodies against neurofilament 200 and CRLF3. As shown in Fig. 4 I, all cell lines expressed neurofilament 200, which is generated in the cell body cytosol and transported into axons. CRLF3-immunoreactivity appeared in dot-like patterns in cell bodies and along axons of WT and Ig-Ctrl cells but not in *CRLF3* KO cells.

## Discussion

The cytokine Epo mediates neuroprotection and promotes regeneration in mammalian nervous systems. Animal models and clinical observations identified Epo as a promising treatment to prevent neurodegenerative cell loss. While Epo itself co-activates adverse effects such as overproduction of blood cells increasing the risk of thrombosis and promotion of tumour growth, some Epo-mimetics including EV-3 selectively stimulate tissue protection without activating homodimeric EpoR-associated side effects. Hence, identification and selective targeting of tissue-protective Epo receptors should be attempted for therapies against neurodegenerative diseases. The present study identifies EV-3/CRLF3-signalling in human neurons as a promising neuroprotective option.

Previous studies on insects suggested that the evolutionary conserved orphan cytokine receptor CRLF3 may serve as neuroprotective receptor for Epo in the mammalian nervous system (Hahn *et al.*, 2017; Hahn, Büschgens, Schwedhelm-Domeyer, Bank, Bart R.H. Geurten, *et al.*, 2019). CRLF3 has been associated with a variety of diseases including neurofibromatosis type I, cutaneous Leishmaniasis, cutaneous squamous cell carcinoma, amyotrophic lateral sclerosis, autism and cancer (Dang *et al.*, 2006; Serra *et al.*, 2019; Castellucci *et al.*, 2021; Kehrer-Sawatzki *et al.*, 2021; Wegscheid *et al.*, 2021). Apart from this, studies on PC12 cells and iPSC-derived cerebral organoids indicated that CRLF3 regulates the development and differentiation of neurons (Wegscheid *et al.*, 2021). However, concrete functions of CRLF3 and the nature of its ligand remained unknown. Insect CRLF3 initiates anti-apoptotic neuroprotective mechanisms upon activation with both human Epo and EV-3 (Hahn *et al.*, 2017; Hahn, Büschgens, Schwedhelm-Domeyer, Bank, Bart R. H. Geurten, *et al.*, 2019). While the endogenous ligand for insect CRLF3 is still unknown (Knorr *et al.*, 2021) current knowledge suggests that CRLF3 is the only Epo/EV-3-responsive receptor in insects. In contrast, mammals express classical homodimeric EpoR activated by Epo and alternative tissue-protective Epo receptors activated by Epo and selective ligands such as EV-3. EV-3 is a natural splice variant that lacks the entire third exon of the *Epo* transcript which prevents activation of homodimeric EpoR and heteromeric EpoR/ $\beta$ CR (Bonnas, 2009; Bonnas *et al.*, 2017). EV-3 is present in human serum and brain and elicits anti-apoptotic effects on rat hippocampal neurons (Bonnas *et al.*, 2017). Using EV-3 in our study prevented the activation of EpoR which is expressed in both iPSC lines and iPSC-derived neurons used in this study, while  $\beta$ CR expression was only detected in undifferentiated iPSC. Demonstrating that EV-3 mediates neuroprotection via human CRLF3 not only deorphanizes CRLF3 but also identifies the previously proposed neuroprotective receptor for EV-3. Since Epo can be regarded as the more general ligand that stimulates both erythropoiesis and tissue protection and insect CRLF3 is activated by both Epo and EV-3, it can be assumed that human CRLF3 will also be stimulated by EV-3 and Epo.

EV-3 protects insect and rat neurons at similar or lower concentrations than Epo (Miljus *et al.*, 2014, 2017; Hahn *et al.*, 2017; Heinrich, Günther and Miljus, 2017; Bonnas *et al.*, 2017)). Both Epo and EV-3 protect neurons in an optimum-type dose response, with both lower and higher concentrations being less neuroprotective and very high concentrations even exerting deleterious effects on cell survival (Siren *et al.*, 2001; Chong, Kang and Maiese, 2003; Weishaupt *et al.*, 2004; Bonnas *et al.*, 2017; Hahn *et al.*, 2017; Heinrich, Günther and Miljus, 2017). Optimal concentrations may vary between species (e.g. brain neurons of *L. migratoria* and *T. castaneum*) and even between different cell types within the same organism and tissue (brain neurons and glia of *L. migratoria*). Such differences were also detected between the two lines of iPSC-derived neurons used in our study. While rotenone-stressed neurons of iPSC#1 were best protected by 41,5 ng/ml EV-3, the most neuroprotective concentration for iPSC#2 was 33,3 ng/ml. Apoptosis-induction with rotenone has frequently been used in studies with various cell types including neurons and Epo-mediated neuroprotection of rotenone-stressed neurons has been reported in vitro (Wen *et al.*, 2002; Cheng *et al.*, 2020). It is important to note, that iPSC#2 cells differentiated not as efficiently as cells originating from iPSC#1. This could account for the higher concentration of rotenone needed, in order to stress the cells.

To our knowledge, the neuroprotective role of Epo or EV-3 in human neurons has not been directly studied. Aiming to explore the potential of Epo mediated cytoprotection in human cells, we generated iPSC-derived neurons that recapitulate essential aspects of in vivo human neurons. Both lines of iPSC-

derived neurons assumed neuron-like morphologies and expressed neuron-specific proteins including  $\beta$ -III-tubulin and neurofilament 200. We strived to understand if (1) EV-3 elicits neuroprotective functions in human neuron-like cells and (2) if this neuroprotection requires the presence of human CRLF3. We demonstrate that EV-3 administration 12 h before and during rotenone-exposure protects WT and Ig-Ctrl neuron-like cells from stress-induced apoptosis. For both cell lines used in this study the apoptotic effect of rotenone was entirely compensated, resulting in cell survival close to control (untreated cells) levels. Importantly, EV-3 mediated neuroprotection was completely absent in CRLF3 KO cells. This data provides evidence that EV-3 (and likely also Epo) and CRLF3 represent a ligand-receptor pair that stimulates protective mechanisms in human cells.

Physiological and/or pathological stress elevates *EpoR* expression in neuronal cell cultures (Chin *et al.*, 2000; Chen *et al.*, 2010; Merelli *et al.*, 2019a), in spinal cord (Cohrs *et al.*, 2018) and brain (Pascal E Sanchez *et al.*, 2009; Merelli *et al.*, 2019a; Wakhloo *et al.*, 2020). Additionally, increased presence of EpoR/ $\beta$ cR in renal cells after ischemic reperfusion injury were also reported (Yang *et al.*, 2013). Cell-protective Epo receptors were either upregulated (Xu *et al.*, 2009) or downregulated (Yang *et al.*, 2013) by the presence of Epo or receptor-activating Epo mimetic molecules in some studies. Hence, we asked whether *CRLF3* expression in iPSC-derived neurons was similarly affected by rotenone-induced stress and EV-3 application. Western blot analysis of iPSC#1 WT and Ig-Ctrl neurons indicated increased CRLF3 levels following rotenone-exposure and partial prevention of this increase by co-application of EV-3. In contrast to the survival assays that selectively analysed neuron-like cells, Western blot analysis non-selectively included all cells in these cultures. Nevertheless, the data suggest that CRLF3 is upregulated under apoptogenic conditions. The presence of EV-3 reduced apoptosis induction by rotenone causing no or reduced upregulation of CRLF3 protein. However, no rotenone and/or EV-3 effects on CRLF3 levels were detected in iPSC#2 WT and Ig-Ctrl neurons. This result is probably caused by lower differentiation efficiency of iPSC#2 (compared to iPSC#1) and more diluted effects by higher portions of non-neuronal cell types.

The data presented here identify human CRLF3 as a neuroprotective receptor for the natural Epo splice variant EV-3. Expression of CRLF3 in various human tissues suggests that CRLF3-stimulated transduction pathways can interfere with apoptotic processes in other cell types besides neurons. The involvement of CRLF3 in human iPSC-derived neuroprotection will initiate a variety of studies to uncover the protective molecular pathways. Furthermore, it facilitates the identification of additional Epo-like ligands to be applied as specific neuro- or other tissue-protective agents. Using iPSC-derived cell types from healthy and diseased donors enables focussed studies on cell-protective mechanisms in cell-specific molecular settings.

## References

- Bonnas, C. et al. (2017) 'EV-3, an endogenous human erythropoietin isoform with distinct functional relevance', *Scientific Reports*, 7(3684), pp. 1–15. doi: 10.1038/s41598-017-03167-0.
- Bonnas, C. B. (2009) Identification of erythropoietin isoforms and evaluation of their biological importance., Dissertation Charité Berlin.
- Boulay, J. L., O'Shea, J. J. and Paul, W. E. (2003) 'Molecular phylogeny within type I cytokines and their cognate receptors', *Immunity*. Cell Press, pp. 159–163. doi: 10.1016/S1074-7613(03)00211-5.
- Brines, M. et al. (2004) 'Erythropoietin mediates tissue protection through an erythropoietin and common b -subunit heteroreceptor', *PNAS*, 101(41).
- Brines, M. et al. (2008) 'Nonerythropoietic, tissue-protective peptides derived from the tertiary structure of erythropoietin', *Proceedings of the National Academy of Sciences of the United States of America*, 105(31), pp. 10925–10930. doi: 10.1073/pnas.0805594105.
- Cao, Y. (2013) 'Erythropoietin in cancer: A dilemma in risk therapy', *Trends in Endocrinology and Metabolism*. Trends Endocrinol Metab, pp. 190–199. doi: 10.1016/j.tem.2012.10.007.
- Castellucci, L. C. et al. (2021) 'A Genome-wide Association Study Identifies SERPINB10, CRLF3, STX7, LAMP3, IFNG-AS1, and KRT80 As Risk Loci Contributing to Cutaneous Leishmaniasis in Brazil', *Clinical infectious diseases : an official publication of the Infectious Diseases Society of America*, 72(10), pp. e515–e525. doi: 10.1093/cid/ciaa1230.
- Chamorro, M. E. et al. (2013) 'Signaling pathways of cell proliferation are involved in the differential effect of erythropoietin and its carbamylated derivative', *Biochimica et Biophysica Acta - Molecular Cell Research*. Biochim Biophys Acta, 1833(8), pp. 1960–1968. doi: 10.1016/j.bbamcr.2013.04.006.
- Chateauvieux, S. et al. (2011) 'Erythropoietin, erythropoiesis and beyond', *Biochemical Pharmacology*. Elsevier Inc., 82(10), pp. 1291–1303. doi: 10.1016/j.bcp.2011.06.045.
- Chen, A. Y. et al. (2010) 'Role of Erythropoietin Receptor Signaling in Parvovirus B19 Replication in Human Erythroid Progenitor Cells', *JOURNAL OF VIROLOGY*, 84(23), pp. 12385–12396. doi: 10.1128/JVI.01229-10.
- Cheng, X. Y. et al. (2020) 'Human iPSCs derived astrocytes rescue rotenone-induced mitochondrial dysfunction and dopaminergic neurodegeneration in vitro by donating functional mitochondria', *Translational Neurodegeneration*. Translational Neurodegeneration, 9(1), pp. 1–14. doi: 10.1186/s40035-020-00190-6.
- Chin, K. et al. (2000) 'Production and processing of erythropoietin receptor transcripts in brain', *Molecular Brain Research*. Brain Res Mol Brain Res, 81(1–2), pp. 29–42. doi: 10.1016/S0169-328X(00)00157-1.
- Chong, Z. Z. et al. (2013) 'Targeting erythropoietin for chronic neurodegenerative diseases', *Expert Opinion on Therapeutic Targets*, 17(6), pp. 707–720. doi: 10.1517/14728222.2013.780599.
- Chong, Z. Z., Kang, J. Q. and Maiese, K. (2003) 'Erythropoietin fosters both intrinsic and extrinsic neuronal protection through modulation of microglia, Akt1, Bad, and caspase-mediated pathways', *British Journal of Pharmacology*, 138(6), pp. 1107–1118. doi: 10.1038/sj.bjp.0705161.
- Cirulli, E. T. et al. (2015) 'Exome sequencing in amyotrophic lateral sclerosis identifies risk genes and pathways', *Science*. American Association for the Advancement of Science, 347(6229), pp. 1436–1441. doi: 10.1126/science.aaa3650.
- Cohrs, G. et al. (2018) 'Spatial and Cellular Expression Patterns of Erythropoietin-Receptor and Erythropoietin during a 42-Day Post-Lesional Time Course after Graded Thoracic Spinal Cord Impact Lesions in the Rat', *Journal of Neurotrauma*. Mary Ann Liebert Inc., 35(3), pp. 593–607. doi: 10.1089/neu.2017.4981.
- Constantinescu, S. N., Ghaffari, S. and Lodish, H. F. (1999) 'The erythropoietin receptor: Structure, activation and intracellular signal transduction', *Trends in Endocrinology and Metabolism*. Elsevier Current Trends, pp. 18–23. doi: 10.1016/S1043-2760(98)00101-5.
- Dang, C. et al. (2006) 'Identification of dysregulated genes in cutaneous squamous cell carcinoma', *Oncology Reports*, 16(3), pp. 513–519. doi: 10.3892/or.16.3.513.
- Debowski, K. et al. (2015) 'Non-viral generation of marmoset monkey iPS cells by a six-factor-in-one-vector approach', *PLoS ONE*. Public Library of Science, 10(3), p. 118424. doi: 10.1371/journal.pone.0118424.
- Ding, J. et al. (2017) 'Neuroprotection and CD131/GDNF/AKT Pathway of Carbamylated Erythropoietin in Hypoxic Neurons', *Molecular Neurobiology*. Humana Press Inc., 54(7), pp. 5051–5060. doi: 10.1007/s12035-016-0022-0.

- Doss, M. X. and Sachinidis, A. (2019) 'Current Challenges of iPSC-Based Disease Modeling and Therapeutic Implications', *Cells*. MDPI AG, 8(5), p. 403. doi: 10.3390/cells8050403.
- Ehrenreich, H. et al. (2009) 'Recombinant human erythropoietin in the treatment of acute ischemic stroke', *Stroke*. Stroke, 40(12). doi: 10.1161/STROKEAHA.109.564872.
- Genc, S., Koroglu, T. F. and Genc, K. (2004) 'Erythropoietin and the nervous system', *Brain Research*, 1000(1–2), pp. 19–31. doi: 10.1016/j.brainres.2003.12.037.
- Ghezzi, P. and Brines, M. (2004) 'Erythropoietin as an antiapoptotic, tissue-protective cytokine', *Cell Death and Differentiation*. Nature Publishing Group, pp. S37–S44. doi: 10.1038/sj.cdd.4401450.
- Hahn, N. et al. (2017) 'The Insect Ortholog of the Human Orphan Cytokine Receptor CRLF3 Is a Neuroprotective Erythropoietin Receptor', *Front. Mol. Neurosci.*, 10(July), pp. 1–11. doi: 10.3389/fnmol.2017.00223.
- Hahn, N., Büschgens, L., Schwedhelm-Domeyer, N., Bank, S., Geurten, Bart R. H., et al. (2019) 'The Orphan Cytokine Receptor CRLF3 Emerged With the Origin of the Nervous System and Is a Neuroprotective Erythropoietin Receptor in Locusts', *Frontiers in Molecular Neuroscience*, 12. doi: 10.3389/fnmol.2019.00251.
- Hardee, M. E. et al. (2006) 'Erythropoietin biology in cancer', *Clinical Cancer Research*. Clin Cancer Res, pp. 332–339. doi: 10.1158/1078-0432.CCR-05-1771.
- Hashimoto, Y. et al. (2012) 'Uncovering genes required for neuronal morphology by morphology-based gene trap screening with a revertible retrovirus vector', *The FASEB Journal*, 26, pp. 4662–4674. doi: 10.1096/fj.12-207530.
- Heinrich, R., Günther, V. and Miljus, N. (2017) 'Erythropoietin-Mediated Neuroprotection in Insects Suggests a Prevertebrate Evolution of Erythropoietin-Like Signaling', in *Vitamins and Hormones*. Academic Press Inc., pp. 181–196. doi: 10.1016/bs.vh.2017.02.004.
- Jelkmann, W. and Metzén, E. (1996) 'Erythropoietin in the control of red cell production', *Annals of Anatomy*. Gustav Fischer Verlag Jena GmbH, 178(5), pp. 391–403. doi: 10.1016/S0940-9602(96)80124-5.
- Kästner, A. et al. (2012) 'Common variants of the genes encoding erythropoietin and its receptor modulate cognitive performance in schizophrenia.', *Molecular medicine (Cambridge, Mass.)*. BioMed Central, 18(6), pp. 1029–1040. doi: 10.2119/molmed.2012.00190.
- Kehrer-Sawatzki, H. et al. (2021) 'Atypical nfl microdeletions: Challenges and opportunities for genotype/phenotype correlations in patients with large nfl deletions', *Genes*, 12(10). doi: 10.3390/genes12101639.
- Knorr, D. Y. et al. (2021) 'Locust Hemolymph Conveys Erythropoietin-Like Cytoprotection via Activation of the Cytokine Receptor CRLF3', *Frontiers in Physiology*, 12(April). doi: 10.3389/fphys.2021.648245.
- Kretz, A. et al. (2005) 'Erythropoietin promotes regeneration of adult CNS neurons via Jak2/Stat3 and PI3K/AKT pathway activation', *Molecular and Cellular Neuroscience*, 29(4), pp. 569–579. doi: 10.1016/j.mcn.2005.04.009.
- Liongue, C. and Ward, A. C. (2007) 'Evolution of Class I cytokine receptors', *BMC Evolutionary Biology*, 7. doi: 10.1186/1471-2148-7-120.
- Lundby, C. and Olsen, N. V. (2011) 'Effects of recombinant human erythropoietin in normal humans', *Journal of Physiology*. Wiley-Blackwell, pp. 1265–1271. doi: 10.1113/jphysiol.2010.195917.
- Maiese, K., Chong, Z. Z. and Shang, Y. C. (2008) 'RAVES AND RISKS FOR ERYTHROPOIETIN', *Cytokine Growth Factor Rev.*, 19(2), pp. 145–155.
- Mangiafico, S. S. (2019) 'Package "recompanion"', (September 2016).
- Merelli, A. et al. (2019) 'Convulsive Stress Mimics Brain Hypoxia and Promotes the P-Glycoprotein (P-gp) and Erythropoietin Receptor Overexpression. Recombinant Human Erythropoietin Effect on P-gp Activity', *Frontiers in Neuroscience*. Frontiers Media S.A., 13(JUL), p. 750. doi: 10.3389/fnins.2019.00750.
- Miljus, N. et al. (2014) 'Erythropoietin-mediated protection of insect brain neurons involves JAK and STAT but not PI3K transduction pathways', *Neuroscience*. IBRO, 258, pp. 218–227. doi: 10.1016/j.neuroscience.2013.11.020.
- Miljus, N. et al. (2017) 'Neuroprotection and endocytosis: erythropoietin receptors in insect nervous systems', *Journal of neurochemistry*, 141, pp. 63–74. doi: 10.1111/jnc.13967.
- Miller, J. L. et al. (2015) 'Discovery and characterization of nonpeptidyl agonists of the tissue-protective erythropoietin receptors', *Molecular Pharmacology*. American Society for Pharmacology and Experimental Therapy, 88(2), pp. 357–367. doi: 10.1124/mol.115.098400.

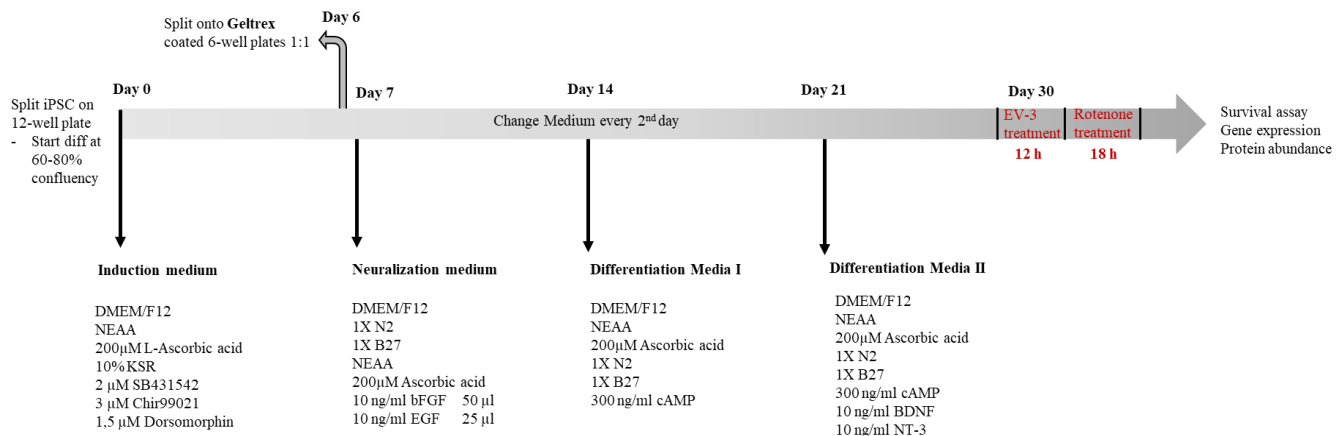
- Miskowiak, K. et al. (2008) 'Differential effects of erythropoietin on neural and cognitive measures of executive function 3 and 7 days post-administration', *Experimental Brain Research. Exp Brain Res*, 184(3), pp. 313–321. doi: 10.1007/s00221-007-1102-1.
- Miskowiak, K., O'Sullivan, U. and Harmer, C. J. (2007) 'Erythropoietin enhances hippocampal response during memory retrieval in humans', *Journal of Neuroscience. J Neurosci*, 27(11), pp. 2788–2792. doi: 10.1523/JNEUROSCI.5013-06.2007.
- Miskowiak, K. W. et al. (2016) 'Cognitive enhancement treatments for bipolar disorder: A systematic review and methodological recommendations', *European Neuropsychopharmacology. Elsevier B.V.*, pp. 1541–1561. doi: 10.1016/j.euroneuro.2016.08.011.
- Morishita, E. et al. (1996) Anti-Erythropoietin Receptor Monoclonal Antibody: Epitope Mapping, Quantification of the Soluble Receptor, and Detection of the Solubilized Transmembrane Receptor and the Receptor-Expressing Cells. Available at: <http://ashpublications.org/blood/article-pdf/88/2/465/844520/465.pdf> (Accessed: 28 March 2022).
- Nadam, J. et al. (2007) 'Neuroprotective effects of erythropoietin in the rat hippocampus after pilocarpine-induced status epilepticus', 25, pp. 412–426. doi: 10.1016/j.nbd.2006.10.009.
- Okita, K. et al. (2011) 'A more efficient method to generate integration-free human iPS cells', *Nature Methods. Nature Publishing Group*, 8(5), pp. 409–412. doi: 10.1038/nmeth.1591.
- Ostrowski, D. and Heinrich, R. (2018) 'Alternative Erythropoietin Receptors in the Nervous System'. doi: 10.3390/jcm7020024.
- Pedroso, I. et al. (2012) 'Use of Cuban recombinant human erythropoietin in Parkinson's disease treatment', *MEDICC Review. MEDICC Rev*, 14(1), pp. 11–17. doi: 10.37757/mr2012v14.n1.4.
- Qi, Y. et al. (2017) 'Combined small-molecule inhibition accelerates the derivation of functional, early-born, cortical neurons from human pluripotent stem cells', *Nature biotechnology. NIH Public Access*, 35(2), p. 154. doi: 10.1038/NBT.3777.
- R Core Team (2019) 'An Introduction to dplyr', *Industrial and Commercial Training*, 10(1), pp. 11–18. doi: 10.1108/eb003648.
- Rey, F. et al. (2019) 'Erythropoietin as a Neuroprotective Molecule: An Overview of Its Therapeutic Potential in Neurodegenerative Diseases', *ASN Neuro. SAGE Publications Inc.* doi: 10.1177/1759091419871420.
- Rodriguez-Polo, I. et al. (2019) 'Baboon induced pluripotent stem cell generation by piggyBac transposition of reprogramming factors', *Primate Biology. Copernicus GmbH*, 6(2), pp. 75–86. doi: 10.5194/pb-6-75-2019.
- Rodriguez-Polo, I. et al. (2021) 'A piggyBac-based platform for genome editing and clonal rhesus macaque iPSC line derivation', *Scientific Reports. Nature Research*, 11(1), p. 15439. doi: 10.1038/s41598-021-94419-7.
- Sanchez, Pascal E. et al. (2009) 'Erythropoietin receptor expression is concordant with erythropoietin but not with common  $\beta$  chain expression in the rat brain throughout the life span', *The Journal of Comparative Neurology. John Wiley & Sons, Ltd*, 514(4), pp. 403–414. doi: 10.1002/cne.22020.
- Sanchez, Pascal E et al. (2009) 'Optimal neuroprotection by erythropoietin requires elevated expression of its receptor in neurons', *PNAS*, 106(24), pp. 1–6.
- Serra, G. et al. (2019) 'NF1 microdeletion syndrome: Case report of two new patients', *Italian Journal of Pediatrics. Italian Journal of Pediatrics*, 45(1), pp. 1–7. doi: 10.1186/s13052-019-0718-7.
- Siren, A.-L. et al. (2001) 'Erythropoietin prevents neuronal apoptosis after cerebral ischemia and metabolic stress', *Proceedings of the National Academy of Sciences*, 98(7), pp. 4044–4049. doi: 10.1073/pnas.051606598.
- Stauske, M., Rodriguez Polo, I., et al. (2020) 'Non-Human Primate iPSC Generation, Cultivation, and Cardiac Differentiation under Chemically Defined Conditions', *Cells. NLM (Medline)*, 9(6), p. 1349. doi: 10.3390/cells9061349.
- Team, Rs. (2015) 'RStudio: Integrated Development for R. RStudio, Inc., Boston, MA'. Available at: <http://www.rstudio.com/>.
- Ueba, H. et al. (2010) 'Cardioprotection by a nonerythropoietic, tissue-protective peptide mimicking the 3D structure of erythropoietin', *Proceedings of the National Academy of Sciences of the United States of America*, 107(32), pp. 14357–14362. doi: 10.1073/pnas.1003019107.
- Wakhloo, D. et al. (2020) 'Functional hypoxia drives neuroplasticity and neurogenesis via brain erythropoietin', *Nature Communications. Springer US*, 11(1), pp. 1–12. doi: 10.1038/s41467-020-15041-1.



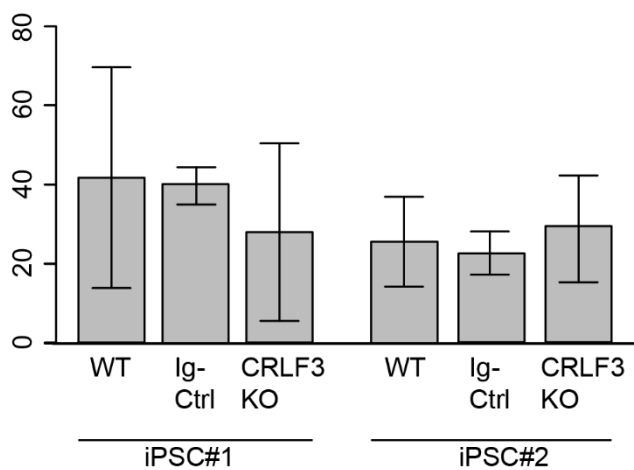
## Chapter 4

- Wegscheid, M. L. et al. (2021) 'Patient-derived iPSC-cerebral organoid modeling of the 17q11.2 microdeletion syndrome establishes CRLF3 as a critical regulator of neurogenesis', *Cell Reports*. Elsevier B.V., 36(1), p. 109315. doi: 10.1016/j.celrep.2021.109315.
- Weishaupt, J. H. et al. (2004) 'Effect of erythropoietin axotomy-induced apoptosis in rat retinal ganglion cells', *Investigative Ophthalmology and Visual Science*. The Association for Research in Vision and Ophthalmology, 45(5), pp. 1514–1522. doi: 10.1167/iops.03-1039.
- Wen, T. C. et al. (2002) 'Erythropoietin protects neurons against chemical hypoxia and cerebral ischemic injury by up-regulating Bcl-xL expression', *Journal of Neuroscience Research*, 67(6), pp. 795–803. doi: 10.1002/jnr.10166.
- Wiegand, C. and Banerjee, I. (2019) 'Recent advances in the applications of iPSC technology', *Current Opinion in Biotechnology*. Elsevier Ltd, pp. 250–258. doi: 10.1016/j.copbio.2019.05.011.
- Wu, Yuanyuan et al. (2013) 'Protective effects of HBSP on ischemia reperfusion and cyclosporine a induced renal injury', *Clinical and Developmental Immunology*, 2013. doi: 10.1155/2013/758159.
- Xu, X. et al. (2009) 'Carbamylated erythropoietin protects the myocardium from acute ischemia/reperfusion injury through a PI3K/Akt-dependent mechanism', *Surgery*. Mosby, 146(3), pp. 506–514. doi: 10.1016/j.surg.2009.03.022.
- Yang, C. et al. (2013) 'Helix B surface peptide administered after insult of ischemia reperfusion improved renal function, structure and apoptosis through beta common receptor/erythropoietin receptor and PI3K/Akt pathway in a murine model', *Experimental Biology and Medicine*. SAGE PublicationsSage UK: London, England, 238(1), pp. 111–119. doi: 10.1258/ebm.2012.012185.
- Yang, F. et al. (2009) 'Cloning and characterization of a novel intracellular protein p48.2 that negatively regulates cell cycle progression', *The International Journal of Biochemistry & Cell Biology*, 41(11), pp. 2240–2250. doi: 10.1016/j.biocel.2009.04.022.
- Yu, X. et al. (2002) 'Erythropoietin receptor signalling is required for normal brain development', 516, pp. 505–516.
- Zeileis, A. et al. (2008) 'Implementing a class of permutation tests: The coin package', *Journal of Statistical Software*, 28(8). Available at: <http://epub.wu.ac.at/4004/%5Cnpapers3://publication/uuid/BF1BBE55-2A35-44D0-96DA-FCCC209A5334>.
- Zhang, Y. et al. (2014) 'Erythropoietin action in stress response, tissue maintenance and metabolism', *International Journal of Molecular Sciences*. MDPI AG, pp. 10296–10333. doi: 10.3390/ijms150610296.

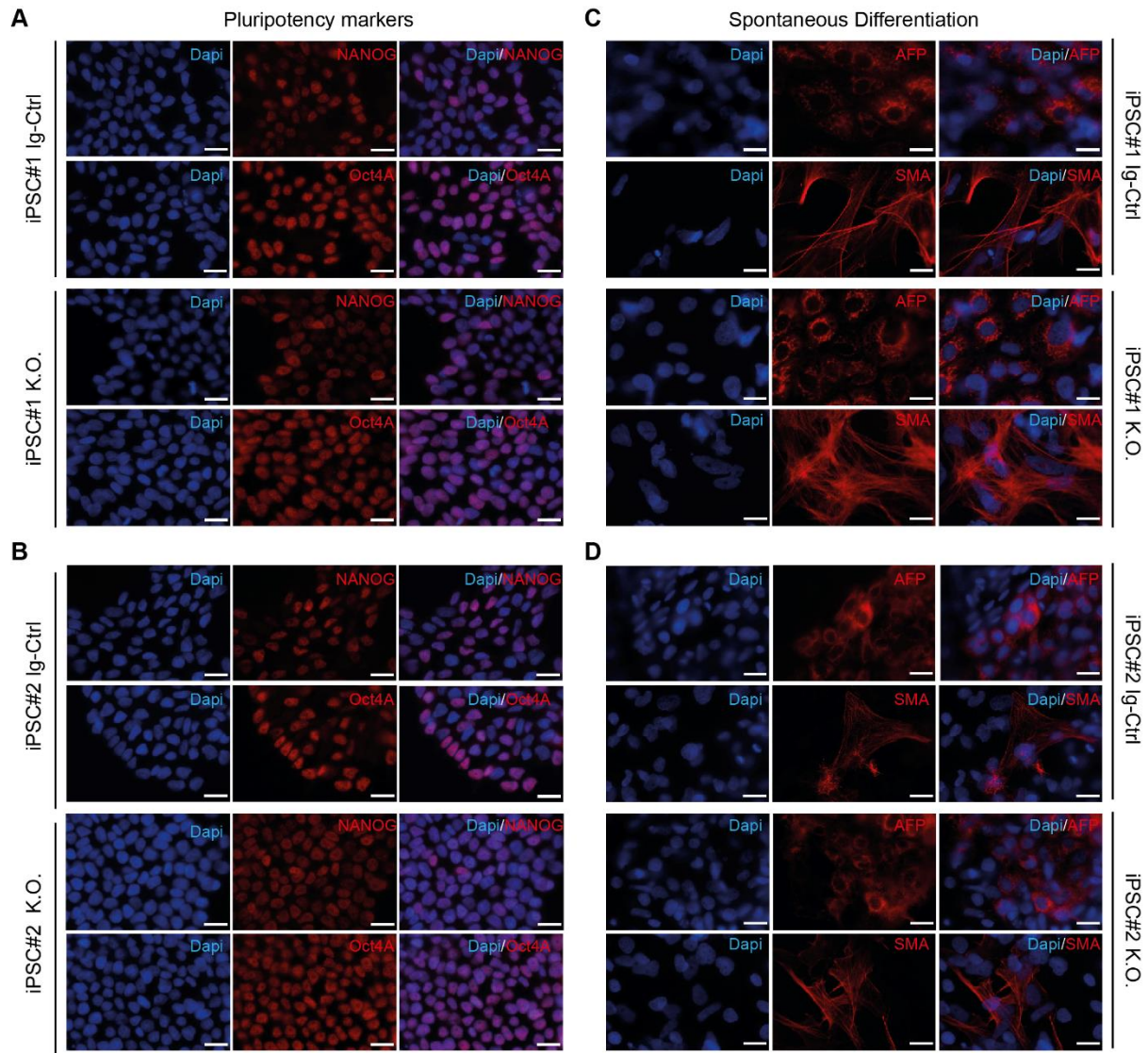
## Supplementary Figures



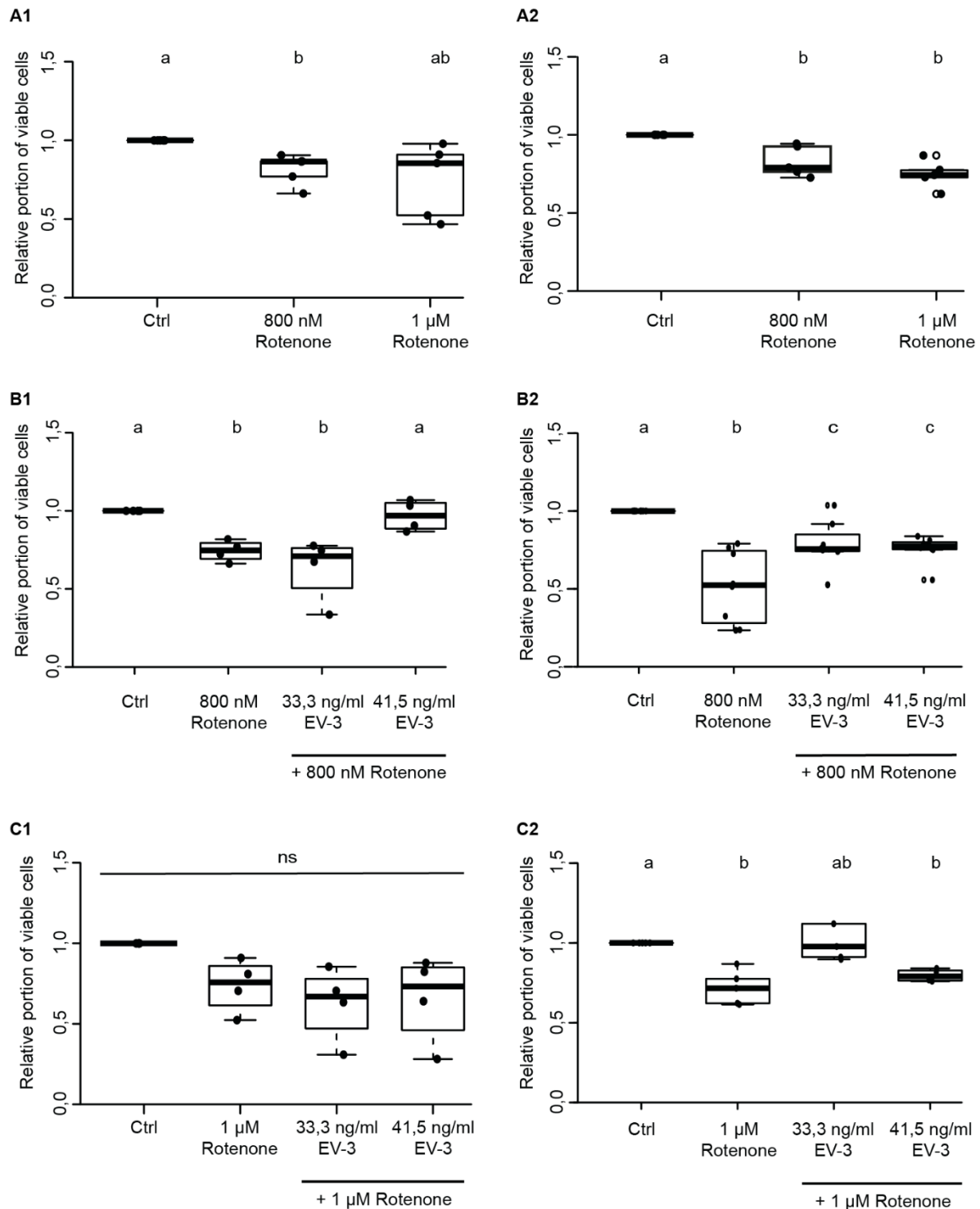
**Supp. Figure 1:** Schematic overview of differentiation process and experimental treatment



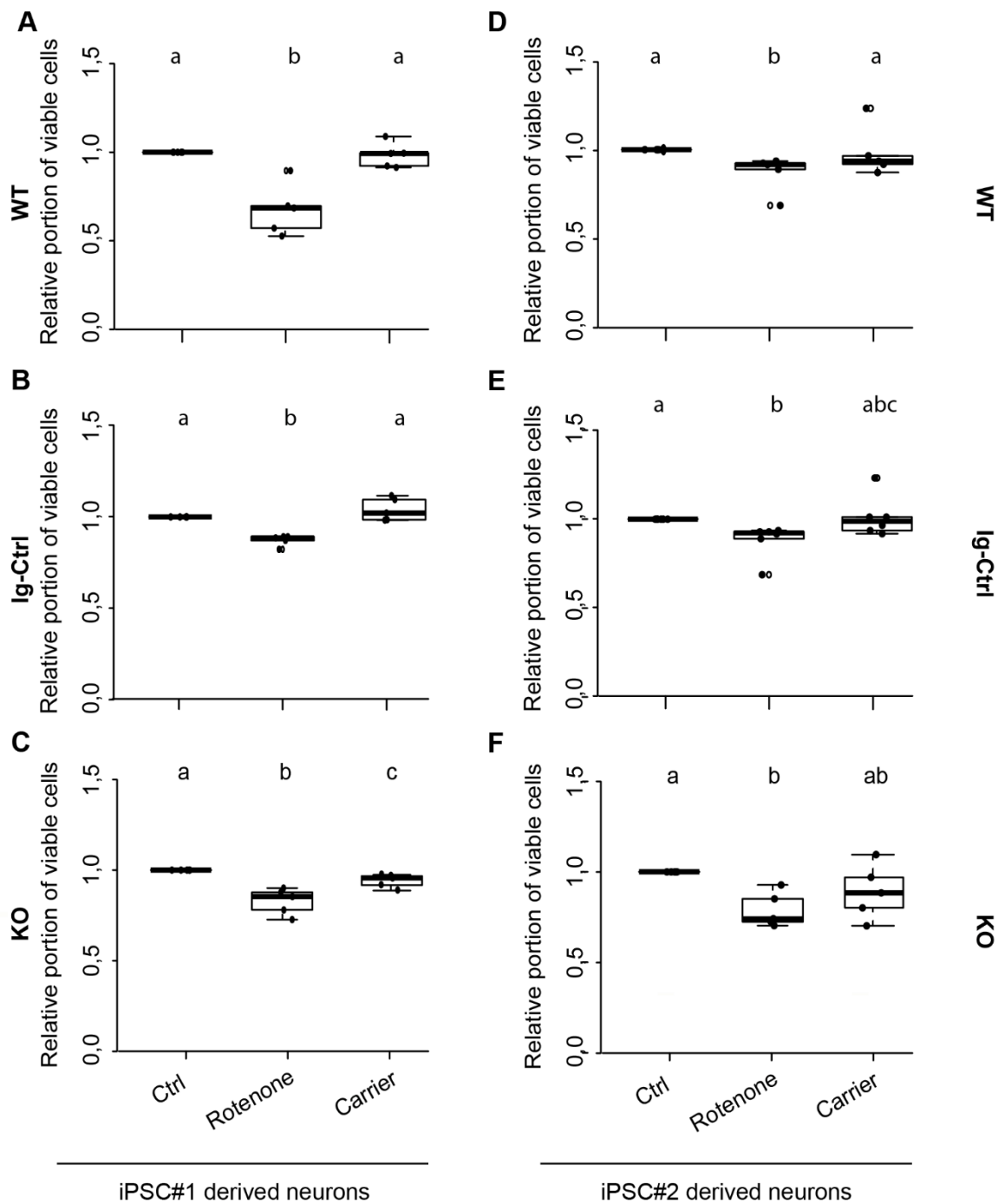
**Supp. Figure 2:** Neuronal differentiation efficiencies between the different iPSC lines. WT and Ig-Ctrl cells originating from iPSC#1 differentiate the most efficient. Cells originating from iPSC#2 reach a max average differentiation efficiency of 40%.



**Supp. Figure 3:** Characterization of newly generated iPSC lines. For both line 1 and 2, Ig-Ctrl and *CRLF3* KO cells were examined to ensure full pluripotency. **A, B:** iPSC of all four lines were stained for two characteristic pluripotency markers. All cells show clear nuclear staining for Nanog and OCT4A. **C, D:** Ig-Ctrl and KO cells of both lines were used to form embryoid bodies and allow spontaneous differentiation. Cells were stained for characteristic markers of the three germ layers. All four lines generate immunopositive cells for alpha-fetoprotein (AFP) representing endodermal tissue and smooth muscle actin (SMA) representing mesoderm.  $\beta$ -III-tubulin stainings for ectodermal differentiation are presented in **Figure 2** of the main manuscript. Scale bars: 20  $\mu$ M.



**Supp. Figure 4:** Survival assays with iPSC-derived neurons. iPSC lines 1 and 2 were differentiated into neurons and subsequently (on day 30 of differentiation) treated with either rotenone alone or rotenone and EV-3. **A1, A2:** iPSC-derived neurons were treated with either 800 nM or 1  $\mu$ M rotenone for 18 h. Cell survival was measured using FACS. Survival in both cell lines is significantly reduced when cells receive 800 nM rotenone. 1  $\mu$ M rotenone significantly decreases cell survival in line 2, however not in line 1.  $n=5$  for both lines. **B1:** Cell death induced by 800 nM rotenone is unaffected by 33,3 ng/ml EV-3 but completely prevented by 41,5 ng/ml EV-3 in iPSC-derived neurons of line 1 ( $n=4$ ). **B2:** Cell death induced by 800 nM rotenone is partially prevented by both concentrations of EV-3 in line 2 iPSC-derived neurons ( $n=8$ ). **C1:** Cell death induced by 1  $\mu$ M rotenone is unaffected by EV-3 in line 1 iPSC-derived neurons ( $n=4$ ). **C2:** Cell death induced by 1  $\mu$ M rotenone is unaffected by 41,5 ng/ml EV-3 but partially reduced by 33,3 ng/ml EV-3 ( $n=5$ ). Statistics: pairwise permutation test with Benjamini-Hochberg correction for multiple comparison. Significant differences ( $p<0,05$ ) are indicated by differing letters.



**Supp. Figure 5:** Neuron-like cells from both iPSC lines used in this study were analysed for cell survival responses on DMSO treatment (rotenone was dissolved in DMSO). **A, B, C:** Cell survival of iPSC-derived neurons originating from iPSC#1. Exposure to Carrier (same concentration of DMSO as rotenone-containing treatments) had no impact on the survival of WT (A) and Ig-Ctrl (B) neurons but reduced survival of KO neurons (C), however survival is higher than in rotenone treated cells. **D, E, F:** Cell survival of iPSC-derived neurons originating from iPSC#2. Exposure to Carrier (same concentration of DMSO as rotenone-containing treatments) had no impact on the survival of WT, Ig-Ctrl and KO neurons. However, cell survival of Ig-Ctrl and KO cells was not significantly different to rotenone treated cells. Statistics: pairwise permutation test with Benjamini-Hochberg correction for multiple comparison. Significant differences ( $p < 0,05$ ) are indicated by differing letters.

## Additional experiments and discussion

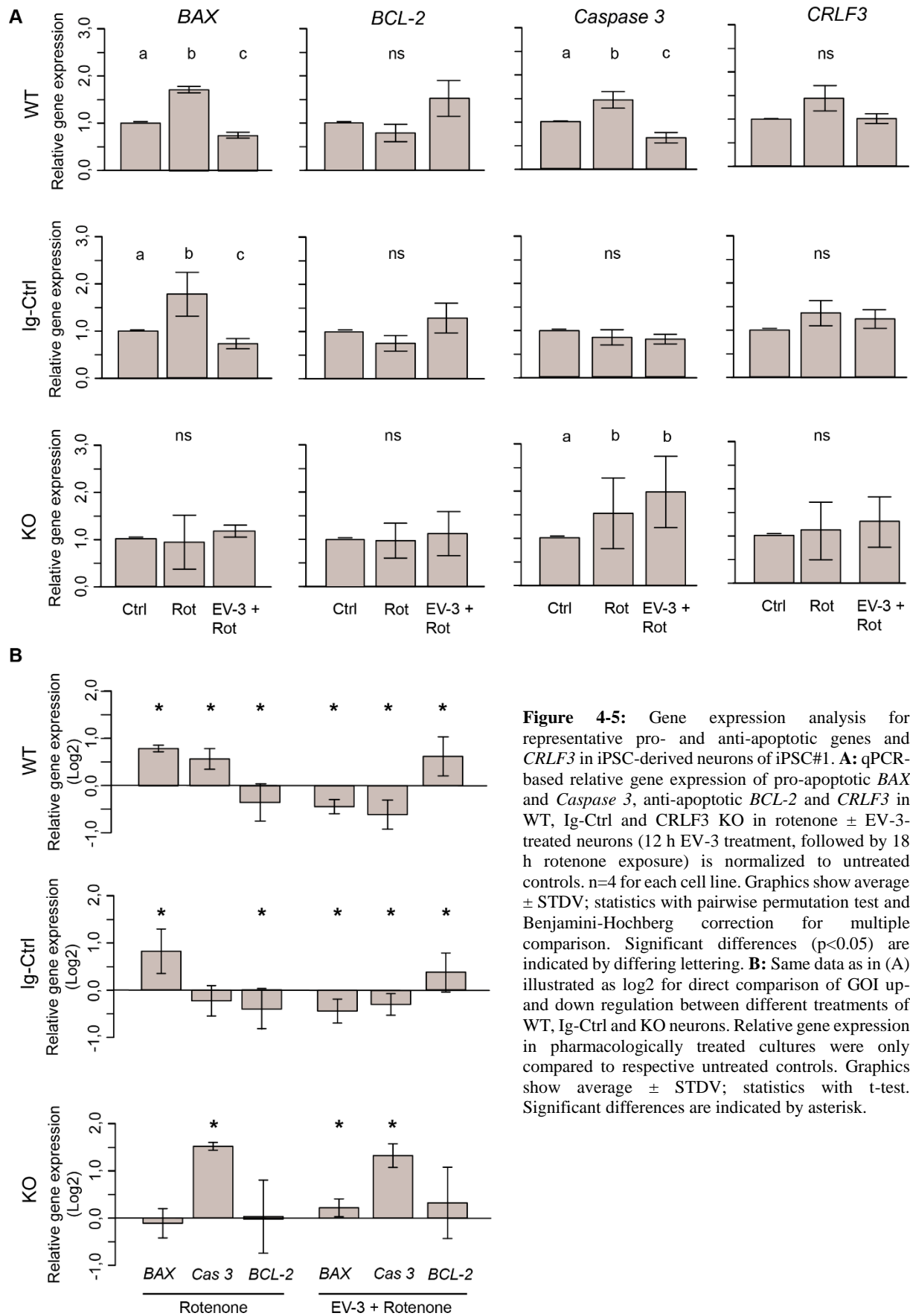
Not all data collected within the human CRLF3 project could be included into the main manuscript. Additional experiments, their results and discussion of such can be found in the following. All methods associated with this work can be found in the Supplementary sub-chapter “Methods iPSC molecular analysis”. Data presented in Figure 4-5 was collected and analysed by myself. Data in Figure 4-6 was collected and analysed by Hanna S. Pies under my supervision.

### Results

#### *Characterization of CRLF3 involvement in EV-3 mediated neuroprotection*

In order to characterize the nature of EV-3-mediated neuroprotection in iPSC-derived neurons, we analysed the expression of pro- and anti-apoptotic genes in untreated, rotenone-exposed and rotenone plus EV-3-treated cells. Analysis included early pro-apoptotic *BAX*, late pro-apoptotic *Caspase 3*, anti-apoptotic *BCL-2* and *CRLF3*. Figure 4-5 displays the data of iPSC#1-derived neurons as average relative gene expression with standard deviation.

First, expression of each gene of interest was separately analysed for different treatments of all lines (Fig. 4-5 A). Expression of pro-apoptotic *BAX*, a marker of early apoptosis, increased during exposure to the apoptogenic rotenone stimulus in WT (1,7 fold  $\pm$  0,06 STDV) and Ig-Ctrl neurons (1,76 fold  $\pm$  0,46 STDV) compared to respective untreated cultures. Co-application of EV-3 not only prevented rotenone-induced *BAX* overexpression but even caused a slight decrease of relative expression compared to untreated controls (WT 0,74  $\pm$  0,06, Ig-Ctrl 0,74  $\pm$  0,12 STDV). In contrast, *BAX* expression in CRLF3-deficient KO neurons was neither altered by rotenone (0,93  $\pm$  0,56 STDV) nor by combined treatment with rotenone and EV-3 (1,16  $\pm$  0,13 STDV). Expression of executioner *Caspase 3* in WT iPSC-derived neurons increased during rotenone exposure (1,47  $\pm$  0,17 STDV) and was reduced below control level following exposure of rotenone with EV-3 (0,66  $\pm$  0,11 STDV). Neither of the two treatments altered *Caspase 3* expression in Ig-Ctrl cells. CRLF3 KO cells increased *Caspase 3* expression during rotenone exposure (1,52  $\pm$  0,74 STDV). In contrast to WT neurons, this increase was not prevented by co-treatment with EV-3 (1,97  $\pm$  0,75 STDV, not different from rotenone-treated neurons). On the contrary, *Caspase 3* expression was further elevated in this condition. *BCL-2* and *CRLF3* expression were not significantly altered by exposure to rotenone or rotenone plus EV-3 in WT, Ig-Ctrl and CRLF3 KO iPSC-derived neurons. However, *BCL-2* expression in rotenone/EV-3-treated WT (1,52  $\pm$  0,18 STDV) and Ig-Ctrl cells (1,3  $\pm$  0,32 STDV) seems to be elevated (not significant), especially compared to rotenone-only treated cultures. WT and Ig-Ctrl lines also demonstrate slightly elevated *CRLF3* expression (not significant) upon exposure to the rotenone stressor (1,46  $\pm$  0,27 and 1,39  $\pm$  0,27 STDV respectively). For direct comparison of treatment-related changes of gene expressions in the three different cell lines, we rearranged the data in Figure 5B and plotted it as the log<sub>2</sub> of relative gene expression. While WT cells seem to increase the expression of both early and late apoptosis genes when stressed (0,55  $\pm$  0,22 *Caspase 3* to 0,77  $\pm$  0,07 *BAX*). Ig-Ctrl and KO cells overexpress either *Caspase 3* or *BAX*. *BCL-2* expression remains low for all lines. When cells are treated with EV-3, the overexpression of pro-apoptotic genes is prevented and anti-apoptotic *BCL-2* is overexpressed in WT and Ig-Ctrl samples (0,6  $\pm$  0,4 and 0,38  $\pm$  0,4 STDV respectively). KO cells, on the other hand, overexpress *Caspase 3* when treated with EV-3 (1,29  $\pm$  0,25 STDV). *BCL-2* and *BAX* expression remain on are slightly elevated in comparison to control (0,31  $\pm$  0,74 and 0,22  $\pm$  0,18 STDV respectively).

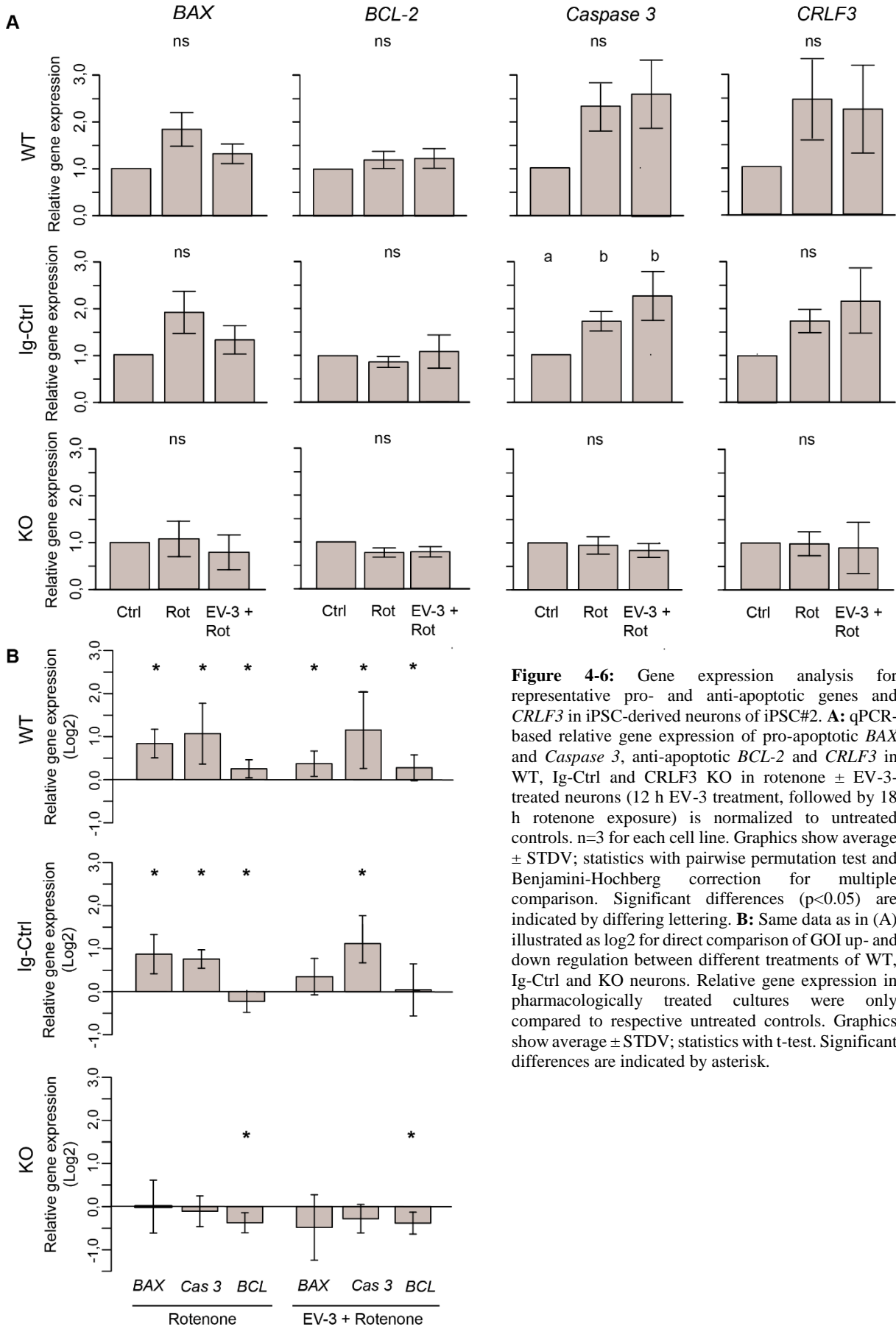


qPCR analysis of *BAX*, *Caspase 3*, *BCL-2* and *CRLF3* were additionally performed for iPSC-derived neurons originating from iPSC#2 (see Fig. 4-6). Even though clear upregulation of pro-apoptotic genes was detected in WT and Ig-Ctrl cells treated with rotenone (Average expression *BAX*  $1,83 \pm 0,35$  for



WT and  $1,89 \pm 0,44$  for Ig-Ctrl), only Ig-Ctrl cells showed significant upregulation of *Caspase 3* ( $1,7 \pm 0,21$ ). For WT and Ig-Ctrl cells originating from iPSC#2 *Caspase 3* expression remained elevated when cells were treated with EV-3 before rotenone-induced stressing ( $2,65 \pm 1,46$  and  $2,23 \pm 0,51$  respectively). *BCL-2* transcript levels were not altered by any of the treatments. CRLF3 KO cells showed no significant differential expression of any of the examined GOIs. Contrary to cells originating from iPSC#1, WT and Ig-Ctrl cells derived from iPSC#2 showed upregulation of *CRLF3* both in rotenone and EV-3 + rotenone exposed cells. These differences in expression however, were not statistically relevant.

When analysing the log2 of relative gene expression for direct comparison of GOIs in iPSC#2 derived neuron-like cells, differential expression becomes more evident (Fig 4-6 B). Both WT and Ig-Ctrl cells show significant upregulation of early and late apoptosis markers when cells receive rotenone (WT cell: *BAX*  $0,84 \pm 0,33$  , *Caspase 3*  $1,07 \pm 0,71$  ; Ig-Ctrl cells: *BAX*:  $0,87 \pm 0,46$  , *Caspase 3*:  $0,76 \pm 0,21$ ). For both lines *BAX* expression dropped when cells were pre-treated with EV-3, however expression in WT cells remains significantly upregulated (WT  $0,37 \pm 0,29$  , Ig-Ctrl  $0,35 \pm 0,42$ ). *Caspase 3* expression remained significantly upregulated in WT and IG-Ctrl cells receiving EV-3 prior to rotenone ( $1,16 \pm 0,9$  and  $1,12 \pm 0,45$  respectively). CRLF3 KO cells do not show upregulation of either apoptosis marker investigated. However, *BCL-2* transcript levels were significantly downregulated both in purely rotenone treated and EV-3 + rotenone treated cells ( $-0,37 \pm 0,233$  and  $-0,38 \pm 0,25$  respectively).



## Discussion

Both Bax and Caspase 3 are established proteins within the apoptotic machinery (reviewed in Elmore, 2007). Initiation and progress of apoptosis has furthermore been correlated with differential gene expression of these proteins (Persad *et al.*, 2004; Naseri *et al.*, 2015; He, Sun and Huang, 2018; Hu *et al.*, 2021). Our data suggest that 18 h rotenone-induced stress leads to overexpression of both “early” and “late” pro-apoptotic genes (namely *BAX* and *Caspase 3*, respectively) in WT cells. It is highly intriguing that in contrast to iPSC#1 WT cells, iPSC#1 Ig-Ctrl neuron-like cells seem to initiate apoptosis later, which is underlined by the lack of *Caspase 3* overexpression but a pronounced overexpression of the early apoptosis marker *BAX*. Since active caspases are rapidly degraded within the cell (Tawa *et al.*, 2004), the overexpression of caspases is essential for the progression of apoptosis and has been described in multiple other studies (Yakovlev *et al.*, 1997, 2001; Clark *et al.*, 2000). For both WT and Ig-Ctrl cells, EV-3 prevented rotenone-induced elevation of *Caspase 3* and/or *BAX* and even reduced expression levels below untreated controls while increasing expression of anti-apoptotic *BCL-2*. This data suggests that EV-3 mediates neuroprotection by upregulation of anti- and downregulation of pro-apoptotic genes, equipping the cells to counteract apoptotic processes induced by rotenone. The counteracting of Bcl-2 to Bax and Caspase-3 is well established within studies covering the mechanisms of apoptosis (Newmeyer *et al.*, 2000; Liang, Yan and Schor, 2001; Vazanov *et al.*, 2018) (reviewed in (Elmore, 2007)). Interestingly, the iPSC#1 KO cells analysed in this study do not display these protective gene expression profiles. *CRLF3* KO cells show a rather dysregulated transcriptional program, indicated by a high variance amongst the different samples. Rotenone treatment did not result in overexpression of *BAX* but in a clear overexpression of *Caspase 3*. Neither *BAX* nor anti-apoptotic *BCL-2* are differentially expressed when KO cells are treated with EV-3, however, quite strikingly *Caspase 3* remained strongly overexpressed as in cells that were exposed to rotenone only. The lack of *BCL-2* overexpression in EV-3 treated cells further underlines the absence of any EV-3 mediated cell-protective effects. iPSC-derived neurons originating from the second iPSC line analysed in this study unfortunately do not follow these expression patterns. However, it is to be noted that differentiation efficiencies for cells originating from iPSC#2 were lower in comparison to cells originating from iPSC#1. Given that samples for molecular analysis were taken as bulk from the experimental plate, the cell population analysed in qPCR and Western blot analysis was composed not only of neurons. As mentioned above, optimal concentrations of EV-3 may vary between different tissues within the same organism. We cannot exclude that EV-3 concentrations used in this study had deleterious effects on other cell types like glia or neuronal-precursor cells, which might be present in the mixed neuronal population we generated. The presence of non-neuronal cell types might account for the contradictory expression data we observed with iPSC#2.

Studies on the mechanisms of Epo/EpoR-mediated cell protection demonstrated elevated *EpoR* expression under physiologically stressful conditions (Mohyeldin *et al.*, 2007; Merelli *et al.*, 2019b; Su *et al.*, 2019). Hence, we asked whether *CRLF3* expression in iPSC-derived neurons was similarly affected by rotenone-induced stress. *CRLF3* expression was not significantly altered by rotenone or rotenone plus EV-3 in any of the studied cell lines of iPSC#1. While expression is slightly elevated in WT and Ig-Ctrl cells when cells receive rotenone, these effects are not statistically relevant. In contrast, the cellular abundance of *CRLF3* protein significantly increased in rotenone-stressed WT and Ig-Ctrl cells originating from iPSC#1 (see Chapter 4, Fig 4). Increased *CRLF3* protein levels without elevated levels of respective transcripts might be achieved by storage of *crlf3* transcript with blocked translation (Hinnebusch and Natarajan, 2002; Jovanovic *et al.*, 2015; Perl *et al.*, 2017; Courel *et al.*, 2019). By a mechanism termed “translation-on-demand” stored transcripts can be rapidly translated for fast cell responses in harmful conditions (reviewed in (Liu, Beyer and Aebersold, 2016)). These mechanisms have been generally described for proteins relevant in cell survival processes and rapid cell responses (Beyer *et al.*, 2004; Liu, Beyer and Aebersold, 2016). It is also possible that *CRLF3* protein is stored within the intracellular membrane of the cells, allowing fast translocation to the outer membrane. This mechanism has been previously described for EpoR, potentiating the intracellular effects of Epo/EpoR binding (Becker *et al.*, 2010). However, if this were the sole mode of activity for *CRLF3*, the intercellular protein portion would have been detected by western blot. Taking all of the presented data into consideration, we hypothesize that proper functioning and presence of *CRLF3* plays a crucial role in many aspects of functional, healthy organisms, including development, cell maintenance and, obviously, cell protection and regeneration of damaged tissue.

**References**

- Becker, V. et al. (2010) 'Covering a broad dynamic range: Information processing at the erythropoietin receptor', *Science*, 328(5984), pp. 1404–1408. doi: 10.1126/science.1184913.
- Beyer, A. et al. (2004) 'Post-transcriptional expression regulation in the yeast *Saccharomyces cerevisiae* on a genomic scale', *Molecular and Cellular Proteomics*. DOI, 3(11), pp. 1083–1092. doi: 10.1074/mcp.M400099-MCP200.
- Clark, R. S. B. et al. (2000) 'Caspase-3 mediated neuronal death after traumatic brain injury in rats', *Journal of Neurochemistry*, 74(2), pp. 740–753.
- Courel, M. et al. (2019) 'Gc content shapes mRNA storage and decay in human cells', *eLife*, 8, pp. 1–32. doi: 10.7554/eLife.49708.
- Elmore, S. (2007) 'Apoptosis: A Review of Programmed Cell Death', *Toxicologic Pathology*, 35(4), pp. 495–516. doi: 10.1080/01926230701320337.
- He, X. I. N., Sun, J. and Huang, X. (2018) 'Expression of caspase-3, Bax and Bcl-2 in hippocampus of rats with diabetes and subarachnoid hemorrhage', pp. 873–877. doi: 10.3892/etm.2017.5438.
- Hinnebusch, A. G. and Natarajan, K. (2002) 'Gcn4p, a master regulator of gene expression, is controlled at multiple levels by diverse signals of starvation and stress', *Eukaryotic Cell*. American Society for Microbiology (ASM), pp. 22–32. doi: 10.1128/EC.01.1.22-32.2002.
- Hu, X. et al. (2021) 'Guidelines for Regulated Cell Death Assays : A Systematic Summary , A Categorical Comparison , A Prospective', 9(March), pp. 1–28. doi: 10.3389/fcell.2021.634690.
- Jovanovic, M. et al. (2015) 'Dynamic profiling of the protein life cycle in response to pathogens', *Science*. American Association for the Advancement of Science, 347(6226). doi: 10.1126/science.1259038.
- Liang, Y., Yan, C. and Schor, N. F. (2001) 'Apoptosis in the absence of caspase 3', *Oncogene*, 20(45), pp. 6570–6578. doi: 10.1038/sj.onc.1204815.
- Liu, Y., Beyer, A. and Aebersold, R. (2016) 'On the Dependency of Cellular Protein Levels on mRNA Abundance', *Cell*. Cell Press, pp. 535–550. doi: 10.1016/j.cell.2016.03.014.
- Merelli, A. et al. (2019) 'Convulsive Stress Mimics Brain Hypoxia and Promotes the P-Glycoprotein (P-gp) and Erythropoietin Receptor Overexpression. Recombinant Human Erythropoietin Effect on P-gp Activity', *Frontiers in Neuroscience*. Frontiers, 13, p. 750. doi: 10.3389/fnins.2019.00750.
- Mohyeldin, A. et al. (2007) 'Survival and invasiveness of astrocytomas promoted by erythropoietin', *Journal of Neurosurgery*, 106(2), pp. 338–350. doi: 10.3171/jns.2007.106.2.338.
- Naseri, M. H. et al. (2015) 'Up regulation of Bax and down regulation of Bcl2 during 3-NC mediated apoptosis in human cancer cells', *Cancer Cell International*. Cancer Cell International, pp. 1–9. doi: 10.1186/s12935-015-0204-2.
- Newmeyer, D. D. et al. (2000) 'Bcl-x(L) does not inhibit the function of Apaf-1', *Cell Death and Differentiation*, 7(4), pp. 402–407. doi: 10.1038/sj.cdd.4400665.
- Perl, K. et al. (2017) 'Reduced changes in protein compared to mRNA levels across non-proliferating tissues', *BMC Genomics*. BioMed Central Ltd., 18(1), p. 305. doi: 10.1186/s12864-017-3683-9.
- Persad, R. et al. (2004) 'Overexpression of caspase-3 in hepatocellular carcinomas', pp. 861–867. doi: 10.1038/modpathol.3800146.
- Su, T. et al. (2019) 'HIF1 $\alpha$ , EGR1 and SP1 co-regulate the erythropoietin receptor expression under hypoxia: An essential role in the growth of non-small cell lung cancer cells', *Cell Communication and Signaling*. BioMed Central Ltd., 17(1), pp. 1–12. doi: 10.1186/s12964-019-0458-8.
- Tawa, P. et al. (2004) 'Catalytic activity of caspase-3 is required for its degradation: Stabilization of the active complex by synthetic inhibitors', *Cell Death and Differentiation*, 11(4), pp. 439–447. doi: 10.1038/sj.cdd.4401360.
- Vazanova, A. et al. (2018) 'Differential mRNA expression of the main apoptotic proteins in normal and malignant cells and its relation to in vitro resistance', *Cancer Cell International*. BioMed Central, 18(1), pp. 1–10. doi: 10.1186/s12935-018-0528-9.
- Yakovlev, A. G. et al. (1997) 'Activation of CPP32-like caspases contributes to neuronal apoptosis and neurological dysfunction after traumatic brain injury', *Journal of Neuroscience*, 17(19), pp. 7415–7424. doi: 10.1523/jneurosci.17-19-07415.1997.
- Yakovlev, A. G. et al. (2001) 'Differential expression of apoptotic protease-activating factor-1 and caspase-3 genes and susceptibility to apoptosis during brain development and after traumatic brain injury', *Journal of Neuroscience*, 21(19), pp. 7439–7446. doi: 10.1523/jneurosci.21-19-07439.2001.

## General Discussion

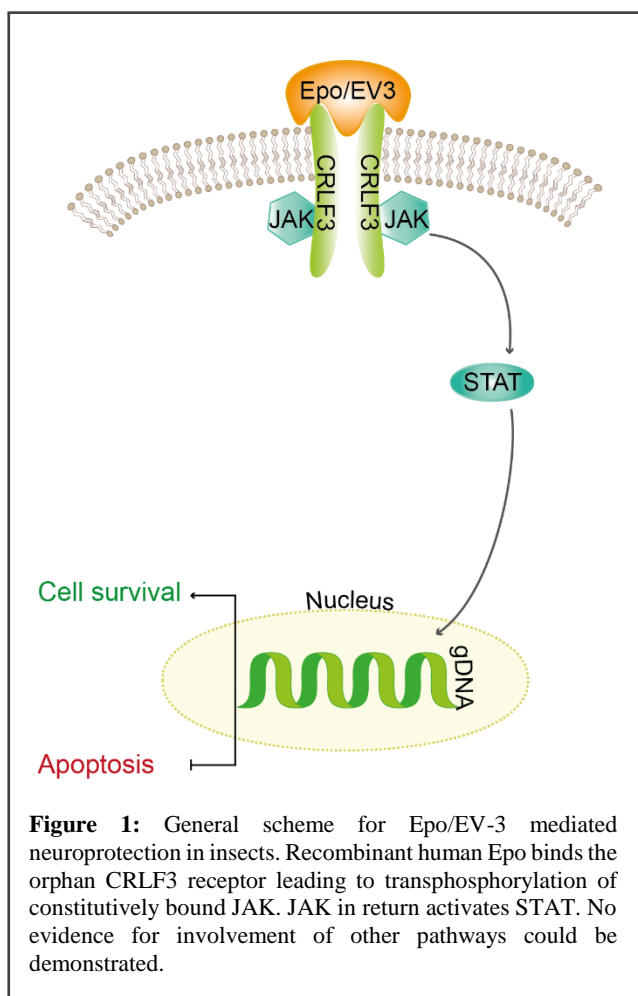
Non-hematopoietic functions of Epo are well established and recognized within the scientific community. Epo has been described to play crucial roles in neurodevelopment (Jacobs *et al.*, 2021; Khalid *et al.*, 2021), neuroprotection and as a promising drug to treat various diseases (reviews: (Kaur *et al.*, 2021; Vittori *et al.*, 2021)). Clinical trials administering Epo to patients with traumatic brain injury, schizophrenia, multiple sclerosis, depression and Alzheimer's disease have shown beneficial effects with respect to recovery and slowing of disease progression. In light of the promising results from these studies, the community started considering Epo as a serious candidate for treatment. However, the canonical, EpoR-mediated functions of Epo cause severe side effects concerning thrombosis and promotion of tumor growth (Ehrenreich *et al.*, 2009; Pedroso *et al.*, 2012). Our lack of understanding the full scope of Epo's biological modes of action hinder progress in the development of Epo-based treatments outside of anaemia patients.

One open question concerns the identity of Epo receptor/s responsible for its cytoprotective actions. While studies have identified both a EpoR homodimer and a heterodimer build of EpoR and  $\beta$ -common receptor ( $\beta$ cR) to stimulate neuroprotection (Brines *et al.*, 2004; Chamorro *et al.*, 2013; Miller *et al.*, 2015; Bonnas *et al.*, 2017; Ding *et al.*, 2017; Wakhloo *et al.*, 2020) these receptors only account for some reported anti-apoptotic functions of Epo. Evidence that recombinant human Epo (rhEpo) elicits neuroprotection in insects (Ostrowski, Ehrenreich and Heinrich, 2011; Miljus *et al.*, 2014; Hahn *et al.*, 2017; Heinrich, Günther and Miljus, 2017; Hahn *et al.*, 2019) in the absence of both EpoR and  $\beta$ cR indicated the presence of additional Epo-responsive receptors possibly shared by insects and mammalian species.

The cytokine receptor-like factor 3 (CRLF3) was identified to bind rhEpo and initiate anti-apoptotic cellular responses in insects (Hahn *et al.*, 2017; Hahn, *et al.*, 2019). Epo-mediated neuroprotection coincided with the presence of CRLF3 in insect species, both being absent in flies. The CRLF3 cytokine receptor is widely present in eumetazoans and highly conserved throughout evolution. Nonetheless, its ligands and functions are widely uncharacterized. In recent years altered regulation of *CRLF3* expression was associated with multiple human diseases, including amyotrophic lateral sclerosis (Cirulli *et al.*, 2015), autism spectrum disorders (Wegscheid *et al.*, 2021) and *Leishmania* infections (Castellucci *et al.*, 2021). However, evidence for Epo/CRLF3-mediated neuroprotection in vertebrate species was missing.

Understanding the activation and downstream effectors of CRLF3 and other tissue-protective receptors could aid in the design of synthetical Epo-like cytokine ligands, which would selectively activate tissue-protective processes without coactivation of unwanted side effects of Epo itself. Furthermore, the identification of other natural CRLF3 ligands is worth investigating in the context of neuroprotection studies.

Figure 1 depicts the general mechanism of Epo-mediated neuroprotection in insects. Even though we knew that CRLF3 was activated by rhEpo and elicited anti-apoptotic effects in insect neurons by



intracellular JAK/STAT signaling (Miljus *et al.*, 2014; Hahn *et al.*, 2017; Hahn *et al.*, 2019), we did not fully understand how Epo was able to inhibit apoptosis and allow damaged neurons to regenerate. Furthermore, activation of CRLF3 by rhEpo can be considered an “artificial model”, given that invertebrate species do not express Epo or any cytokine with detectable sequence similarity. The endogenous ligand of CRLF3 was unknown across all animal species, terming CRLF3 an orphan receptor.

### ***AChE is a molecular target of Epo-mediated anti-apoptotic effects***

Epo-mediated anti-apoptotic mechanisms in vertebrates involve activation of STAT5, PI3K, NFkB and AKT amongst others (Pregi *et al.*, 2009; Wenker *et al.*, 2010; Jia *et al.*, 2014; Si *et al.*, 2019). For insects, the involvement of JAK/STAT has been demonstrated, however, no involvement of PI3K or AKT could be observed (Miljus *et al.*, 2014). Furthermore, pro- and anti-apoptotic mechanisms involved in this system were unknown.

The enzyme acetylcholinesterase (AChE; *ace*) has only recently emerged as a crucial player in vertebrate apoptosis, disease and non-synaptic cell homeostasis (Small, Michaelson and Sberna, 1996; Karczmar, 2010; Zhang and Greenberg, 2012; Rotundo, 2017; Toiber *et al.*, 2008; Walczak-Nowicka and Herbet, 2021). Within the apoptotic machinery, the esterase acts as a promotor for apoptosome formation. The apoptosome is a large multiprotein complex consisting of Apaf-1, cytochrome c, and procaspase 9, and is generally regarded as the point-of-no-return in apoptosis. It was demonstrated that cytochrome c only interacts with Apaf-1 after association with AChE and that the absence of AChE inhibits apoptosome formation (Park, Kim and Yoo, 2004; Park *et al.*, 2008; Zhang and Greenberg, 2012). Furthermore, AChE was described to translocate to the nucleus and act as a DNase during apoptosis (Du *et al.*, 2015).

Since many crucial cell regulatory mechanisms are well conserved throughout evolution, and adapted in their complexity corresponding to the organisms, I hypothesized that AChE has similar pro-apoptotic functions in insects as in vertebrates. The data presented in this thesis demonstrates that both locusts and beetles require AChE in their apoptotic programs. While the AChE isoform relevant for mammalian apoptosis remains controversial (some studies describe AChE-S (Zhang *et al.*, 2002a; Du *et al.*, 2015) others describe AChE-R (Härtel, Gleinich and Zimmermann, 2011) to be relevant in apoptosis progression), the data collected here points towards a combinational role of both types of esterases present in insects.

Given that Epo positively regulates the erythrocytic AChE splice variant in mammals during erythrocyte differentiation (Xu *et al.*, 2018), I hypothesized that a similar mechanism might take place in Epo-mediated neuroprotection, but in a negative regulatory manner. In the mammalian system, the positive feedback loop of Epo on AChE-E expression was mediated by GATA-1 (Xu *et al.*, 2019). GATA factors have been described in insects (Uvell and Engström, 2007) and might account for *ace* transcription regulation in insects as well. Indeed, I was able to demonstrate that hypoxic stress induced overexpression of the pro-apoptotic AChE in insect neurons and that this overexpression is prevented by pre-treatment with protective concentrations of rhEpo. This is the first evidence that Epo/CRLF3 exerts a negative regulatory mechanism on pro-apoptotic AChE expression in a neuroprotection model. Since AChE involvement in apoptosis, as well as Epo(-like-ligand)-mediated neuroprotection, seem to be conserved it is possible that Epo regulates pro-apoptotic AChE in vertebrate species. This inhibitory action might account for reports in which Epo interrupted the apoptotic machinery and rescued vertebrate cells (Siren *et al.*, 2001; Kretz *et al.*, 2005).

### ***Deorphanizing CRLF3 – A quest for an unknown cytokine***

As mentioned previously, invertebrate species do not express Epo, and lack homologs of vertebrate identified Epo-responsive receptors. Nonetheless, the presence of cytokines involved in cellular responses, in particular immunity, is well-established in insects (Beschin *et al.*, 2001; Ottaviani, Malagoli and Franchini, 2004; H. S. Wang *et al.*, 2007; Altincicek, Knorr and Vilcinskis, 2008; Duressa *et al.*, 2015; Kodrík *et al.*, 2015; Shears and Hayakawa, 2019; Watari *et al.*, 2019). Many insect cytokines are released from the fat body and travel with the hemolymph through the open body cavity of the organism. Hemocytes and the solute composition of hemolymph fluid are highly dynamic and can react rapidly to exogenous and endogenous insults (Hillyer and Christensen, 2002; C. Wang *et al.*, 2007; Welchman *et al.*, 2009; Kingsolver, Huang and Hardy, 2013). Considering that CRLF3 is expressed in insect neurons, myocytes and hemocytes (Hahn *et al.*, 2019; Knorr *et al.*, 2021), we hypothesized that

the unknown ligand might be present in the insect hemolymph, allowing the cytokine to interact with its different target locations. Cytokines are considered a monophyletic group in evolution, nonetheless, this group of humoral factors shares little sequence and structural similarities amongst each other. This characteristic makes bioinformatical approaches for the identification of novel cytokines challenging. Functional approaches seem to have greater chances for the identification of cytokine/cytokine receptor signalling. However, unambiguous identification of cytokine functions is problematic considering the pleiotropic effects and promiscuous interactions of cytokine ligands with different cytokine receptors. During my work on the modes of CRLF3 action, I made use of our previous knowledge on its activation by rhEpo. Performing direct comparisons of cell survival in hypoxia-challenged neuron cultures, I demonstrated that locust hemolymph mediates similar neuroprotective effects as rhEpo does. This data allowed me to deduce the presence of an Epo-like cytokine in the insect hemolymph. Further evidence pointed towards equivalent biological functions, given that, similar to Epo, this unknown ligand acted in a dose-dependent manner and the protective functions were entirely dependent on the presence of CRLF3.

Given the nature of cytokines, it is unlikely that only one ligand can activate CRLF3 (already noticeable with Epo, EV-3 and the hemolymph-contained cytokine being able to). The evidence that two protein fractions collected from hemolymph show neuroprotective properties, both mediated *via* CRLF3, suggests the presence of more than one insect endogenous ligand contained within hemolymph. Even though I am not able to give a full characterization of these ligands, it is undoubted that they share profound similarities with Epo, investigated in the experimental approaches performed here. If recombinant expression studies are successful, it would be highly intriguing to test the effects of the insect CRLF3 ligand on human neuroprotection models, especially on human cells that express CRLF3. Given that rhEpo can activate insect CRLF3, it is possible that *vice versa*, the insect neuroprotective cytokine could also activate anti-apoptotic mechanisms in mammalian cells.

#### ***Prospects for Epo-mediated neuroprotection in humans***

With the increasing association of dysregulated *CRLF3* in human diseases, the potential importance of this receptor in cell survival and homeostasis becomes apparent. From an evolutionary perspective, CRLF3 emerged together with the nervous system in cnidarians and prevailed in all major groups of animal species, including humans (Hahn *et al.*, 2019). The fact that this receptor withstood evolutionary pressure over millions of years raises the question: Why? What makes this receptor so pivotal within the nervous system to not be eliminated during evolution? CRLF3 belongs to the same class of cytokine receptors as EpoR (Liongue and Ward, 2007) and includes the conserved cytokine binding domain (WSXWS) and a constitutive intracellular JAK binding site typical for this receptor family (Boulay, O'Shea and Paul, 2003; Liongue and Ward, 2007). Our previous experiments furthermore highlight, that both CRLF3 sequence and function were conserved (seeing that human Epo can activate the insect receptor). In light of our previous studies on Epo/CRLF3-mediated neuroprotection in insects, it was highly intriguing to study the potential involvement of CRLF3 in human neuroprotection.

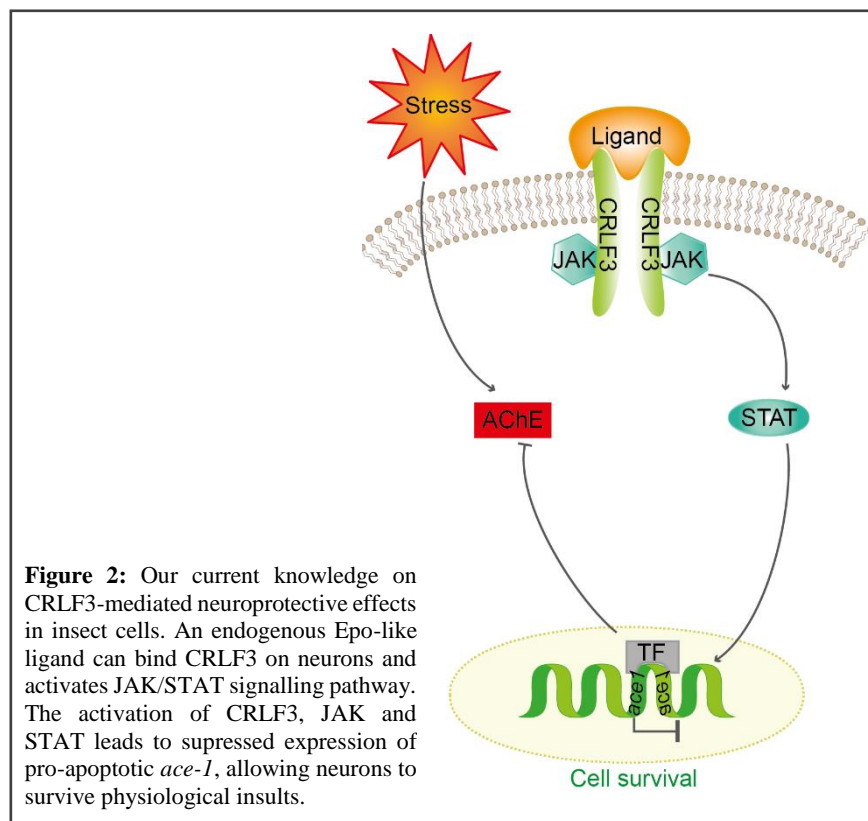
Using iPSC versatility to generate a model of human neuronal apoptosis, I am able to show that CRLF3 activation is a potent survival mechanism for neurons in physiologically harmful conditions *in vitro*. In humans, the administration of rhEpo can lead to co-activation of homodimeric EpoR and heterodimeric EpoR/ $\beta$ cR. While *CSF2RB* ( $\beta$ cR) expression was not detected in human iPSC-derived neurons, *EpoR* expression was clearly present. In light of this, administering Epo itself could result in co-activation of EpoR in iPSC-derived neurons, undermining potential effects of CRLF3 activation. In order to avoid this co-activation, I administered EV-3, a naturally occurring human Epo splice variant. EV-3 was previously shown to protect mouse and insect neurons from stress-induced apoptosis to similar levels as Epo (Bonnas *et al.*, 2017; Hahn *et al.*, 2017; Heinrich, Günther and Miljus, 2017). In the present context, usage of EV-3 was of particular interest, given that it is endogenously present in humans and does not activate erythropoietic responses by binding to EpoR (Bonnas *et al.*, 2017). Using CRISPR/Cas9 I was able to abolish CRLF3 in two independent human iPSC lines and analyse the corresponding responses to EV-3 in the mutants under physiological stress. My data demonstrate that while WT (and Isogenic Control) cells were protected by EV-3 from chemically induced hypoxic stress, KO cells lacking CRLF3 were not protected. This data is the first evidence that human CRLF3 is a neuroprotective receptor that stimulates anti-apoptotic processes. Furthermore, molecular analysis of all cell lines used in this study revealed that CRLF3 KO cells showed highly dysregulated gene expression patterns and higher



susceptibility to exogenous insults. Together with data from other groups reporting *CRLF3* associated alterations in human diseases, these results indicate that CRLF3 might be responsible for tissue protection under challenging conditions and plays a role in general cell homeostasis under normal conditions. The data presented here elucidated the involvement of basic pro- and anti-apoptotic proteins regulated by EV-3/CRLF3 in human neurons. Both WT and Ig-Ctrl cells showed an upregulation of the early pro-apoptotic *Bax* gene when challenged with rotenone. WT cells furthermore upregulated *Caspase 3*, which is involved in the apoptosis execution pathway. For both WT and Ig-Ctrl cells upregulation of the pro-apoptotic proteins was inhibited by EV-3 treatment. Instead, I observed a significant upregulation of anti-apoptotic *Bcl-2*. CRLF3 KO cells on the other hand demonstrated the strongest *Caspase 3* upregulation amongst the tested cell lines. Treatment with EV-3 did not abolish increased *Caspase 3* expression and did not affect anti-apoptotic *Bcl-2* expression. Even though I am able to make a basic molecular analysis of the mechanisms occurring upon EV-3 treatment during stress, more efforts have to be put into unravelling the exact mechanism behind it. In insects, CRLF3 is also activated by the Epo-mimetic P16, resulting in neuroprotection (Hahn, 2019). This mimetic, together with others, should be considered for testing in human neurons in order to exclude specific interaction of only EV-3 with CRLF3. Additionally, the generated transgenic human iPSC can further be utilized to study CRLF3 functions in other human tissues and cell types. Given that CRLF3 is expressed in a vast majority of human tissue, it is likely that general tissue-protective properties could be attributed to the receptor. Moreover, the emerging complexity and relevance of organoid technologies could further be employed together with these cells in order to recapitulate the relevance of CRLF3 in organ development and functioning.

#### ***A hypothetical model for cytokine/CRLF3-mediated neuroprotection***

The work presented in this thesis extends our knowledge of Epo- and Epo-like cytokine-mediated neuroprotective mechanisms. We are now able to draw a clearer picture of the underlying mechanisms and biological modes of action. We have identified an additional receptor that mediates neuroprotective effects of Epo, connected anti-apoptotic mechanisms of CRLF3 activation with downregulation of AChE and showed that insect hemolymph contains endogenous CRLF3 ligands that will be identified in future studies. Figure 2 is an adaption of Figure 1, with the addition of the new findings presented here.

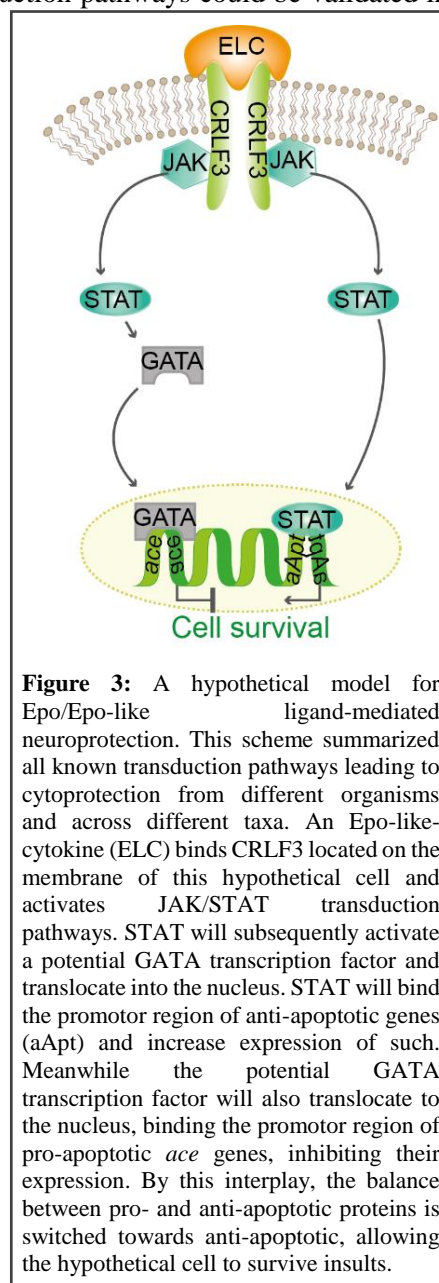


Seeing that vertebrate Epo-mediated neuroprotection and transduction pathways could be validated in insect species and that EV-3/CRLF3 mediated neuroprotection in insects could be reproduced in human neuron-like cells, it is likely that the cytokine-mediated neuroprotection system is an evolutionarily ancient and conserved mechanism of cytoprotection. In order to make these findings and their implications more accessible, I would like to introduce a hypothetical model, condensing all available information into one hypothetical chimeric insect/human cell. Figure 3 depicts this hypothetical cell, with a currently unknown pathway shown in grey.

In harmful conditions, an Epo-like cytokine (ELC) is released into the circulatory system and will bind CRLF3 located on the hypothetical cell membrane. CRLF3 might be built up as a homodimer or a heterodimer, with the second component currently unknown. Interaction of ELC and CRLF3 will lead to intracellular transphosphorylation of constitutively bound JAK, which in return will activate STAT as a transcription factor. STAT will translocate into the nucleus and activate transcription of anti-apoptotic proteins. Simultaneously other intracellular transduction pathways will be activated, further strengthening the anti-apoptotic functions of ELC. A candidate transcription factor activated as a result of this cascade might be part of the family of GATA transcription factors.

GATA transcription factors are generally known to either inhibit or activate gene expression depending on the family member and their target (Ogilvie *et al.*, 2000; Zhao *et al.*, 2006; Obara *et al.*, 2008; Rogers *et al.*, 2008; Jun *et al.*, 2013). Epo itself has previously been described to act on multiple of the GATA transduction activation family members (Ogilvie *et al.*, 2000; Zhao *et al.*, 2006; Obara *et al.*, 2008; Rogers *et al.*, 2008; Jun *et al.*, 2013). GATA transcription factors have been described in invertebrate species (Uvell and Engström, 2007). However, an involvement in Epo-mediated insect neuroprotection has to be validated in the future. The hypothetical ELC might act similarly and activate a GATA family member, which in return will also translocate into the nucleus, where it will bind the promoter region of pro-apoptotic *ace* genes, inhibiting transcription. The transcriptional regulation by STAT and GATA will shift the balance of pro- and anti-apoptotic genes toward anti-apoptotic proteins, allowing the cell to sustain itself during physiological stress.

Both Epo and the endogenous insect cytokine show toxic effects when applied in too high concentrations. While protective functions of Epo are well studied, barely any information can be found on underlying mechanisms of Epo overdose. My data shows that toxic concentrations of Epo reactivate pro-apoptotic *ace-1* gene expression. This means that neuroprotective concentrations of Epo/unknown ligand /ELC bind CRLF3 and inhibit *ace* gene expression, but toxic concentrations of these cytokines lead to overexpression of *ace* by means yet unknown. It cannot be excluded that a yet unidentified alternative receptor/s with lower binding affinities might be responsible for these effects.



***Final remarks***

With increasing numbers of patients suffering from neurodegenerative and -physiological diseases, the lack of appropriate treatments becomes more evident. High hopes were set into Epo after first studies identified neuroprotective and regenerative properties of this natural cytokine. Albeit striking evidence of beneficial functions, severe side effects of Epo administration hinder clinical application in the context of neuroprotection and regeneration. Even though non-erythropoietic Epo mimetics stimulate similar protective effects while lacking erythropoietic and tumorigenic effects, our understanding of the cytokines' full potential, transduction pathways and regulatory properties is far from being complete. The work presented in this thesis does not complete the picture of Epo-mediated neuroprotective mechanisms, but it contributes substantial knowledge to the field.

Our understanding of cytokine evolution and cell survival strategies is limited, because it is generally considered troublesome to translate invertebrate studies to vertebrate species. However, the data presented here highlight the importance of understanding evolution and the underestimated conservation of crucial cell homeostasis mechanisms. By translating our knowledge of invertebrate Epo-mediated neuroprotection into mammalia it was shown that the insect Epo-responsive CRLF3 receptor is also a neuroprotective receptor in humans. Furthermore, it builds a new target for clinical approaches in the context of neuro-physiological and -degenerative disease treatments.

## References General Introduction and Discussion

- Abdel-Aal, R. et al. (2021) 'Celecoxib effect on rivastigmine anti-Alzheimer activity against aluminum chloride-induced neurobehavioral deficits as a rat model of Alzheimer's disease; novel perspectives for an old drug', *Journal of Medical and Life Science*, 0(0), pp. 44–82. doi: 10.21608/jmals.2021.210630.
- Altincicek, B., Knorr, E. and Vilcinskas, A. (2008) 'Beetle immunity: Identification of immune-inducible genes from the model insect *Tribolium castaneum*', *Developmental and Comparative Immunology*, pp. 585–595. doi: 10.1016/j.dci.2007.09.005.
- Arcasoy, M. O. (2008) 'The non-haematopoietic biological effects of erythropoietin', *British Journal of Haematology*. John Wiley & Sons, Ltd, 141(1), pp. 14–31. doi: 10.1111/j.1365-2141.2008.07014.x.
- Arnoult, D. (2007) 'Mitochondrial fragmentation in apoptosis', *Trends in Cell Biology*, pp. 6–12. doi: 10.1016/j.tcb.2006.11.001.
- Arnoult, D. (2007) 'Mitochondrial fragmentation in apoptosis', *Trends in Cell Biology*, pp. 6–12. doi: 10.1016/j.tcb.2006.11.001.
- Bender, C. E. et al. (2012) 'Mitochondrial pathway of apoptosis is ancestral in metazoans', *Proceedings of the National Academy of Sciences*, 109(13), pp. 4904–4909. doi: 10.1073/pnas.1120680109.
- Bernaudin, M. et al. (2000) 'Neurons and astrocytes express EPO mRNA: Oxygen-sensing mechanisms that involve the redox-state of the brain', *Glia*, 30(3), pp. 271–278. doi: 10.1002/(SICI)1098-1136(200005)30:3<271::AID-GLIA6>3.0.CO;2-H.
- Beschin, A. et al. (1999) 'Convergent evolution of cytokines', *Nature*, 400(6745), pp. 627–628. doi: 10.1038/23164.
- Beschin, A. et al. (2001) 'On the existence of cytokines in invertebrates', *Cellular and Molecular Life Sciences*, 58(5–6), pp. 801–814. doi: 10.1007/PL00000901.
- Bonnas, C. et al. (2017) 'EV-3, an endogenous human erythropoietin isoform with distinct functional relevance', *Scientific Reports*, 7(3684), pp. 1–15. doi: 10.1038/s41598-017-03167-0.
- Boulay, J. L., O'Shea, J. J. and Paul, W. E. (2003) 'Molecular phylogeny within type I cytokines and their cognate receptors', *Immunity*. Cell Press, pp. 159–163. doi: 10.1016/S1074-7613(03)00211-5.
- Brines, M. et al. (2004) 'Erythropoietin mediates tissue protection through an erythropoietin and common  $\beta$ -subunit heteroreceptor', *PNAS*, 101(41).
- Brines, M. et al. (2008) 'Nonerythropoietic, tissue-protective peptides derived from the tertiary structure of erythropoietin', *Proceedings of the National Academy of Sciences of the United States of America*, 105(31), pp. 10925–10930. doi: 10.1073/pnas.0805594105.
- Brines, M. and Cerami, A. (2005) 'Emerging biological roles for erythropoietin in the nervous system', *Nature Reviews Neuroscience*. Nature Publishing Group, pp. 484–494. doi: 10.1038/nrn1687.
- Buchmann, K. (2014) 'Evolution of innate immunity: Clues from invertebrates via fish to mammals', *Frontiers in Immunology*, 5(SEP), pp. 1–8. doi: 10.3389/fimmu.2014.00459.
- Castellucci, L. C. et al. (2021) 'A Genome-wide Association Study Identifies SERPINB10, CRLF3, STX7, LAMP3, IFNG-AS1, and KRT80 As Risk Loci Contributing to Cutaneous Leishmaniasis in Brazil', *Clinical infectious diseases : an official publication of the Infectious Diseases Society of America*, 72(10), pp. e515–e525. doi: 10.1093/cid/ciaa1230.
- Chamorro, M. E. et al. (2013) 'Signaling pathways of cell proliferation are involved in the differential effect of erythropoietin and its carbamylated derivative', *Biochimica et Biophysica Acta - Molecular Cell Research*. Biochim Biophys Acta, 1833(8), pp. 1960–1968. doi: 10.1016/j.bbamcr.2013.04.006.
- Chateauvieux, S. et al. (2011) 'Erythropoietin, erythropoiesis and beyond', *Biochemical Pharmacology*. Elsevier Inc., 82(10), pp. 1291–1303. doi: 10.1016/j.bcp.2011.06.045.
- Chu, C. Y. et al. (2008) 'Erythropoietins from teleosts', *Cellular and Molecular Life Sciences*, 65(22), pp. 3545–3552. doi: 10.1007/s00018-008-8231-y.
- Cirulli, E. T. et al. (2015) 'Exome sequencing in amyotrophic lateral sclerosis identifies risk genes and pathways', *Science*. American Association for the Advancement of Science, 347(6229), pp. 1436–1441. doi: 10.1126/science.aaa3650.
- Ding, J. et al. (2017) 'Neuroprotection and CD131/GDNF/AKT Pathway of Carbamylated Erythropoietin in Hypoxic Neurons', *Molecular Neurobiology*. Humana Press Inc., 54(7), pp. 5051–5060. doi: 10.1007/s12035-016-0022-0.

## References

- Doss, M. X. and Sachinidis, A. (2019) 'Current Challenges of iPSC-Based Disease Modeling and Therapeutic Implications', *Cells*. MDPI AG, 8(5), p. 403. doi: 10.3390/cells8050403.
- Du, A. et al. (2015) 'A novel role for synaptic acetylcholinesterase as an apoptotic deoxyribonuclease', *Cell Discovery*. Nature Publishing Groups, 1. doi: 10.1038/celldisc.2015.2.
- Duressa, T. F. et al. (2015) 'Identification and functional characterization of a novel locust peptide belonging to the family of insect growth blocking peptides', *Peptides*, 74, pp. 23–32. doi: 10.1016/j.peptides.2015.09.011.
- Ehrenreich, H. et al. (2007) 'Exploring recombinant human erythropoietin in chronic progressive multiple sclerosis', *Brain*, 130(10), pp. 2577–2588. doi: 10.1093/brain/awm203.
- Ehrenreich, H. et al. (2009) 'Recombinant human erythropoietin in the treatment of acute ischemic stroke', *Stroke*. Stroke, 40(12). doi: 10.1161/STROKEAHA.109.564872.
- Ghezzi, P. and Conklin, D. (2013) 'Tissue-protective cytokines: Structure and evolution', *Methods in Molecular Biology*. Humana Press Inc., 982, pp. 43–58. doi: 10.1007/978-1-62703-308-4\_3.
- Gilboa-geffen, A. et al. (2007) 'The thymic theme of acetylcholinesterase splice variants in myasthenia gravis', *Blood*, 109(10), pp. 4383–4392. doi: 10.1182/blood-2006-07-033373.The.
- Grisaru, D. et al. (1999) 'Structural roles of acetylcholinesterase variants in biology and pathology', *European Journal of Biochemistry*, pp. 672–686. doi: 10.1046/j.1432-1327.1999.00693.x.
- Hahn, N. et al. (2017) 'The Insect Ortholog of the Human Orphan Cytokine Receptor CRLF3 Is a Neuroprotective Erythropoietin Receptor', *Front. Mol. Neurosci.*, 10(July), pp. 1–11. doi: 10.3389/fnmol.2017.00223.
- Hahn, N. et al. (2019) 'The Orphan Cytokine Receptor CRLF3 Emerged With the Origin of the Nervous System and Is a Neuroprotective Erythropoietin Receptor in Locusts', *Frontiers in Molecular Neuroscience*. Frontiers Media S.A., 12. doi: 10.3389/fnmol.2019.00251.
- Hahn, N (2019): "Erythropoietin-mediated neuroprotection and potential contribution of the cytokine receptor CRLF3 in insects"; Dissertation Georg-August-University Göttingem
- Hall, L. M. and Spierer, P. (1986) 'The Ace locus of *Drosophila melanogaster*: structural gene for acetylcholinesterase with an unusual 5' leader.', *The EMBO Journal*, 5(11), pp. 2949–2954. doi: 10.1002/j.1460-2075.1986.tb04591.x.
- Härtel, R., Gleinich, A. and Zimmermann, M. (2011) 'Dramatic increase in readthrough acetylcholinesterase in a cellular model of oxidative stress', *Journal of Neurochemistry*, 116, pp. 1088–1096. doi: 10.1111/j.1471-4159.2010.07164.x.
- Heinrich, R., Günther, V. and Miljus, N. (2017) 'Erythropoietin-Mediated Neuroprotection in Insects Suggests a Prevertebrate Evolution of Erythropoietin-Like Signaling', in *Vitamins and Hormones*. Academic Press Inc., pp. 181–196. doi: 10.1016/bs.vh.2017.02.004.
- Hicks, D. et al. (2011) 'Membrane targeting, shedding and protein interactions of brain acetylcholinesterase', *Journal of Neurochemistry*, 116(5), pp. 742–746. doi: 10.1111/j.1471-4159.2010.07032.x.
- Hillyer, J. F. and Christensen, B. M. (2002) 'Characterization of hemocytes from the yellow fever mosquito, *Aedes aegypti*', pp. 431–440. doi: 10.1007/s00418-002-0408-0.
- Huising, M. O., Kruiswijk, C. P. and Flik, G. (2006) 'Phylogeny and evolution of class-I helical cytokines', *Journal of Endocrinology*, 189(1), pp. 1–25. doi: 10.1677/joe.1.06591.
- Jacobs, R. A. et al. (2021) 'Erythropoietin promotes hippocampal mitochondrial function and enhances cognition in mice', *Communications Biology*, 4(1). doi: 10.1038/s42003-021-02465-8.
- Jang, W. et al. (2014) 'Safety and efficacy of recombinant human erythropoietin treatment of non-motor symptoms in Parkinson's disease', *Journal of the Neurological Sciences*. Elsevier B.V., 337(1–2), pp. 47–54. doi: 10.1016/j.jns.2013.11.015.
- Jelkmann, W. (2011) 'Regulation of erythropoietin production', *Journal of Physiology*. *J Physiol*, pp. 1251–1258. doi: 10.1113/jphysiol.2010.195057.
- Jia, Y. et al. (2014) 'EPO-dependent activation of PI3K/Akt/FoxO3a signalling mediates neuroprotection in in vitro and in vivo models of Parkinson's disease', *Journal of Molecular Neuroscience*, 53(1), pp. 117–124. doi: 10.1007/s12031-013-0208-0.
- Jun, J. H. et al. (2013) 'Erythropoietin prevents hypoxia-induced GATA-4 ubiquitination via phosphorylation of serine 105 of GATA-4', *Biological and Pharmaceutical Bulletin*, 36(7), pp. 1126–1133. doi: 10.1248/bpb.b13-00100.

- Karczmar, A. G. (2010) 'Cholinesterases (ChEs) and the cholinergic system in ontogenesis and phylogenesis, and non-classical roles of cholinesterases-A review', *Chemico-Biological Interactions*. Elsevier Ireland Ltd, 187(1–3), pp. 34–43. doi: 10.1016/j.cbi.2010.03.009.
- Kaur, D. et al. (2021) 'Unravelling the potential neuroprotective facets of erythropoietin for the treatment of Alzheimer's disease', *Metabolic Brain Disease*. Springer US. doi: 10.1007/s11011-021-00820-6.
- Khalid, K. et al. (2021) 'Erythropoietin stimulates gabaergic maturation in the mouse hippocampus', *eNeuro*, 8(1), pp. 1–20. doi: 10.1523/ENEURO.0006-21.2021.
- Kim, Y. H. and Lee, S. H. (2013) 'Which acetylcholinesterase functions as the main catalytic enzyme in the Class Insecta?', *Insect biochemistry and molecular biology*, 43(1), pp. 47–53. doi: 10.1016/j.ibmb.2012.11.004.
- Kingsolver, M. B., Huang, Z. and Hardy, R. W. (2013) 'Insect antiviral innate immunity: Pathways, effectors, and connections', *Journal of Molecular Biology*. Elsevier Ltd, 425(24), pp. 4921–4936. doi: 10.1016/j.jmb.2013.10.006.
- Knorr, D. Y. et al. (2021) 'Locust Hemolymph Conveys Erythropoietin-Like Cytoprotection via Activation of the Cytokine Receptor CRLF3', *Frontiers in Physiology*. Frontiers Media S.A., 12. doi: 10.3389/fphys.2021.648245.
- Kodrík, D. et al. (2015) 'Hormonal regulation of response to oxidative stress in insects—an update', *International Journal of Molecular Sciences*. MDPI AG, pp. 25788–25817. doi: 10.3390/ijms161025788.
- Kretz, A. et al. (2005) 'Erythropoietin promotes regeneration of adult CNS neurons via Jak2/Stat3 and PI3K/AKT pathway activation', *Molecular and Cellular Neuroscience*, 29(4), pp. 569–579. doi: 10.1016/j.mcn.2005.04.009.
- Liongue, C. and Ward, A. C. (2007) 'Evolution of Class I cytokine receptors', *BMC Evolutionary Biology*, 7. doi: 10.1186/1471-2148-7-120.
- Lu, Y., Park, Y., et al. (2012) 'Cholinergic and non-cholinergic functions of two acetylcholinesterase genes revealed by gene-silencing in *Tribolium castaneum*', *Scientific Reports*, 2, pp. 1–7. doi: 10.1038/srep00288.
- Lu, Y., Pang, Y.-P., et al. (2012) 'Genome organization, phylogenies, expression patterns, and three-dimensional protein models of two acetylcholinesterase genes from the red flour beetle.', *PloS one*. Public Library of Science, 7(2), p. e32288. doi: 10.1371/journal.pone.0032288.
- Marti, H. H. et al. (1996) 'Erythropoietin gene expression in human, monkey and murine brain', *European Journal of Neuroscience*, 8(4), pp. 666–676. doi: 10.1111/j.1460-9568.1996.tb01252.x.
- Miljus, N. et al. (2014) 'Erythropoietin-mediated protection of insect brain neurons involves JAK and STAT but not PI3K transduction pathways', *Neuroscience*. IBRO, 258, pp. 218–227. doi: 10.1016/j.neuroscience.2013.11.020.
- Miller, J. L. et al. (2015) 'Discovery and characterization of nonpeptidyl agonists of the tissue-protective erythropoietin receptors', *Molecular Pharmacology*. American Society for Pharmacology and Experimental Therapy, 88(2), pp. 357–367. doi: 10.1124/mol.115.098400.
- Noguchi, C. T. et al. (2007) 'Role of erythropoietin in the brain', *Critical Reviews in Oncology/Hematology*. Elsevier, pp. 159–171. doi: 10.1016/j.critrevonc.2007.03.001.
- Obara, N. et al. (2008) 'Repression via the GATA box is essential for tissue-specific erythropoietin gene expression', *Blood*, 111(10), pp. 5223–5232. doi: 10.1182/blood-2007-10-115857.
- Oda, Y. et al. (2010) 'Adaptor protein is essential for insect cytokine signaling in hemocytes', *Proceedings of the National Academy of Sciences of the United States of America*. National Academy of Sciences, 107(36), pp. 15862–15867. doi: 10.1073/pnas.1003785107.
- Ogilvie, M. et al. (2000) 'Erythropoietin stimulates proliferation and interferes with differentiation of myoblasts', *Journal of Biological Chemistry*. J Biol Chem, 275(50), pp. 39754–39761. doi: 10.1074/jbc.M004999200.
- Okita, K. et al. (2011) 'A more efficient method to generate integration-free human iPS cells', *Nature Methods*. Nature Publishing Group, 8(5), pp. 409–412. doi: 10.1038/nmeth.1591.
- Ostrowski, D., Ehrenreich, H. and Heinrich, R. (2011) 'Erythropoietin promotes survival and regeneration of insect neurons in vivo and in vitro', *Neuroscience*, pp. 95–108. doi: 10.1016/j.neuroscience.2011.05.018.
- Ottaviani, E., Malagoli, D. and Franchini, A. (2004) 'Invertebrate humoral factors: cytokines as mediators of cell survival.', *Progress in molecular and subcellular biology*, 34, pp. 1–25. doi: 10.1007/978-3-642-18670-7\_1.
- Pang, Y. et al. (2015) 'Structure of the apoptosome: Mechanistic insights into activation of an initiator caspase from *Drosophila*', *Genes and Development*, 29(3), pp. 277–287. doi: 10.1101/gad.255877.114.

## References

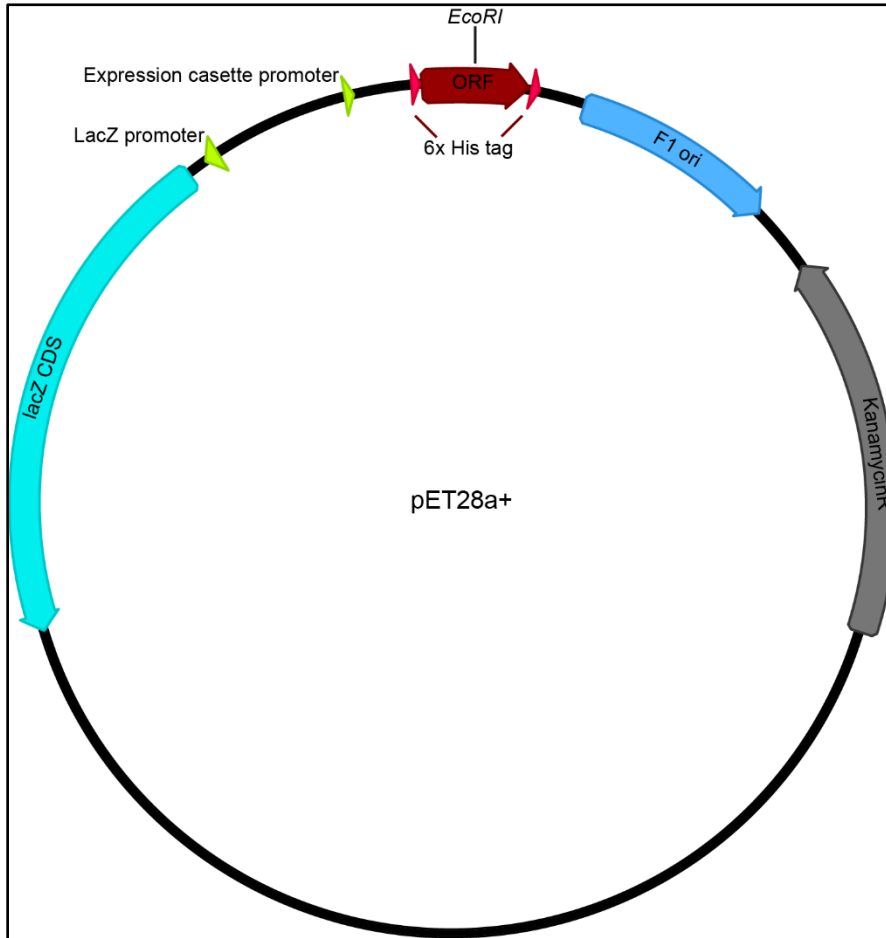
- Park, S. E. et al. (2008) 'Interactions of acetylcholinesterase with caveolin-1 and subsequently with cytochrome c are required for apoptosome formation', *29*(4), pp. 729–737. doi: 10.1093/carcin/bgn036.
- Park, S. E., Kim, N. D. and Yoo, Y. H. (2004) 'Advances in Brief Acetylcholinesterase Plays a Pivotal Role in Apoptosome Formation', *Cancer Res*, *64*, pp. 2652–2655.
- Pedroso, I. et al. (2012) 'Use of Cuban recombinant human erythropoietin in Parkinson's disease treatment', *MEDICC Review. MEDICC Rev*, *14*(1), pp. 11–17. doi: 10.37757/mr2012v14.n1.4.
- Pregi, N. et al. (2009) 'TNF-alpha-induced apoptosis is prevented by erythropoietin treatment on SH-SY5Y cells', *Experimental Cell Research. Elsevier Inc.*, *315*(3), pp. 419–431. doi: 10.1016/j.yexcr.2008.11.005.
- Revuelta, L. et al. (2009) 'RNAi of ace1 and ace2 in *Blattella germanica* reveals their differential contribution to acetylcholinesterase activity and sensitivity to insecticides', *Insect Biochemistry and Molecular Biology*, *39*(12), pp. 913–919. doi: 10.1016/j.ibmb.2009.11.001.
- Riedl, S. J. and Salvesen, G. S. (2007) 'The apoptosome : signalling platform of cell death', *8*(May), pp. 405–413. doi: 10.1038/nrm2153.
- Rodriguez-Polo, I. et al. (2019) 'Baboon induced pluripotent stem cell generation by piggyBac transposition of reprogramming factors', *Primate Biology. Copernicus GmbH*, *6*(2), pp. 75–86. doi: 10.5194/pb-6-75-2019.
- Rogers, H. M. et al. (2008) 'Hypoxia alters progression of the erythroid program', *Exp Hematol.*, *36*(1). doi: 10.1016/j.exphem.2007.08.014.
- Rotundo, R. L. (2017) 'Biogenesis, assembly and trafficking of acetylcholinesterase', *Journal of Neurochemistry*, *142*(Suppl 2), pp. 52–58. doi: 10.1111/jnc.13982.
- Sendoel, A. and Hengartner, M. O. (2014) 'Apoptotic cell death under hypoxia', *Physiology. American Physiological Society*, pp. 168–176. doi: 10.1152/physiol.00016.2013.
- Sepodes, B. et al. (2006) 'Recombinant human erythropoietin protects the liver from hepatic ischemia-reperfusion injury in the rat', *Transplant International. John Wiley & Sons, Ltd*, *19*(11), pp. 919–926. doi: 10.1111/J.1432-2277.2006.00366.X.
- Shears, S. B. and Hayakawa, Y. (2019) 'Functional Multiplicity of an Insect Cytokine Family Assists Defense Against Environmental Stress', *Frontiers in Physiology. Frontiers Media S.A.*, *10*(MAR), p. 222. doi: 10.3389/fphys.2019.00222.
- Shields, D. C. et al. (1995) 'The evolution of haematopoietic cytokine/receptor complexes', *Cytokine*, *7*(7), pp. 679–688. doi: 10.1006/cyto.1995.0080.
- Si, W. et al. (2019) 'Erythropoietin protects neurons from apoptosis via activating PI3K/AKT and inhibiting Erk1/2 signaling pathway', *3 Biotech. Springer International Publishing*, *9*(4), pp. 1–8. doi: 10.1007/s13205-019-1667-y.
- Siren, A.-L. et al. (2001) 'Erythropoietin prevents neuronal apoptosis after cerebral ischemia and metabolic stress', *Proceedings of the National Academy of Sciences*, *98*(7), pp. 4044–4049. doi: 10.1073/pnas.051606598.
- Small, D. H., Michaelson, S. and Sberna, G. (1996) 'non-classical actions of cholinesterases: Role in cellular differentiation, tumorigenesis and Alzheimer's Disease', *Neurochem. Int.*, *28*(5), pp. 453–483.
- Stauske, M. et al. (2020) 'Non-Human Primate iPSC Generation, Cultivation, and Cardiac Differentiation under Chemically Defined Conditions', *Cells*, *9*(6).
- Takahashi, K. and Yamanaka, S. (2006) 'Induction of Pluripotent Stem Cells from Mouse Embryonic and Adult Fibroblast Cultures by Defined Factors', *Cell*, *126*(4), pp. 663–676. doi: 10.1016/j.cell.2006.07.024.
- Toiber, D. et al. (2008) 'N-acetylcholinesterase-induced apoptosis in alzheimer's disease', *PLoS ONE*, *3*(9). doi: 10.1371/journal.pone.0003108.
- Ueba, H. et al. (2010) 'Cardioprotection by a nonerythropoietic, tissue-protective peptide mimicking the 3D structure of erythropoietin', *Proceedings of the National Academy of Sciences of the United States of America*, *107*(32), pp. 14357–14362. doi: 10.1073/pnas.1003019107.
- Uvell, H. and Engström, Y. (2007) 'A multilayered defense against infection: combinatorial control of insect immune genes', *Trends in Genetics*, *23*(7), pp. 342–349. doi: 10.1016/j.tig.2007.05.003.
- Vittori, D. C. et al. (2021a) 'Erythropoietin and derivatives: Potential beneficial effects on the brain', *Journal of Neurochemistry*, *158*(5), pp. 1032–1057. doi: 10.1111/jnc.15475.
- Wakhloo, D. et al. (2020) 'Functional hypoxia drives neuroplasticity and neurogenesis via brain erythropoietin', *Nature Communications. Springer US*, *11*(1), pp. 1–12. doi: 10.1038/s41467-020-15041-1.



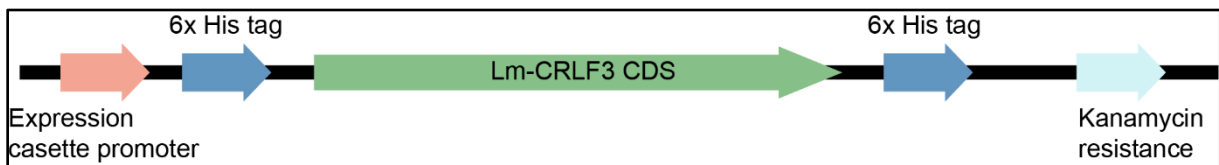
- Walczak-Nowicka, Ł. J. and Herbet, M. (2021) 'Acetylcholinesterase inhibitors in the treatment of neurodegenerative diseases and the role of acetylcholinesterase in their pathogenesis', *International Journal of Molecular Sciences*, 22(17). doi: 10.3390/ijms22179290.
- Wang, C. et al. (2007) 'Differentially-expressed glycoproteins in *Locusta migratoria* hemolymph infected with *Metarhizium anisopliae*', *Journal of Invertebrate Pathology*, 96(3), pp. 230–236. doi: 10.1016/j.jip.2007.05.012.
- Wang, H. S. et al. (2007) 'cDNA cloning of heat shock proteins and their expression in the two phases of the migratory locust', *Insect Molecular Biology*, 16(2), pp. 207–219. doi: 10.1111/j.1365-2583.2006.00715.x.
- Watari, H. et al. (2019) 'A novel sponge-derived protein thrombocortin is a new agonist for thrombopoietin receptor', *Comparative Biochemistry and Physiology Part C: Toxicology & Pharmacology*, 221, pp. 82–88. doi: 10.1016/j.cbpc.2019.04.003.
- Wegscheid, M. L. et al. (2021) 'Patient-derived iPSC-cerebral organoid modeling of the 17q11.2 microdeletion syndrome establishes CRLF3 as a critical regulator of neurogenesis', *Cell Reports*. Elsevier B.V., 36(1), p. 109315. doi: 10.1016/j.celrep.2021.109315.
- Welchman, D. P. et al. (2009) 'Insect Immunity: From Pattern Recognition to Symbiont-Mediated Host Defense', in *Cell Host and Microbe*. Cell Press, pp. 107–114. doi: 10.1016/j.chom.2009.07.008.
- Wenker, S. D. et al. (2010) 'Differential antiapoptotic effect of erythropoietin on undifferentiated and retinoic acid-differentiated SH-SY5Y cells', *Journal of Cellular Biochemistry*, 110(1), pp. 151–161. doi: 10.1002/jcb.22521.
- Wiegand, C. and Banerjee, I. (2019) 'Recent advances in the applications of iPSC technology', *Current Opinion in Biotechnology*. Elsevier Ltd, pp. 250–258. doi: 10.1016/j.copbio.2019.05.011.
- Wiegand, C. and Banerjee, I. (2019) 'Recent advances in the applications of iPSC technology', *Current Opinion in Biotechnology*. Elsevier Ltd, pp. 250–258. doi: 10.1016/j.copbio.2019.05.011.
- Wu, Yuanyuan et al. (2013) 'Protective effects of HBSP on ischemia reperfusion and cyclosporine a induced renal injury', *Clinical and Developmental Immunology*, 2013. doi: 10.1155/2013/758159.
- Wyder, S. et al. (2007) 'Quantification of ortholog losses in insects and vertebrates', *Genome Biology*, 8(11). doi: 10.1186/gb-2007-8-11-r242.
- Xu, M. L. et al. (2018) 'Erythropoietin regulates the expression of dimeric form of acetylcholinesterase during differentiation of erythroblast', *JOURNAL OF NEUROCHEMISTRY*, 146(November), pp. 390–402. doi: 10.1111/jnc.14448.
- Xu, M. L. et al. (2019) 'Differentiation of erythroblast requires the dimeric form of acetylcholinesterase: Interference with erythropoietin receptor', *Chemico-Biological Interactions*, 308(April), pp. 317–322. doi: 10.1016/j.cbi.2019.06.006.
- Yamaji, R. et al. (1996) 'Brain capillary endothelial cells express two forms of erythropoietin receptor mRNA', *European Journal of Biochemistry*, 239(2), pp. 494–500. doi: 10.1111/j.1432-1033.1996.0494u.x.
- Ye, W. et al. (2010) 'AChE deficiency or inhibition decreases apoptosis and p53 expression and protects renal function after ischemia/reperfusion', *Apoptosis*, 15(4), pp. 474–487. doi: 10.1007/s10495-009-0438-3.
- Yilmaz, S. et al. (2004) 'The protective effect of erythropoietin on ischaemia/reperfusion injury of liver', *HPB*. Elsevier, 6(3), pp. 169–173. doi: 10.1080/13651820410026077.
- Zhang, X.-J. and Greenberg, D. S. (2012) 'Acetylcholinesterase Involvement in Apoptosis', *Frontiers in Molecular Neuroscience*. doi: 10.3389/fnmol.2012.00040.
- Zhang, X. J. et al. (2002) 'Induction of acetylcholinesterase expression during apoptosis in various cell types', *Cell Death and Differentiation*, 9(8), pp. 790–800. doi: 10.1038/sj.cdd.4401034.
- Zhao, W. et al. (2006) 'Erythropoietin stimulates phosphorylation and activation of GATA-1 via the PI3-kinase/AKT signaling pathway', *Blood*, 107(3), pp. 907–915. doi: 10.1182/blood-2005-06-2516.
- Zhou, X. and Xia, Y. (2009) 'Cloning of an acetylcholinesterase gene in *Locusta migratoria manilensis* related to organophosphate insecticide resistance', *Pesticide Biochemistry and Physiology*, pp. 77–84. doi: 10.1016/j.pestbp.2008.11.007.

## Supplements

### Vector maps for recombinant protein expression



**Supp. Figure 1:** pET28a+ expression vector used for recombinant expression studies stated in Chapter 3.1. ORF= Open reading frame



**Supp. Figure 2:** Schematic of pET28a+ vector carrying locust CRLF3 CDS for recombinant expression.

*Mass spectrometry data*

Description	Sum PEP Score	Coverage [%]	# Peptides	# PSMs	# Unique Peptides	Fragment 10 stressed			Fragment 16 stressed		Fragment 19 Ctrl			Supplements
						F10.1	F10.2	F10.3	F16.1	F16.2	F19.1	F19.2	F19.3	
Q9U943 APLP_LOCM1	1145,715	56	164	2114	164	High	High	High	High	High	High	High	High	
Q25313 DFP_LOCM1	88,102	29	9	1257	9	High	High	High	High	High	High	High	High	
E0WBM7 E0WBM7_LOCM1	376,697	70	53	1071	12	High	High	High	High	High	High	High	High	
A0A2R2Q2F2 A0A2R2Q2F2_LOCM1	314,587	71	47	901	7	NF	High	NF	High	High	High	High	High	
A0A2Z6FI57 A0A2Z6FI57_LOCM1	382,936	67	53	700	51	NF	NF	NF	High	High	High	High	High	
A0A4Y5R7W2 A0A4Y5R7W2_LOCM1	299,496	42	44	503	44	High	High	High	High	High	High	High	High	
A0A1L5LBJ0 A0A1L5LBJ0_LOCM1	302,5	36	36	388	36	High	High	High	High	High	NF	High	High	
E0WBM8 E0WBM8_LOCM1	147,226	67	23	366	6	High	High	High	High	High	High	High	High	
COLV92 COLV92_LOCM1	194,705	46	32	264	32	High	High	High	High	High	High	High	High	
D6WVY4 D6WVY4_TRICA	145,77	64	16	104	11	High	NF	High	High	High	NF	NF	High	
Q94607 Q94607_LOCM1	80,61	32	18	97	18	High	High	High	High	High	High	High	High	
W8EC24 W8EC24_LOCM1	65,165	28	12	89	12	NF	NF	NF	High	High	High	High	High	
A0A1L7XZ70 A0A1L7XZ70_LOCM1	70,078	42	20	81	17	High	High	High	High	High	High	High	High	
H8YU84 H8YU84_LOCM1	86,894	63	13	71	13	High	High	High	High	High	NF	High	NF	
P10762 APL3_LOCM1	42,763	21	6	65	6	High	High	High	High	NF	High	High	NF	
D6WFR9 D6WFR9_TRICA	28,386	16	3	62	3	NF	NF	NF	NF	NF	NF	NF	NF	
A0A6G5XGE6 A0A6G5XGE6_LOCM1	36,659	34	8	57	3	High	High	High	NF	NF	NF	NF	NF	
X5MPI2 X5MPI2_LOCM1	25,797	24	3	50	3	NF	High	High	High	High	High	High	High	
F4YUJ0 F4YUJ0_LOCM1	37,873	57	12	44	9	High	High	NF	NF	NF	NF	NF	NF	
D6WSV2 D6WSV2_TRICA	87,401	47	14	40	5	NF	NF	NF	NF	NF	NF	NF	NF	
Q86QM8 Q86QM8_LOCM1	60,036	20	10	39	3	High	High	High	NF	NF	NF	NF	NF	

Supplements

A0A139W9W1														
A0A139W9W1_TRICA	23,508	9	5	36	2	NF	NF	High	NF	NF	NF	NF	NF	NF
Q6SXP5 Q6SXP5_LOCFI	53,193	20	14	35	14	High	High	High	NF	NF	High	High	NF	
D6WYT2 D6WYT2_TRICA	22,568	25	5	34	3	NF	NF	NF	NF	NF	High	High	NF	
D6W835 D6W835_TRICA	9,128	12	3	33	1	High	High	NF	NF	NF	High	NF	NF	
D6WPR3 D6WPR3_TRICA	72,695	48	14	33	5	NF	NF	NF	NF	NF	NF	NF	NF	
F4YUJ2 F4YUJ2_LOCFI	29,182	49	10	31	6	High	NF	NF	NF	NF	NF	NF	NF	
E0WBM9 E0WBM9_LOCFI	25,103	16	10	30	10	High	High	High	High	High	High	NF	NF	
V9Q315 V9Q315_LOCFI	19,751	43	8	30	7	High	High	High	High	High	High	High	NF	
D6WJW7 D6WJW7_TRICA	14,958	16	4	30	1	NF	NF	NF	NF	NF	NF	NF	NF	
P61210 ARF1_LOCFI	29,182	53	7	29	4	High	High	High	NF	NF	NF	NF	NF	
A0A139WAS5 A0A139WAS5_TRICA	60,298	22	10	28	3	NF	NF	NF	NF	NF	NF	NF	NF	
D6WBLO D6WBLO_TRICA	93,045	51	13	27	3	NF	NF	NF	NF	NF	NF	NF	NF	
P41509 FABPM_LOCFI	58,02	60	10	27	10	NF	High	NF	NF	NF	NF	NF	NF	
A0A139W9I4 A0A139W9I4_TRICA	15,182	34	4	27	1	NF	NF	High	NF	High	NF	NF	NF	
A0A1B3PEJ4 A0A1B3PEJ4_LOCFI	43,848	37	13	26	13	NF	NF	NF	High	High	NF	NF	NF	
A0A139WAX1 A0A139WAX1_TRICA	12,052	5	3	26	1	NF	NF	NF	NF	NF	High	NF	NF	
A0A6G9W3U8														
A0A6G9W3U8_LOCFI	43,188	41	13	25	13	NF	NF	NF	High	NF	High	High	High	
V9Q487 V9Q487_LOCFI	11,45	24	5	24	2	NF	NF	NF	High	NF	NF	High	NF	
DYPNLAELK	0,066279 9	0,0036449 1	1	1	5	NF	High	NF	NF	High	NF	High	NF	
A6M9J4 A6M9J4_LOCFI	26,396	25	7	24	7	High	High	High	High	NF	NF	NF	NF	
F4YUJ3 F4YUJ3_LOCFI	16,415	38	6	22	3	NF	NF	NF	NF	NF	NF	NF	NF	
A0A6G5XI97 A0A6G5XI97_LOCFI	65,498	37	11	21	1	NF	NF	NF	NF	NF	NF	NF	NF	
A0A139WNV6 A0A139WNV6_TRICA	21,981	5	5	20	5	High	High	NF	High	NF	NF	High	High	
D7EKP1 D7EKP1_TRICA	14,984	18	4	20	4	NF	High	High	NF	High	NF	NF	NF	
E7BTM5 E7BTM5_LOCFI	40,437	49	9	18	9	NF	NF	NF	NF	NF	NF	NF	NF	
A0A139WNV5 A0A139WNV5_TRICA	18,669	26	4	18	1	NF	NF	NF	NF	NF	NF	NF	NF	
E0WBM6 E0WBM6_LOCFI	20,423	15	8	17	7	NF	NF	NF	High	High	NF	NF	NF	

A0A0A1EAU6 A0A0A1EAU6_LOCFMI	33,794	24	4	16	4	NF	NF	NF	NF	NF	NF	NF	NF	NF
D6WI91 D6WI91_TRICA	1,596	2	1	15	1	High	High	NF	High	High	NF	High	High	
F4YUJ4 F4YUJ4_LOCFMI	21,609	27	6	15	3	NF	NF	NF	NF	NF	NF	NF	NF	
A0A0B5GZN2 A0A0B5GZN2_LOCFMI	16,57	21	4	14	4	High	NF	NF	NF	NF	High	High	NF	
Q8T8P6 Q8T8P6_LOCFMI	26,364	21	7	13	7	NF	NF	NF	High	High	NF	High	NF	
D6WHK2 D6WHK2_TRICA	6,659	8	1	13	1	NF	NF	NF	High	High	High	High	High	
A0A0B5HB40 A0A0B5HB40_LOCFMI	9,615	2	3	13	3	NF	High	High	High	High	High	NF	NF	
D6W9I6 D6W9I6_TRICA	13,155	11	6	12	6	High	High	High	NF	NF	NF	NF	NF	
A0A139WMW3 A0A139WMW3_TRICA	12,993	9	3	12	3	High	NF	NF	NF	NF	NF	NF	High	
O96558 O96558_LOCFMI	21,094	18	5	12	5	High	High	High	NF	NF	NF	NF	NF	
D6WP52 D6WP52_TRICA	12,141	18	3	12	1	NF	NF	High	NF	NF	NF	NF	NF	
F4YUJ6 F4YUJ6_LOCFMI	16,02	34	5	11	5	High	High	NF	NF	NF	NF	NF	NF	
D2A4R3 D2A4R3_TRICA	36,232	18	7	10	7	NF	NF	NF	NF	NF	NF	NF	NF	
D6W8B6 D6W8B6_TRICA	13,687	46	5	10	5	NF	NF	NF	NF	NF	NF	NF	NF	
W8E8J1 W8E8J1_LOCFMI	18,699	12	5	10	5	NF	NF	NF	NF	NF	High	High	High	
D6WQP8 D6WQP8_TRICA	9,11	20	3	10	1	NF	NF	NF	NF	NF	NF	NF	NF	
X5MBK6 X5MBK6_LOCFMI	7,397	9	1	10	1	High	NF	NF	High	NF	NF	NF	NF	
L7WRS4 L7WRS4_LOCFMI	16,953	9	4	10	4	NF	High	NF	High	High	NF	NF	NF	
D6WRR0 D6WRR0_TRICA	19,736	9	7	10	7	NF	NF	NF	NF	High	NF	NF	High	
A0A139WEI6 A0A139WEI6_TRICA	4,941	2	2	9	2	NF	NF	NF	High	High	NF	NF	NF	
A0A1L4A1S1 A0A1L4A1S1_LOCFMI	23,577	14	7	9	7	NF	NF	NF	NF	NF	High	High	NF	
W8EH35 W8EH35_LOCFMI	19,548	11	6	9	6	NF	NF	NF	High	High	NF	High	High	
D6WV64 D6WV64_TRICA	5,519	10	2	9	1	NF	High	NF	NF	NF	NF	NF	NF	
D6WJQ8 D6WJQ8_TRICA	7,379	15	3	8	3	High	High	High	NF	NF	NF	NF	NF	
L0APJ7 L0APJ7_LOCFMI	18,399	10	5	8	5	NF	High	NF	High	NF	High	High	NF	
D6WHK3 D6WHK3_TRICA	1,496	1	1	8	1	NF	High	High	NF	High	NF	NF	High	
L7SU46 L7SU46_LOCFMI	7,726	9	3	7	3	NF	NF	NF	NF	NF	High	High	High	
A0A139WJ47 A0A139WJ47_TRICA	18,932	5	4	7	4	High	High	High	NF	NF	NF	NF	NF	
D6WTD3 D6WTD3_TRICA	22,439	11	6	7	6	NF	NF	NF	NF	NF	NF	NF	NF	

Supplements

D7GXZ9 D7GXZ9_TRICA	3,521	10	2	7	2	High	High	High	NF	NF	NF	NF	NF
Q0ZLZ3 Q0ZLZ3_LOCM	13,682	36	4	6	4	NF	NF	NF	NF	NF	NF	NF	NF
D2A4Q0 D2A4Q0_TRICA	7,831	16	2	6	2	NF	NF	NF	NF	NF	NF	NF	NF
A0A0F7IQ20 A0A0F7IQ20_LOCM	20,283	16	4	6	4	NF	NF	NF	NF	NF	NF	NF	NF
D6WCX5 D6WCX5_TRICA	10,818	5	2	6	2	NF	NF	NF	NF	NF	NF	NF	NF
A0A6G5XH10 A0A6G5XH10_LOCM	13,038	7	4	6	4	NF	NF	NF	High	NF	NF	NF	NF
V9Q318 V9Q318_LOCM	12,523	29	5	6	4	NF	NF	NF	NF	NF	NF	NF	NF
D7EIM3 D7EIM3_TRICA	5,621	11	2	6	2	High	High	High	NF	NF	NF	NF	NF
D6WKA5 D6WKA5_TRICA	13,772	12	4	6	4	NF	NF	High	NF	NF	NF	NF	NF
E2GDJ8 E2GDJ8_TRICA	11,535	12	2	6	1	NF	NF	NF	NF	NF	NF	NF	NF
X5MFI1 X5MFI1_LOCM	4,673	5	1	5	1	NF	NF	NF	NF	NF	NF	High	High
X5MNU7 X5MNU7_LOCM	5,596	5	1	5	1	NF	NF	NF	NF	NF	NF	High	NF
G8XSQ5 G8XSQ5_LOCM	17,963	5	3	5	2	NF	NF	NF	NF	NF	NF	NF	NF
D2A0P2 D2A0P2_TRICA	4,294	2	2	5	2	High	High	NF	High	NF	NF	NF	NF
V9Q3X9 V9Q3X9_LOCM	7,703	14	3	5	2	NF	NF	NF	NF	NF	NF	NF	NF
V9TLV5 V9TLV5_LOCM	20,5	4	4	5	4	NF	NF	NF	NF	NF	NF	NF	NF
A0A4D5SEZ2 A0A4D5SEZ2_LOCM	13,187	19	4	5	4	NF	NF	NF	NF	NF	NF	NF	NF
D6WZ25 D6WZ25_TRICA	13,666	29	2	4	1	NF	NF	NF	NF	NF	NF	NF	NF
D2A4R4 D2A4R4_TRICA	12,151	8	2	4	2	NF	NF	NF	NF	NF	NF	NF	NF
M1PFE4 M1PFE4_LOCM	9,708	31	3	4	3	NF	NF	NF	NF	NF	NF	High	NF
E5DWM0 E5DWM0_LOCM	12,124	23	4	4	4	NF	NF	NF	NF	NF	NF	NF	NF
D6WU92 D6WU92_TRICA	7,683	9	2	4	2	NF	NF	NF	NF	NF	NF	NF	NF
D6X0W4 D6X0W4_TRICA	2,715	3	1	4	1	High	NF	High	NF	NF	High	High	NF
D6WB91 D6WB91_TRICA	11,8	11	1	4	1	NF	NF	NF	NF	NF	NF	NF	NF
A0A139W8V5 A0A139W8V5_TRICA	11,77	6	2	4	1	NF	NF	NF	NF	NF	NF	NF	NF
D2A0S3 D2A0S3_TRICA	8,602	12	3	4	3	NF	NF	NF	NF	NF	NF	NF	NF
A0A139WNN1													
A0A139WNN1_TRICA	5,447	2	2	4	2	NF	High	High	NF	NF	NF	NF	NF
A0A139WLA3 A0A139WLA3_TRICA	11,906	4	2	4	1	NF	NF	NF	NF	NF	NF	NF	NF
A0A6B9BK63 A0A6B9BK63_LOCM	13,61	10	3	4	3	NF	NF	NF	NF	High	NF	NF	NF

W0C415 W0C415_LOCFI	3,29	9	1	4	1	NF	High	NF	NF	NF	NF	NF	NF
K4Q3F5 K4Q3F5_LOCFI	14,138	9	4	4	4	NF	NF	NF	NF	NF	NF	NF	NF
V9Q3X5 V9Q3X5_LOCFI	4,706	12	3	4	3	NF	NF	NF	NF	NF	NF	NF	NF
D6WA84 D6WA84_TRICA	3,189	7	1	4	1	High	NF	NF	NF	NF	NF	NF	NF
D6W7G0 D6W7G0_TRICA	6,435	1	1	4	1	NF	NF	NF	NF	NF	High	NF	NF
A0A139WAL9 A0A139WAL9_TRICA	1,547	3	1	4	1	NF	NF	NF	NF	NF	NF	NF	High
A0A139WG19 A0A139WG19_TRICA	10,394	17	2	4	2	NF	NF	High	NF	NF	NF	NF	NF
Q3LB77 Q3LB77_LOCFI	10,28	25	4	4	4	NF	NF	NF	NF	NF	NF	NF	NF
D7EI38 D7EI38_TRICA	10,525	27	2	3	2	NF	NF	NF	NF	NF	NF	NF	NF
D2A5H8 D2A5H8_TRICA	13,903	8	2	3	2	NF	NF	NF	NF	NF	NF	NF	NF
A0A139WNJ1 A0A139WNJ1_TRICA	2,308	2	1	3	1	NF	High	High	NF	High	NF	NF	NF
D6WGX8 D6WGX8_TRICA	7,539	8	2	3	2	NF	NF	NF	NF	NF	NF	NF	NF
D6WLU7 D6WLU7_TRICA	4,919	12	3	3	3	NF	NF	NF	NF	NF	NF	NF	NF
E7CIJ0 E7CIJ0_LOCFI	2,101	13	1	3	1	High	NF	NF	NF	NF	High	NF	NF
D2A5W6 D2A5W6_TRICA	1,4	1	1	3	1	High	High	High	NF	NF	NF	NF	NF
A0A139WCQ8 A0A139WCQ8_TRICA	6,76	1	1	3	1	NF	NF	NF	NF	NF	NF	NF	NF
D6WSI9 D6WSI9_TRICA	8,84	7	3	3	1	NF	NF	NF	NF	NF	NF	NF	NF
D2A651 D2A651_TRICA	1,221	2	1	3	1	NF	NF	NF	High	NF	NF	NF	NF
V9Q2Q3 V9Q2Q3_LOCFI	3,423	9	2	3	2	High	High	NF	NF	NF	NF	NF	NF
D6X1D2 D6X1D2_TRICA	5,492	17	1	3	1	NF	NF	NF	NF	NF	NF	NF	NF
A0A3Q8CKT9 A0A3Q8CKT9_LOCFI	4,032	11	1	3	1	NF	NF	High	NF	High	NF	High	NF
S4VDE6 S4VDE6_LOCFI	9,915	7	3	3	1	NF	NF	NF	NF	NF	NF	NF	NF
A0A139WF25 A0A139WF25_TRICA	1,998	3	1	3	1	NF	NF	NF	High	NF	NF	NF	NF
D6WR75 D6WR75_TRICA	2,094	5	1	3	1	High	NF	High	NF	NF	NF	NF	NF
A0A1P8BK01 A0A1P8BK01_LOCFI	5,607	1	2	3	2	NF	High	High	NF	NF	NF	NF	NF
T1VXB0 T1VXB0_LOCFI	5,11	3	2	3	2	NF	NF	NF	NF	NF	High	High	High
D6WHC6 D6WHC6_TRICA	8,764	8	1	3	1	NF	NF	NF	NF	NF	NF	NF	NF
A0A1S6Q344 A0A1S6Q344_LOCFI	7,351	6	2	3	2	NF	NF	NF	NF	NF	NF	High	NF
D2A198 D2A198_TRICA	12,867	7	3	3	3	NF	NF	NF	NF	NF	NF	NF	NF



Supplements

D6W9B0 D6W9B0_TRICA	5,182	4	1	2	1	NF	NF	NF	NF	NF	High	High	NF
A0A139WJ64 A0A139WJ64_TRICA	3,913	5	1	2	1	NF	NF	NF	NF	NF	NF	NF	NF
D6WA44 D6WA44_TRICA	3,72	6	1	2	1	NF	NF	NF	High	NF	NF	NF	NF
D6X550 D6X550_TRICA	8,211	16	2	2	2	NF	NF	NF	NF	NF	NF	NF	NF
D2A142 D2A142_TRICA	3,651	4	2	2	2	NF	NF	NF	NF	NF	NF	NF	NF
X5MFH0 X5MFH0_LOCFI	2,442	6	1	2	1	NF	NF	NF	High	NF	NF	NF	NF
W8EH13 W8EH13_LOCFI	5,051	5	2	2	2	NF	NF	NF	NF	NF	High	NF	NF
X5MBK1 X5MBK1_LOCFI	6,786	9	1	2	1	NF	NF	NF	NF	NF	NF	NF	NF
A9LC94 A9LC94_LOCFI	4,298	2	1	2	1	NF	NF	NF	NF	NF	NF	NF	High
D6WC52 D6WC52_TRICA	1,181	3	1	2	1	NF	NF	NF	NF	NF	NF	NF	NF
D6WNV1 D6WNV1_TRICA	1,746	2	1	2	1	NF	NF	NF	NF	NF	High	NF	NF
D6WAC0 D6WAC0_TRICA	2,671	8	1	2	1	NF	NF	NF	NF	NF	NF	NF	NF
D6WAC2 D6WAC2_TRICA	3,101	7	1	2	1	NF	High	NF	NF	NF	NF	NF	NF
D6WY26 D6WY26_TRICA	1,465	1	1	2	1	NF	NF	NF	High	High	NF	NF	NF
D6WKA1 D6WKA1_TRICA	3,299	11	2	2	2	NF	NF	NF	NF	NF	NF	NF	NF
D6W7V9 D6W7V9_TRICA	4,57	12	2	2	2	NF	NF	NF	NF	NF	NF	NF	NF
V9Q3Y3 V9Q3Y3_LOCFI	3,789	9	2	2	2	NF	High	NF	NF	NF	NF	NF	NF
C0KJ6 C0KJ6_LOCFI	1,592	2	1	2	1	NF	High	High	NF	NF	NF	NF	NF
A0A1B0Y0A8 A0A1B0Y0A8_LOCFI	2,584	2	1	2	1	NF	High	High	NF	NF	NF	NF	NF
H8YU82 H8YU82_LOCFI	5,59	4	1	2	1	NF	NF	NF	NF	High	NF	High	NF
D6X4H8 D6X4H8_TRICA	2,842	1	1	2	1	NF	NF	NF	NF	NF	NF	NF	NF
D7EK09 D7EK09_TRICA	1,259	4	1	2	1	NF	NF	NF	NF	NF	NF	NF	NF
D6WQ48 D6WQ48_TRICA	1,251	2	1	2	1	NF	NF	NF	NF	NF	NF	NF	NF
D6WMJ9 D6WMJ9_TRICA	4,638	6	1	2	1	High	NF	NF	NF	NF	NF	NF	NF
C0KJ8 C0KJ8_LOCFI	2,218	2	1	2	1	High	NF	High	NF	NF	NF	NF	NF
A0A6G5XGQ5 A0A6G5XGQ5_LOCFI	3,104	4	1	2	1	NF	NF	NF	NF	NF	NF	NF	NF
A0A139WJ91 A0A139WJ91_TRICA	3,352	1	2	2	2	NF	High	High	NF	NF	NF	NF	NF
D2A203 D2A203_TRICA	1,178	2	1	2	1	NF	NF	NF	NF	NF	NF	NF	NF
V5RE76 V5RE76_LOCFI	5,778	5	2	2	2	NF	NF	NF	High	NF	NF	NF	NF

A0A139WI27 A0A139WI27_TRICA	2,115	3	1	2	1	NF	NF	NF	NF	High	NF	NF	NF
D6X2X9 D6X2X9_TRICA	1,826	1	1	2	1	NF	NF	NF	High	NF	NF	NF	NF
D6WLS9 D6WLS9_TRICA	2,019	5	1	2	1	NF	NF	NF	NF	NF	NF	NF	NF
A0A139WC21 A0A139WC21_TRICA	2,148	1	1	2	1	High	High	NF	NF	NF	NF	NF	NF
D2A3W2 D2A3W2_TRICA	3,621	5	1	2	1	High	NF	NF	High	NF	NF	NF	NF
B1NMW4 B1NMW4_9EURO	3,449	8	1	2	1	NF	NF	NF	NF	NF	NF	NF	NF
L7WSJ0 L7WSJ0_LOCFI	4,358	14	2	2	2	High	NF	NF	NF	NF	NF	NF	NF
A0A023ZYJ9 A0A023ZYJ9_TRICA	2,837	5	1	2	1	NF	High	NF	NF	NF	NF	NF	NF
D6WTD4 D6WTD4_TRICA	1,6	2	1	2	1	NF	NF	NF	NF	NF	NF	High	High
D2A4T5 D2A4T5_TRICA	1,725	4	1	2	1	High	NF	NF	NF	NF	NF	NF	NF
J7G7F5 J7G7F5_9EURO	2,62	10	1	2	1	NF	NF	NF	NF	NF	NF	NF	NF
A0A139WDE4 A0A139WDE4_TRICA	1,863	1	1	2	1	NF	NF	NF	NF	NF	NF	High	NF
D6WPP3 D6WPP3_TRICA	4,164	3	1	2	1	NF	NF	NF	NF	NF	NF	NF	NF
D6WUV2 D6WUV2_TRICA	3,686	10	2	2	2	NF	NF	NF	NF	NF	NF	NF	NF
D6WKP5 D6WKP5_TRICA	3,163	2	1	2	1	NF	NF	NF	High	High	NF	NF	NF
A0A139WHJ3 A0A139WHJ3_TRICA	8,449	1	2	2	2	NF	NF	NF	High	NF	NF	NF	NF
D6X0G0 D6X0G0_TRICA	10,26	13	2	2	2	NF	NF	NF	NF	NF	NF	NF	NF
X5MI43 X5MI43_LOCFI	2,023	9	1	1	1	NF	NF	NF	NF	NF	NF	NF	NF
A0A139WLM4 A0A139WLM4_TRICA	1,395	3	1	1	1	NF	NF	NF	NF	NF	NF	NF	High
X5MFH4 X5MFH4_LOCFI	3,64	8	1	1	1	NF	NF	NF	NF	NF	NF	NF	NF
D6WD83 D6WD83_TRICA	3,146	4	1	1	1	High	NF	NF	NF	NF	NF	NF	NF
A0A139WDN6 A0A139WDN6_TRICA	1,48	1	1	1	1	NF	NF	High	NF	NF	NF	NF	NF
D6WS19 D6WS19_TRICA	1,138	4	1	1	1	High	NF	NF	NF	NF	NF	NF	NF
V9Q2Q7 V9Q2Q7_LOCFI	1,69	5	1	1	1	NF	NF	NF	NF	NF	NF	NF	NF
D6WEM3 D6WEM3_TRICA	1,324	4	1	1	1	NF	NF	NF	NF	NF	NF	NF	NF
C0KJ5 C0KJ5_LOCFI	2,397	2	1	1	1	NF	NF	High	NF	NF	NF	NF	NF
D6WBX0 D6WBX0_TRICA	1,582	1	1	1	1	NF	NF	NF	NF	NF	NF	NF	NF
A0A139WDC8 A0A139WDC8_TRICA	1,428	4	1	1	1	NF	NF	NF	NF	NF	NF	NF	NF

## Supplements

D6WJB9 D6WJB9_TRICA	3,958	7	1	1	1	NF	NF	NF	NF	NF	NF	NF	NF
D6WMI1 D6WMI1_TRICA	1,402	1	1	1	1	NF	NF	NF	NF	NF	NF	NF	NF
D6WXI4 D6WXI4_TRICA	1,559	6	1	1	1	NF	NF	High	NF	NF	NF	NF	NF
V5RF49 V5RF49_LOCFI	4,932	4	1	1	1	NF	NF	NF	NF	NF	NF	NF	NF
D2A297 D2A297_TRICA	5,885	12	1	1	1	NF	NF	NF	NF	NF	NF	NF	NF
H8YU83 H8YU83_LOCFI	1,526	1	1	1	1	NF	NF	NF	NF	NF	NF	High	NF
A0A0G3F535 A0A0G3F535_LOCFI	1,925	4	1	1	1	NF	NF	NF	High	NF	NF	NF	NF
A0A139WJG0 A0A139WJG0_TRICA	1,309	0	1	1	1	NF	NF	NF	NF	NF	NF	NF	NF
A0A139WPG1 A0A139WPG1_TRICA	3,599	0	1	1	1	NF	NF	NF	NF	NF	NF	High	NF
D6WUS6 D6WUS6_TRICA	5,251	5	1	1	1	NF	NF	NF	NF	NF	NF	NF	NF
D6WRY5 D6WRY5_TRICA	1,222	3	1	1	1	NF	NF	NF	NF	NF	NF	NF	NF
D6W7E6 D6W7E6_TRICA	3,539	4	1	1	1	NF	NF	NF	NF	NF	NF	NF	NF
D6W794 D6W794_TRICA	1,407	4	1	1	1	NF	NF	NF	NF	NF	NF	NF	NF
D2A013 D2A013_TRICA	1,604	4	1	1	1	NF	NF	NF	NF	NF	NF	NF	NF
D6WFE2 D6WFE2_TRICA	2,112	5	1	1	1	NF	NF	NF	NF	NF	NF	High	NF
D6W9B2 D6W9B2_TRICA	2,164	4	1	1	1	NF	NF	NF	NF	NF	NF	NF	NF
A0A222NTC4 A0A222NTC4_LOCFI	1,654	7	1	1	1	NF	NF	NF	NF	NF	NF	High	NF
D6WW84 D6WW84_TRICA	1,194	3	1	1	1	NF	NF	NF	NF	NF	NF	NF	NF
W8EH07 W8EH07_LOCFI	2,857	5	1	1	1	NF	NF	NF	NF	NF	NF	High	NF
D6WDF4 D6WDF4_TRICA	1,673	3	1	1	1	NF	NF	NF	NF	NF	NF	NF	NF
D1ZZ88 D1ZZ88_TRICA	4,246	3	1	1	1	NF	NF	NF	NF	High	NF	NF	NF
B0FJK9 B0FJK9_LOCFI	2,848	3	1	1	1	NF	NF	NF	NF	NF	NF	High	NF
A0A139WCJ6 A0A139WCJ6_TRICA	1,392	3	1	1	1	NF	NF	NF	NF	NF	NF	NF	NF
D6X293 D6X293_TRICA	1,279	1	1	1	1	NF	NF	NF	NF	High	NF	NF	NF
A0A139WBH3 A0A139WBH3_TRICA	1,76	3	1	1	1	NF	NF	NF	NF	NF	NF	NF	NF
D6WEK6 D6WEK6_TRICA	4,281	3	1	1	1	NF	NF	NF	High	NF	NF	NF	NF
D7EKM4 D7EKM4_TRICA	4,899	5	1	1	1	NF	NF	NF	NF	NF	NF	NF	NF
D6X202 D6X202_TRICA	2,677	1	1	1	1	NF	NF	NF	NF	NF	NF	NF	NF
A0A139WIK4 A0A139WIK4_TRICA	1,841	2	1	1	1	NF	NF	NF	NF	NF	NF	NF	NF
X5MBK8 X5MBK8_LOCFI	2,581	3	1	1	1	NF	NF	NF	NF	NF	NF	NF	NF

D6WRR8 D6WRR8_TRICA	1,387	1	1	1	1	NF	NF	NF	High	NF	NF	NF	NF
V5RDW2 V5RDW2_LOCFMI	6,671	3	1	1	1	NF	NF	NF	NF	NF	NF	NF	NF
D6WVU4 D6WVU4_TRICA	2,259	4	1	1	1	NF	NF	NF	NF	NF	NF	NF	NF
D6X4W2 D6X4W2_TRICA	1,437	2	1	1	1	NF	NF	NF	NF	NF	NF	NF	NF
D6WB31 D6WB31_TRICA	1,81	7	1	1	1	NF	NF	NF	NF	NF	NF	NF	NF
A0A139WD26 A0A139WD26_TRICA	2,907	1	1	1	1	NF	NF	NF	NF	NF	NF	NF	NF
D6WR02 D6WR02_TRICA	1,271	4	1	1	1	NF	NF	NF	NF	NF	NF	NF	NF
D6WTQ4 D6WTQ4_TRICA	5,022	12	1	1	1	NF	NF	NF	NF	NF	NF	NF	NF
D6WFZ1 D6WFZ1_TRICA	2,983	4	1	1	1	NF	High	NF	NF	NF	NF	NF	NF
A0A139W942 A0A139W942_TRICA	1,246	0	1	1	1	NF	NF	NF	NF	NF	NF	NF	NF
A0A139WPQ7 A0A139WPQ7_TRICA	1,672	1	1	1	1	NF	NF	NF	NF	NF	NF	NF	NF
A0A139W8C1 A0A139W8C1_TRICA	1,692	2	1	1	1	NF	NF	NF	NF	NF	NF	NF	NF
D6WM75 D6WM75_TRICA	3,287	2	1	1	1	NF	NF	NF	NF	NF	NF	NF	NF
D6W7D3 D6W7D3_TRICA	2,001	2	1	1	1	NF	NF	NF	High	NF	NF	NF	NF
D6WCL3 D6WCL3_TRICA	2,2	7	1	1	1	NF	NF	NF	NF	NF	NF	NF	NF
D6X3F5 D6X3F5_TRICA	1,22	5	1	1	1	High	NF	NF	NF	NF	NF	NF	NF
D6X4R1 D6X4R1_TRICA	1,647	2	1	1	1	NF	NF	NF	NF	NF	NF	NF	NF
D6WYY8 D6WYY8_TRICA	1,321	2	1	1	1	NF	NF	NF	High	NF	NF	NF	NF
D1ZZP5 D1ZZP5_TRICA	4,199	3	1	1	1	NF	NF	NF	NF	NF	NF	High	NF
D6WL33 D6WL33_TRICA	3,42	8	1	1	1	NF	NF	NF	NF	NF	NF	NF	NF
D2A090 D2A090_TRICA	2,775	6	1	1	1	High	NF	NF	NF	NF	NF	NF	NF
D7EIU4 D7EIU4_TRICA	3,468	2	1	1	1	NF	NF	NF	NF	High	NF	NF	NF
D6X4D8 D6X4D8_TRICA	3,68	9	1	1	1	NF	NF	NF	NF	NF	NF	NF	NF
D6WFQ2 D6WFQ2_TRICA	1,283	2	1	1	1	NF	NF	NF	NF	NF	NF	NF	NF
D6WSR2 D6WSR2_TRICA	2,818	8	1	1	1	NF	NF	NF	NF	NF	NF	NF	NF
D6WIT1 D6WIT1_TRICA	1,137	4	1	1	1	NF	NF	NF	NF	NF	NF	NF	NF
V9Q3Y6 V9Q3Y6_LOCFMI	2,943	4	1	1	1	NF	NF	NF	NF	NF	NF	NF	NF
D6WBM8 D6WBM8_TRICA	6,249	8	1	1	1	High	NF	NF	NF	NF	NF	NF	NF
D6WW25 D6WW25_TRICA	2,079	4	1	1	1	NF	NF	NF	High	NF	NF	NF	NF
D7EIK6 D7EIK6_TRICA	1,208	2	1	1	1	NF	NF	NF	NF	NF	NF	NF	NF

Supplements

D6WCG2 D6WCG2_TRICA	1,289	2	1	1	1	NF	NF	NF	NF	NF	NF	NF	NF
D6WN12 D6WN12_TRICA	2,135	6	1	1	1	NF	NF	NF	NF	NF	NF	NF	NF
A0A139WAR2 A0A139WAR2_TRICA	1,489	4	1	1	1	NF	NF	High	NF	NF	NF	NF	NF
A0A1L7NZM8 A0A1L7NZM8_LOCFI	2,687	3	1	1	1	High	NF	NF	NF	NF	NF	NF	NF
D7ELD3 D7ELD3_TRICA	2,948	2	1	1	1	NF	NF	NF	High	NF	NF	NF	NF
A0A139W8B2 A0A139W8B2_TRICA	4,76	2	1	1	1	NF	NF	NF	NF	NF	NF	NF	NF
D6X3U4 D6X3U4_TRICA	2,415	3	1	1	1	NF	NF	NF	NF	NF	NF	NF	NF
D6WGS1 D6WGS1_TRICA	1,204	4	1	1	1	NF	NF	NF	NF	NF	NF	NF	NF
D2A5J2 D2A5J2_TRICA	1,147	17	1	1	1	NF	NF	NF	NF	NF	NF	NF	NF
A0A139WMQ2 A0A139WMQ2_TRICA	1,267	0	1	1	1	NF	NF	NF	NF	NF	NF	NF	High
X5MPI3 X5MPI3_LOCFI	1,394	4	1	1	1	NF	NF	NF	NF	NF	NF	NF	NF
A0A139WL15 A0A139WL15_TRICA	2,532	3	1	1	1	NF	NF	NF	NF	NF	NF	NF	NF
D6WRI6 D6WRI6_TRICA	7,04	14	1	1	1	NF	NF	NF	NF	NF	NF	NF	NF
A0A1B1MRN4 A0A1B1MRN4_LOCFI	1,654	6	1	1	1	NF	NF	NF	NF	NF	NF	NF	NF
A0A139WIH0 A0A139WIH0_TRICA	2,211	1	1	1	1	NF	NF	High	NF	NF	NF	NF	NF
D6WGA0 D6WGA0_TRICA	2,541	6	1	1	1	NF	NF	NF	NF	NF	NF	NF	NF
A0A139WEI4 A0A139WEI4_TRICA	2,676	2	1	1	1	NF	NF	NF	High	NF	NF	NF	NF
D6WTN7 D6WTN7_TRICA	1,494	1	1	1	1	NF	NF	NF	NF	NF	NF	NF	NF
D6X3T6 D6X3T6_TRICA	1,142	1	1	1	1	NF	NF	NF	High	NF	NF	NF	NF

### Methods iPSC molecular analysis

#### Analysis of gene expression and CRLF3 abundance

In order to further analyse gene expression patterns for pro- and anti-apoptotic genes within iPSC-derived neurons, Real-time quantitative PCR (qPCR) was run. CRLF3 protein abundance was analysed via Western blot and staining for CRLF3 in iPSC-derived neurons.

#### RNA isolation and cDNA synthesis

For all treatment groups within survival assays two wells of a 6-well plate were pelleted for further molecular analysis. RNA was isolated by means of Trizole/Chloroform protocol as described in Knorr et al. (Knorr *et al.*, 2020). In brief, 1 ml Trizole (Thermo Fisher Scientific; #15596026) was added to each cell pellet and cells were disrupted in a tissue lyser. 200 µl Chloroform (Labsolute; #2475) was added and the samples were shaken vigorously for 20 sec in tissue lyser. Samples were incubated on ice for 15 min before centrifugation at 12.000 x g for 15 min at 4°C. The top translucent phase of each sample was transferred to a fresh Eppendorf cup and mixed with 1 ml ice-cold 75% EtOH. Samples were incubated at -20°C for at least 1 h before centrifugation at 10.000 x g for 15 min at 4°C. The resulting RNA pellet was washed three times in ice-cold EtOH before pellets were dried and resuspended in 30 µl ddH<sub>2</sub>O. RNA concentrations were measured by Nanodrop (Thermo Fisher Scientific).

cDNA was synthesised using the LunaScript RT SuperMixKit (New England BioLabs; #E3010) according to the manufactures instructions. For all samples 1 µg RNA was reverse transcribed.

#### qPCR

qPCR analysis for *BAX*, *Caspase 3*, *BCL-2* and *CRLF3* were run using specific primers (see oligonucleotide list Table 1). *B-Actin* was used as housekeeping gene (HKG). All primers were analysed for their efficiencies previously. All samples were loaded in triplicates and (-) RT controls and water were run as negative controls on every plate. qPCRs reactions were prepared with final concentrations of 5 µl Luna® Universal qRT-PCR Master Mix (New England Bio- Lab; #M3003), 0,1 mM forward and reverse primers and 10 ng cDNA. qPCRs were pipetted in a 96-well clear well plates (StarLab; #E1403-5200) and run using a Bio-Rad CFX Connect Real-Time system (Bio-Rad; #1855201). The following qPCR program was employed for specific gene amplification (see table 2).

**Table 9:** Oligonucleotides used in this study

Application	Gene	Oligonucleotide 5'-3'	Tm	Accession number
qPCR	Bax-fwd	CGAGTGGCAGCTGACATGTT	61°C	ENST00000293288.12
qPCR	Bax-rev	TCCAGCCCATGATGGTTCTG		
qPCR	Caspase 3-fwd	GGAGGCCGACTTCTTGTATG	61°C	ENST00000308394.9
qPCR	Caspase 3-rev	TGCCACCTTTCGGTTAACCC		
qPCR	BCL-2-fwd	CGTTATCCTGGATCCAGGTG	61°C	ENST00000398117.1
qPCR	BCL-2-rev	GTGTGTGGAGAGCGTCAAC		
qPCR	bActin-fwd	GCGAGAAGATGACCCAGATC	61°C	ENST00000674681.1
qPCR	bActin-rev	GGGCATACCCCTCGTAGATG		

## Supplements

**Table 2:** qPCR program used for this study

	<b>Step</b>	<b>Temperature [°C]</b>	<b>Time [s]</b>	
PCR	Initial denaturation	95	180	
	Denaturation	95	10	
	Annealing	61	30	x40
Melting curve reaction	Elongation	72	30	
	Denaturation	95	60	
	Annealing	55	60	
	Melting curve	55	10	0.5 °C per cycle up to 95 °C

Ct values were analysed using the Pfaffl method (Pfaffl, 2001) and data was normalized to the corresponding HKG value of each sample and further to the corresponding gene of interest (GOI) control value. Relative gene expression data is represented as Bar plots showing the geometric mean and standard deviations.

### *Western blot*

Western blot analysis of iPSC-derived neurons was performed as described previously. Quantification of protein band intensities was performed using ImageJ. Band intensities were normalized to the corresponding  $\alpha$ Tubulin band intensity of each sample and then towards control samples within treatment groups. Data is shown as bar plots representing the average band intensities measured together with the calculated standard deviation.

## Acknowledgements

*“So long, and thanks for all the fish!”* – The Dolphins [Douglas Adams]

3,5 years, a fried hard drive, a pandemic, a wrist operation of the useful hand and countless hours later I can finally call it a thesis. Many people have accompanied and supported me on my way and I would like to take the chance to pay them justice.

First and foremost, I want to express my deep gratitude and thank to my PhD supervisor Ralf Heinrich. Over the last years we have built a team that cannot be beat (except maybe in badminton due to me). I am so unbelievably thankful for the opportunity to work with you again and the trust you have put into me, allowing me to basically do whatever I wanted. You supported me in all the right ways and moments and let me roam free when I needed to. You challenged me whenever I got too confident and reassured me, when I was doubting myself- and that is what makes a great supervisor. Thank you so, so much for all the laughs, cakes, beers and dinners (and of course for being a major driver in carrying furniture during my moving) but also for our show-worthy discussions about titles and wording. You are fantastic and I could not have asked or hoped for anyone better to guide me through this adventure.

I furthermore would like to express my gratitude to Rüdiger Behr and Gregor Bucher for supporting me as members of my thesis advisory committee. Special thanks go out to Rüdiger, for following my path since the masters and allowing me to work in his lab as part of my thesis.

To Steffi, Nicola and Gudrun- You lovely ladies! You have helped me so much during my PhD. May it have been contracts, money problems, experiments I simply did not have time to do myself or keeping me sane and healthy with food. I will always appreciate that cupboard that mysteriously filled with food and sweets when you noticed that I was running night shifts again. I cannot thank you enough for your friendship and support!

To all the others in the lab: Thank you for holding up with me, with 20 experiments running at the same time and a wild Debbie running from lab to lab trying to keep everything in order. Special shoutout to Phil and Bart who have not only enlightened many days with conversation, scientific discussions and advise but who have turned out to be friends and people whose opinions matter a lot! And especially to Bart: Thank you for programming that AI, my wrist might never be the same again, but at least it won't get any worse by clicking 1000s of cells anymore. Charon is my true queen!

During my time as a PhD student, many, many students have passed the lab and I would like to thank all of them for the work and effort they have put into their experiments. It has been a pleasure to supervise every single one of you and I believe that I learned at least as much as you guys did during supervision.

To the Behr Lab: Thank you for hosting me during my iPSC project. I know that I took up chronically sparse space. Nonetheless, you all have welcomed me in your space, have shared laughs and advise with me and bared with the crazy that I was during that project. A big shoutout to Angelina, Charis and Nicole for being utterly fantastic humans, with such big hearts that I sometimes really wondered how you could be real. Thank you for all the lab support, even more for all the moral support and the most for your friendship. Having you on my team kept me going, thank you!!

To my friends and family: You people are truly and utterly incredible! Many of you have been at my side since the beginning of my academic journey. You have watched me grow from a sloppy bachelor student to a workaholic and back to sloppy writhing periods. You have supported me, stood by my side, held my back, pushed me when I had to be pushed and held back, when I was in moments of wanting to be alone. From near and far I have always felt your love and your trust into me, and I could not hope for a more supportive group of humans to call my friends.



## Acknowledgements

To Ignacio- the weird Spanish guy who smoothly slid into my life and decided to stay: THANK YOU! Thank you for everything you have held up with, for late night dinners and grumpy morning Debbies. For chaos in flats, being locked in a way to small place during a pandemic, for ginger shots and ice cream overloads. Thank you for respecting my me time and holding me like no other human could in times in which I felt like falling apart. I would have been able to this without you, but I do have to admit, that it was a much better time with you!

To my mother Vicdan: You are an incredible woman, you make your way and you fight your fights. I thank you so much for equipping me with the skills of handling this life and its drawbacks, but also for knowing when to celebrate. I thank you for your limitless and unconditional support, for food packages and warming words. For your love and for holding up with the mess I have been at times. You pushed me and you held me, and I will never be able to repay you for all your kindness, love and support.

To my father Roland: Look what I did! There is nothing that I wouldn't give to have one last beer with you, to have one last talk on how I am supposed to tackle the rest, to hear your voice again. Somewhere deep down I know that you are still there, that you are protecting me and that you are always rooting for me. One day we will celebrate this, and we will bicker as we used to.

This journey has been a long one and even though I did not finish everything that I wanted to, I believe that I achieved a lot. Over the last 3,5 years I have not only earned my PhD title, I made incredible friends, I grew my family my many biologically unrelated members, I have learned so much and started to understand what I can reach if I only stay true to myself. I have figured out that the humans in my close vicinity are the most precious thing and that love and empathy can take you to places you would never have imagined. I don't know what lays ahead of my road, but I know that I could not have asked for anything more to equip me to withstand it. Thank you again to all those people mentioned here but also to all those that did not find mentioning by name- you guys all know! You all are incredible and every day again I am thankful to have you in my own little microcosmos. THANK YOU and always remember: DON'T LET THE MUGGLES GET YOU DOWN! [Ron Weasley]

# Curriculum Vitae

Name: Debra Yasemin Knorr

E-Mail: debbrayasemin.knorr@uni-goettingen.de

Date & place of birth: 27.06.1992, Cape Town, South Africa

Language skills: German (native)  
English (native)  
Turkish (fluent in word)

## Education

---

2018-2022: Georg-August-University, Göttingen  
Gauss PhD program  
Graduating May 2022

2016-2018: Georg-August-University, Göttingen  
M.Sc Developmental, Neural and Behavioural Biology  
Graduated September 2018, Total mark 1,2

2016: Field Guide Level 1 and Trails Guide Training,  
Ulovane Environmental Trainer, Paterson, South Africa

2012-2016: Georg-August-University, Göttingen  
B.Sc Biology  
Graduated February 2016, Total mark 2.3

## Laboratory work experience

---

2022: PhD thesis in the Schwann-Schleiden-Institute Göttingen, **Department of Cellular Neurobiology** under the supervision of Prof. Dr. Ralf Heinrich  
Thesis title: *“Anti-apoptotic & neuroprotective erythropoietin/CRLF3-signalling in insects and humans”*

2018: Master thesis in the **Platform for Degenerative Diseases**, German Primate Center, Göttingen,  
Department of Prof. Rüdiger Behr, working on: *“Enhancing the maturation of human and non-human primate iPS cell-derived cardiomyocytes by hormones and increased calcium levels”*

- 2017: **Platform for Degenerative Diseases**, German Primate Center, Göttingen  
Department of Prof. Rüdiger Behr, working on: “*Cardiac differentiation of induced pluripotent stem cells from Macaca mulatta and Papio Anubis*”
- 2017: **Department of Infectious Diseases and Molecular Medicin**, University of Cape Town, South Africa  
Department of Prof. Jonathan Blackburn, working on: “*The Effect of Rifampicin and Isoniazid on Differentiated Human Neuronal Stem Cells*”
- 2017: Schwann-Schleiden-Institute Göttingen, Department of **Cellular Neurobiology**  
Working group of Prof. Andreas Stumpner, working on: „*Neurotransmitters in Ensifera auditory Neurons*”, focusing on *Grillus bimaculatus* and *Ancistrura nigrovittata*
- 2017: **German Center for Neurodegenerative Diseases**, University Medical Center Göttingen, Department of Psychiatry and Psychotherapy  
Department of Prof. Andre Fischer, working on: “*The epigenetics of Alzheimers disease- A time dependant effect of SAHA and TSA on histone and protein acetylation in M.musculus primary neuronal cell culture*”
- 2016: Schwann-Schleiden-Institute Göttingen, **Department of Cellular Neurobiology**  
Working group of Prof. Ralf Heinrich, working on: „*Erythropoietin-mediated neuroprotection of insect neurons after knockdown of the orphan cytokine receptor CRLF3*”, focusing on *Tribolium castaneum* as model organism
- 2014-2015: Schwann-Schleiden-Institute Göttingen, **Department of Cellular Neurobiology**  
Working group of Prof. Ralf Heinrich, working on:  
*Identification of signaling pathways involved in Epo-mediated neuroprotection in the Locust Locusta migratoria*

## Teaching experience

---

- Since 2018:* Independent supervision of Bachelor and Master students in the Department for Cellular Neurobiology
- 6 Bachelor students
  - 7 Master students
  - 1 International exchange student
- March 2017:* Tutor for bachelor students  
Teaching assistance in “Animal physiology” course
- March 2016:* Tutor for bachelor students  
Teaching assistance in “Animal physiology” course
- Dec 2015:* Tutor for Msc/PhD Neuroscience students  
Teaching assistance in “Sensory and behavioural physiology” course

## Publications

---

**Knorr DY**, Hartung D, Schneider K, Hintz L, Pies HS and Heinrich R (2021) “Locust Hemolymph Conveys Erythropoietin-Like Cytoprotection via Activation of the Cytokine Receptor CRLF3”, *Front. Physiol.* 12:648245. doi: 10.3389/fphys.2021.648245

**Knorr DY**, Georges NS, Pauls S, Heinrich R (2020) “Acetylcholinesterase promotes apoptosis in insect neurons”, *Apoptosis*; <https://doi.org/10.1007/s10495-020-01630-4>

Stauske M, Rodriguez Polo I, Haas W, **Knorr DY**, Borchert T, Streckfuss-Bömeke K, Dressel R, Bartels I, Tiburcy M, Zimmermann W-H, Behr R; (2020) “Non-Human Primate iPSC Generation, Cultivation, and Cardiac Differentiation under Chemically Defined Conditions.”, *Cells* 9, 1349; <https://doi.org/10.3390/cells9061349>

Stumpner A, Gubert S, **Knorr DY**, Göpfert, M; (2020) “Auditory DUM neurons in a bush-cricket: inhibited inhibitors.”, *Comp Physiol A* 206, 793–807; <https://doi.org/10.1007/s00359-020-01438-2>

Hahn N, **Knorr DY**, Liebig J, Wüstefeld L, Peters K, Büscher M, Bucher G, Ehrenreich H, Ralf Heinrich; (2017) “The Insect Ortholog of the Human Orphan Cytokine Receptor CRLF3 Is a Neuroprotective Erythropoietin Receptor”, *Frontiers in Molecular Neuroscience*, 10:1-11; doi: 10.3389/fnmol.2017.00223

*Under review:*

**Knorr DY**, Schneider K., Büschgens L., Förster J., Georges N.S., Geurten B.R.H. and Heinrich R.; “Protection of insect neurons by erythropoietin/CRLF3-mediated regulation of pro-apoptotic acetylcholinesterase”, Submitted to *Molecular Neurobiology* (2022)

*Submitted:*

**Knorr DY**, Rodriguez Polo I, Pies HS., Behr R. and Heinrich R. “Human Epo splice variant EV-3 mediates neuroprotective effects in human iPSC derived neurons by activation of CRLF3”

## Oral & Poster presentations

---

2021: 14<sup>th</sup> Göttingen meeting of the German Neuroscience Society; Poster  
“Neuroprotection in insects: Roles of ancestral erythropoietin-like proteins and acetylcholinesterase”; **Debra Y. Knorr**, Luca Büschgens, Kristin Schneider, Jan Förster, Nadine Georges, Denise Hartung, Luzia Hintz, Hanna S. Pies, Henning Jelten, Sonja Pribicevic, Ralf Heinrich

2020: 12<sup>th</sup> FENS Forum for Neuroscience; Posters  
“Acetylcholinesterase in apoptosis: Common functions in insects and vertebrates”;  
**Debra Y. Knorr**, Nadine S. Georges, Jan Förster, Luca Büschgens & Ralf Heinrich

“CRLF3-mediated neuroprotection by insect hemolymph: Unraveling ancient erythropoietin precursor proteins”; Ralf Heinrich, Denise Hartung, Kristin Schneider, Luzia Hintz, Sonja Pribicevic & **Debra Y. Knorr**

## CV

2020: Gönomix seminar series; Talk  
“Beyond classical roles: Acetylcholinesterase is a conserved key player in apoptosis”

2019: 30<sup>th</sup> NeuroDoWo; Poster  
“Mechanisms of Epo-mediated cell protection”; **Debbra Y. Knorr**, Denise Hartung, Nadine Georges, Hanna Pies, Nicola Schwedhelm-Domeyer, Nina Hahn & Ralf Heinrich

13<sup>th</sup> Göttingen meeting of the German Neuroscience Society; Poster  
“Ancient functions of “erythropoietin-like” neuroprotective signalling in insects: Receptors, transduction pathways & anti-apoptotic effects”; **Debbra Y. Knorr**, Bitu Massih, Luca Büschgens, Ruoyu Huang, Hanna Pies, Franziska Schmitt, Nicola Schwedhelm-Domeyer, Nina Hahn, Ralf Heinrich

## Awards & Funding

---

2022: FAZIT PhD finalization scholarship for 6 months  
Monthly 1100,-€

2020: FENS-IBRO/PERC travelling grant  
Endowed at 130,-€

2018: Scientific Photo Contest of the German primate institute, Göttingen  
Winning photo titled: “*The big bang*”, endowed at 200,-€

2017: PROMOS: Program for the enhancement of the mobility of students of german institutes of higher education of the DAAD; Travelling grant, endowed at 1675,-€